Universidade de Aveiro Departamento de Química
2018

Elisabete Valente da Costa

Produtos de alto valor em macroalgas: lípidos como compostos bioativos

High value-added products from macroalgae: lipids as bioactive compounds

Universidade de Aveiro Departamento de Química
2018

Elisabete Valente da Costa

Produtos de alto valor em macroalgas: lípidos como compostos bioativos

High value-added products from macroalgae: lipids as bioactive compounds

Tese apresentada à Universidade de Aveiro para cumprimento dos requisitos necessários à obtenção do grau de Doutor em Química Sustentável, realizada sob a orientação científica da Doutora Maria do Rosário Gonçalves dos Reis Marques Domingues, Professora Associada com Agregação do Departamento de Química da Universidade de Aveiro e da Doutora Maria Helena Abreu, Diretora e Cofundadora da empresa ALGAplus, Produção e Comércio de Algas e derivados, Lda.

Apoio financeiro do POCTI no âmbito do III Quadro Comunitário de Apoio.

Apoio financeiro da FCT e do FSE no âmbito do III Quadro Comunitário de Apoio.

Dedico este trabalho às minhas filhas Maria e Matilde, ao meu marido e à minha mãe.

"O que sabemos, saber que o sabemos. Aquilo que não sabemos, saber que não o sabemos: eis o verdadeiro saber."

Confúcio

o júri

presidente

Prof. Doutor Vítor António Ferreira da Costa
Professor Catedrático do Departamento de Mecânica da Universidade de Aveiro

Prof. Doutor Artur Manuel Soares da Silva
Professor Catedrático do Departamento de Química da Universidade de Aveiro

Doutor Ricardo Jorge Guerra Calado
Investigador Principal em regime laboral do Departamento de Biologia da Universidade de Aveiro

Prof. Doutora Maria Teresa Teixeira da Cruz Rosete
Professora auxiliar no Centro de Neurociências e Biologia Celular (CNC) da Faculdade de Farmácia da Universidade de Coimbra

Doutor Philippe Potin
Investigador Principal no Centro Nacional para a Investigação Científica (CNSR), Roscoff Marine Station

Prof. Doutora Maria Manuel Silva Oliveira
Professora Auxiliar do Departamento de Química da Universidade de Trás-os-Montes e Alto Douro

Doutora Pi Nyvall Collen
Investigadora Responsável por R & D, OLMIX, Amadéite SAS

Prof. Doutora Maria do Rosário Gonçalves Reis Marques Domingues
Professora Associada com agregação do Departamento de Química da Universidade de Aveiro

agradecimentos

Em primeiro lugar uma palavra de especial reconhecimento e uma profunda gratidão à Professora Doutora Maria do Rosário Domingues e à Doutora Helena Abreu pela orientação científica, pelo rigor, pela confiança e pelo incentivo. Por serem exemplo de responsabilidade, cordialidade, perseverança e de sucesso. Pela amizade.

A todos os colegas do grupo de Espetrometria de Massa agradeço a colaboração e o excelente espírito de equipa que nos une. À Dra. Cristina Barros agradeço também todo o apoio laboratorial. Às doutoras Tânia Melo, Ana Moreira e Elisabete Maciel agradeço a amizade, a presença constante e o apoio nos momentos mais fáceis e mais difíceis.

Agradeço a toda a equipa da ALGAplus Lda., particularmente ao doutor Rui Pereira à Mestre Andreia Rego pela disponibilidade, integração e espírito de ajuda.

Agradeço a todos os que colaboraram nos trabalhos apresentados nesta tese e sempre que solicitados, particularmente ao Professor Doutor Pedro Domingues, ao Professor Doutor Ricardo Calado, à Professora Doutora Luísa Helguero, à Doutora Carina Bernardo, à Mestre Isabel Ferreira e à Professora Doutora Teresa Cruz.

À minha mãe por ser o meu modelo de vida, de quem herdei tantas qualidades, agradeço profundamente tudo quanto sempre fez por mim e o orgulho que sente por tudo o que faço.

Às minhas filhas Matilde e Maria, sentido essencial da minha existência, dedico este trabalho, na esperança de que consiga demonstrar o que consegui construir e justificar tantas vezes a minha ausência e o porquê deste modo de vida: ter sempre trabalho para fazer. Nós conseguimos, nós somos capazes!

Agradeço a quem tem sido a minha força maior, o meu maior crítico, o meu melhor colega, o meu saco de boxe, o meu amparo e o meu guia. O pai presente e o esposo compreensivo. Muito obrigada Mendes de Sousa.

Agradeço à Universidade de Aveiro, ao Departamento de Química, às unidades Química Orgânica, Produtos Naturais e Agroalimentares (QOPNA, UID/QUI/00062/2013), Centro de Espetrometria de Massa e Rede Nacional de Espetrometria de Massa (REDE/1504/REM/2005) que me acolheram e proporcionaram os meios necessários para a realização do doutoramento.

Ao programa doutoral em Química Sustentável, particularmente ao Professor Doutor Artur Silva, Coordenador deste Doutoramento, agradeço a oportunidade, o incentivo e prontidão na resolução de todos os formalismos.

Agradeço à Fundação para a Ciência e a Tecnologia (FCT, Portugal) o financiamento da bolsa de doutoramento (SFRH/BD/52499/2014).

palavras-chave

Macroalgae, lípidos, glicolípidos, fosfolípidos, compostos bioativos, espetrometria de massa, IMTA.

resumo

As macroalgas marinhas são consideradas alimentos interessantes pelas suas propriedades nutricionais e como fonte de compostos bioativos. Estes incluem lípidos polares tais como glicolípidos (GLs), betaínas e fosfolípidos (PLs), considerados lípidos com elevado valor nutricional e ingredientes funcionais com reconhecidos benefícios para a saúde. A sua biossíntese depende de diversos fatores ambientais como a sazonalidade, a nutrição e o habitat, aumentando a complexidade estrutural do lipidoma das macroalgas, pelo que a sua identificação é um desafio da atualidade. A espectrometria de massa (MS) é uma técnica bem-sucedida e promissora no estudo detalhado da assinatura lipidómica de distintas matrizes, que pode ser alargada à identificação das centenas de espécies no lipidoma das macroalgas e permitir que estas possam finalmente ser valorizadas como fonte de lípidos.

Neste trabalho pretende-se identificar o lipidoma de macroalgas representativas do filo das Chlorophyta (*Codium tomentosum*), das Rhodophyta (*Gracilaria* sp. e *Porphyra dioica*) e das Ochrophyta (*Fucus vesiculosus)*, algas existentes na costa marítima portuguesa e recentemente cultivadas num sistema multi-trófico integrado em aquacultura (IMTA), usando estratégias de análise por espectrometria de massa acoplada a métodos cromatográficos. Pretende-se ainda avaliar as propriedades bioativas dos lípidos polares das macroalgas nomeadamente as suas propriedades biológicas como agentes anti-inflamatórios e antiproliferativos/antitumorais.

Para alcançar os objetivos propostos, foram realizados estudos de caracterização dos extratos lipídicos por HILIC–MS e MS/MS. Os resultados do trabalho permitiram identificar cerca 238 espécies moleculares distribuídas por doze classes na macroalga *Codium tomentosum*, 147 espécies moleculares em catorze classes na *Gracilaria* sp., 110 espécies moleculares em catorze classes na *Porphyra dioica* e 181 espécies moleculares distribuídas em dezassete classes na *Fucus vesiculosus*. De modo geral, o lipidoma destas macroalgas inclui os glicolípidos (GLs) monogalactosil diacilglicerol (MGDG), digalactosil diacilglicerol (DGDG), sulfoquinovosil diacilglicerol (SQDG) e a forma liso (SQMG); inclui os fosfolípidos (PLs) fosfatidilcolina (PC) e forma liso (LPC), fosfatidilglicerol (PG) e a forma liso (LPG), ácido fosfatidico (PA), fostatidilinositol (PI) e as betaínas (diacilglicerol trimetil-homoserina, DGTS). As algas verdes diferenciam-se pela predominância de espécies moleculares que contêm ácidos gordos polinsaturados com 16, 18 e 20 átomos de carbono, como o 16:3, o 18:3 e o 20:5 na família *n*-3, e pela presença da forma liso das betaínas, a classe monoacilglicerol trimetil-homoserina (MGTS), identificadas pela primeira vez no lipidoma de macroalgas.

resumo

As macroalgas vermelhas diferenciam-se pelo elevado número de espécies moleculares que incluem cadeias de ácidos gordos C_{20} da família *n*-3 e *n*-6, principalmente na composição dos GLs, e pela presença das classes fosfatidiletanolamina (PE) e inositolfosfoceramida (IPC), apenas identificada nestas algas, pelo que podem ser consideradas um biomarcador deste filo. Neste trabalho, foi avaliada a variação na assinatura lipidómica em duas fases do ciclo de vida (gametófita e esporófita) tomando como alga de estudo a *Porphyra dioica*. Os resultados obtidos indicaram variações a nível molecular nas classes PC, PA, PE e PG. Em ambas as fases não se observam variações na assinatura dos GLs. O estudo do perfil em ácidos gordos desta alga mostrou que ambas as fases contêm ácidos gordos do tipo 20:4(*n*-6) e 20:5(*n*-3), pelo que apresentam elevado valor nutricional. Na composição da macroalga castanha *Fucus vesiculosus*, as espécies moleculares combinam diversos ácidos gordos polinsaturados com 18 e 20 átomos de carbono da família *n*-3 (18:3, 18:4 e 20:5), e 20:4 da família *n*-6. As algas castanhas apresentam várias espécies moleculares na categoria das betaínas nomeadamente a classe diacilglicerol trimetil-β-alanina (DGTA) e a sua forma liso MGTA, identificada pela primeira vez no lipidoma de macroalgas, ambas não detetadas no lipidoma dos restantes filo.

O efeito da sazonalidade na variação da assinatura lipidómica foi estudado para a *Fucus vesiculosus* colhida em duas estações do ano: inverno e primavera. Os resultados obtidos mostram que o lipidoma desta macroalga mantém o mesmo número de espécies moleculares em todas as classes de lípidos polares, observando-se um aumento da abundância relativa das espécies moleculares que combinam ácidos gordos polinsaturados C_{18} e C_{20} (18:3, 18:4, 20:4 e 20:5), em especial nas categorias GLs e betaínas na macroalga de inverno. Assim, podemos concluir que a sazonalidade tem efeito no lipidoma, manifestado pelo aumento de ácidos gordos incorporados nos lípidos polares na macroalga de inverno, muito benéfico em termos nutricionais. Quanto à bioprospecção, avaliaram-se as atividades anti-inflamatória e antiproliferativa do extrato lipídico total da macroalga *Gracilaria* sp.. A atividade anti-inflamatória foi avaliada pela capacidade de inibição dos extratos na produção de NO em macrófagos RAW 264.7 estimulados com o lipopolissacarídeo bacteriano e a atividade anti proliferativa foi testada quanto à capacidade inibitória na proliferação de células T-47D, originadas a partir de um carcinoma ductal humano (cancro da mama) e de células 5637 originadas a partir do carcinoma humano da bexiga. Os extratos totais demonstraram atividade anti-inflamatória e antiproliferativa, pelo que se avaliou o efeito do extrato rico em glicolípidos e a capacidade inibitória na proliferação de células T-47D, verificando-se uma capacidade inibitória da mesma ordem obtida para o extrato total, pelo que poderão ter particular interesse como fitoquímicos.

Assim, os resultados obtidos podem contribuir para a valorização das macroalgas como fonte natural e renovável de alimentos, tendo em consideração o valor nutricional como fonte de ácidos gordos *n*-3 e *n*-6, e de compostos bioativos a ser utilizados como ingredientes funcionais, fitoquímicos e noutras potenciais aplicações na indústria alimentar e farmacêutica.

keywords

Macroalgae, polar lipids, glicolipids, phospholipids, bioactivity, mass spectrometry, IMTA.

abstract

Marine macroalgae are considered to be interesting for food in Western countries and an important supply of novel natural bioactive compounds. Among these are polar lipids such as glycolipids, betaine lipids and phospholipids recognized as high valued lipids for nutrition and as functional ingredient with recognized health benefits. Its biosynthesis depends on several environmental factors such as seasonality, nutrition and habitat, increasing the structural complexity of macroalga lipidome, so that its identification is a current challenge. Mass spectrometry (MS) is a promising tool successfully applied in the study of lipidomic signature of distinct organisms, which can be extended to identify the hundreds of species in the lipidome of macroalgae, and allow them to finally be explored as potential source of lipids.

In this work we aim to identify the lipidome of macroalgae representative of Chlorophyta (*Codium tomentosum*), Rhodophyta (*Gracilaria* sp. and *Porphyra dioica*) and Ochrophyta (*Fucus vesiculosus*). These algae thrive in the Portuguese coast but are recently being cultivated on an integrated multi-trophic aquaculture system (IMTA). The characterization of the lipidome will be performed by using mass spectrometry analysis tools coupled to chromatographic methods. We aim to evaluate the bioactive properties of the polar lipids from macroalgae fostering the potential application of these compounds in function of its biological properties as anti-inflammatory and antiproliferative/antitumor agents.

The main goals of this project were achieved after the characterization by using HILIC–MS and MS/MS approaches of the lipid extracts carrying on different extraction protocols. The results of this study allowed to identify about 238 molecular species distributed by twelve classes in the macroalgae *Codium tomentosum*, 147 molecular species in fourteen classes in *Gracilaria* sp., 110 molecular species in fourteen classes in *Porphyra dioica* and 181 molecular species distributed by seventeen classes in *Fucus vesiculosus*. Overall, the lipidome of these macroalgae included GLs monogalactosyl diacylglycerol (MGDG), digalactosyl diacylglycerol (DGDG), sulfoquinovosyl diacylglycerol (SQDG) and its lyso-form (SQMG); phosphatidylcholine (PC) and lyso-PC, phosphatidylglycerol (PG), lyso-PG (LPG), phosphatidic acid (PA), phosphatidylinositol (PI) and betaines (diacylglyceryl trimethyl-homoserine, DGTS). Green macroalgae may be differentiated by the predominance of molecular species including C_{16} – C_{20}, polyunsaturated fatty acids (PUFA) such as 16:3, 18:3 and 20:5 from *n*-3 FA family. It contains several molecular species belonging to GLs and betaines including monoacylglyceryl trimethyl-homoserine (MGTS), never reported before in the lipidome of macroalga.

Red macroalgae are differentiated by molecular species that incorporate C_{20} FA chains of *n*-3 and *n*-6 families, mainly reflected on the composition of GLs.

abstract

Red algae contained phosphatidylethanolamine (PE) and inositol phosphoceramides (IPC), only identified in red algae and therefore to be considered putative biomarker of this phylum. Among intra-taxonomic groups, the differentiation is reflected by the high number of molecular species within the PE class and the lowest number of molecular species composing betaine lipids present in the lipidome of genus *Porphyra*. The brown macroalgae *Fucus vesiculosus* hold molecular species mainly combining C_{18} and C_{20} *n*-3 type such as 18:3, 18:4 and 20:5 and 20:4(*n*-6) PUFA. Brown algae contain several molecular species within the category of betaine lipids, namely the diacylglyceryl trimethyl-β-alanine class (DGTA) and the lyso-DGTA (MGTA), class never reported before in the lipidome of macroalga, not detected in the lipidome of the remaining phyla.

In this work, the differentiation between the lipidic signature from two life cycle stages (gametophyte and sporophyte) was evaluated, taking *Porphyra dioica* as the case-study. The results showed dissimilarities at the molecular level in PC, PA, PE and PG classes. In both stages GLs preserve its signature. The FA profile of this macroalgae showed that both stages contained 20:4(*n*-6) and 20:5(*n*-3) FA that infers high nutritional value to *Porphyra dioica*.

Season effect on the lipid profile from *Fucus vesiculosus* was evaluated (winter and spring seasons). The results unveil that the lipidomic signature of this macroalga is maintained considering the number of molecular species and polar lipid classes, and season effect was reflected by the increase of the relative abundance of the molecular species that combine C_{18} and C_{20} (18:3, 18:4, 20:4, and 20:5 FA) in the lipidome of *F. vesiculosus* harvested in winter, particularly displayed by GLs and betaine lipids, that enhance the nutritional value of this macroalgae.

After the identification of the different macroalgae and bioprospection of the identified molecular species, the anti-inflammatory and antiproliferative activities of the total lipid extract of the macroalga *Gracilaria* sp. were screened. The anti-inflammatory activity was evaluated by the inhibitory effect of the extracts in the production of NO in RAW 264.7 macrophage cells after bacterial cell-wall component lipopolysaccharide (LPS) stimulation. Antiproliferative activity was assessed as inhibitory capacity of lipid extracts in the proliferation of T-47D cells, originating from a human ductal carcinoma (breast cancer) and 5637 cancer cells from the human bladder carcinoma. The total extracts showed anti-inflammatory and antiproliferative activity, and effect of the glycolipid-rich extract and the inhibitory capacity on the proliferation of T-47D cells was evaluated resulting similar between both extracts. With this work, we were able to identify putative biomarkers for taxonomy, season effect and life cycle stages of macroalgae. It was identified species that from the point of view of bioprospecting may be considered interesting phytochemicals, and that, in fact, have proved to be related with anti-inflammatory and antiproliferative activity of the extracts. These results may contribute to the valorization of macroalgae as a natural and renewable source of food and feed, considering the nutritional value as a source of *n*-3 and *n*-6 FA but also as a source of bioactive compounds to be used as functional ingredients, phytochemicals or in new formulations for food and pharma industries.

Publications and communications

The results presented in this thesis originated four publications in international scientific journals with Referee, one book chapter, as well as oral and poster communications (as first author) in national and international meetings.

Publications in international scientific journals with Referee

Elisabete da Costa, Tânia Melo, Ana S. P. Moreira, Carina Bernardo, Luisa Helguero, Isabel Ferreira, Maria Teresa Cruz, Andreia M. Rego, Pedro Domingues, Ricardo Calado, Maria H. Abreu and Maria Rosário Domingues, *Valorization of Lipids from* Gracilaria *sp. through lipidomics and decoding of antiproliferative and anti-Inflammatory activity*. Marine Drugs (2017), 15(3), 62 (F.I. 3.637).

Elisabete da Costa, Tânia Melo, Ana S.P. Moreira, Eliana Alves, Pedro Domingues, Ricardo Calado, Maria H. Abreu, Maria Rosário Domingues. *Decoding bioactive polar lipid profile of the macroalgae* Codium tomentosum *from a sustainable IMTA system using a lipidomic approach*. Algal Research (2015), 12 (F.I. 4.694).

Elisabete da Costa, Vitor Azevedo, Tânia Melo, Andreia M. Rego, Pedro Domingues, Dmitry V. Evtuguin, Ricardo Calado, Maria H. Abreu and Maria Rosário Domingues, *High-Resolution lipidomics of the early life stages of the red seaweed* Porphyra dioica, on "Phytochemicals: Biosynthesis, Metabolism and Biological Activities". Molecules (2018), 23 (F.I. 2.861).

Elisabete da Costa, Joana Silva, Sofia Hoffman Mendonça, Maria H. Abreu, Maria Rosário Domingues et al. *Lipidomic approach towards deciphering glycolipids from microalgae as a reservoir of bioactive lipids*, Marine Drugs (2016), 14 (F.I. 3.637).

Book Chapter

Elisabete da Costa, Elisabete Maciel, Pedro Domingues, Miguel Leal, Ricardo Calado, Ana Lillebø, Maria H. Abreu, Maria Rosário Domingues. *Chapter 15. Mass spectrometry analysis of polar lipid components in seaweed*, in the international book "Seaweed Bioactives: Extraction and Characterization Techniques" (ISBN: 987-1-138-19753-4) to be published by the CRC Press under “Functional Foods and Nutraceuticals Series. Under revision.

Oral communications

Elisabete da Costa et al. Deciphering the lipidomic profile of the seaweed *Codium tomentosum* toward the bioprospection of bioactive phytochemicals. 4th Workshop in Lipidomics. May, 2015. University of Aveiro, Portugal.

Elisabete da Costa. Potential application of *Gracilaria* and *Ulva* in food and cosmetics. Closing session of CIGArRA e ALGADOURADA projects, 10th December, 2015. CIEMAR, Ilhavo, Portugal.

Elisabete da Costa et al. Bioprospection of glycolipids from macroalgae using mass spectrometry-based approaches, Workshop of carbohydrates, 8th May, 2016. University of Aveiro.

Elisabete da Costa et al. Deciphering the lipidome of the seaweed *Gracilaria* sp. from a land-based IMTA system in the lagoon of Aveiro, International seaweeds symposium, 23st June, 2016. Copenhagen, Denmark.

Elisabete da Costa et al. High added value products from macroalgae: Lipids as bioactive compounds. 1st Scientific Meeting of the Doctoral Programme in Sustainable Chemistry, 26th September, 2016. University of Aveiro, Portugal.

Elisabete da Costa et al. How to use lipidomic tools in red and green seaweeds signature and bioprospection? *Codium tomentosum* and *Gracilaria* sp. as showcases. The 5th International Seaweed Conference, 27-28th September, 2016. Aveiro, Portugal.

Poster communications

Elisabete da Costa et al. Unraveling the lipidome of the seaweed *Gracilaria* sp. from the IMTA system in the lagoon of Aveiro as a source of bioactive polar lipids, Research day, 15th June, 2016. University of Aveiro, Portugal.

Elisabete da Costa et al. How to use lipidomic tools in red and green seaweeds signature and bioprospection? *Codium tomentosum* and *Gracilaria* sp. as showcases, The 5th International Seaweed Conference, 27-28th September, 2016. Aveiro, Portugal.

Elisabete da Costa et al. The life cycle of *Porphyra dioica*: a lipidomics approach, EU COST action 'The quest for tolerant varieties: phenotyping at plant and cellular level (FA1306) 3rd General COST Meeting, 27-28th March, 2017. Oeiras, Portugal.

Index of Contents

List of Figures……...…….....V

List of Tables……...……..XIII

Abbreviations……...……XVII

In Chapter I

I. Introduction……..…….....3

I.1 State of the art……...……4

I.1.1. Macroalgae …….4

I.1.2. Lipids in macroalgae…….……...…..…9

I.1.2.1. Non-polar lipids……10

I.1.2.2. Polar lipids……12

I.1.2.3. Pathways of polar lipids biosynthesis…….....19

I.1.2.4. Polar lipid profile dependence with growth conditions……..…..22

I.1.3. Lipidomic–based approaches applied to macroalgae……...…...…...…….25

I.1.3.1. Analytical strategies to identify the lipid profile of macroalgae…..26

I.1.3.2. Identification of the lipidome of macroalgae by mass spectrometry…...…….....…….32

I.1.3.3. Studies uncovering the lipidome of macroalgae…..……35

I.1.4. Biological properties of polar lipids……38

I.1.4.1. Antioxidant properties…..……....40

I.1.4.2. Anti-inflammatory properties……..……....41

I.1.4.3. Antitumoral activity…..……...42

I.1.4.4. Antimicrobial activity……..……....44

I.2. Aims of the work……....45

In Chapter II

II. Materials and methods…….……47

II.1. Macroalgae material……...…..50

II.2. Total lipid extraction…….....51

II.3. Thin-layer chromatography (TLC)……...…53

II.4. Solid Phase extraction (SPE)……...…….....53

II.5. Extraction and quantification of pigments……..…....54

II.6. Quantification of glycolipids……..…....54

II.7. Quantification of phospholipids…….…..54

II.8. Fatty acid methyl esters (FAMEs) analysis by gas chromatography–mass spectrometry (GC–MS)……..55

II.9. Mass spectrometry and hyphenated approaches……...56

II.10. Evaluation of the biological activity……...…58

II.10.1. Antiproliferative activity……..…,…….....59

II.10.2. Anti-inflammatory activity……..……...…….59

II.10.3. Antioxidant Capacity……..…….…61

II.11. Statistical Analysis……..62

II.12. Nutritional Indexes……..…...63

II.13. Standards and Reagents……..……....63

In Chapter III

III. Results and Discussion…….……...…65

III.1. The lipidomic approach……...67

III.1.1. The lipidome of Chlorophyta: *Codium tomentosum*…….……...…69

III.1.1.1. Polar lipids from *Codium tomentosum*……..……....71

III.1.1.2. Fatty acid profile……..……..……....84

III.1.1.3. Discussion…….....86

III.1.2. The lipidome of Rhodophyta……..……...…...89

III.1.2.1. The lipidome of *Gracilaria* sp……..……91

III.1.2.1.1. Polar lipids from *Gracilaria* sp…….……..93

III.1.2.1.2. Fatty acid profile……..……101

III.1.2.1.3. Photosynthetic pigments……..……102

III.1.2.2. The lipidome of *Porphyra dioica*……..……105

III.1.2.2.1. Polar lipids from *Porphyra dioica*……..……..108

III.1.2.2.2. Fatty acids profile….……118

III.1.2.3. Discussion on the lipidome of Rhodophyta…….……121

III.1.3. The lipidome of Ochrophyta: *Fucus vesiculosus*...……...……127

III.1.3.1. Polar lipids from *Fucus vesiculosus*...……129

III.1.3.2. Fatty acids profile……..……...……...147

III.1.3.3. Discussion……..……...……...149
III.2. Bioprospection of polar lipids……..…….153
III.2.1. Anti-inflammatory activity on nitrite production in RAW 264.7 cells…..155
III.2.1.1. Introduction……..…….....155
III.2.1.2. Results…….....157
III.2.2. Activity of lipid extract on human cancer cell viability……..……...159
III.2.2.1. Introduction…….159
III.2.2.2. Results……...……..160
III.2.3. Discussion……...……162
In Chapter IV
IV. Conclusions……...……..165
In Chapter V
V. References……171
In Supplementary Information
Appendix A. Supplementary material of Chapter III.1.1……..….195
Appendix B. Supplementary material of Chapter III.1.2……..….198
Appendix C. Supplementary material of Chapter III.1.3……..….202
Appendix D. Supplementary resume table of the identification of polar lipids.....….204

List of Figures

In Chapter I

Figure I. 1. *Porphyra* spp. life cycle: The gametophytic blade phase reproduces sexually through fertilization of the carpogonium by the spermatium and subsequent carpospores formation; the development of these spores gives rise to the filamentous sporophyte conchocelis phase, which produces conchospores that are release into seawater and germinate forming new blades……7

Figure I. 2. Chemical composition of macroalgae……..8

Figure I. 3. Polar lipid classes in macroalgae. Glycolipids (GLs): monogalactosyl diacylglycerol (MGDG), digalactosyl diacylglycerol (DGDG), sulfoquinovosyl diacylglycerol (SQDG), sulfoquinovosyl monoacylglycerol (SQMG); Phospholipids (PLs): phosphatidylglycerol (PG) and lyso-PG (LPG), phosphatidylcholine (PC) and lyso-PC (LPC), phosphatidylinositol (PI), phosphatidic acid (PA), inositol phosphorylceramide (or inositol phosphoceramide) (IPC); Betaine lipids: diacylglyceryl trimethyl-homoserine (DGTS), monoacylglyceryl trimethyl-homoserine (MGTS), diacylglyceryl hydroxymethyltrimethyl-alanine (DGTA), diacylglyceryl carboxyhydroxymethyl-choline (DGCC). R_1 and R_2 represent fatty acyl chains; R represents fatty acyl and R´ the long-chain base……17

Figure I. 4. Simplified diagram of the pathways of the biosynthesis of glycerolipids in macroalgae that include chloroplastic (‘‘prokaryotic” pathway) reactions and endoplasmic - ER (‘‘eukaryotic” pathway) reactions. Orange arrows refer to the biosynthetic pathway of transport of ER-derived glycerolipid to chloroplasts. ACP, acyl carrier protein; PA, phosphatidic acid; DAG, diacylglycerol; PC, phosphatidylcholine; MGD, MGDG synthases; DGD, DGDG synthases; UDP, uridine diphosphate galactose intermediate in the production of polysaccharides (-Gal galactose, -Sq sulfoquinovose); GPAT, glycerol-3-phosphatase acyltransferase; LPAAT, lysophosphatidic acid acyltransferase; PA, phosphatidic acid; PP, phosphatidate phosphatase; DAG-CPT, diacylglycerol synthetase-choline: diacylglycerol cholinephosphotransferase; SLS, sulfolipid synthase; SQDG, sulfoquinovosyl diacylglycerol; PE, phosphatidylethanolamine; DGTS, diacylglyceryl trimethyl-homoserine; TAG, triacylglycerol; Δ, degree of unsaturation ranging from 1 - 4 double bonds (adapted from da Costa et al., 2016)……..20

Figure I. 5. LC–MS approach in the lipidomic analysis of polar lipids from macroalgae……...26

Figure I. 6. Schematic representation of mass spectrometer components. Mass analyser referred to a) Ion trap and b) Orbitrap (adapted from https: //www.thermofisher.com/pt/en/home/industrial/mass-spectrometry.htm)……27

Figure I. 7. Schematic fragmentation pathways of digalactosyl diacylglycerol observed in the MS/MS spectra of the $[M + Na]^+$ ions that support their structural characterization……33

Figure I. 8. Schematic fragmentation of sulfoquinovosyl diacylglycerol. The lines indicate the product ions formed. The fragment ion at *m/z* 225 is attributed to the sulfoquinovose head group.33

Figure I. 9. Schematic fragmentation of glycerophospholipids. The dotted lines indicate the most labile bonds where fragmentation may occur. The table includes the product ions and neutral losses that provide the structural information and allow the identification of PLs classes.....34

Figure I. 10. Schematic fragmentation of betaine lipids DGTS. Characteristic product ion at *m/z* 236 results from $[M + H]^+$ or $[M + Na]^+$. Fragmentation of polar head may occur in $[M + Na]^+$: neutral loss of 59 Da (loss of the $-N^+(CH_3)_3$), 73 Da (loss of the $-CH_2N^+(CH_3)_3$), and 87 Da (loss of $-CH_2CH_2N^+(CH_3)_3$)…….....…….35

In Chapter II

Figure II. 1. Schematic representation of the workflow that include extraction of total lipids extract (crude extract) and identification polar lipids from macroalgae. Lipids from *Gracilaria* sp. were isolated from the total extract by SPE (solid phase extraction). ESI-electrospray ionization, MS-mass spectrometry, HILIC-hydrophilic interaction liquid chromatography, MS-mass spectrometry, UV-ultraviolet, LC-liquid chromatography, GC-gas chromatography, Si-silica, TLC-thin layer chromatography, MTBE-Methyl-tert-butyl ether, UAE-ultrasound assisted extraction……...49

Figure II. 2. Macroalgae species targeted on this Ph.D., produced in a land-based IMTA system.....……51

In Chapter III

Figure III. 1. LC–MS spectrum and general structure of the sulfoquinovosyl diacylglycerol (SQDG) species, observed by HILIC–ESI–MS as $[M - H]^-$ ions…….73

Figure III. 2. ESI–MS/MS spectra of the SQDG molecular species observed as $[M - H]^-$ at *m/z* 737.4 identified as SQDG 28:0 (SQDG 12:0/16:0 and 14:0/14:0) (A), and at *m/z* 833.4 identified as SQDG 35:2 (SQDG 17:0/18:1 and 16:0/19:1) (B)……73

Figure III. 3. LC–MS spectrum of monogalactosyl diacylglycerol (MGDG) molecular species observed by HILIC−ESI−MS as $[M + NH_4]^+$ ions. *Eluent contamination. A general structure is also represented…….74

Figure III. 4. ESI–MS/MS spectrum of the ion $[M + Na]^+$ of MGDG 34:1(MGDG 16:0/18:1 and 16:1/18:0) at *m/z* 779.7……..74

Figure III. 5. LC–MS spectrum and general structure of the digalactosyl diacylglycerol (DGDG) molecular species, observed by HILIC−ESI−MS as $[M + NH_4]^+$ ions……..75

Figure III. 6. LC–MS/MS spectra of the DGDG molecular species observed as $[M + Na]^+$ at *m/z* 927.7 identified as DGDG 33:1 (DGDG 16:0/17:1) and DGDG 32:2-OH (DGDG 14:0/18:2-OH) (A), and at *m/z* 955.8 identified as DGDG 35:1 (DGDG 16:0/19:1 and 17:0/18:1) (B)……...76

Figure III. 7. LC–MS spectrum and general structure of the phosphatidylglycerol (PG) species observed by HILIC−ESI−MS as $[M - H]^-$ ions……78

Figure III. 8. ESI–MS/MS spectra of the PG 34:2 (A), LPG 16:0 (B), PI 34:2 (C), PA 36:4 (D), PC 36:2 (E) and LPC 18:3 (F)……79

Figure III. 9. LC–MS spectrum and general structure of the phosphatidylcholine (PC) molecular species, observed by HILIC−ESI-MS as $[M + H]^+$ ions……...80

Figure III. 10. LC–MS spectrum and general structure of the phosphatidylinositol (PI) molecular species observed by HILIC−ESI−MS as $[M - H]^-$ ions……....80

Figure III. 11. LC–MS spectrum and general structure of the diacylglyceryl-*N*,*N*,*N*-trimethyl-homoserines (DGTS) species, observed by HILIC−ESI−MS as $[M + H]^+$ ions……...82

Figure III. 12. ESI–MS/MS spectra of the DGTS 34:2 (A), DGTS 35:1 (B), MGTS 18:2 (C) and MGTS 19:1 (D)……83

Figure III. 13. LC–MS spectra of the classes a) monogalactosyl diacylglyceride (MGDG) and b) digalactosyl diacylglyceride (DGDG) observed by HILIC−ESI−MS as $[M + NH_4]^+$ ions, and c) sulfoquinovosyl diacylglyceride (SQDG) observed as $[M - H]^-$ ions……..94

Figure III. 14. LC–MS spectra of the classes a) phosphatidylcholine (PC) and b) lyso phosphatidylcholine (LPC) observed as $[M + H]^+$ ions; c) phosphatydilglycerol (PG) and d) lyso phosphatidylglycerol (LPG) observed as $[M - H]^-$ ions; e) phosphatidic acid (PA) observed as $[M - H]^-$ ions and f) phosphatidilethanolamine (PE) observed as $[M + H]^+$ ions……..97

Figure III. 15. a) LC-MS spectrum of inositol phosphoceramide (IPC) observed by HILIC–ESI–MS as $[M - H]^-$ ions; b) LC–MS/MS spectrum of $[M - H]^-$ ions of IPC at *m/z* 920.6 (IPC (t18:1/24:1-OH)……...100

Figure III. 16. LC–MS spectra of a) diacylglyceryl-*N*,*N*,*N*-trimethyl-homoserine species (DGTS) and b) monoacylglyceryl-*N*,*N*,*N*-trimethyl-homoserine (MGTS), observed by HILIC–ESI–MS as $[M + H]^+$ ions……...100

Figure III. 17. LC–MS chromatograms of *Porphyra dioica* blade (B) and conchocelis (C) stages observed by HILIC–MS, acquired in the positive mode and blade (B′) and conchocelis (C′) acquired in the negative mode…….109

Figure III. 18. LC–MS spectra of glycolipids from *Porphyra dioica* blade (B) and conchocelis (C) stages: a) MGDG and b) DGDG observed by HILIC–LC–MS as $[M + NH_4]^+$ ions, c) SQDG and d) SQMG observed as $[M – H]^–$ ions……..…….110

Figure III. 19. LC–MS spectra of phospholipids from *Porphyra dioica* blade (B) and conchocelis (C) stages: a) PC, b) LPC observed by HILIC–LC–MS as $[M + H]^+$ ions and c) PE, d) LPE, e) PG, f) LPG, g) PA, and (h) IPC observed as $[M – H]^–$ ions……...114

Figure III. 20. LC–MS spectra of betaine lipids from *Porphyra dioica* blade (B) and conchocelis (C) stages: DGTS observed by HILIC–LC–MS as $[M + H]^+$ ions …….118

Figure III. 21. Number of molecular species identified in the lipidome of *Gracilaria* sp., *Porphyra dioica* – blade and conchocelis phases……122

Figure III. 22. LC–MS chromatograms of lipid extracts obtained from *Fucus vesiculosus* collected in February (mid-winter) and acquired on positive mode (A) and and negative mode (B) and collected on May (end-spring) on positive mode (C) and negative mode (D)……130

Figure III. 23. LC–MS spectra of glycolipids from *Fucus vesiculosus* collected in February (mid-winter) and May (end-spring) observed by LC–MS, respectively a) and e) MGDG, b) and f) DGDG molecular species were identified as $[M + NH_4]^+$ ions, c) and g) SQMG and d) and h) SQDG identified as $[M – H]^–$ ions……..132

Figure III. 24. Percentage of a) MGDG, b) DGDG and c) SQDG plus d) SQMG molecular species identified after LC–MS and MS/MS. The results are expressed as percentage obtained by dividing the ratio between peak areas of each molecular species and internal standards and the total of all ratios. Values are means ± standard deviation of the duplicate of three independent experiments. (***, significantly different $p < 0.001$; **, significantly different $p < 0.01$, * significantly different $p < 0.05$). February refers to *Fucus vesiculosus* collected in mid-winter. May refers to *Fucus vesiculosus* collected in end-spring…….134

Figure III. 25. LC–MS spectra of phospholipids from *Fucus vesiculosus* collected in February (mid-winter) and May (end-spring) observed by LC–MS, respectively a) and g) PC, b) and h) LPC as $[M + H]^+$ ions; c) and i) PG, d) and j) LPG, e) and k) PE, f) and l) PI as $[M - H]^-$ ions…….138

Figure III. 26. Percentage of a) PC, b) LPC and c) PG plus d) LPG, e) PI, f) PE and g) LPE, molecular species identified after LC–MS, MZ mine software and MS/MS analysis. The results are expressed as percentage obtained by dividing the ratio between peak areas of each molecular species and internal standards and the total of all ratios. Values are means ± standard deviation of the duplicate of three independent experiments. (***, significantly different $p < 0.001$; **, significantly different $p < 0.01$, * significantly different $p < 0.05$). February refers to *Fucus vesiculosus* collected in mid-winter. May refers to *Fucus vesiculosus* collected in end-spring…..141

Figure III. 27. LC–MS spectra of betaine lipids from *Fucus vesiculosus* collected in February (mid-winter) and May (end-spring) observed by LC-MS, respectively a) and e) DGTS, b) and f) MGTS; c) and g) DGTA, e) and h) MGTA as $[M + H]^+$ ions…….143

Figure III. 28. Percentage of a) DGTS, b) MGTS and c) DGTA plus d) SQMG molecular species identified after LC–MS, and MS/MS analysis. The results are expressed as percentage obtained by dividing the ratio between peak areas of each molecular species and internal standards and the total of all ratios. Values are means ± standard deviation of the duplicate of three independent experiments. (***, significantly different $p < 0.001$; **, significantly different $p < 0.01$, * significantly different $p < 0.05$). February refers to *Fucus vesiculosus* collected in mid-winter. May refers to *Fucus vesiculosus* collected in end-spring……145

Figure III. 29. Percentage of FAMEs expressed by the ratio between each FAME and the total of all individual areas. Values are means ± standard deviation of the duplicate of three independent experiments. (***, significantly different $p < 0.001$; **, significantly different $p < 0.01$, * significantly different $p < 0.05$). February refers to *Fucus vesiculosus* collected in mid-winter. May refers to *Fucus vesiculosus* collected in end-spring……149

Figure III. 30. Representation of the inhibitory effect on NO production by lipid extracts in macrophages. LPS stimulation induces NF-kB that induce the nucleus translocation and production of iNOS through the activation of iNOS gene in the nucleus. iNOS produces NO and L-citrulline through the precursor L-arginine. NO is released to the extracellular medium. LPS – lypopolysaccharide; TLR4 – toll like receptor 4; NF-kB –nuclear factor kappa; iNOS – inducible nitric oxide synthase……156

Figure III. 31. Cell viability and anti-inflammatory activity of *Gracilaria* sp. lipid extract. (A) Assessment of metabolically active cells was performed using a resazurin bioassay. Results are expressed as a percentage of resazurin reduction relative to the control (Ctrl). (B) Anti-inflammatory activity was measured as inhibition of NO production, quantified by the Griess assay. Nitrite concentration was determined from a sodium nitrite standard curve and the results are expressed as concentration (μM) of nitrite in a culture medium. Each value represents the mean ± SD from at least three independent experiments (** $p < 0.01$ compared to Ctrl; # $p < 0.05$, ### $p < 0.001$ compared to ethanol (EtOH, vehicle) plus lipopolysaccharide (LPS))…….157

Figure III. 32. Effect of lipid extracts *of Gracilaria* sp. on T-47D breast (A) and 5637 bladder (B) cancer cell lines, after 96 h incubation. Results are shown as mean ± SD of three independent determinations (*** $p < 0.001$, compared to control). OD: optical density; a.u.: arbitrary units...161

Figure III. 33. Effect of glycolipid rich extracts of *Gracilaria* sp. on T-47D breast cancer cell lines, after 96 h incubation. Results are shown as mean ± SD of three independent determinations (*** $p < 0.001$, compared to control). OD: optical density; a.u.: arbitrary units……161

In Supplementary information

Appendix A. Supplementary material of Chapter III.1.1

Figure S. 1. LC–MS spectrum of the sulfoquinovosyl monoacylglycerol (SQMG) molecular species observed by HILIC−ESI−MS as $[M - H]^-$ ions. Bold *m/z* values correspond to the most abundant species detected in the LC−MS spectrum. (C means number of carbon atoms and N represents the number of double bonds in the fatty acyl side chains). A general structure is also represented….....195

Figure S. 2. ESI–MS/MS spectrum of the ion $[M - H]^-$ of SQMG 16:0 at *m/z* 555.2 (A)…….195

Figure S. 3. LC–MS spectrum of the lyso phosphatidylglycerol (LPG) molecular species observed by HILIC–ESI–MS as $[M - H]^-$ ions. Bold *m/z* values correspond to the most abundant species detected in the LC−MS spectrum. (C means number of carbon atoms and N represents the number of double bonds in the fatty acyl side chains). *Eluent contamination. A general structure is also represented……..…….196

Figure S. 4. LC–MS spectrum of the lyso phosphatidylcholine (LPC) molecular species. The table includes the molecular species observed by HILIC−ESI−MS as $[M + H]^+$ ions. Bold *m/z* values correspond to the most abundant species detected in the LC-MS spectrum. (C means number of

carbon atoms and N represents the number of double bonds in the fatty acyl side chains). A general structure is also represented..……..…….196

Figure S. 5. LC–MS spectrum of the phosphatidic acid (PA) molecular species. The table includes the molecular species, observed by HILIC-ESI-MS, as $[M - H]^-$ ions. (C means number of carbon atoms and N represents the number of double bonds in the fatty acyl side chains). A general structure is also represented…….197

Figure S. 6. LC–MS spectrum of the monoacylglyceryl-*N,N,N*-trimethylhomoserine (MGTS) molecular species. The table includes the molecular species observed by HILIC–ESI–MS, as $[M + H]^+$. Bold *m/z* values correspond to most abundant species detected in the LC-MS spectrum. (C means number of carbon atoms and N represents the number of double bonds in the fatty acyl side chains). A general structure is also represented……...197

In Appendix B

Figure S. 7. LC–MS spectrum of the pigments species in the total extract of *Gracilaria* sp.as $[M + H]^+$ ions and UV spectrum……...198

In Appendix C

Figure S. 8. Percentage of PA molecular species identified after LC–MS, and MS/MS analysis. The results were expressed as percentage contained by dividing the ratio between peak areas of each molecular species and internal standards and the total of all ratios. Values are means ± standard deviation of the duplicate of three independent experiments. (***, significantly different $p < 0.001$; **, significantly different $p < 0.01$, * significantly different $p < 0.05$)……202

Figure S. 9. LC chromatogram and MS/MS spectra of the betaine molecular species as standard a) and b), respectively. The Figure b) includes the fragmentation of the ion at *m/z* 712.6 as $[M + H]^+$. LC chromatogram c); MS/MS spectrum of the ion at *m/z* 710.6 as $[M + H]^+$ identified in the extract of *Fucus vesiculosus* corresponding to the DGTS d) and MS/MS spectrum of the ion at *m/z* 710.6 as $[M + H]^+$ identified in the extract of *Fucus vesiculosus* corresponding to betaine class DGTA e). The figure f) includes the range of *m/z* between 375 and 550 and was extracted from spectrum e) representing product ions that allow the identification of the fatty acyl composition of $[M + H]^+$ ion at *m/z* 712.6 attributed to DGTA (16:0/16:1) and DGTA (14:0/18:1).....203

List of Tables

In Chapter I

Table I. 1. Lipidomics of Chlorophyta, Rhodophyta and Ochrophyta macroalgae reported in literature…….29

Table I. 2. Polar lipids from macroalgae and their potential biological activities……39

In Chapter III

Table III. 1. Identification of MGDG and DGDG molecular species observed by HILIC–ESI–MS, as $[M + NH_4]^+$ ions and SQDG and SQMG molecular species observed as $[M - H]^-$ ions, with the assignment of the fatty acyl composition of each lipid molecular species, according to the interpretation of the correspondent MS/MS spectra…….....77

Table III. 2. Identification of phospholipids molecular species observed by HILIC–ESI–MS, for PG, LPG, PA and PI as $[M - H]^-$ ions and for PC and LPC as $[M + H]^+$, with the assignment of the fatty acyl composition of each lipid molecular species, according to the interpretation of the correspondent MS/MS spectra…….……..81

Table III. 3. Identification of betaine molecular species observed by HILIC–ESI–MS as $[M + H]^+$, for DGTS and MGTS, with the assignment of the fatty acyl composition of each lipid molecular species, according to the interpretation of the correspondent MS/MS spectra……..……84

Table III. 4. Fatty acid profile of the lipid extract of *Codium tomentosum*.....85

Table III. 5. Composition of lipid extracts of *Gracilaria* sp.....93

Table III. 6. Identification of MGDG and DGDG molecular species observed by HILIC–ESI–MS as $[M + NH_4]^+$ ions and SQDG and SQMG molecular species observed as $[M - H]^-$ ions in *Gracilaria* sp.…….95

Table III. 7. Identification of phospholipid molecular species observed by HILIC–ESI–MS, as $[M + H]^+$ ions for PC, LPC, and PE and as $[M - H]^-$ ions for PG, LPG, PI, PA, and IPC in *Gracilaria* sp.……...98

Table III. 8. Identification of betaine molecular species observed by HILIC–ESI–MS as $[M + H]^+$ ions for DGTS and MGTS in *Gracilaria* sp……..……..101

Table III. 9. Fatty acid profile of lipids from *Gracilaria* sp. determined by GC–MS analysis of fatty acid methyl esters (FAMEs).....102

Table III. 10. UV and MS spectral data of chlorophylls and their derivatives extracted from *Gracilaria* sp……103

Table III. 11. Pigments content on the methanolic extract of *Gracilaria* sp. IMTA cultured…...103

Table III. 12. Identification of glycolipids molecular species observed by HILIC–LC–MS in *Porphyra dioica* blade and conchocelis, MGDG and DGDG as $[M + NH_4]^+$ ions and SQDG and SQMG as $[M – H]^–$ ions……..111

Table III. 13. Identification of phospholipid molecular species observed by HILIC–LC–MS in *Porphyra dioica* blade and conchocelis, PC and LPC as $[M + H]^+$ ions and PE, LPE, PG, LPG, PA, PI, and IPC as $[M – H]^–$ ions……..115

Table III. 14. Identification of betaine molecular species observed by HILIC–LC–MS in *Porphyra dioica* blade and conchocelis, DGTS as $[M + H]^+$ ions……...118

Table III. 15. Fatty acids profile of polar lipids from blade and conchocelis stages of *Porphyra dioica* determined by GC-MS analysis of fatty acid methyl esters (FAMEs).....119

Table III. 16. Identification of glycolipids observed by HILIC–LC–MS in *Fucus vesiculosus*. MGDG and DGDG molecular species were identified as $[M + NH_4]^+$ ions, SQDG and SQMG as $[M – H]^-$ ions …….....135

Table III. 17. Identification of phospholipid molecular species observed by HILIC–LC–MS in *Fucus vesiculosus*. PC and LPC as $[M + H]^+$ ions; PG, LPG, PI, LPI, PE, LPE, and PA as $[M – H]^–$ ions……...139

Table III. 18. Identification of betaine molecular species observed by HILIC–LC–MS in *Fucus vesiculosus*. DGTS, MGTS, DGTA, and MGTA as $[M + H]^+$ ions……146

Table III. 19. Fatty acid profile of *Fucus vesiculosus* determined by GC–MS analysis of fatty acid methyl esters (FAMEs).....……...148

In Supplementary material of Chapter III.1

In Appendix B

Table S. 1. Molecular species observed by HILIC−ESI−MS with the assignment of the total fatty acyl composition of each lipid molecular species, according to the analyses performed by mass accuracy (error < 5 ppm) using the Xcalibur software, exact mass calculator - http://www.sisweb.com/referenc/tools/exactmass.htm, and lipid maps tools

http://www.lipidmaps.org/tools/. C means number of carbon atoms and N represents the number of double bonds in the fatty acyl side chains……...199

In Appendix D

Table S. 2. Molecular species identification observed by HILIC–ESI–MS as $[M + NH_4]^+$, as $[M + H]^+$, and as $[M – H]^–$ ions, with the assignment of the fatty acyl composition of each lipid molecular species, according to the interpretation of the corresponding MS/MS spectra. (C means number of carbon atoms and N represents the number of double bonds in the fatty acyl side chains)……204

Abbreviations, acronyms and symbols

AA	Arachidonic acid
Ac-CoA	Acetyl- coenzyme
ACP	Acyl carrier protein
ALA	Linolenic acid
APCI	Atmospheric pressure chemical ionization
BHT	Tert-butyl-4-hydroxytoluene
BuOH	n-butanol
CAT	Catalase
C:N	Number of acyl carbons: number of double bonds
CSE	Conventional Solvent Extraction
CVDs	Cardiovascular diseases
DAG	Diacylglycerol
DGDG	Digalactosyl diacylglycerol
DGTA	Diacylglyceryl hydroxymethyltrimethyl-β-alanine
DGTS	Diacylglyceryl-3-*O*-4-*N,N,N*-trimethyl-homoserine
DHA	Docosahexaenoic acid
DPPH	2,2-diphenyl-1-picrylhydrazyl
DW	Dry weight
EPA	Eicosapentaenoic acid
ESI	Electrospray ionization
ESI-MS	Electrospray ionization-mass spectrometry
EtOAc	Ethyl acetate
FA	Fatty acid
FAB	Fast Atom Bombardment
FT-ICR-MS	Fourier transform ion cyclotron resonance mass spectrometry
GC	Gas chromatography
GL	Glycolipid
GLA	γ-linolenic acid

GPAT	Glycerol-3-phosphate acyltransferase
GSH	Glutathione
HepG	Hepatocellular carcinoma cell line
HILIC	Hydrophilic interaction liquid chromatography
HPLC	High-performance liquid chromatography
HSV-1	Herpes simplex virus (Oral herpes)
HSV-2	Herpes simplex virus (Genital herpes)
IMTA	Integrated multi-trophic aquaculture
iNOS	Inducible nitric oxid synthase
IPC	Inositol phosphoceramide
LA	Linoleic acid
LC	Liquid chromatography
LDH	Lactase dehydrogenase
LLE	Liquid–liquid extraction
LOX	Lipoxygenase
LPA	Lysophosphatidic acid
LPAT	Lysophosphatidic acid acyltransferase
LPC	Lyso-phosphatidylcholine
LPE	Lyso-phosphatidylethanolamine
LPG	Lyso-phosphatidylglycerol
LPO	Lipid peroxidation
m/z	Mass to charge ratio
MAE	Microwave-assisted extraction
MALDI	Matrix-assisted laser desorption/ionization
MCF-7	Human breast carcinoma
MeOH	Methanol
MGD	MGDG synthase
MGDG	Monogalactosyl diacylglycerol
MGTA	Monoacylglyceryl hydroxymethyltrimethyl-β-alanine

MGTS	Monocylglyceryl-3-*O*-4-(*N,N,N*-trimethyl)-homoserine
MIC	Minimum inhibitory concentration
MS	Mass spectrometry
MS/MS	Tandem mass spectrometry
MTBE	Methyl tert-butyl ether
MUFA	Monounsaturated fatty acid
NF-κB	Factor nuclear kappa B
NL	Non-polar lipid
NO	Nitric oxid
NMR	Nuclear magnetic resonance
NOS	Nitric oxide synthase
NP	Normal phase
ORAC	Oxygen Radical Absorbance Capacity
PA	Phosphatidic acid
PAP	Phosphatidic acid phosphatase
PAR	Incidence photosynthetically radiation
PC	Phosphatidylcholine
PE	Phosphatidylethanolamine
PG	Phosphatidylglycerol
PI	Phosphatidylinositol
Pi	Inorganic phosphate
PL	Phospholipid
PLE	Pressurized liquid extraction
PS	Phosphatidylserine
PSU	Practical salinity units
PUFA	Polyunsaturated fatty acid
Q	Quadrupole
IT	Ion trap
QqQ	Triple quadruple

Q-TOF	Quadrupole-Time of Flight
RAW 264.7	Mouse leukaemic monocyte macrophage cell line
ROS	Reactive oxygen species
RP	Reversed-phase
SFA	Saturated fatty acid
SFE	Supercritical fluid extraction
SLE	Solid–liquid extraction
SQDG	Sulfoquinovosyl diacylglycerol
sp.	Species not specified
SPE	Solid-phase extraction
spp.	Several species
TAG	Triacylglycerol
TLC	Thin-layer chromatography
UAE	Ultrasound assisted extraction
UDP	Uridine diphosphate galactose
UPLC	Ultra performance liquid chromatography

CHAPTER I

INTRODUCTION

Part of this section was included in the chapter in press:

Elisabete da Costa, Elisabete Maciel, Pedro Domingues, Miguel Leal, Ricardo Calado, Ana Lillebø, Maria H. Abreu, Maria Rosário Domingues. **Chapter 15. Mass spectrometry analysis of polar lipid components in seaweed**, in the international book "Seaweed Bioactives: Extraction and Characterization Techniques" (ISBN: 987-1-138-19753-4). In Press to be published (by invitation) by CRC Press under “Functional Foods and Nutraceuticals Series.

Introduction

Macroalgae, also refered to as seaweeds, are a diverse and ubiquitous group of photosynthetic organisms. They are known to produce a large amount of bioactive compounds, involved in the natural defense mechanisms to biotic and abiotic stresses (1–3). Thus, they are considered a promising commercial supply of bioactive compounds, stimulating further research of novel applications for human and animal health and nutrition (1,4–6). The most well-known bioactive compounds of macroalgae include sulfated polysaccharides, proteins such as phycobiliproteins, pigments such as carotenoids, lipids, among others (7–9). Macroalgae lipids are also a group of bioactive compounds (10–13). They can be divided into two main groups: the nonpolar lipids (acylglycerols, sterols, free (nonesterified) fatty acids) and the polar lipids that include glycolipids (GLs) as the major components, phospholipids (PLs) and betaine lipids (14–16).

Polar lipids have essential functions as building blocks of membranes (17,18) and as signaling molecules (15,19). They are a source of polyunsaturated fatty acids (PUFA) (1,20,21) and are considered promising phytochemicals with high nutritional value and with potential health benefits as antibacterial (12,22,23), antifungal (1,12,24), antiviral (23,25), anti-inflammatory (26,27), and antitumor agents (10,12,25,28,29). The biological activity of polar lipids depends on the fatty acids (FA) composition and on the polar head group structure (30). Among polar lipids, GLs are valuable products to be used in functional foods, as well as in the pharmaceutical and cosmetic industries (23,31,32). Phospholipids from algae are used in the cosmetic and pharmaceutical industries, and have been described to alleviate senescence, to be beneficial for cognitive functions and inflammatory diseases (28,32,33).

The high complexity, chemical diversity, and huge difference in the molar abundance of these compounds explains why up to now the characterization and the evaluation of polar lipids profile from macroalgae and their biological properties is still unknown (34–36). The lipidomic approach supported by modern research with MS-based techniques (37–41) is an emerging field in the research of marine lipids (42). It is considered an important molecular tool to understand the features of polar lipids structure as well as structural

changes occurring in the lipids due to metabolic adaptation to environmental stress and starvation conditions (43–45).

Macroalgae employed for bioprospection are commonly collected from the wild and the same species collected in different regions, or sampling periods, may display different chemical compositions (46), tightly dependent on the seasonal, environmental, nutrition and habitat effects. These features could be a drawback considering bioprospection and potential applications of macroalgae as a source of bioactive compounds where replicability of biomass is needed. The use of macroalgae cultivated under controlled conditions, moreover when using integrated multi-trophic aquaculture (IMTA) systems, presents a sustainable solution to this pitfall, as well as to potential replicability issues when larger volumes of biomass are required (47–49).

In this Ph.D., lipidomic-based strategies were used for the analysis of polar lipids, in order to contribute to a better elucidation of the identity of lipids and fostering the valorization of macroalgae obtained from IMTA as a source of promising value-added bioactive compounds for food and health biotechnological applications (37–41).

I.1 State of the art

I.1.1. Macroalgae

Marine macroalgae are photosynthetic organisms, with close to 10,000 identified species that belong to Eukaryota Domain and the Kingdom Plantae (for the green and red algae) and Kingdom Chromista (for the brown algae) (6,50). They can be found along the littoral zone and are classified according to various structural and biochemical characteristics. Nonetheless, the systematic classification of macroalgae within three phyla is primarily based on the color of thallus and thus pigment components: phylum Chlorophyta for green algae, phylum Rhodophyta for red species and phylum Ochrophyta for brown. The most relevant photosynthetic pigments are divide in three categories, chlorophylls, carotenoids and phycobiliproteins (51). Chlorophyll (Chl) a is characteristic of all macroalgae, Chl b is characteristic of green, and Chl c found in brown macroalgae (15,18,52) while carotenoids, which are brown or yellow, are divided into primary (e.g., lutein) and secondary (e.g., carotenes and xanthophylls) carotenoids (52).

The phylum Chlorophyta

Chlorophyta, where green algae belong, includes several species that are characterized by the pigmentation that includes high amounts of chlorophyll a and b, β-carotene (a yellow pigment) and various xanthophylls (yellowish or brownish pigments) (53). Chlorophyta is the phylum with the lowest number of macroalgae species (about 1,500) but include some of the most common ones, like the species *Codium tomentosum*, target of this study. This species is organized in branches that form spongy, dark green, coenocytic thalli of intertwined filaments (54). *Codium tomentosum* thrives in Portugal, commonly found from late spring to the end of summer on semi-exposed rocks and/or deep rock pools on the lower seashore (55). The specimen is native to the North East of the Atlantic Ocean but is also found around the coasts of Africa and in various other parts of the world. Traditionally, it was part of a mixture of macroalgae, the "sargasso", which was used as soil conditioner in northern Portugal. Globally, *Codium* species are used in human nutrition, in cosmetic industry, and as an important source of sulfated galactans (56), and other compounds with bioactive properties, such as antioxidant, antigenotoxic, anti-tumor and hypoglycemic activities (13,57). With a growing interest from these sectors in accessing high quality biomass (e.g., monospecific, native, traceable, certified), together with a lack of availability plus the need of preservation of the wild resources, aquaculture is the only solution. The cultivation of *Codium* species is common in Asia, mostly for human consumption purposes. However, the production of the Atlantic species *Codium tomentosum* is still in its infancy, with aquaculture initiatives of the species occurring in Portugal and southern Spain.

The phylum Rhodophyta

Rhodophyta, where red macroalgae belong, contain photosynthetic pigments such as chlorophyll a, phycobilins (e.g., *R*-phycocyanin and *R*-phycoerythrin) and carotenoids, mostly β-carotene, lutein and zeaxanthin (52). Rhodophyta has the highest diversity of macroalgae species (about 6,500 species) and includes cylindrical and filamentous *Gracilaria* species from Gracilariales order (55). This macroalgae is represented by more than 300 species of which 160 have been accepted taxonomically (58) and is one of the world's most cultivated and valuable macroalgae. *Gracilaria* sp. are the main raw material used for production of agar, mainly in China, Indonesia, and Chile (1,9). *Gracilaria*

species are also abundant in Portugal, namely *G. gracilis*, *G. verrucosa* and *G. vermiculophylla*, and the only way to distinguish them with certainity is by using molecular tools. In Portugal, namely in the region of Aveiro and its coastal lagoon "Ria de Aveiro", *Gracilaria* is a very common species. In this region, its was once harvested for soil conditioning, as it was part of "moliço" - a mixture of algae and seagrasses collected in the lagoon that contained *Gracilaria* spp. (Rhodophyta) among others (59).

This group of seaweeds is well adapted to cultivation on land-based integrated multi-trophic aquaculture (IMTA) systems, allowing its sustainable production under controlled and replicable conditions that provide a secure supply of high-grade seaweed biomass for demanding markets (e.g., food, pharmaceuticals) (49).

The genus *Porphyra* is also one of the more diverse within Rhodophyta macroalgae, exceeding 150 species. It inhabits the intertidal zone of rocky shores throughout the year, with seasonal abundances of the different species (60). *Porphyra* spp. (Bangiales, Rhodophyta) is commercially valuable seaweed used primarily for food and attributed to health and longevity in Asian cultures but also as a source of the red pigment *R*-phycoerythrin (61,62). *Porphyra* (Nori) reputation is firmly established in oriental countries and recently in western countries as new super food and health promoter. Attempts are underway to develop *Porphyra* spp. as aquaculture crops in the United States, South America and Europe. Among the genus, *Porphyra dioica* (J. Brodie & L. M. Irvine, 1997, is one of the most common species in North of Portugal (63,64). The blade of *Porphyra* spp. (gametophytes) is the most commercially relevant phase of the life cycle. This macroalgae has a trimorphic life history (Fig. I.1) that also includes microscopic carposporophyte and uniseriate, branched filamentous conchocelis (sporophyte) (65,66). The development of the filamentous sporophyte phase is commercial interesting due to its molecular plasticity particularly for target molecules and since has the potential to be cultivated on indoor nurseries integrated in aquaculture systems (62).

Rhodophyta species are of paramount interest for industrial and biotechnological uses and are considered economically valuable resources due to their ability to achieve high yields of commercially valuable biomass and due to their use as a food and feed (1,21,67). These algae are also sources of important metabolites with several biological activities, namely anti-inflammatory properties (23,58,68).

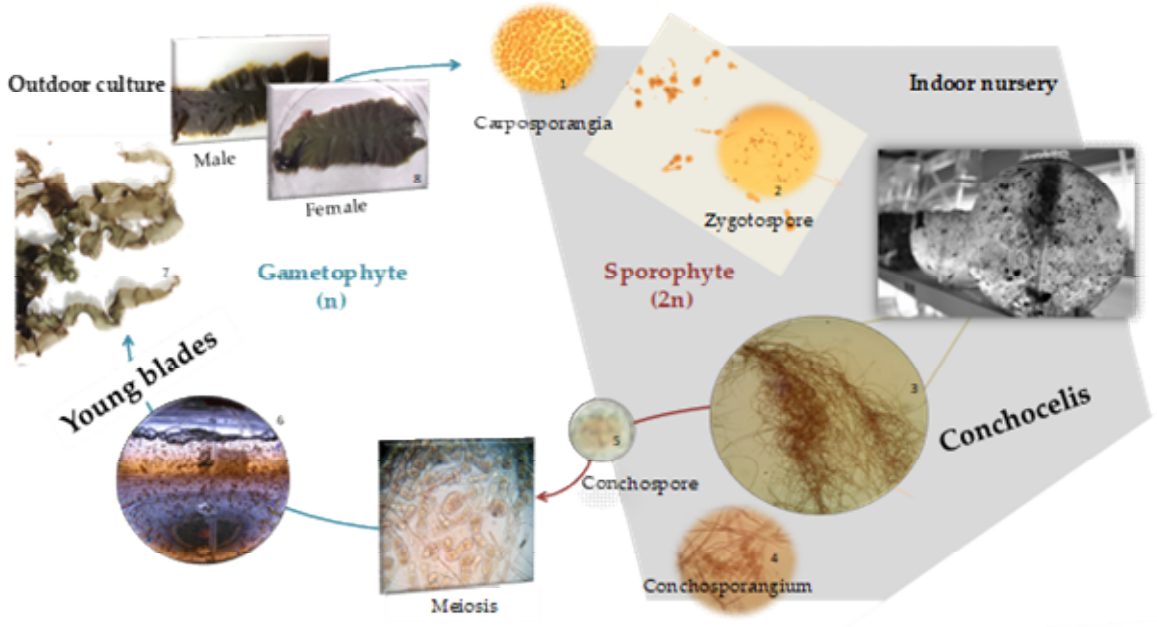

Figure I. 1. *Porphyra* spp. life cycle: The gametophytic blade phase reproduces sexually through fertilization of the carpogonium by the spermatium and subsequent carpospores formation; the development of these spores gives rise to the filamentous sporophyte conchocelis phase, which produces conchospores that are release into seawater and germinate forming new blades.

The phylum Ochrophyta/phaeophyta

The brown algae are members of the Ochrophyta, Class Phaeophyceae. As photosynthetic pigments, besides the normal chlorophylls a and c, brown algae differ for having a high amount of carotenoids, particular fucoxanthin (15,18). Ochrophyta comprise about 1,500 species, common in cold waters along continental coasts (69,70). *Fucus vesiculosus*, also called bladderwrack, is very common in rocky shores of northern temperate regions, also being present in rocky formation of salt marshes. Like the other members of Ochrophyta, their cell walls contain cellulose, alginic acid and sulfated polysaccharides, mostly exploited for commercial applications (1). *Fucus* species are thus an important source of alginates-colloidal extracts with many industrial uses and was also an important source of iodine. Indeed, the great interest of this edible macroalgae is mainly due to their bioactive ingredients that have showed benefits in cosmetic and, recently, in the prevention of chronic diseases (70,71).

The exploitation of marine resources including macroalgae and is one of the critical sectors within the action plan of economic, social and environmental betterment of Portugal (9,72). Although that were recognized the existence of 246 species of

Rhodophytes, 98 Phaeophytes and 60 Chlorophytes were identified in Northern Portugal, the main economic macroalgae in Portugal are the agarophyte *Gelidium sesquipedale*, harvested on the coast of the mainland, and *Pterocladiella capillacea*, which is harvested on the Azores Islands (73,74). Actually, macroalgae are definitely rather underexploited resources considering their great taxonomic diversity and promising source of biologically active compounds (5). There is a recent interest for drugs of marine origin and concomitant investigation is focusing on bioactivity and potential applications of macroalgae for food, feed and health improvement (1,74–77). Macroalgae can be directly consumed by humans and animal foods resembling traditional foods or as functional food possessing physiological benefits and promoting health by reducing the occurrence and incidence of different diseases (cancer, cardiovascular diseases, obesity, and diabetes) (5,11). They also constitute a source of high added-value metabolites (e.g., polysaccharides 50 - 70% of dry biomass), proteins (7 - 30% of dry biomass), lipids (1 - 10% of dry biomass), among others (Fig. I.2) (78).

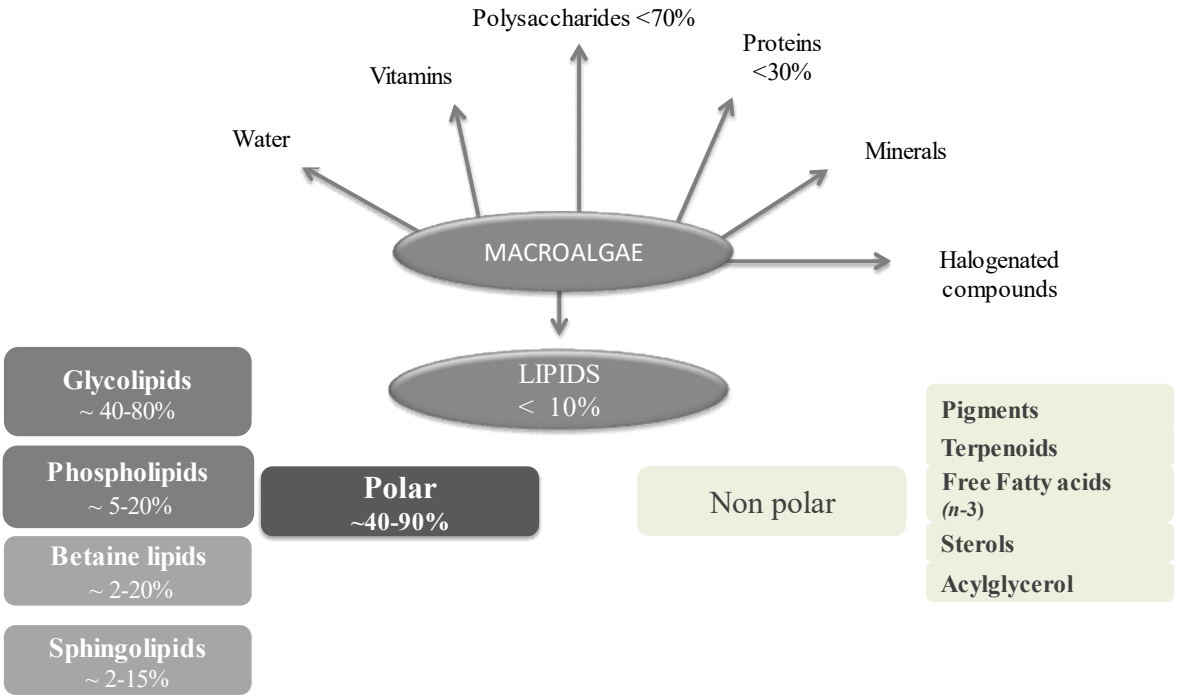

Figure I. 2. Chemical composition of macroalgae.

These metabolites have high nutraceutical value and infer macroalgae´s several applications in agriculture (fertilizers, biostimulants, bioregulators), animal (e.g., feed additives and as bioremediators for nitrogen-rich effluents from fed aquaculture) and

human products (food, cosmetics, pharmaceuticals) (79) and can be added at different stages of the food production process (80).

New markets are interested in the recovery and valorization of algae, as renewable resource, as a source of high value products in a positive integrated sustainable approach (81), that endorse the production of edible macroalgae, namely in aquaculture systems (1). Integrated multi-trophic aquaculture (IMTA) is being proposed as a mean to develop environmentally sound aquaculture practices and resource management through a balanced coastal ecosystem approach (82). IMTA mimics the natural ecosystem as nutrients excreted from one organism are taken up and transformed into resources needed for the growth of others (83). There are different conceptual approaches, the most classical being "fed fish" producing water rich in organic matter that is filtered by oyster and inorganic dissolved nutrients (like ammonia, nitrate, phosphate) that is extracted by photosynthetic organisms (like algae or halophytes). The cleaner water can recirculate back to the fish production or be released into the environment. IMTA can be implemented on land or at sea. In Western countries, macroalgae employed for bioprospecting are commonly collected from the wild, beeing exposed to natural variations of biotic and abiotic factors that will affect their chemical composition (6,83). Meanwhile, macroalgae obtained from aquaculture such as the IMTA system, by being grown in optimized conditions, are expected to guarantee the supply of target metabolites and presents a sustainable solution to potential replicability issues when larger volumes of biomass for high value markets are required (31,48). The valorization of macroalgae aligns with the innovation platform within blue economy for sustainable development of marine products to be the future generation of commercial and industrial applications (6,84).

Among the full diversity of macroalgae, *Codium tomentosum*, Stackhouse, 1797 (green macroalgae), *Gracilaria* sp., Greville, 1830 (red macroalgae), *Porphyra dioica*, J. Brodie & L. M. Irvine, 1997 (red macroalgae), and *Fucus vesiculosus*, Linnaeus, 1753, (brown macroalgae) were characterized in this Ph.D. focusing their lipidome and infering on potential valuable market applications.

I.1.2. Lipids in macroalgae

Lipids are considered potential bioactive components of macroalgae supporting the actual increase in marine lipid research all over the world. They represent less than 10% dry weight biomass (33), provide the structural basis for cell membranes, and fuels for

metabolism. Overall, lipids in macroalgae can be divided into two main groups: the nonpolar lipids (acylglycerols, sterols, free-nonesterified fatty acids, pigments) and polar lipids (phospholipids, sulfolipids, betaine lipids) that can account about 90 % of total lipids (16,18,85,86). Polar lipids are major and vital components of cell membranes and organelles, play a number of roles as mediators in signal transduction, cytoskeletal rearrangement and membrane trafficking (38,87,88). Different cellular compartments of algae have a particular lipid signature: extraplastidial cell membranes are mainly composed by phospholipids and betaines, while plastids membranes mainly contain glycolipids.

I.1.2.1. Non-polar lipids

Triacylglycerols (TAGs)

The triacylglycerols (TAGs) are a class of nonpolar ester-lipids derived from glycerol esterified to three fatty acids. TAGs are storage products and biosynthetic precursors, easily catabolized to provide metabolic energy to cellular activities storing high reducing power and energy (85). TAGs from macroalgae are being considered for biodiesel applications and their content may be manipulated by changing environmental factors (15,89).

Fatty acids (FA)

Fatty acids in macroalgae occurs mainly esterified to glycerolipids whose main classes in algae are the phospholipids, glycolipids and triacylglycerols and barely occur in the free form (1,12,90). Macroalgae contain saturated, monounsaturated and polyunsaturated FA with 8 to 24-carbon chain (91) FA from macroalgae contain high amounts of *n*-3 and *n*-6 families PUFAs such as eicosapentaenoic acid (EPA, 20:5(*n*-3) and eicosatetraenoic acid (or arachidonic AA, 20:4(*n*-6)) (71).

Fatty acids play a number of key roles in metabolism as major metabolic fuel (storage and transport of energy), as essential components of all membranes from cells and organelles, and as gene regulators (92). They confer flexibility, fluidity and selective permeability properties to cellular membranes and are vital important nutraceutical and pharmaceutical targets in human and animal health (93–96). Among FA, PUFA are essential in the food web processes of human and animal nutrition and have various beneficial clinical and nutraceutical applications, such as reducing coronary heart disease

risk and blood cholesterol, thus preventing the risk of arteriosclerosis, inflammation and several carcinomas (76). Otherwise, fatty acid profiles are considered very significant in macroalgae as biomarkers in chemotaxonomy (97).

Sterols

Sterols occur in free form, esterified with fatty acids, or, in minor concentrations, involved in glycosylated conjugates resulting from the development of a defense strategy of macroalgae to survive in a competitive environment (98–100). These compounds are important constituents of cell membranes and responsible for many of the cell functions (15,101). Sterols, namely phytosterols, are occur naturally in plants, animals and fungi, and are indispensable for a multitude of physiological processes in all eukaryotic organisms (98,102).

Pigments

There are considered three basic classes of pigments found in marine algae: chlorophylls, carotenoids and phycobiliproteins (53). Under these categories, many pigments have been described in marine algae and are of commercial interest, mainly used as food colorants and in nutritional supplements (52,53,103).

Chlorophylls are green lipid-soluble pigments found in all algae, higher plants or cyanobacteria that carry out photosynthesis (104–106). Chlorophyll contains a porphyrin stable ring-shaped molecule around which electrons are free to move. The ring has the potential to gain or lose electrons easily, and thus the potential to provide energized electrons to other molecules. This is the fundamental process by which chlorophyll "captures" the energy of sunlight, occurring in the center of the thylakoid, light-harvesting structures in which photosynthesis is carried out further converted into pheophytin, pyropheophytin and pheophorbide in processed vegetable food and following ingestion by humans (52,103). Chlorophyll is confined in chloroplasts, complexed with phospholipids, polypeptides and tocopherols and thus is protected by an hydrophobic membrane [6]. Within this class, as aforementioned, the most important is chlorophyll a, the molecule that makes photosynthesis possible, the second kind is chlorophyll b, and the third form of chlorophyll is chlorophyll c (53,107).

The second group of pigments are carotenoids, part of the photosynthetic apparatus, primarily in the reaction centers of photosystems (or inserted in pigment–protein antenna complexes) where they act as accessory pigments for light-harvesting processes during photosynthesis, as structural stabilizers for protein assembly in photosystems, and as inhibitors of either photo- and free radical oxidation provoked by excess light exposure (104,105). Carotenoids are the most widespread pigments in nature and are present in all algae, higher plants and many photosynthetic bacteria (7,35,108). They include photosynthetic pigments in the red, orange or yellow wavelengths. Green macroalgae species contain β-carotene, lutein, violaxanthin, neoxanthin and zeaxanthin, while red species mainly contain α- and β-carotene, lutein and zeaxanthin while β-carotene, violaxanthin and fucoxanthin are present in brown seaweed (53). Fucoxanthin is a xanthophyll with a unique structure that include an unusual allenic bond and 5,6-monoepoxide in its molecule and is one of the most abundant carotenoids in nature (9,109) It is found in brown algae and has important bioactivities (109).

The third group of pigments are phycobiliproteins, water soluble proteins that form particles (phycobilisomes) on the surface of the thylakoids (4,110). They are linear tetrapyrroles, with different combinations of the two principal phycobilins (phycoerythrobilin (red) and phycocyanobilin (blue) that absorb different regions of wavelengths. Phycobiliproteins play an important role in the photosynthetic process of algae, namely in Rhodophyta (33,111,112), and are currently being used as natural colorants in foods such as chewing gum and in cosmetic applications such as lipsticks and eyeliners (35,111). Moreover, they exhibit important activities such as antioxidant, in liver protecting, in serum lipid reduction, and in lipase inhibition (78).

I.1.2.2. Polar lipids

Polar lipids, as aforementioned, are important structural components in algae cell membranes and organelles, namely chloroplast and thylakoids (Fig. I.3). The polar lipidome is quite diverse and orchestrated by the activity of a panel of biosynthetic enzymes that coordinate the synthesis of each specific lipid, the trafficking of lipid intermediates, the catabolic pathways, and the regulatory processes that ensure the homeostasis of cell membranes (113). Polar lipids are amphipathic and the orientation of their hydrophobic and hydrophilic regions directs their packing and allows the formation of

a double layer, the central architectural feature of biological membranes (18,114). In addition to membrane stability role, some polar lipids may act as key intermediates (or precursors of intermediates) in cell signaling pathways (e.g., inositol lipids, products of oxidation) and play a role in adaptation to changes in the environment (115).

Polar lipids comprise several classes, among are glycolipids, phospholipids and betaine lipids that will be described (32,116,117).

Glycolipids

Glycolipids (GLs) are important classes of membrane lipids synthesized by prokaryotic and eukaryotic organisms and are the most abundant lipids located in photosynthetic membranes: thylakoid and chloroplasts (118). GLs are a category of lipids having a 3-carbon glycerol scaffold (each carbon is numbered following the stereospecific numbering nomenclature *sn*-1, *sn*-2, *sn*-3), anchoring one or two acyl chains esterified (R_1 and R_2) at positions *sn*-1 and *sn*-2, and a sugar moiety or derivative at position *sn*-3 denominated the polar head (119). Distinct classes can be found depending on the sugar moiety (polar head) and several molecular species can result due to the huge variety in the chain lengths, degree of unsaturation, and distribution of FA to the *sn*-1 and *sn*-2 position of the glycerol backbone (hydrophobic part). The properties of GLs straight depend on the polar head and on the structure of the two acyl chains thus the GLs can vary within the intra- and inter-taxonomy and in response to environmental changes (19,120).

Macroalgae biosynthesize three major types of glycolipids that constitute more than half of total polar lipids: the neutral galactolipids 1,2-diacyl-3-*O*-(β-D-galactopyranosyl)-*sn*-glycerol, also called monogalactosyl diacylglycerol (MGDG) and 1,2-diacyl-3-*O*-(α-D-galactopyranosyl-(1→6)-*O*-β-D-galactopyranosyl)-*sn*-glycerol, also called digalactosyl diacylglycerol (DGDG) and the acidic 1,2-diacyl-3-*O*-(6-sulfo-6-deoxy-*α*-D-glucosyl)-*sn*-glycerol also called sulfoquinovosyl diacylglycerol (SQDG) (Fig. I.3) (113,119). Also, glycosphingolipids, lipopolysaccharides and phenolic glycolipids may occur as minor components (113).

Glycolipids such as MGDG and DGDG play important roles for the structural stabilization and function of membranes (44,121), and are fundamental in the trafficking of lipids between subcellular compartments, namely to be transported to extraplastidial membranes (122). Under nutrition starvation and stress conditions, DGDG is exported to

various extraplastidial membranes, substituting phosphoglycerolipids (123,124) and facilitating the survival in stress environments (122). One of the most important features of GLs is in the regulation of homeostasis by the tuning of MGDG/DGDG and SQDG/PG (phosphatidylglycerol) ratios within the thylakoids and chloroplasts, and the galactoglycerolipid/phosphoglycerolipid (or DGDG/PL) ratio at the whole cell level in chloroplast-containing eukaryotes (113).

The class SQDG refers to a monoglucosyl diacylglycerol with a sulfonic acid linked at the monosaccharide moiety (125–127) (Fig. I.3). The sulfoquinovosyl moiety provide distinct properties to SQDG and the charged polar head of SQDG, at physiological pH, is appropriate to maintain the repulsive forces between neighboring membranes (122). The functional role of SQDG in the "membrane mosaic" relies particularly in signaling and coordination between chloroplast lipids (outer envelope membrane) and cytosolic partners. Upon phosphate starvation, SQDG compensate lower PG level and thus SQDG/PG ratio is tuned in response to phosphate availability (124,127).

The class of MGDG tends to adapt a conical shape when fatty acids are highly unsaturated (non- bilayer forming lipid) but if fatty acids are saturated MGDG rather adapt cylindrical form (128). DGDGs constitute the former bilayer lipid of chloroplast and thylakoid membrane (123,124). DGDG and SQDG has a more cylindric structure. Cylindrical shapes are ideally suited for packing side by side in a bilayer (128). The knowledge on structural details of GLs are thus very important to understand for the proper functioning of thylakoid membranes in chloroplasts. To accomplish their role in macroalgae membranes, GLs are known to contain 16- and 18-carbon *n*-3 trienoic acids and very long chain PUFA, with more than 20 carbon atoms and more than 3 double bonds such as eicosapentaenoic acid (EPA) (129–133). The contents of GLs in marine macroalgae may contain high *n*-3/*n*-6 PUFAs ratio.

Red macroalgae contained about 50 - 75% of GLs in total lipids, brown macroalgae contained about 47 - 83% of GLs and green macroalgae contained 68 - 75% of GLs (134). MGDGs generally represented 40 - 55% of GLs in brown and green macroalgae and 20 - 50% of GLs in the red division. DGDG contribute to 10 - 30% of GLs in green algae and 20 - 45% of GLs in brown and red macroalgae (15,122). The profile of GLs at molecular level (class/acyl composition of molecular species) among marine macroalgae was not elucidated until now, and analytical approaches such as TLC and GC–MS were most used

in the analysis of these complex molecular species, giving very limited information (97,135,136). Glycolipids are also known to have important bioactive properties as antitumor agents (132), as potential antiviral (25) and anti-inflammatory agents (137) and the knowledge on structural features is of paramount importance.

Phospholipids

Phospholipids (PLs) are a class of lipids, major components of lipid bilayers of all eukaryotic cell membranes (116,138). They play important structural and metabolic roles in living cells. Cell membranes use the dual hydrophilic and hydrophobic characteristic of PLs to maintain the integrity of membranes and act as structural entities confining subcellular components (139). In addition to their role in cellular structure they play an important part assembling other important molecules within several signaling systems (139).

Phospholipids such as glycerophospholipids commonly have two fatty acids esterified to the glycerol backbone and a phosphorous group that is further linked to the hydrophilic molecule confining the headgroup (Fig. I.3). PLs can be classified by the head group and the simplest form of PLs contains a backbone of phosphatidic acid (PA), formed by 1,2-diacyl-3-phospho-*sn*-glycerol with two fatty acids esterified at the positions *sn*-1 and *sn*-2 (15). When one acyl chain is lacking and then only one hydroxyl group of the glycerol backbone is acylated they are called lyso-phospholipids (140).

The phospholipids from macroalgae are phosphatidylglycerol (PG), phosphatidylcholine (PC), phosphatidylethanolamine (PE) and phosphatidylinositol (PI) that containing glycerol, choline, ethanolamine, myo-inositol, and phosphomonoester as their characteristic head groups, respectively (97,135,136). PLs are mainly located in extra-plastidial membranes, with the exception of phosphatidylglycerol (PG) that is found in significant amounts in plastidial membranes where it plays important role to ensure the efficiency of photosynthesis (32,97). PC was also found in lower amounts on the outer envelope of chloroplasts membrane (38). PLs form many kinds of assemblies such as micelles, liposomes and hexagonal phases depending on molecular shapes of each class (116,141). PC, PG, PA and PI tend to adapt a cylindrical shape, while unsaturated PE adapts a conical form. Lyso-phospholipids are prone to adapt to an inverted cone shape (Fig. I.3) (142).

The quantity and composition of phospholipids is regulated in a way that enables membranes for maintaining their structure and function, in spite of their developmental and environmental changes (15,135). Until now, the distribution of phospholipids along marine macroalgae was not elucidated due to the limitation of the methodology in the analysis of these complex molecular species. The profile of fatty acids of PLs were reported on literature based on GC–MS data revealing that PLs contain C_{16} and C_{18}, C_{20} and C_{22} and their PUFA from *n*-3 and *n*-6 series among are 20:4(*n*-6) and 20:5(*n*-3) FA (19,120). It was stated that FA-profile of PG was comparable to SQDG due to a common biosynthetic pathway of polar lipids from thylakoid membranes (97).

During the latest years, beneficial health effects of PLs are being considered in both animals and humans (28). PLs in diet act as natural emulsifiers, facilitating the digestion and absorption of fatty acids, cholesterol, and other lipophilic nutrients. Besides the nutraceutical relevance, PLs from algae are also used in the cosmetic and pharmaceutical industries [21], and have been described to be beneficial for cognitive functions and inflammatory diseases (32). PLs represent about 10 - 20% of total lipids in macroalgae (143,144), which quantity and composition are directly dependent on phylum, on environmental, and on nutritional growth conditions (143). Amid phyla, it is expected PG to be the most abundant PL in green seaweeds (< 50%), PC the most abundant in red seaweeds (~ 60% of the total PLs content), and both PC and PE classes to dominate in brown seaweed (< 30% of total PLs) (136). PA and PI account for lower percentages (97).

Polar lipid also includes sphingolipids when a group of acyl lipids with a sphingosine-based structure (phytosphingosine) is linked to a phosphoinositol group, corresponding to the inositol phosphoceramides (IPC). IPCs contain long-chain bases 18-carbon phytosphingosine and 14- to 26-carbon of hydroxy and non-hydroxy fatty acids (145,146). IPC is an extraplastidial lipid constituent with important biological functions as cellular messengers. It is considered characteristic of the red macroalgae lipidome signature (88,147,148).

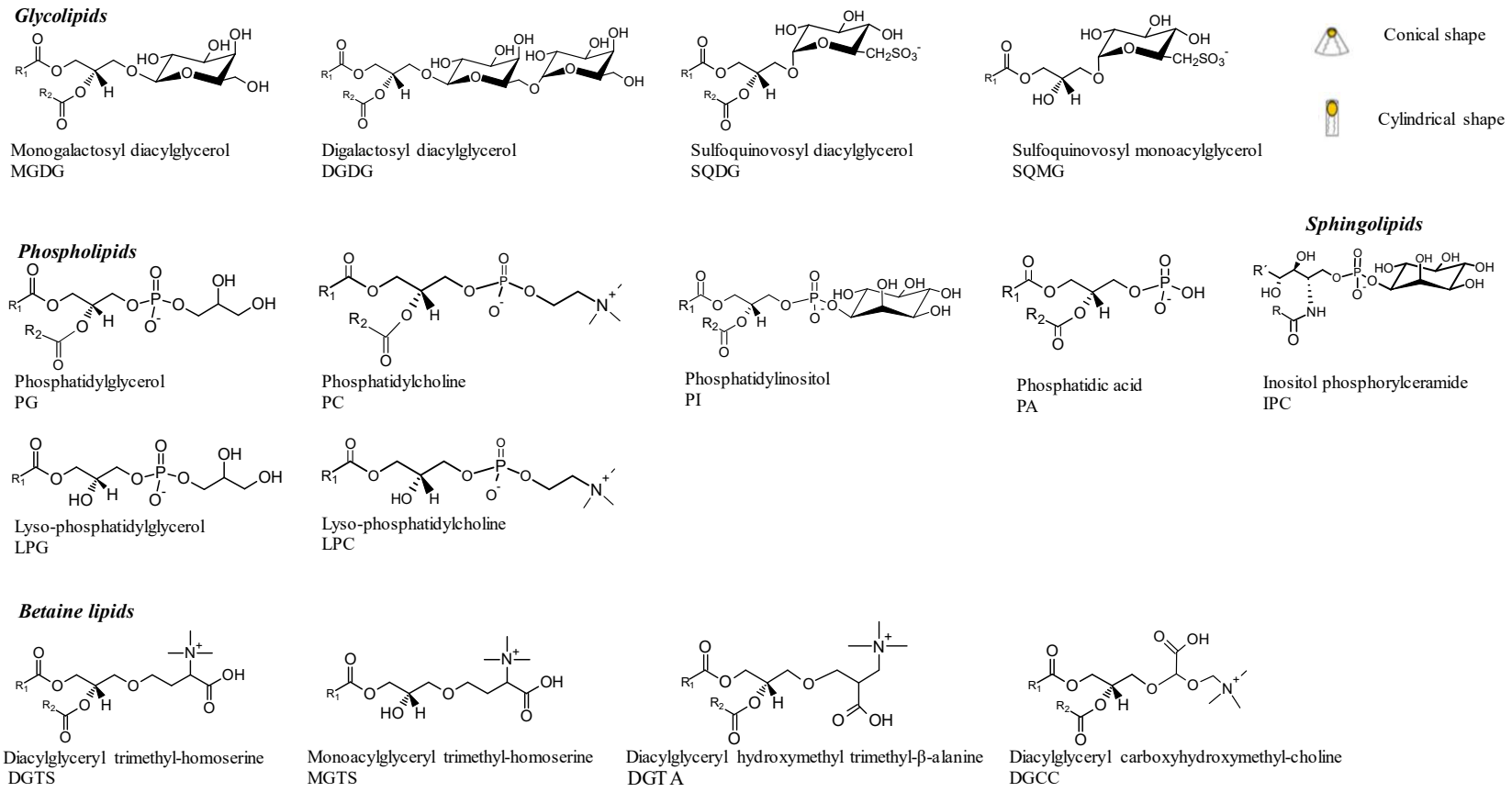

Figure I. 3. Polar lipid classes in macroalgae. Glycolipds (GLs): monogalactosyl diacylglycerol (MGDG), digalactosyl diacylglycerol (DGDG), sulfoquinovosyl diacylglycerol (SQDG), sulfoquinovosyl monoacylglycerol (SQMG); Phospholipids (PLs): phosphatidylglycerol (PG) and lyso-PG (LPG), phosphatidylcholine (PC) and lyso-PC (LPC), phosphatidylinositol (PI), phosphatidic acid (PA), inositol phosphorylceramide (or inositol phosphoceramide) (IPC); Betaine lipids: diacylglyceryl trimethyl-homoserine (DGTS), monoacylglyceryl trimethyl-homoserine (MGTS), diacylglyceryl hydroxymethyltrimethyl-alanine (DGTA), diacylglyceryl carboxyhydroxymethyl-choline (DGCC). R_1 and R_2 represent fatty acyl chains; R represents fatty acyl and R´ the long-chain base.

Betaine Lipids

Betaine lipids are naturally occurring lipids not found in higher plants, but are quite widely distributed in algae (149,150). They are components of extraplastidial membranes and of the outer membrane of chloroplasts (150). Betaine lipids from algae are involved in the transfer of fatty acids from the cytoplasm to the chloroplast, tend to replace phospholipids under conditions of phosphorous limitation, and may contribute as marker for signaling during environmental and nutrition changes (151). This class of acylglycerolipids has a quaternary amine alcohol ether-linked to a diacylglycerol moiety that confers a zwitterionic character at neutral pH due to the positively-charged trimethylammonium group and a negatively-charged carboxyl group, lacking in phosphorous. Until this moment, three types of betaine lipids are known to occur in algae: diacylglyceryl-*N,N,N*-trimethyl-homoserine (DGTS) (Fig. I.3) and its structural isomer diacylglyceryl hydroxymethyl-*N,N,N*-trimethyl-β-alanine (DGTA) and diacylglyceryl carboxyhydroxy methyl-choline (DGCC) (152). Of these, DGTS is considered the most common betaine in nature (153,154). Similarly to PCs, betaine lipids tend to adapt to cylindrical shape (155). Betaine lipids can have attached at the *sn*-1 and *sn*-2 positions of the glycerol saturated fatty acids (14:0 and 16:0), 18-carbon unsaturated fatty acid (predominantly 18:2 and 18:3), and PUFA (e.g., 20:5 FA) (152). Lyso-betaines containing one fatty acid esterified at the glycerol were never described in macroalgae.

Amid phyla, it was suggested that green macroalgae contain great amounts of betaine lipid DGTS (< 20% of total lipids) that act as substitute for PC in extra-chloroplast membranes (36,150). In red algae, DGTS and DGTA were found in small amounts (36,134). Brown algae was found to contain preferentially DGTA species (36).

Betaine lipids are a less reported class when compared with GLs and PLs and there is a great lack in structural and metabolic information about this category of lipids and their role in macroalgae is still unclear. Studies concerning betaine lipids are old and mainly devoted to bacteria, fungi and microalgae, and based on FA profile, thus their role in macroalgae cells stills unclear (150). Betaine lipids from microalgae were suggested to contribute as marker for signaling environmental and nutrition drawbacks that can be tuned, that could be interesting to differentiation between taxonomic clusters or target-biomass production (151).

I.1.2.3. Pathways of polar lipids biosynthesis

Photosyntethic membranes have a unique lipid composition that has been conserved from cyanobacteria to chloroplast (119). The biosynthesis of membrane lipids in eukaryotic algae involves cooperation between the plastid and the extraplastidial compartment (156). The set of reactions of the glycerolipid synthesis occurring within the chloroplast are termed the choroplastic or ‘‘prokaryotic” pathway and those that involve the participation of enzymes of the endoplasmic reticulum (ER) and chloroplast envelope constitute the endoplasmic or ‘‘eukaryotic” pathway (53,156). These enzymes control the type of sugar linked in the polar head in GLs and also the fatty acid position. The fatty acids linked in GLs are primarly biosynthesized *de novo* in the chloroplasts that remain in the plastid to be assembled to complex lipids such as GLs. These FAs can also be exported to the endoplasmic reticulum entering the endoplasmic pathway of the biosynthesis of lipids (Fig. I.4) (122).

GLs are formed in the chloroplast (“prokaryotic” pathway) by the sequential action of acyl-ACP glycerol 3-phosphate acyl transferase and acyl-ACP lysophosphatidic acid acyl-transferase. These enzymes produce phosphatidic acid that assembles almost exclusively C_{16} fatty acids at the *sn*-2 position of glycerol (18). The biosynthesis of GLs is catalyzed by the MGD synthase (galactosylation) that transfer a galactosyl residue from uridine diphospho-galactose (UDP-Gal) onto the *sn*-3 position of diacylglycerol (DAG) to produce MGDG, or to MGDG to form DGDG (114). The anomeric configuration of the first sugar is a β-glycosidic linkage and a α-glycosidic linkage in the second (113,119). SQDG is produced in the chloroplast´s envelope by the assemblage of a sulfoquinovose head group from the UDP-sulfoquinovose conjugated to DAG (113). DAG may also be derived from the ER, where it is formed during the glycerolipid biosynthetic pathway, followed by subsequent transfer of DAG moieties into the chloroplast to be used in the endoplasmic or “eukaryotic” pathway.

In the endoplasmic reticulum, the microsomal acyl-transferases are responsible for phosphatidic acid synthesis in the ER and give rise to lipids that contain C_{18} fatty acids exclusively at the *sn*-2 position and either C_{16} or C_{18} fatty acids at the *sn*-1 position (53,156,157) providing a signature of ER origin of a DAG.

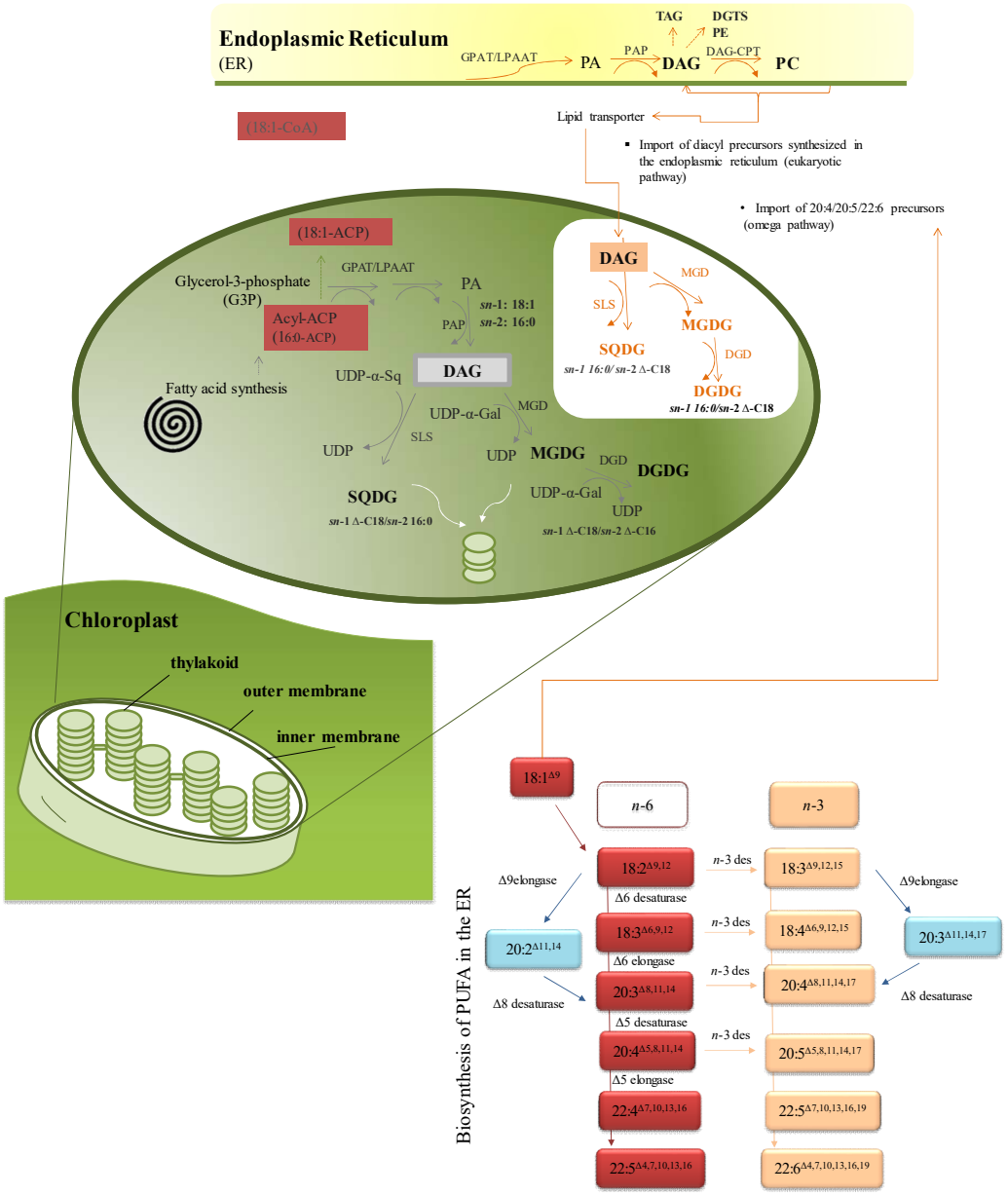

Figure I. 4. Simplified diagram of the pathways of the biosynthesis of glycerolipids in macroalgae that include chloroplastic (‘‘prokaryotic” pathway) reactions and endoplasmic - ER (‘‘eukaryotic” pathway) reactions. Orange arrows refer to the biosynthetic pathway of transport of ER-derived glycerolipid to chloroplasts. ACP, acyl carrier protein; PA, phosphatidic acid; DAG, diacylglycerol; PC, phosphatidylcholine; MGD, MGDG synthases; DGD, DGDG synthases; UDP, uridine diphosphate galactose intermediate in the production of polysaccharides (-Gal galactose, -Sq sulfoquinovose); GPAT, glycerol-3-phosphatase acyltransferase; LPAAT, lysophosphatidic acid acyltransferase; PA, phosphatidic acid; PAP, phosphatidate phosphatase; DAG-CPT, diacylglycerol synthetase-choline: diacylglycerol cholinephosphotransferase; SLS, sulfolipid synthase; SQDG, sulfoquinovosyl diacylglycerol; PE, phosphatidylethanolamine; DGTS, diacylglyceryl trimethyl-homoserine; TAG, triacylglycerol; Δ, degree of unsaturation ranging from 1 - 4 double bonds (adapted from da Costa et al., 2016).

Glycolipids can also include PUFAs like 20:4(*n*-6), 20:5(*n*-3) and 22:6(*n*-3) (Fig. I.4) formed by the desaturation and elongation reactions occurring in the ER (via omega pathway, Fig. I.4) or C_{14} FA that can be biosynthesized via "prokaryotic" and/or "eukaryotic" routes (114,158). In the chloroplast, glycolipids can undergo little turnover by deacylation–reacylation reactions. Furthermore, the newly formed galactolipids are redistributed to the thylakoid membranes and, under certain growth or stress conditions, DGDG may also exported to extraplastidial membranes (53). Based on the positional distribution of fatty acids on the individual molecular species of GLs is possible to identify the pathway of biosynthesis (114,119,139,158).

A resumed biosynthesis pathway of GLs, PLs and betaine lipids in the macroalgae is proposed on Figure I. 4, adapted by da Costa et al. (159) according to Okazaky et al. (156), Boudiére et al. (113) and Yan et al. (160). The current knowledge of the membrane lipids biosynthesis was mainly based on green microalgae-model *Chlamydomonas reinhardtii* (15,45,113) and on the plant-model of *Arabidopsis* (113,119,156,161).

Phospholipids are mainly biosynthesized in the endoplasmic reticulum. The simplest structure of PL is phosphatidic acid (PA) that is biosynthesized from glycerol-3-phosphate via sequential acylation at the *sn*-1 and *sn*-2 hydroxyl groups by glycerol-3-phosphate acyl transferase and acylglycerol-3-phosphate acyl transferase. Following the pathway, it diverts onto two main branches: one that leads to the formation of the PI, and the other where PA is dephosphorylated by PA-phosphatase (PAP) to diacylglycerol (DAG). DAG serves as a precursor of PC and PE. DAG can also be converted into triacylglycerol (TAG) to be a reservoir of DAG and fatty acids, or DAG can convert to ceramides via the incorporation of serine (not showed in the Fig. I.4). PLs may be imported from endoplasmic reticulum to the chloroplastic compartment to be part of the biosynthetic pathway of the GLs. The chloroplast system is responsible for the production of GLs and for the production of phospholipids such as PA and PG, all incorporated in chloroplast membranes. Ensuing chloroplast pathways, PA biosynthesis participate in the formation of phosphatidylglycerol (PG) or, by a secondary pathway, can be dephosphorylated by a PAP to DAG that serves as a precursor of GLs (32,38).

Regarding DGTS, the biosynthesis is not completely elucidated until this moment, but it was hypothesized to be close to PLs pathway occurring in the ER. One of the most important issues about the biosynthesis of the betaine lipids concerns the origin of the polar

group and the mechanism of formation of the ether linkage between the glycerol and the hydroxyamino acids. Methionine is considered the precursor needed for the formation of the polar group of betaine lipids (150). Similar to PLs route, it was suggested that these lipids may be imported from ER to the chloroplastic compartment to be part of the biosynthetic pathway of the GLs.

I.1.2.4. Polar Lipid profile dependence with growth conditions

Macroalgae can be found in natural habitats with harsh environment and experience a variety of stressful conditions such as nutrient limitation, salinity variations, intense radiation, temperature fluctuation, and repeated immersion due to tidal fluctuation, desiccation, and chemical pollution (49,57,79,83). These parameters have great interference in the biochemical composition, distribution, production, and fecundity of macroalgae (19,124).

Regarding lipid composition, they are directly dependent on seasonal changes that include environmental factors such as temperature, light, nutrient availability, and also of the physiological state of the macroalgae (19). These variables and stressful environmental conditions have been shown to be associated with the increase in the formation of reactive oxygen species (ROS) in cells as a consequence of photosynthetic inhibition with excess energy, resulting in the production of singlet oxygen that causes 'oxidative' stress (15,162). Such climatic stresses disturb the fluidity of cell membranes due to changes in the metabolism and lead to changes in membrane composition and in the physiological properties of membrane bilayer for maintaining normal cell functioning (ion permeability, photosynthesis, respiration and other metabolic activities). The alteration in lipid species and lipid classes, namely by changing the chain length and/or the degree of saturation and content, and the modification of the metabolism pathways were the most commonly observed changes in membrane lipids following adverse environmental conditions in macroalgae (15,162).

Polar lipids PLs, GLs and DGTSs are recognized as signaling biomarkers when algae are exposed to different conditions, adapting the expression levels and the polar group and fatty acyl composition towards the regulation of homeostasis. The effects of the nutrients regime and environmental changes on the lipidome of macroalgae are reviewed.

Polar lipids and Nutrients Regime

Nutritional stress effects caused by limitation of nutrients such as nitrate and phosphate alter the metabolic pathways involved in lipid biosynthesis by shifting of lipid classes, fatty acids, and production of oxylipins (124,163). Salinity is an important environmental factor that affects growth and productivity of algae. Salinity fluctuations influence algae by altering membrane permeability and fluidity (124). Under salt stress, the restructuration of membrane lipid composition occurs and is mainly attained by increasing the unsaturation of the fatty acids from PLs (124). Salt stress cause decrease in the PLs content, namely of PC and PG classes, essential lipid for the assembly of light harvesting proteins in photosystems. The decrease of PL content is associated with an increase of the SQDG content (123). Salt stress may also lead to increasing of the expression levels of GLs (MGDG and DGDG) that protect the normal function of membrane under stress condition. An increase of DGDG/MGDG ratio is considered crucial for maintaining membrane stability and functional activity of membrane proteins (123).

The differential nitrate and phosphate uptake and their storage are part of adaptive strategies of macroalgae for their successful sustenance (164). Phosphate (inorganic phosphate, Pi) is an essential nutrient for all plants, including marine species. Under Pi deprivation, the uptake of exogenous Pi increase making use of membrane phospholipids as an internal Pi source (157). Benning et al. revealed that Pi starvation strongly decreases the relative content of overall phospholipids and increases certain non-phosphorus lipids, particularly SQDG species (133). Stress and deprivation of Pi relates to the decrease of PLs content, probably by the regulation of PC and PG under stress adaptation. Recently, Kumari et al. (164) reported that nutritional deprivation of *Ulva lactuca* inferred the accumulation of DGDG, SQDG and DGTS species when deprived of either nitrate, phosphate or both. Meanwhile, supplementation of nutrients, especially nitrate, infer the recovery of MGDG. PLs biosynthesis is very dependent on phosphate availability and deprivation leads to the degradation of PLs and production of PA or lyso-phospholipids (164). The deficiency of both N and Pi leads to the to the increase in the DGDG/MGDG ratio concomitant with the degradation of PLs that also is reflected in the increase of PA and of lyso- lipids.

Under nitrogen starvation of algae, there is as increase of DGTS species containing monounsaturated fatty acid (MUFA) moieties such as 18:1, and PUFAs such as 18:2, while

DGTS species exhibiting PUFAs moieties, such as 18:3(*n*-3) and 18:4(*n*-3) decreases (150). Nitrate deprivation may also accomplish the accumulation of non-polar lipids (triacylglycerol; TAG) while an increase in nitrate leads to the increase of the galactolipid biosynthesis, especially of MGDG species (15).

Polar lipids and environmental changes

Like other biochemical components of algae, the lipid content varies with the season and environmental factors like temperature, pH and light exposure (19,120,124,151). The research on the effect of seasonality and thermo-adaption on macroalgae Ochrophyta (*Egregia menziesii*), Rhodophyta (*Chondracanthus canaliculatus*) and Chlorophyta (*Ulva lobata*) suggested that the relative amount of polar lipids increased in winter, which coincided with highest unsaturated fatty acids unsaturation (18,120). Higher percentage of PUFAs, high unsaturation index, and higher relation *n*-3/*n*-6 PUFAs in algae are more related to winter than to summer season (97,120,165-167) due to low-temperature acclimatization and photosynthetic machinery protection from low temperature (15).

Generally, it was suggested that algae can accumulate PUFAs when there is a decrease in the environmental temperature (91). During the change in season from summer to winter occurs a substitution of *n*-6 by *n*-3 PUFAs that is accomplished by the partial substitution of C_{20} by C_{18} PUFAs in the molecular species of GLs and PG in contrast to PC and PE. Otherwise, it has been reported that PLs and SQDG increased while MGDG content decreases with the decrease of temperatures (15-16,165). However, this was not observed within all taxonomic species and the temperature effect on polar lipids alterations deserves to be better understood (162,166).

The effect of light has been reported to interfere with algal lipid metabolism and polar lipid composition (166,168). Changes in the quality and quantity of lipids from both storage and structural lipids and in the chloroplast development can occur due to alterations of light conditions (15). Exposure to low light intensity, with shade about 8 - 10% of the incident photosynthetically active radiation (PAR), increases content of SQDG, PG, and PC membrane lipids (146). High light effect decreases the level of PLs as well as the content of EPA in MGDG and PG species. The green algae *Ulva fenestrata* increased amounts of MGDG, SQDG and PG were observed when grown at 24% PAR compared to the same specimen cultured at 80% PAR. The content of DGDG and betaine lipids

displayed little dependence on light intensity. However, aforementioned behaviors were supported by scarce studies, the light effects, environmental effects such as extreme pH conditions on polar lipids from macroalgae is still not well documented.

I.1.3. Lipidomic–based approaches applied to macroalgae

Mass-spectrometry- based lipidomics is nowadays the analytical approach that allows the elucidation of lipid profile in macroalgae and identification of their structural deviations. “Lipidomics” refers to the detailed and comprehensive profiling of lipid classes and molecular structures considering the plethora of cellular functions mediated by lipids (169,170). Polar lipids are a diverse group of highly complex biomolecules due to the various combinations of polar headgroups and fatty acyl species (114). They enclose distinct roles within the biological system attending their specific structures (42,43,170). The knowledge of their biological role is thus a great challenge that is dependent on lipid analysis at molecular level. The full characterization of polar lipids includes isoforms and isobaric compounds of intact and also modified structures (169). The advantage of mass spectrometry such as increased sensitivity, resolution, and speed of analysis boosted the development of lipidomics and the structural characterization of the lipidome. New perspectives in the understanding of the roles of lipids in human health and disease (171–174), plants (38,156,157,175–177) and bacteria (38,171,178) have been reported. Based on these knowledge, MS-based analytical techniques provided comparable and amenable quantification of high through put data analysis, the knowledge of lipid classes and acyl chains featuring molecular species, and allow to distinguish composition at molecular level, ideal for traceability and taxonomic differentiation (179). The new era of marine lipidomic is in progress on the lipidome of microalgae (40,44,123,151,180), and is flourishing decoding lipid profiles of macroalgae (145,164,166,181).

Lipidomics based on mass spectrometry approaches (e.g., liquid chromatography (LC)-mass spectrometry (MS)) is rapid in comparison to “traditional” methods of lipid analysis (thin layer chromatography (TLC), gas chromatography GC, nuclear magnetic resonance NMR) and requires relatively small amounts of material (169). It allows the identification and quantification of hundreds of lipid species, directly from a total lipid extracts of biomass without chemical modification (145). The Figure I.5 presents a general workflow

for lipidomics-approach based adapted to the identification of polar lipids from macroalgae.

First step on the methodology is the extraction of the total lipids from the dried or fresh biomass, in some cases followed by direct analysis by LC–MS. Some cases, when specific classes are the focus of the study, fractionation of lipid extracts by TLC or solid phase extraction (SPE) may be useful, and fractions will be further analyzed by MS or LC–MS. Moreover, fatty acids esterified to polar lipids are achieved by MS-approaches, either from the total extracts or selected fractions of polar lipids, or the profile of fatty acids can also be obtained by GC–MS or GC–FID analysis.

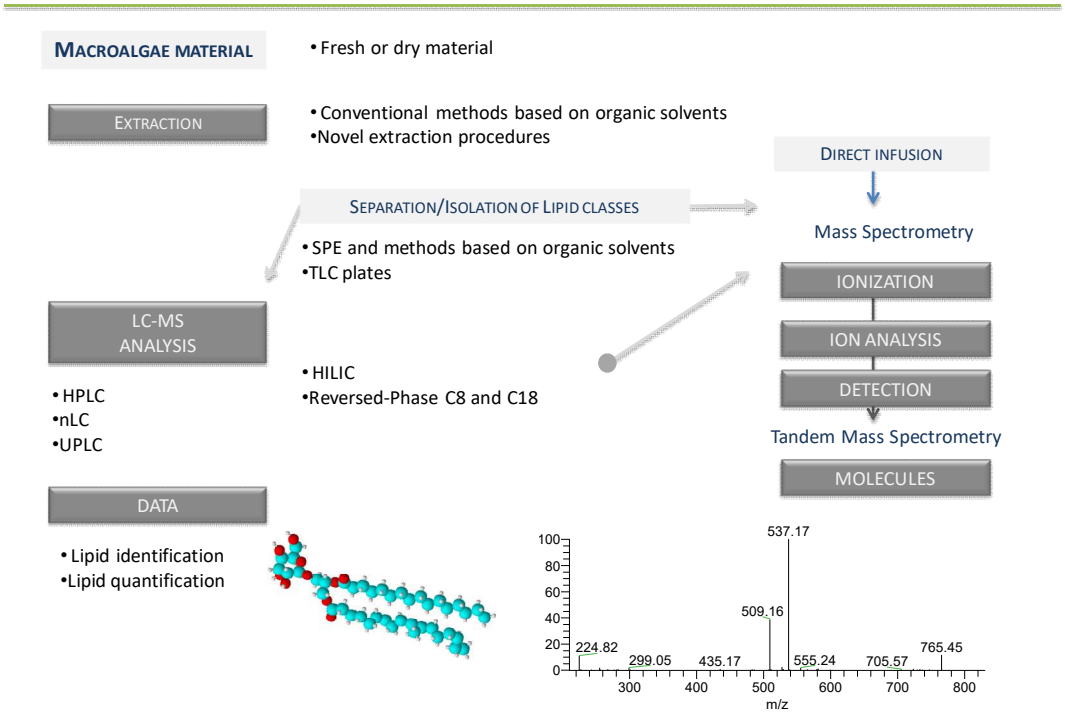

Figure I. 5. LC–MS, approach in the lipidomic analysis of polar lipids from macroalgae.

I.1.3.1. Analytical strategies to identify the lipid profile of macroalgae

Lipid extraction protocols commonly use well-known solid-liquid extraction methods with methanol or combinations of methanol and chloroform such as Bligh and Dyer (1:2, per volume) (182) and Folch (2:1, per volume) (183) methods. The use of other solvents ethyl acetate, acetone, butanol or methyl-*tert*-butyl ether (MTBE) have been reported aiming to avoid organochlorides (184,185). It gives rise to lipid extracts with different compositions and extractions with dissimilar yields. In attempt to avoid the use of toxic

solvents hazardous for health, or not compatible with food processing, novel "green" extraction techniques are being considered for the extraction of polar lipids from macroalgae (81,186). Supercritical fluid extraction (SFE) (187,188), microwave-assisted extraction (MAE) (189,190), ultrasound- assisted extraction (UAE) (35,151,191) and pressurized liquid extraction PLE (192,193) are some of these novel "green" extraction techniques. The advantages of use these methods have to consider to be low cost, safety and the ability to scale up and easy to apply on the industrial scale for the extraction of lipids biomass. These novel extraction technologies may provide an alternative to the traditional methods whereas that must to attend that polar lipids are sensitive, thermolabile and are found in low concentrations. The development of novel extraction technologies must guarantee that alternative extractions won´t interfere with the structure of these lipids.

Most common lipidomics include ESI source and different analysers such as IT, Q-TOF and orbitrap (Fig. I.6) (194).

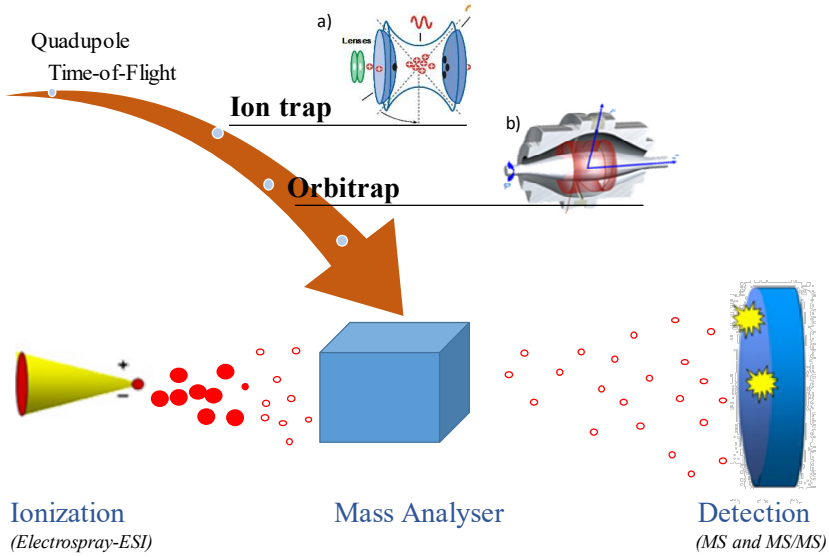

Figure I. 6. Schematic representation of mass spectrometer components. Mass analyser referred to a) Ion trap and b) Orbitrap (adapted from https: //www.thermofisher.com/pt/en/home/industrial/mass-spectrometry.htm).

Two main strategies for the analysis of polar lipids by MS have been reported: untargeted lipidomics that usually uses chromatographic-based separation techniques prior to the MS analysis of lipids (160,195); targeted (shotgun) lipidomics by direct infusion analysis of a crude lipid extract (196). Both methods have their advantages and disadvantages with shotgun approach being more prone to strong ion suppression effects.

These effects can be partially compensated by large sample dilutions and by the use of internal reference compounds. Chromatography-based methods (off-line TLC, off-line silica columns, on-line HPLC, on-line UPLC) are less prone to these suppression effects, due to the previous chromatographic separation (41,197).

Untargeted-lipidomics supported by modern advanced MS-based techniques allows to identify and quantify several molecular species from distinct polar lipid classes. Hydrophilic interaction chromatography (HILIC) allows the separation of lipids depending on their polar head group and fatty acyl composition. HILIC has been introduced as a variant of normal phase chromatography (198,199). Elution is performed by a binary eluent of organic solvent/ water. HILIC–MS (acquired in a LIT–MS–analyser) successfully applied decoding the lipidome of the red macroalgae *Chondrus crispus* (145). It allowed the identification of more than 100 molecular species in the lipidome of this macroalgae. Other works were published about target-lipidomics to identify molecular species/classes from previous isolated extracts of macroalgae and have used distinct mass analysers (Q–TOF, LTQ, and QqQ) (Table I. 1) (40,200,201). MS-based approach was fundamental to characterize glycolipids and further evaluate the relation between their structure and biological activity (23,25,30). Some case-studies were marine *Palmaria palmata* (181), marine *Osmundaria* sp. (202), *Chondria armata* (203), cultivated *Chondrus crispus* (30,145), marine brown algae *Sargassum* sp. (25,204), and *Fucus spiralis* (27). MS-based lipidomics was used to identify the polar lipid profile of macroalgae during growth, showing the high potential on the screening of molecular changes occurring under nutrition quality and environmental stress (164) or even as an important tool to profile fatty acids biosynthesized by macroalgae. This work allowed to establish and manipulate the distinct biotechnological applications, namely by the content in *n*-3 PUFA (15) (Table I.1).

In the field of algae, the great improvement to lipidomics is paramount to accomplish the analysis of the hundreds of different species that are compose the lipidome of a single matrix. However, the full profile at molecular level of distinct classes of polar lipids across different taxonomic categories (green, red and brown) is far from being elucidated and, attending the great biotechnological potential of lipids, it deserves to be further explored.

Table I. 1. Lipidomics of Chlorophyta, Rhodophyta and Ochrophyta macroalgae reported in literature

Macroalgae	Extraction protocols	Polar lipid classes, *and total number of molecular species identified within each class*			Reference
		Glycolipids	Phospholipids	Betaine lipids	
CHLOROPHYTA					
Enteromorpha intestinalis	Folch	1 SQDG, 1 SQMG			(33)
Ulva armoricana	Methanol/Chloroform	1 DGDG			(205)
Ulva fasciata	Bligh and Dyer		1 PS, 1 PA		(116)
	Bligh and Dyer	1 SQDG, 1 MGDG			(127)
Ulva lactuca*	Bligh and Dyer	MGDG, DGDG, SQDG	PG, LPG, PC, LPC, PS (#), PA (#), PI (*)	DGTS	(164)
Ulva rigida	Folch	1 SQDG	4 PCs, 1 LPE	-	(33)
RHODOPHYTA					
Asparagopsis taxiformis	Folch	1 SQMG			(33)
Chondrus crispus	Methyl *tert*-butyl ether/Methanol	19 DGDGs, 14 SQDGs	18 PGs, 60 PCs, 8 LPCs, 14 PAs, 2 LPGs	14 DGTS	(145)
Chondria armata	Methanol Chloroform Butanol	2 MGMGs, 3 MGDGs, 2 SQMGs	4 DPGs		(203)
Chondrus crispus	Methanol Ethyl acetate	8 MGDGs			(30)

Galaxoura cylindriea	Bligh and Dyer		1 PG, 1 PE, 1PA	(116)
	Bligh and Dyer	1 SQDG, 1 MGDG		(127)
Laurencia papillose	Bligh and Dyer		1 PE	(116)
	Bligh and Dyer	1 SQDG,1 MGDG		(127)
Osmundaria obtusiloba	Acetone Methanol/Chloroform	1 MGDG, 1 DGDG, 1 SQDG, 1 SQMG		(202)
Palmaria palmata	Methanol/Chloroform Ethyl acetate	2 MGDGs, 3 DGDGs, 2 SQDGs	2 PGs, 1 PE	(181))
Pterocodiella capillacea	Folch	1 DGDG, 1 SQDG, 1 SQMG	2 PGs, 11 PCs, 1 PI, 1 LPI, 2 PS, 1 LPE	(33)
Porphyra haitensis	Methanol/Formic acid/Water		7 PCs, 5 LPCs, 1 LPE	(206)
Solieria chordalis	Methanol/Chloroform	1 MGDG		(205)
		Ochrophyta		
Fucus spiralis	Methanol	2 MGDGs		(27)
Sargassum horneri	Ethyl acetate	10 MGDG		(207)
Sargassum thunbergii	Methanol/ Butanol 2:1 (v/v)	2 MGDGs		(204)
Sargassum vulgare	Methanol/Chloroform 2:1 and 1:2	6 SQDGs		(25)
Stypocaulum scoparium	Folch		2 PGs, 2 PCs, 2 PS	(33)
Dictyota dicotoma	Folch	1 SQDG, 1 SQMG	11 PCs, 1 LPE	(33)

Colpomenia sinuosa	Folch	1 SQMG	8 PCs, 1 PI, 1 LPE	(33)
Cystoseyra brachicarpa	Folch	1 SQDG	2 PGs, 2 PCs	(33)
Dilophys fasciola	Bligh and Dyer		PG, PC (#), PE, PI (*)	(116)
	Bligh and Dyer	1 SQDG,1 SQMG		(127)
Taonia atomaria	Bligh and Dyer		PG, LPC (#)	(116)
	Bligh and Dyer	1 SQDG,1 SQMG		(127)

MGDG, monogalactosyl diacylglycerol; MGMG, monogalactosyl monoacylglycerol; DGDG, digalactosyl diacylglycerol; SQDG, sulfoquinovosyl diacylglycerol; SQMG, sulfoquinovosyl monoacylglycerol; PC, phosphatidylcholine; LPC, lyso phosphatidylcholine; PG, phosphatidylglycerol; LPG, lysophosphatidylglycerol; PE, phosphatidylethanolamine: PI. Phosphatidylinositol; PA, phosphatidic acid.;(*) detailed composition not included; (#) uncertain assignments; Folch (183); Bligh and Dyer (182).

I.1.3.2. Identification of the lipidome of macroalgae by mass spectrometry

LC–MS spectra typically contains several ions and, based on their mass-to-charge ratios, it is possible to calculate the molecular weight of the correspondent lipid molecular species (170,208). Molecular weight is determined by the identification of the type of the ions that are present in the MS data such as protonated, deprotonated or adducted ions. Polar lipids are able to ionize as positive ions or negative ions, depending on the chemical nature of their polar head groups (209). Following, detailed structural characterization is achieved by using Tandem MS, based on the isolation of a specific *m/z* value (precursor ion) that may be submitted to dissociation and subsequent production of ion fragments (41).

Concerning the polar lipids from algae lipids there are three categories: anionic (PA, PI, PS, SQDG), weakly anionic (ceramide, PE, PG) and 'neutral' lipids (MGDG, DGDG, DGTS) (136). Thus, due to their chemical structure, different molecular ions are observed in MS spectra of each class, as will be described. According to the pattern of fragmentation obtained by tandem MS, the structure of molecular species from distinct classes is built based on the polar heads and fatty acyl fragments. The typical fragmentation is identified by comparison with databases and literature or by analyzing the detailed fragmentation of standards.

The glycolipids MGDG and DGDG preferably ionize in the positive mode *via* the formation of adduct cations (e.g., Na^+, NH_4^+). The detailed fragmentation of the precursor ion $[M+Na]^+$ yield the product ion galactosyl glycerol head group $[C_9H_{16}O_6 + Na]^+$ at *m/z* 243 (MGDG and DGDG) and the digalactosyl glycerol head group $[C_{15}H_{26}O_{11} + Na]^+$ at *m/z* 405 (DGDG) (Fig. I.7) (123,145,156,210,211). The neutral loss of the hexose residue (Y_1, Fig. II.4) plus the hexose unit (Z_1, Fig. I.7) in the case of MGDG and DGDG, and the loss of the dimer (Y_0, Z_0, Fig. I.7) in the structure of the DGDG assign the identification of these glycolipids. Otherwise, the fatty acid composition as well as the determination of their position on the glycerol backbone is obtained from the loss of the fatty acyl moieties, described by the product ions D_1 (loss of the R_1COOH) and D_2 (loss of the R_2COOH) in the Figure I.7. The fragmentation of GLs as $[M + NH_4]^+$ may be identified by the product ions resulting from the loss of NH_3, loss of hexose residue (-162 Da, $-Hex_{res}$), and hexose moiety (-180 Da, -Hex) (123,156,210,211). Product ions formed by combined loss of the

one FA and the hexose yield a typical acylium ions plus 74 $(RCO + 74)^+$ that allows to identify the FA composition.

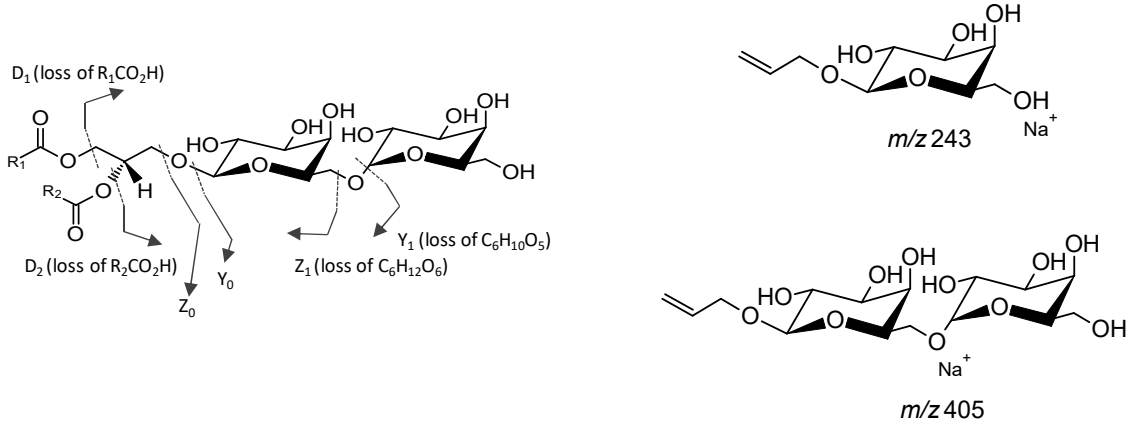

Figure I. 7. Schematic fragmentation pathways of digalactosyl diacylglycerol observed in the MS/MS spectra of the $[M + Na]^+$ ions that support their structural characterization.

Sulfoquinovosyl diacylglycerol ionize preferably as $[M - H]^-$ and showed in tandem MS the typical product ion at *m/z* 225, attributed to the sulphoquinovosyl anion, and ions due to the loss of fatty acyl chains (Product ions D_1 and D_2, Fig. I.8), both as acid and keto derivatives (127,131,145). The product ions attributed to carboxylate anions ($RCOO^-$) can also be found in the MS/MS spectra.

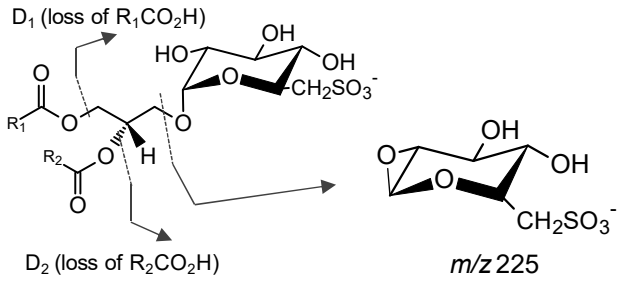

Figure I. 8. Schematic fragmentation of sulfoquinovosyl diacylglycerol. The lines indicate the product ions formed. The typical product ion at *m/z* 225 is attributed to the sulfoquinovose head group.

The fragmentation of PLs showed characteristic product ions or neutral losses (Fig. I.9) deriving from the head group that are useful since they allow specific identification of the distinct classes. PE and LPE ionize as $[M + H]^+$ and as $[M - H]^-$ ions. $[M + H]^+$ fragments yield the loss of the head group (phosphoethanolamine) as a neutral fragment of 141 Da, used to confirm this class in spectra. PG and LPG are seen as $[M - H]^-$ ions and the MS/MS shows the neutral loss of 74 Da and the formation of the product ions such as

glycerol phosphate anion at *m/z* 171 together with glycerophosphate glycerol anion minus H_20 at *m/z* 227 that confirm the class. PI is identified as $[M - H]^-$ and the fragmentation yields the product ion at *m/z* 297 arising from consecutive losses of the fatty acyl substituents. The product ions at *m/z* 223 and *m/z* 241 the inositol head group (138,212–214). PA is identified as $[M - H]^-$ ion by the product ion of glycerophosphate (*m/z* 153) (138,213,214). PC and LPC ionize as $[M + H]^+$ ions in positive ion mode and fragmentation of PC ions generate the product ion at *m/z* 184 (138,214,215). structural features are confirmed in the negative-ion mode as $[M + CH_3COO]^-$ ions.

The induced cleavage of the ester bonds linking alkyl chains to the glycerol moiety of molecular anions yields product ions such as fatty acid carboxylate anions, lyso-PL produced leading neutral loss of a fatty acid residue as a ketene and a lyso-PL-like due to the neutral loss of a free fatty acid (138), providing direct information of the alkyl substituents.

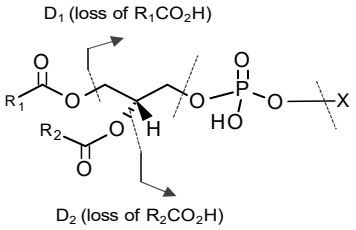

X	Phospholipid	Precursor ion	Neutral loss/product ion (*m/z*)
H	PA	$[M - H]^-$	Product ion *m/z* 153 Product ions R_1COO^-; R_2COO^-
Choline	PC	$[M + H]^+$ $[M - H]^-$	Product ion *m/z* 184 Product ions R_1COO^-; R_2COO^-
Ethanolamine	PE	$[M + H]^+$ $[M - H]^-$	Neutral loss 141 Da Product ions R_1COO^-; R_2COO^-
Glycerol	PG	$[M - H]^-$	Neutral loss 74 Da Product ions R_1COO^-; R_2COO^-
Inositol	PI	$[M - H]^-$	Product ion *m/z* 241 Product ions R_1COO^-; R_2COO^-

Figure I. 9. Schematic fragmentation of glycerophospholipids. The dotted lines indicate the most labile bonds where fragmentation may occur. The table includes the product ions and neutral losses that provide the structural information and allow the identification of PLs classes.

Betaine lipids are seen in MS as the $[M + H]^+$. They can be identified by characteristic product ion at *m/z* 236 that results from the combined loss of the two fatty acyl chains as ketenes (loss of R_1CO+R_2CO) (Fig. I.10) (216) in the classes DGTS, MGTS, DGTA, and MGTA. Betaine lipids can also form adducted ions, such as $[M + Na]^+$ with characteristics fragments resulting from the neutral loss of 87 Da (loss of $-CH_2CH_2N^+(CH_3)_3$), loss of 74

Da (loss of $-CH_2N^+(CH_3)_3$), and a loss of 59 Da representing the loss of trimethylamine - $N(CH_3)_3$.

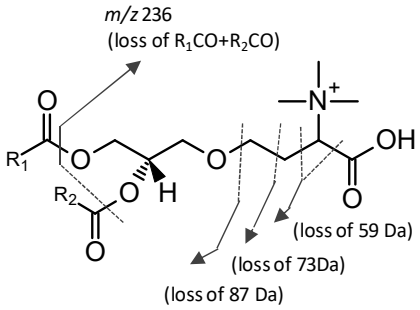

Figure I. 10. Schematic fragmentation of betaine lipids DGTS. Characteristic product ion at *m/z* 236 results from loss of fatty acyl as $[M + H]^+$ or $[M + Na]^+$. Fragmentation of polar head may occur in $[M + Na]^+$ ions: neutral loss of 59 Da (loss of the $-N^+(CH_3)_3$), 73 Da (loss of the - $CH_2N^+(CH_3)_3$), and 87 Da (loss of $-CH_2CH_2N^+(CH_3)_3$).

I.1.3.3. Studies uncovering the lipidome of macroalgae

Mass spectrometry based lipidomic analysis of green, red and brown seaweeds were reported in literature. The aforementioned works scarcely identified polar lipids species considering the diversity expected within polar classes. In fact, some studies reported the identification of only few molecular species (two to ten) while one other account around two hundred different lipid species in seaweeds lipidome. This section describes current state-of-the-art on lipidomics of seaweeds (Table I. 1), and attempts to pinpoint new findings regarding polar lipidome of seaweeds within phylum and taxa.

Lipidomic analysis of Chlorophyta

Lipidomics studies on green macroalgae (Chlorophyta) by using MS-based approach were focused on the lipidome of *Ulva* sp. and *Enteromorpha intestinalis*, presently accepted as *Ulva intestinalis* Linnaeus, 1753 (22,33,164). By using MS-based on target analysis (direct infusion-shotgun lipidomics) of lipid extracts of *Ulva lactuca*. The screening of neutral loss and precursor ions of PLs and GLs allowed the identification of glycolipids MGDG, DGDG and SQDG and the phospholipids PG, LPG, PC, LPC and PI. However, the study reported only the total relative amount of each class of lipid and did not provide the identification at the molecular level (164). The authors also refer to the identification of PA and phosphatidylserine (PS), however they made an incorrect

identification of these classes. PS class was identified in positive ion mode as $[M + H]^+$ with neutral loss of 153 Da and PA as $[M – H]^-$ in negative ion mode with neutral loss of 120 Da. These assignments differ from the detailed fragmentation pattern established for these classes (138,214).

This study also showed the advantage of MS to evaluate the effect of nutrition limitation and environmental stress on the lipid profile. By profiling the distinct classes, it was suggested that the biosynthesis of PLs is dependent on phosphate availability and under P-limitation occurs degradation of PLs to PA or lyso-phospholipids. When limited by nitrogen (nitrate, NO_3-N), or by phosphorus (phosphate, PO_4-P) or both, *U. lactuca* also accumulates DGDG, SQDG and DGTS concomitant with the decrease of the content in PLs. Supplementation of nutrients, especially nitrate, increase the content of MGDG and also of the DGDG/MGDG ratio concomitant with the degradation of PLs.

Non-target lipidomics was used to characterize the lipidome of *Ulva rigida* and *Enteromorpha intestinalis* (33). LC–MS analysis of the lipidome of *Ulva* sp. allowed the identification of up to six molecular species distributed by sulfolipids and PLs such as PC and LPE and two molecular species from sulfolipids, respectively. Amid lipidomics platform, other studies reported the FA composition within each class obtained by GC–MS and suggested that green macroalgae were rich in 16- and 18-carbon PUFAs, namely 16:3(*n*-3) and 18:3(*n*-3) (97,164,217).

Overall, the lipidome of the green macroalgae stills a less studied phylum far from being completely deciphered. Polar lipids vary according intra and inter taxonomy, but are also directly dependent on stress factors that deserve to be explored. The application of advanced MS-based lipidomics and accurate-deep knowledge on the detailed analysis of the high throughput data and structural features of molecular species of green seaweed is actually an emergent and promising field of research of green macroalgae´ lipidome.

Lipidomic analysis of Rhodophyta

The characterization of polar lipidome by target lipidomics and untarget LC–MS approaches was reported on Rhodophyta macroalgae. Methanol/chloroform extracts of *Palmaria palmata* (181), *Chondrus crispus* (218), *Osmundaria obtusiloba* (185), *Chondria armata* (203), and *Asparagopsis taxiformis* (33) were fractioned by using different liquid-liquid extraction protocols and the fractions-rich in glycolipids obtained were further analyzed by MS. Few glycolipids were identified in each study (less than ten species)

distributed by MGDG, DGDG, SQDG, and SQMG classes. After MS-based identification, GLs extracted from some red seaweeds were further screened for bioprospection (218). PLs such as PG, PE, PI, and LPE were assigned in lipidome of some reported red macroalgae (33,181) as shown in the Table I. 1. Based on MS-data and mass accuracy, LC–MS was used to identify metabolites of different life cycle stages of *Porphyra haiatanensis* that included conchocelis, sporangial branchlets and conchosporangia phases (206). Few classes of PLs were identified and molecular species from PC, LPC, and LPE were considered important biomarkers differentiating life cycle phases, showing other important application of MS-based approaches to be explored.

An accurate and complete identification of the profile of *Chondrus crispus* was achieved by LC–MS/MS. Results allowed the identification of 180 molecular species distributed by 19 DGDGs, 32 SQDGs, 14 PAs, 60 PCs, and 18 PGs, including lyso-PC and lyso-PG subclasses, and 14 DGTS lipids species provided by a single extract (145). By using MS–based approaches, several molecular species were for the first time reported in DGTS class. Betaine lipids profile at molecular level was never mentioned before on the lipidome of Rhodophyta and, in macroalgae, its identification was poorly characterized by TLC and GC–MS (36). In the category of sphingolipids, inositol phosphoceramides (IPCs) and hexosyl ceramides (HexCer) were detected in *C. crispus* and were considered a specific marker for Rhodophyta phylum (147). Lipidomic study of *C. crispus* demonstrated the great potential of MS-based approaches profiling detailed molecular species of polar lipids and less abundant classes in complex lipid matrices.

The profile of FA from polar lipids of Rhodophyta have been characterized by GC–MS, and were reported to be 14-, 16-, 18- and 20-carbon of saturated and unsaturated fatty acids (97) with GLs and PLs including eicosapolyenoic acid 20:4(*n*-6) and 20:5(*n*-3) (30,97). Odd numbered fatty acid species and 20-carbons hydroxy-fatty acids were found (36). Overall, the lipidome of red macroalgae was reported generally based on FA profiles but characterization of the full lipidome was poorly explored. Considering the great potential of LC–MS and MS/MS approaches, not only to complete the lipidome signature or differentiating intra and inter Rhodophyta taxonomy, but also attending environmental and stress effects on polar lipids response, there is an open field to research.

Lipidomics analysis of Ochrophyta

In the Ochrophyta phylum, the lipidome of *Fucus spiralis* (27), *Sargassum* spp. (207), *Stypocaulon scoparium* presently accepted as *Halopteris scoparia* (33), *Dictyota dichotoma* (33), *Colpomenia sinuosa* (33), *Cystoseira brachycarpa* (33), *Dilophus fasciola* (22) presently accepted as *Dictyota fasciola* (22) and *Taonia atomaria* (22) were characterized by MS–based approaches, as reported in Table I. 1. Fractionated extracts of *Sargassum* spp. and *Fucus* sp. obtained after chromatographic separation on silica column were further analyzed by LC–MS and a small number of molecular species from MGDG were identified (up to ten), meanwhile SQDGs (six species) was only found in lipidome of *Sargassum* sp. (25,27,207,219). The identification of PLs or betaines were not reported by these authors, because these studies were focused on MS–based approaches to differentiate the regiospecific distribution of fatty acyl species in glycolipids and elucidation about the relation structure/bioactivity of GLs.

LC–MS approach was used to identify the lipidic fraction of *Stypocaulon scoparium* and three molecular species of GLs and seventeen PLs as PG, PC, LPI and LPE, were tentatively identified (33). There are no findings on betaine lipids in brown macroalgae by using MS-based tools. Typical approaches based on TLC and GC–MS analysis reported that betaine lipids such as DGTA were present (97,149). The profile of FA in the lipid extracts, determined by GC-MS, included 14-, 16-, 18- and 20-carbon saturated and unsaturated fatty acids, and included octapolyenoic acids (18:3(*n*-3) and 18:4(*n*-3)) and eicosapolyenoic acid (20:5(*n*-3)) PUFA (97).

Deep knowledge is needed to full assign the lipidome of Ochrophyta, to understand metabolic biosynthetic pathways of polar lipids, namely of betaine lipids present in the lipidome, as well as to evaluate environmental stress. To decipher brown macroalgae´s lipidome is an open field regarding the role of polar lipids for taxonomic differentiation and bioprospection.

I.1.4. Biological properties of polar lipids

Based on Asian diets, the intake of macroalgae seems to contribute to a lower incidence of cancer, namely lower occurrence of breast cancer, and relative longevity and low incidence of cardiovascular diseases of the populations. This supports the functional and nutraceutical concept of algae in nutrition to provides beneficial effects on human health

all over the world (3,13,28,220). Thus, many studies have been done about naturally-occurring phytochemicals in macroalgae that were reported as being beneficial for human health and with potential to replace those used in therapeutics for which are many resistances (5,13). Amid are lipids, metabolites produced for a myriad of functions such as UV protection, protection against pathogens, improvement of plant survivability, and bioactivities such as antioxidant, anti-inflammatory, and antimicrobial, among others, (3,35,221). Beneficial effects have been reported recently to dietary polar lipids, namely GLs and PLs from macroalgae (28,32,132,222).

Table I. 2. Polar lipids from macroalgae and their potential biological activities

Species Name	Lipid Class	Inhibitory effects	Ref.
Antitumoral			
Ulva fasciata	SQDG	MCF-7 and HepG2 cells	(127)
Ulva armoricana	DGDG	NSCLC-N6 CELLS	(205)
Galaxoura cylindriea	SQDG	MCF-7 and HepG2 cells	(127)
Porphyra crispata	SQDG	HepG2	(132)
Solieria chordalis	MGDG	NSCLC-N6 CELLS	(205)
Dilophys fasciola	SQDG	MCF-7 and HepG2 cells	(127)
Sargassum horneri	SQDG, DGDG	Caco-2 cell	(223)
Anti-inflammatory			
Chondrus crispus	MGDG, DGDG	Production of NO via iNOS	(30)
Chondrus crispus *Palmaria palmata* *Porphyra dioica*	GLs	Dowregulation of cytokine IL-6 and IL-8	(224)
Palmaria palmata	SQDG, PG	Production of NO via iNOS	(181)
Fucus spiralis	MGDG	Production of NO via iNOS	(27)
Antimicrobial/antiviral*/antifungal**			
Ulva fasciata	SQDG	*B. subtilis* and *E. coli*	(127)
Chondria armata	MGDG	*Klebsiella* sp /*C. albicans*	(203)
Galaxoura cylindriea	SQDG	*B. subtilis* and *E. coli*)	(127)
Osmundaria obtusiloba	SQDG	HSV-1 and HSV-2*	(202)
Dilophys fasciola	SQDG	*B. subtilis* and *E. coli*	(127)
Sargassum thumbergii	MGDG	*Candida albicans***	(204)
Sargassum wightii	SQDG	*X. oryzae* pv.	(225)
Taonia atomaria	SQDG	*B. subtilis* and *E. coli*	(127)

Novel works emerged on the study of the properties related with these polar lipids extracted from macroalgae (21,26,27,116,127,202), from halophytes (132) and microalgae (137), among other natural sources (25).

Hypothesis about structure and biological activities of total lipid extracts or fractionated-extracts from the macroalgae have been suggested (127,202,204,225) (Table I.2). Structural information obtained by MS-based approaches to identify target molecules from isolate extracts of marine macroalgae and evaluate their bioactive properties seems promising tool in the bioprospection of the polar lipidome (21,207,226).

In the following section, it will be reported the current knowledge that has been gathered so far for the antioxidant, anti-inflammatory, antitumoral, and antimicrobial activities from macroalgae.

I.1.4.1. Antioxidant properties

Oxidative stress has been associated with several diseases such as atherosclerosis, diabetes, neurodegenerative diseases, chemical carcinogenesis, intoxication with certain xenobiotics, and aging (4,35). Oxidative stress is currently defined as the discrepancy that occurs between pro-oxidant reactions, which produce free radicals, and antioxidant mechanisms, which inactivate free radicals (227). This imbalance can be caused by increased production of free radicals, so one way to counter the process is through supplying antioxidant substances.

Free radicals are defined as molecules with an odd or unpaired electron in the external orbital of their atomic structures. They are very important due to their redox characteristic and interfere directly with oxidation-reduction reactions in cellular processes by reacting aggressively with other biomolecules to produce highly reactive species within cells (221,227). Reactive oxygen species (ROS) include peroxyl radical ($RCOO^{\cdot}$), superoxide anion (O_2^{-}), hydrogen peroxide (H_2O_2), singlet oxygen ($^1O_2$), hydroxyl radical ($HO^{\cdot}$), and peroxynitrite ($ONOO^{-}$) (228).

Lipid extracts from marine macroalgae are considered a source of natural antioxidants (109,229) and were mainly attributed to PUFAs (74,96,230). However, since FA from macroalgae are mainly assembled to polar lipid structures, macroalgae polar lipids deserve to be investigated as a potential source of natural antioxidants (231). Regarding macroalgae, antioxidant activity of polar lipids from macroalgae has been barely investigated. However, the fractionated lipidic extract of the microalgae *Porphyridium cruentum* showed antioxidant activity of polar lipids by the strongly inhibition of the production of superoxide anion generated by peritoneal leukocytes primed with phorbol

myristate acetate (232). Thus, supported by the antioxidant properties related to the SQDG isolated from microalgae and the known antioxidant properties attributed to PUFAs, the potential of polar lipids as antioxidants was scarcely addressed and deserves to be explored.

I.1.4.2. Anti-inflammatory properties

Inflammation is the response of vascular tissues to harmful stimuli such as injury, pathogens or irritants, and reactive species are produced. In long term, exaggerated misdirected response adversely affect health such in the case of inflammatory bowel disease, arthritis, or asthma (137). Chronic and acute inflammation is a complex biological process mediated by the activation of immune cells such as neutrophils, eosinophils, mononuclear phagocytes and macrophages (13). Under inflammatory conditions, cytokines and enzymes induce cell and tissue damage and activate cells involved in several chronic diseases as hepatitis, atherosclerosis and rheumatoid arthritis (233).

The inflammation process is controlled by a group of substances called chemical mediators that consist of vasoactive amines, cytokines, bradikinin, fibrin, eicosanoids, platelet activating factor (PAF), nitric oxide (NO) and neuropeptides (12,234). Eicosanoids, reactive oxygen species (ROS) and nitrogen radicals play a crucial role in every step of inflammation. Nitric oxide (NO) is an important signaling molecule that, in many tissues, regulates a diverse range of physiological processes (235). NO is highly permeable and diffuses rapidly across membranes. In inflammatory responses, NO can modulate the release of a wide range of anti-inflammatory modulators, enzymes activity, blood flow and adhesion of leucocytes to the vascular endothelium (12,234). Under pathological conditions undesirable effects can result from the overproduction of NO such as vasodilatation, inflammation, and tissue damage. NO is produced through its precursor, L-arginine, by the action of the specific enzyme NOS like the inducible nitric oxide synthase (iNOS). This isoform is typically synthesized in response to inflammatory or pro-inflammatory mediators, such as cytokines or endotoxins (e.g., bacteria products) (234).

Excessive production of NO is involved in tissue damage, septic shock, organ dysfunction, and carcinogenesis processes (27). Effective inhibition of NO accumulation represents a beneficial therapeutic strategy for the treatment of NO-mediated disorders (235). Macrophages are a major component of the mononuclear phagocyte system and play

a critical role in initiation, maintenance and resolution of inflammation and usually start the production of NO, for example, when exposed to bacterial LPS (235).

There is an enormous demand for new and potent anti-inflammatory drugs in view of the fact that inflammation triggers a multitude of human diseases and macroalgae constitute an endless source of bioactive secondary metabolites such as lipids with promising effects for human health (28,181). In this context, some works were published and suggested that lipids extracted from macroalgae have anti-inflammatory activity (Table I. 2). Lopes *et al*, 2014 were able to isolate two species of MGDG from *Fucus spiralis* lipids, MGDG (20:5/18:3) and MGDG (20:5/18:3), that expressed the capacity to reduce NO release in a dose-dependent manner (27). Banskota et al. (30) evaluated the anti-inflammatory activity of isolated fractions of extracts-rich in galactolipids from *Chondrus crispus,* that exhibit inhibitory activity against lipopolysaccharide (LPS)- inducible nitric oxide synthase (iNOS) production in murine RAW264.7 cells. The molecular species identified include MGDG (20:5/20:5), MGDG (20:5/20:4), MGDG (18:4/16:0) and MGMG 20:4. The extract also contained MGDG (20:4/16:0) and MGDG (20:5/16:0) and DGDG analogues. Some authors evaluated the fraction isolated from the methanolic extract of *Palmaria palmata* (181), rich in SQDG (20:5/14:0), PG (20:5/16:0), and PG (20:5/16:1), that showed suppression effect on NO production through down-regulation of iNOS. Underlying anti-inflammatory activity of glycolipids, they are considered as novel anti-inflammatory agents potentially useful for human pathologies related to inflammation (137). However, a better understanding of lipids structures and correspondent action on the treatment of inflammatory diseases still represents a scientific challenge for further advances in the resolution of pathologies (220).

I.1.4.3. Antitumoral activity

Cancer incidences is increasing and, therefore, effective therapies are needed to control these malignant diseases (236). Cancer is the most common and serious disease, and there are six properties that make cells capable of cancerous growth; they are not under the control of signals that regulate cell proliferation, they are resistant to apoptosis, they overcome the limitations on proliferation by avoiding replicative senescence and evading differentiation, they are genetically unstable, are able to invade surrounding tissues and are capable of metastasis. The cancerous tumor develops when cancer cells overcome

replicative cell senescence and become "immortalized" *i.e*. continue dividing indefinitely (237).

Chemotherapy is usually the first line treatment to cure cancers and a group of drugs are used to kill or inhibit the growth of cancer cells (238). Many side effects are related to chemotherapeutic drugs and comprise baldness, vomiting, diarrhea, loss of appetite, nausea and fatigue, consequently new anticancer agents should be investigated from various resources (239). Thus, alternative to chemotherapy drugs and side effects, the research in anticancer activities of non-toxic biological macromolecules seems a solution to this pitfall (236,238).

Marine algae are considered a potential source of natural bioactive substances and efforts have been done towards the identification of compounds with antiproliferative effects (236,237,240,241). The antitumor effect of lipids is usually expressed in function of the fatty acyl profile due to limitations on the isolation of polar lipids and their characterization (67,97). PUFA have been considered biologically active compounds and, in macroalgae, are abundant components of glycolipids (97). Some researchers are now focusing on the antitumoral and the immunosuppressive effect of macroalgae polar lipid extracts on distinct cell lines of cancer (Table I. 2) (127,132). Among polar lipids, sulfolipids have been suggested to prevent human cancer diseases (132). Sulfonoquinovosyl acyl glycerols, particular those combining PUFAs, were suggested to be clinically promising agents (127). An extracted fraction-rich in sulfolipids was separated from the glycolipidic fraction of *P. crispata* containing MGDG, DGDG, and SQDG glycolipids (132). Isolated SQDGs inhibit the grow of human hepatocellular carcinoma cell line (HepG2) due to its high proportion of PUFAs and its *n*-3/*n*-6 ratio in addition to its sulfolipid structure and content (132). Aside from the essential sulfate moiety of SQDG, eicosapolyenoic moieties seemed to be more critical against the carcinoma. SQDGs and DGDGs from *Sargassum horneri* were found to induce apoptosis of the human colon carcinoma Caco-2 cell (223).

Therefore, it has been hypothesized that not only fatty acids but also the polar head may be responsible for biological activities highlighted from glycolipids (127). On general point of view, the bioactivities of glycoglycerolipids seems to be related to the sugar moiety, the position of the glycerol linkage to the sugar, the length and location of the acyl chain, and the anomeric configuration of the sugar (241). Biological activity from SQDGs is

suggested to be due to the presence of the unsaturated fatty acids and sulfonate moieties (127), meanwhile the antiviral and antitumor activities may be more related to the presence of the sulfonate group (25). It is noteworthy that the distribution of PUFAs in glycolipids from seaweeds depends on their taxonomic position, and on seasonality, among others factors, it may then be logical to expect some taxa to be more active than others (19,120).

Phospholipids showed *in vitro* anticancer activity against breast (MCF-7) and liver human (HepG2) cancer cells and were attributed to PG class (116). Algal phospholipids of *D. fasciola, L. papillose* and *G. cylindriea* presented high inhibition of MCF-7 cell line growth. The antitumor activity of phospholipids was suggested to be related to not only PUFA but to phosphorus contents. So far, the characterization of PLs structure evolving fatty acyl and polar head composition, the activity associated with PLs as well as metabolic pathways related were not well explored.

I.1.4.4. Antimicrobial activity

Mainstream medicine is increasingly receptive to the use of antibacterial and other drugs derived from plants and algae, since traditional antibiotics (products of microorganisms or their synthesized derivatives) become ineffective and new diseases remain intractable to this type of drug (228). Secondary metabolites with potential antimicrobial activity in seaweeds have been attributed to a wide range of compounds including fatty acids, halogenated compounds, sulfur-containing heterocyclic compounds and phlorotannin (242). The functions attributed to macroalgae metabolites included defense against herbivores, fouling organisms and pathogens in addition to protection from UV radiation and allelopathic agents (12,94).

Within bacteria there are two main domains, the Gram positive (Gram+) and the Gram negative (Gram-), containing a thin peptidoglucan cell wall only surrounded by a second layer of LPS and proteins, respectively, inferring Gram- to be more toxic than Gram+ (102,243). The use of antibacterial agents (antibiotics), usually small molecules, will interfere with the normal life of bacteria without damaging human cells. Lipid-soluble extracts from marine macroalgae have been investigated as a source of substances with antibacterial activity showing antibacterial activity against Gram+ and Gram- pathogenic strains. Some extracts-rich in glycolipids and phospholipids, namely from Ochrophyta, exhibit antimicrobial activity (231). The brown macroalgae *Sargassum wightii* was found

to contain SQMGs featuring C_{16} fatty acids with antimicrobial properties, useful in the inhibition of the growth of the bacterium *Xanthomonas oryzae pv. Oryzae*, which causes bacterial blight of rice (225). Baz et al. also suggested that sulfolipids from Rhodophyta *(Laurencia popillose, Galaxoura cylindrie*a); Chlorophyta *(Ulva fasciata*), and Ochrophyta *(Dilophys fasciola, Taonia atomaria*) from Mediterranean macroalgae had antimicrobial activity (127). Thus, sulfolipids from macroalgae are potential sources of natural antibiotics to be explored. Recently, a great deal of interest has been expressed regarding polar lipids from macroalgae as potential antiviral compounds. SQDG from the red macroalgae *Osmundaria obtusiloba* and from brown macroalgae *Sargassum vulgare* exhibited potent anti-HSV-1 and HSV-2 activities (25,202).

Phospholipids as PG from different macrophytes display antiviral activity of simplex virus type 1 (116). *U. fasciata* and *L. papillose* phospholipids inhibit virus replication and adsorption of virus on host cells. The antivirus activities of phospholipids seem to be related to unsaturated fatty acid and phosphorus contents. So far, the characterization of PLs structure evolving fatty acyl and polar head composition, the activity associated with PLs as well as metabolic pathways was not much developed.

Due to their biological activities as anti-inflammatory, antibacterial, and anti-tumor promoters, marine algae have notably a great potential to be used in food and pharmaceutical products (5,19,26). In the future, polar lipids from macroalgae will certainly be part of the target bioactive compound to explore for drug discovery, and marine algae incorporation as functional food may provide a natural source of health promoting benefits against disease.

I.2. Aims of the work

The polar lipidome from macroalgae comprise a plethora of complex lipids with potential biological properties that is far away from being fully elucidated, preventing the discovery of the full potential of macroalgae as a functional food and as a source of bioactive compounds. Thus, the main aim of this Ph.D. work is to give some insights in this field and contribute to the elucidation of the composition in polar lipids of macroalgae native to the Portuguese coast but produced under semi controlled conditions in a land-based IMTA system, by using mass spectrometry (MS)-based analytical strategies. On the

basis of the current knowledge, it can be stated that the complete identification of polar lipids is hampered by their diversity and the structural complexity of the structures formed.

The variability in the chemical composition of macroalgae, aside from the species, may be the result of its developmental stage, geographical location, habitat, season and associated water quality (inorganic nutrients, salinity). The use of macroalgae cultivated under semi controlled conditions under the IMTA concept presents a sustainable solution to this pitfall, guaranteeing abundance and replicability issues of targeted biomass. Thus, in this Ph.D. work it is aimed *to enhance the high value of macroalgae produced in land-based IMTA by means of their polar lipidome as well as to enhance their biological activities, supported by powerful lipidomic approaches and new analytical strategies.*

Having this in mind, the main goals of this Ph.D. were:

- Characterize the lipid signature of the selected edible macroalgae, representative of each phylum, namely *Codium tomentosum* (Chlorophyta), *Gracilaria* sp. and *Porphyra dioica* (two distinct phases of life cycle) Rhodophyta) and *Fucus vesiculosus* (two different seasons of the year, Ochrophyta). The identification of the lipidomic signature was accomplished by MS-based strategies, and edible macroalgae were produced in a land-based IMTA system (ALGAplus Lda., Portugal).

- Evaluate the biological activities of polar lipids from macroalgae extracts attending the antitumor and anti-inflammatory properties fostering potential applications of macroalgae in cosmetic, nutraceutical and functional food industries, and encourage the optimization of the production of high-value macroalgae in IMTA system. The biological activity of specific lipid classes fractionated from the total lipid extract (glycolipids) were tested.

This work was developed by using MS-facilities in the Mass Spectrometry Centre from QOPNA Research unit (Chemistry Department, Aveiro University). The evaluation of biological properties of lipid extracts were performed in collaboration with the Biology Department of Aveiro University - Institute for Research in Biomedicine (iBiMED) and Center for Neuroscience and Cell biology (CNC), University of Coimbra. All the macroalgae biomass, as well as associated informations, was produced and kindly given by the company ALGAplus, Produção e Comercialização de Algas e seus derivados Lda.

CHAPTER II

MATERIALS AND METHODS

II. Materials and methods

II.1. Macroalgae material

II.2. Total lipid extraction

II.3. Thin-layer chromatography (TLC)

II.4. Solid Phase extraction (SPE)

II.5. Extraction and quantification of pigments

II.6. Quantification of glycolipids

II.7. Quantification of phospholipids

II.8. Fatty acid methyl esters (FAMEs) analysis by gas chromatography–mass spectrometry (GC–MS)

II.9. Mass spectrometry and hyphenated approaches

II.10. Evaluation of the biological activity

II.11. Statistical Analysis

II.12. Nutritional Indexes

II.3. Standards and Reagents

Materials and methods

The polar lipids were extracted from the selected species *Codium tomentosum*, *Gracilaria* sp., *Porphyra dioica* and *Fucus vesiculosus*. These macroalgae are edible macroalgae (WHO - FAO) (59,244,245) cultivated on open land based IMTA system using nutrient-rich water from sea-bass and sea-bream ponds at ALGAplus Lda. facilities. Total lipids were obtained by using conventional protocols of extraction that were further characterized by HILIC–LC–MS and MS/MS. The anti-inflammatory, antioxidant and antiproliferative effects of the extract of *Gracilaria* sp. were evaluated. Partial lipid extract (glycolipids-rich fractions) of *Gracilaria* sp. were obtained, characterized, and antiproliferative effect of the fraction-rich in glycolipids was tested. Figure II.1 represents the schematic workflow designed to achieve the goals of the Ph.D. plan.

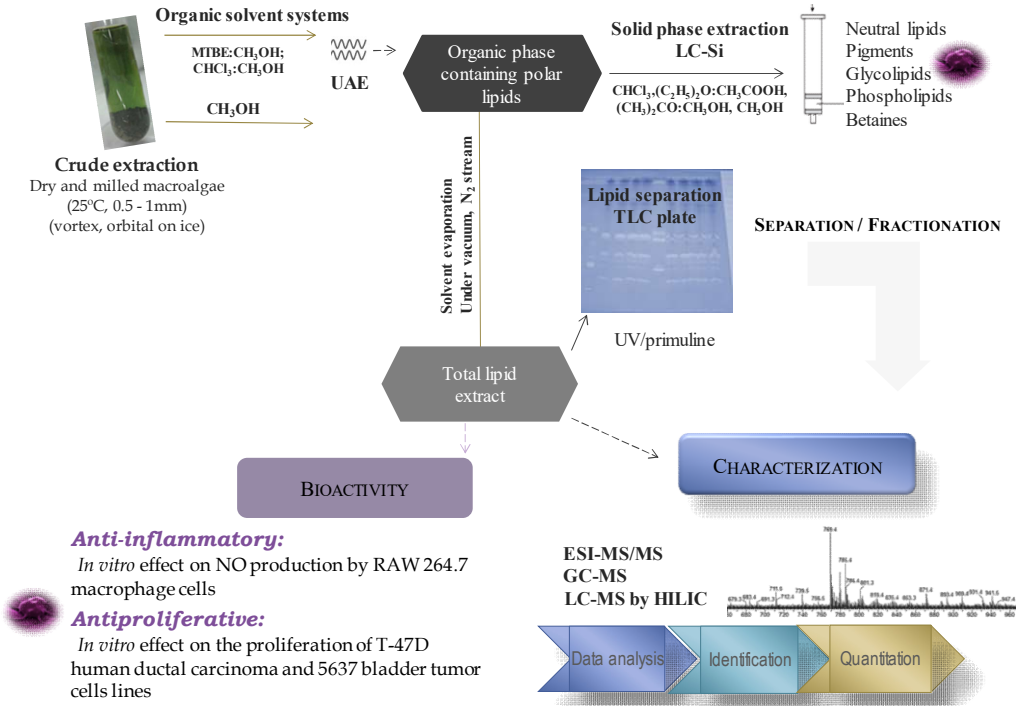

Figure II. 1. Schematic representation of the workflow that include extraction of total lipids extract (crude extract) and identification polar lipids from macroalgae. Lipids from *Gracilaria* sp. were isolated from the total extract by SPE (solid phase extraction). ESI-electrospray ionization, MS-mass spectrometry, HILIC- hydrophilic interaction liquid chromatography, MS-mass spectrometry, UV-ultraviolet, LC-liquid chromatography, GC-gas chromatography, Si-silica, TLC-thin layer chromatography, MTBE-Methyl-tert-butyl ether, UAE-ultrasound assisted extraction.

II.1. Macroalgae material

Dried samples (25 °C, up to 12% moisture content) of cultivated macroalgae were provided by ALGAplus Ltd. (production site in Ria de Aveiro, mainland Portugal, 40°36′43″N, 8°40′43″W). The biomass was produced in tanks by clonal propagation (asexual reproduction strategy) and with lower variability in terms of chemical quality than would be expected from wild harvested biomass. Production factors as stocking densities and water renewal rates were controlled in order to maintain the lowest level of variation in abiotic factors as temperature, salinity, as well as availability of light and inorganic nutrients.

The samples of macroalgae were representative of the bulk in production. Still at ALGAplus Lda, macroalgae were cleaned in filtered seawater, and dried at low temperature (25ºC) in an air tunnel, until reaching 10 – 12% total moisture. Dried material was milled into 0.5 – 1 mm flakes. *Codium tomentosum* was collected in June 2012, *Gracilaria* sp. (G1.3214M) was collected in August 2014 (*G. gracilis* or *G. vermiculophylla*, identification pending confirmation by DNA barcode analysis). ALGAplus is a successful pioneer in the cultivation of *Porphyra dioica*. Gametophyte stage of *Porphyra dioica* (blades) was cultivated on outdoor IMTA tanks (1000L) at ALGAplus under stable conditions of pH, temperature, and salinity. Blade samples were collected on 6th March of 2014 (P1.1014). During the period of cultivation (up to 3 weeks), IMTA guaranteed production of seaweed under controlled conditions of water renewal, pH (8.0 – 8.2), salinity (average salinity 22.1 PSU (Practical Salinity Units), and temperature (13.8 ± 0.93ºC). The conchocelis phase of *P. dioica* was collected in November 2015 (P1.00.10.4.151103). This sample was cultivated indoor nursery of ALGAplus Lda, under vegetative mode (at 15ºC, irradiance of 25 - 30 µmol photons m^2 s^{-1} and long day growth (16:8 h light-dark conditions) from June 2014 till November 2015. The biomass was dried at 25 °C up to 12% moisture content, and about 250 mg were used to extract lipids. *Fucus vesiculosus* is harvested within the margins of the fish ponds and the exit channels of the aquaculture site. Before processing for food, the seaweed biomass is maintained in tanks with controlled conditions for 1 to 2 weeks. *Fucus vesiculosus* samples were collected in February 2016 representing the mid-winter - F1.0716M, and in the end of May 2016, representing end-spring season - F1.2116D. Mid-winter *Fucus* was maintained at 13.2 ± 1.17ºC, average salinity 27.0 PSU, and an average irradiance of 177 µmol photons m^2 s^{-1};

end-spring macroalgae was cultivated at 17.4 ± 1.36ºC, average salinity of 27.5 PSU, and average irradiance of 424 µmol photons m^2 s^{-1}. The samples were stored at -20 ºC prior to extraction. The extraction of lipids is detailed in section II.2.

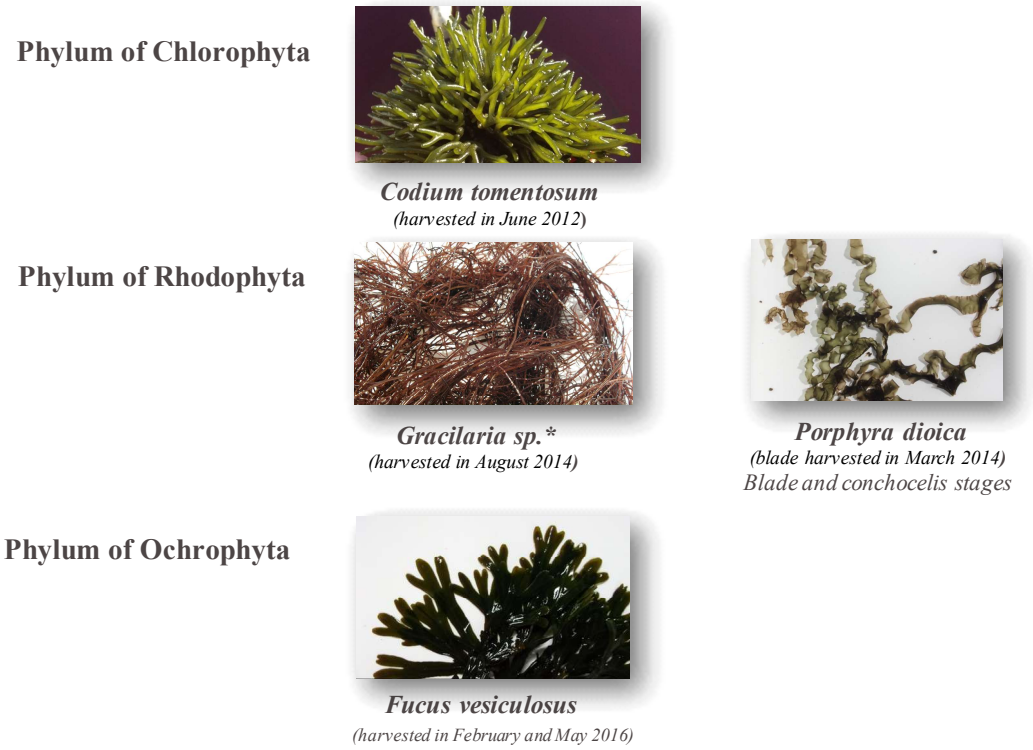

Figure II. 2. Macroalgae species targeted on this Ph.D., produced in a land-based IMTA system. **Gracilaria* sp. corresponds either to *G.vermiculophylla or gracilis,* currently pending on DNA results

II.2. Total lipid extraction

Total lipid extraction was performed by using conventional solvent extraction protocols (CSE) (105,246–248). In the literature, the Bligh and Dyer protocol for extraction is currently used to extract total lipid from macroalgae (34,249). Methanol/methyl-*tert*-butyl ether (MTBE) were used to extract lipids from different type of samples (30,145,184). However, MTBE extraction requires large volume of solvent and are required time and energy to evaporate the solvent. In this Ph.D. work total lipid extracts of macroalgae biomass was performed by using distinct adapted methods from CSE as follows:

Method 1. Methanol extraction

The macroalgae *Codium tomentosum* material (500 mg) was homogenized with liquid nitrogen in a glass mortar and mixed with 20 mL of MeOH (25 mg of biomass/mL of

MeOH) by vortexing 15 s and then incubated on an orbital shaker for 1 h. The MeOH lipid extract was obtained after centrifugation (Mixtasel Centrifuge, JP Selecta, Spain) for 10 min at 1500 rpm.

Method 2. Methanol/Methyl *tert*-butyl ether (MeOH/MTBE) extraction
250 milligrams *Codium tomentosum* biomass was weighed and a mixture of MeOH/MTBE (3:7, v/v) was added, soaking the sample to homogenize it as much as possible and further transferred to a glass PYREX tube, homogenized by vortexing 15 s and then incubated on an orbital shaker for 1 h. Then, 2 mL of milli-Q water are added to induce phase separation followed by centrifugation during 10 min at 1500 rpm, collecting the organic (upper) phase to a new tube. The aqueous (lower) phase was re-extracted with 2 mL of solvent mixture (MeOH/MTBE/H_2O) (10:3:2.5 per volume), repeating the previous steps, collecting the upper phase back into the tube, thus combining the two organic phases extracted.

Method 3. Methanol/Chloroform extraction
A mixture of methanol/chloroform (1:2, per volume) was added to 250 mg of macroalgae (*Codium tomentosum*, *Gracilaria* sp., *Porphyra dioica* (blade and conchocelis) and *Fucus vesiculosus*). The mixture was transferred to a glass tube with a Teflon-lined screw cap and, after addition of 3.75 mL of a mixture methanol/chloroform (2:1, per volume), was homogenized by vortexing 2 min plus one minute in ultrasonics bath (Selecta, Spain) and then incubated in ice on an orbital shaker (STR6 Stuart, UK) during 2h30. The mixture was centrifuged at 2000 rpm for 10 min and organic phase was collected. The biomass residue is re-extracted twice with 1.5 mL of the mixture and 2.3 mL of water are added to the total collected organic phase to induce phase separation, followed by centrifugation for 10 min at 2000 rpm, collecting the organic (lower) phase to a new tube.

Three independent replicates were performed to extract macroalgae. The extractions and analyses were performed on different days. Solvents were evaporated under a stream of nitrogen gas and under vacuum (i.e., methanol extract) and. The total lipid content was estimated by gravimetry. Lipid extracts were stored at -20 °C prior to analysis by LC–MS. Lipid extracts were analyzed by HILIC–LC–MS and MS/MS, as will be described. The polar lipids of *Codium tomentosum* were separated from pigments by thin layer chromatography (TLC) and polar lipids were fractionated from *Gracilaria* by using solid phase extraction (SPE) followed by LC–MS analysis and structural identification.

II.3. Thin-layer chromatography (TLC)

TLC is a method routinely used in the separation and isolation of lipid extracts (170,250). This method was widely used to separate the polar lipid classes from algae followed by MS-based instrumental approaches (30,97,100,150,207).

In this work, chlorophyll and other pigments were separated from the polar lipids by TLC using silica gel plates. Prior to separation, the plates were washed with chloroform/MeOH (1:1, per volume) and activated (sprayed or impregnated) with 2.3% boric acid in ethanol and placed in an oven at 100 ºC for 15 min. Plates with spots containing 20 µg of total lipid extract were eluted in a solvent mixture of chloroform/ethanol/water/triethylamine (30:35:7:35, per volume). Spots corresponding to polar lipids were visualized with a UV lamp (254 and 366 nm; Camag, Germany) after exposing the plates to primuline (50 mg in 100 mL of acetone/water, 80:20, per volume), are scrapped off from the silica and gathered for further extraction (251). The extraction of total polar lipids from silica was made by using chloroform/MeOH (2:1, per volume) and the identification of polar lipids is obtained by mass spectrometry.

II.4. Solid Phase extraction (SPE)

Solid phase extraction is one of the most powerful techniques available for rapid and selective sample preparation (252–258). The most widely cited SPE packing for simple separation of glycolipids, phospholipids and neutral lipids are silica packing columns (38,100,117,259,260). In this work, total lipid extract of *Gracilaria* sp. was fractionated in distinct lipid-rich fractions by solid phase extraction in SUPELCLEAN™ LC-SI SPE Tube, bed wt. 500 mg, volume 3mL cartridges (SUPELCO). Fractionation of total lipid extract was performed using a modification of Pacetti´s method [61]. A sample of lipid extract (1 mg) was dissolved in 300 µL of chloroform and transferred to a Supelclean™ LC-Si SPE Tube (bed wt. 500 mg, volume 3 mL cartridges; SUPELCO, Sigma-Aldrich, St Louis, MO, USA), followed by sequential elution with 4 mL of chloroform, 3 mL of ether diethyl ether/acetic acid (98:2, per volume), 5 mL of acetone/methanol (9:1 per volume), and 4 mL of methanol. Fractions 3 and 4, rich in glycolipids and in phospholipids plus betaines, respectively, were recovered, separated, dried under nitrogen, and stored at –20 °C prior to analysis by ESI–MS. Fractions 1 and 2, corresponding to neutral lipids and pigments, were discarded after the analysis by ESI–MS.

The content in phospholipids and glycolipids was determined by using colorimetric methods. Fraction-rich in glycolipids was used to evaluate antiproliferative effect.

II.5. Extraction and quantification of pigments

The macroalgae *Gracilaria* sp. (50 mg) was extracted with methanol (1.5 mL) (three independent replicates), homogenized by vortexing 2 min and then incubated on ice in an orbital shaker for 2h30. The mixture was centrifugated at 2000 rpm for 10 min and organic phase was collected. The extracts obtained were immediately analyzed in a UV/visible light spectrometer between 400 nm and 700 nm (Multiskan GO, Thermo Scientific, Hudson, NH, USA). The absorbance values at 666, 653 and 470 nm in methanol extract were used to calculate, respectively, the levels of Chl a and total carotenoids according to the corresponding equation, according with Lichtenthaler & Wellburn (1983) (261–263).

II.6. Quantification of glycolipids

Glycolipids were estimated by using a modified colorimetric method of resorcinol, determining the concentration of the total sugars in the lipid extract (CyberLipids, (264)). This method determines both reducing and non-reducing sugars due to the presence of strongly oxidizing sulfuric acid. Sugars react with the resorcinol reagent under acidic conditions and its absorbance is measured at 505 nm.

Dry lipid extracts were heated at 80 °C for 20 min with 2 mL of a solution of resorcinol (5-methylresorcinol (Sigma-Aldrich), 2 mg/mL of 70% sulfuric acid, per volume). After cooling, the absorbance of the solution was measured at 505 nm (Multiskan GO, Thermo Scientific, Hudson, NH, USA). A blank sample was analyzed simultaneously. The amount of sugar was obtained by using the calibration curve of glucose after reaction under acidic conditions (stock solution 5 mg/mL of sugar). The factor 100/35 was chosen to convert hexoses to GL (265).

II.7. Quantification of phospholipids

Quantification of phospholipids in the total lipid extract of macroalgae were assessed by a molybdovanadate method for the simultaneous assay of orthophosphate and organic phosphates, as described by Bartlett and Lewis (266).

Concentrated perchloric acid (125 µL, 70% m/v) was added to the samples in acid-washed glass tubes and the mixture is incubated for 60 min at 170 ºC in a heating block (Block Heater SBH200D/3, StuartW, Bibby Scientific Ltd., Stone, UK). After incubation, 825 µL of water, 125 µL of 2.5% of ammonium molybdate and 10% of ascorbic acid were added. The reaction mixture was well homogenized in a vortex mixer after each addition and incubated for 10 min at 100 ºC in a water bath (Precisterm, JP Selecta S.A.). Standards from 0.1 to 2 µg of phosphate (standard solution of $NaH_2PO_4.2H_2O$, 100 µg P/mL) underwent the same treatment as the samples. Finally, the absorbance of the standards and samples was measured at 797 nm, at room temperature, in a microplate UV–Vis spectrophotometer (Multiskan GO, Thermo Scientific, Hudson, NH, USA) with PL being calculated as P x 25 (265).

II.8. Fatty acid methyl esters (FAMEs) analysis by gas chromatography–mass spectrometry (GC–MS)

The analysis by gas chromatography has been used as a rapid and sensitive method of analysis to identify the lipids composition in FA of macroalgae, as was recently demonstrated, for example, to *Chondrus crispus*, *Ulva* sp. *Laminaria* sp., *Sargassum* sp., *Zostera* sp. (30,97,203,267,268). To obtain the profile of the FA they can be derivatized to fatty acid methyl esters (FAMEs) by alkaline hydrolysis and direct transesterification further analyzed by GC or GC–MS (97,269,270).

In this work, FAMEs were prepared by using 30 µg of total lipid extracts and a methanolic solution of potassium hydroxide (2.0 M) to perform the derivatization, according to the methodology previously described (145). The FAMEs recovered were dried using a nitrogen flow. Volumes of 2.0 µL of the hexane solution containing FAMEs were analyzed by gas chromatography–mass spectrometry (GC–MS) on an Agilent Technologies 6890 N Network (Santa Clara, CA) equipped with a DB–FFAP column with the following specifications: 30 m long x 0.32 mm internal diameter x 0.25 µm film thickness (123-3232, J&W Scientific, Folsom, CA). The GC equipment was connected to an Agilent 5973 Network Mass Selective Detector operating with an electron impact mode at 70 eV and scanning the range *m/z* 40 – 500 in a 1 s cycle in a full scan mode acquisition. The oven temperature was programmed as follows: (1) the initial temperature was set up to 80 ºC for 3 min; (2) a linear increase to 160 ºC at 25 ºC/min; (3) a linear increase at 2

ºC/min to 210 ºC; and (4) a linear increase at 30 ºC/min to 250 ºC followed by 10 min at this temperature. The injector and detector temperatures were 220 and 280 °C, respectively. Helium was used as carrier gas at a flow rate of 1.7 mL min^{-1}.

The injector and detector temperatures were 220 and 280 °C, respectively. Helium was used as the carrier gas at a flow rate of 0.5 mL/min. At least, three replicates were performed. Internal standard methyl heptadecanoate ≥ 99% from Sigma (USA) was used. The identification of each FA was performed by mass spectrum comparison with those in the Wiley 275 library and confirmed by its interpretation and comparison with the literature (AOCS Lipid Library). The relative amounts of FAs were calculated by the percent area method with proper normalization, considering the sum of all areas of the identified FAs.

II.9. Mass spectrometry and hyphenated approaches

Hydrophilic interaction liquid chromatography–ESI–mass spectrometry based (LC–MS) in a linear ion trap (LIT)

In this work, hydrophilic interaction liquid chromatography analysis of total lipid extracts was performed on a Waters Alliance 2690 HPLC system (Waters Corp., Milford, MA, USA) coupled to a Finnigan LXQ electrospray LIT spectrometer (Thermo Fisher, San Jose, CA, USA). Mobile phase A consisted of 25% water, 50% acetonitrile and 25% MeOH, with 10 mM ammonium acetate, and mobile phase B consisted of 60% acetonitrile and 40% MeOH with 10 mM ammonium acetate. The lipid extracts (12.5 µg) was diluted in mobile phase B (90 µL) and 10 µL of the reaction mixture is introduced into an Ascentis Si HPLC Pore column (15 cm x 1.0 mm, 3 µm; Sigma-Aldrich). The solvent gradient was programmed as follows: gradient started with 0% of A and 100% of B, linearly increased to 100% of A in 20 min, and isocratically held for 35 min, returning to the initial conditions in 5 min. The flow rate through the column was 7.5 µL min^{-1} obtained using a pre-column split (Accurate, LC Packings, San Francisco, CA, USA). Polar lipid analysis is carried out by negative- and positive-ion electrospray ionization mass spectrometry (ESI-MS). The electrospray voltage was 4.7 kV in the negative-ion mode and 5.0 in the positive-ion mode. The capillary temperature was 275 °C, and the sheath gas (He) flow rate was 25 units. A precursor ion isolation width of 0.5 *m/z* units was used, with a 30 ms activation time for MS/MS experiments. Full scan MS spectra and MS/MS spectra were acquired

with a maximum ionization time of 50 ms and 200 ms, respectively. The normalized collision energy (CE) varied between 17 and 20 (arbitrary units) for MS/MS. Data acquisition and treatment of results are carried out with the Xcalibur® Data System 2.0 (Thermo Scientific, San Jose, CA, USA).

Hydrophilic interaction liquid chromatography–mass spectrometry based (LC–MS) in high resolution Orbitrap

High performance LC (HPLC) system (Thermo scientific Accela™) with an autosampler coupled online to the Q-Exactive® mass spectrometer with Orbitrap® technology was used. The solvent system consisted of two mobile phases as follows: mobile phase A (acetonitrile/methanol/water 50:25:25, *per volume*) with 1 mM ammonium acetate) and mobile phase B (acetonitrile/methanol 60:40, *per volume*) with 1 mM ammonium acetate). Initially, 0% of mobile phase A was held isocratically for 8 min, followed by a linear increase to 60% of A within 7 min and a maintenance period of 15 min, returning to the initial conditions in 10 min. A volume of 5 µL of each sample containing 5 µg of lipid extract and 95 µL of eluent B was introduced into the Ascentis® Si column (15 cm × 1 mm, 3 µm, Sigma-Aldrich) with a flow rate of 40 µL min^{-1} and at 30 ºC.

The mass spectrometer with an Orbitrap® analyser was operated in simultaneous positive (electrospray voltage 3.0 kV) and negative (electrospray voltage –2.7 kV) modes with high resolution with 70000 and automatic gain control (AGC) target of 1E6, the capillary temperature was 250 ºC and the sheath gas flow was 15 U. In MS/MS experiments, a resolution of 17,500 and AGC target of 1E5 was used and the cycles consisted in one full scan mass spectrum and ten data-dependent MS/MS scans were repeated continuously throughout the experiments with the dynamic exclusion of 60 seconds and intensity threshold of 1E4. Normalized collision energy™ (CE) ranged between 25, 30 and 35 eV. Data acquisition was carried out using the Xcalibur data system (V3.3, Thermo Fisher Scientific, USA). All the analyses were performed in triplicate. The identification of molecular species of polar lipids was based on the assignment of the molecular ions observed in LC-MS/MS spectra. In order to identify molecular species, mass accuracy (Qual Browser) was determined with ≤ 5 ppm allowed in possible elemental composition calculation of empirical formula. Furthermore, and in the case of the lipidome

of *Fucus vesiculosus*, HPLC-MS raw data were preprocessed by *s*pectral filtering stage, *p*eak detection, alignment, normalization and further integration into the MZmine 2 (271) software, with a tolerance of 5 ppm of exact mass error, *after* identification of the lipids based on the calculation of their theoretical monoisotopic mass and subsequent analysis of the MS/MS spectrum. The analysis of polar lipids was performed after normalization in relation to the internal standards.

Electrospray-Mass Spectrometry (ESI-MS) Conditions

Fractions 3 and 4 recovered from total lipid extract of *Gracilaria* were analyzed by ESI-MS on a Q-Tof 2 quadrupole time of flight mass spectrometer (Micromass, Manchester, UK) operating in positive mode. Each sample, diluted in 195 µL of methanol, was introduced through direct infusion with the following electrospray conditions: flow rate of 10 mL/min, voltage applied to the needle at 3 kV, a cone voltage at 30 V, source temperature of 80 °C, and solvation temperature of 150 °C [62]. The resolution was set to about 9000 FWHM (full width at half maximum). Tandem mass spectra (MS/MS) were acquired by collision induced dissociation (CID), using argon as the collision gas (pressure measured as the setting in the collision cell 3.0×10^5 Torr). The collision energy was between 30 and 60 eV. Both MS and MS/MS spectra were recorded for 1 min. Data acquisition was carried out with a MassLynx 4.0 data system.

II.10. Evaluation of the biological activity

Considering the great biological potential of marine species, it is of great interest use of appropriate methodologies that can rapidly screen different marine sources for bioactive compounds. *In vitro* screening of anti-inflammatory and antiproliferative activities of macroalgae extracts were evaluated. The first approach was the evaluation of total lipids extract from *Gracilaria sp.* and further the evaluation of the fraction-rich in GLs obtained from *Gracilaria* by SPE separation (section II.4). Antioxidant activity of total lipid extract from *Gracilaria* was evaluated by DPPH bioassay.

II.10.1. Antiproliferative activity

Cell Viability Assay on T-47D and 5637 Tumor Cell Lines

The antiproliferative activity of lipid extracts was examined by the effect of *Gracilaria* sp. lipid extracts on the T-47D human breast cancer and urinary bladder cancer cell lines' metabolism using the Prestoblue colorimetric assay (Invitrogen Life Sciences, Paisley, UK). Tumor cells were cultivated in Dulbecco's Modified Eagle Medium (DMEM-F12, Invitrogen Life Technologies, Paisley, UK) with 10% fetal bovine serum (FBS; Gold, PAA) and 5 mg/L 1% penicillin/steptomicin (Invitrogen) in a humidified incubator at 37 °C under an atmosphere of 5% CO_2. Cells were plated on 96-well plates and allowed to attach for 24 h, 100 µL of cell suspension (1–2 × 10^4 cell/mL in complete medium) were used. Following this step, 200 µL of the treatment solution in a range of 5–20 µg/mL were applied to the culture. The lipid extract was dissolved in DMSO and diluted to a final concentration of 0.1% DMSO in a phenol-red free RPMI 1640 medium supplemented with 2% charcoal treated FBS (DCC), 1% glutamate, and 1% PEST. The same concentration of DMSO was used in untreated controls [63]**.** The treatment medium was changed 48 h later, and was removed from each well after 48 h for viability assay using PrestoBlue Absorbance measured at 570 nm and 600 nm at 1, 2, 3, 4, and 5 h on a plate reader, which gave a linear absorbance range. Experiments were carried out in quadruplicate and three independent experiments were carried out for each cell line.

II.10.2. Anti-inflammatory activity

Immunomodulatory effects of total lipid and fractionated extracts was evaluated on Raw 264.7, a mouse leukaemic monocyte macrophage cell line macrophages, key cell of immune responses (272). The evaluation *in vitro* of the anti-inflammatory activity of extracts on macrophages was accessed by exposing to the bacterial cell-wall component lipopolysaccharide (LPS) that subsequently leads to the production of a broad array of pro-inflammatory mediators, namely cytokines, chemokines and NO (272,273). The production of NO is measured by the accumulation of nitrite in the culture supernatants, using a colorimetric reaction with the Griess reagent (274). Test solutions of *Gracilaria* sp. lipid extracts (stock solution 25 mg/mL) were prepared in ethanol and stored at –20 °C until used. Serial dilutions of tested solutions with culture medium in a range of 25–200

μg/mL were prepared and sterilized by filtration immediately before in vitro assays. Ethanol concentrations ranged from 0.1% to 0.8% (*v/v*).

RAW 264.7, a mouse leukemic monocyte macrophage cell line from American Type Culture Collection (ATCC TIB-71), was supplied by Otília Vieira (Centro de Neurociências e Biologia Celular, Universidade de Coimbra, Coimbra, Portugal) and cultured in Dulbecco's Modified Eagle Medium (Invitrogen Life Technologies, Paisley, UK) supplemented with 10% non-inactivated fetal bovine serum, 100 U/mL penicillin, and 100 μg/mL streptomycin at 37 °C in a humidified atmosphere of 95% air and 5% CO_2. During the experiments, cells were monitored through microscope observation to detect any morphological change. Assessment of metabolically active cells was performed using a resazurin bioassay [64]. Briefly, cell duplicates were plated at a density of 0.1×10^6/well, in a 96-well plate and allowed to stabilize overnight. Following this period, cells were either maintained in a culture medium (control) or pre-incubated with various concentrations of *Gracilaria* sp. lipid extracts or its vehicle for 1 h, and later activated with 50 ng/mL LPS for 24 h. After the treatments, resazurin solution (50 μM in culture medium) was added to each well and incubated at 37 °C for 1 h, in a humidified atmosphere of 95% air and 5% CO_2. As viable cells are able to reduce resazurin (a non-fluorescent blue dye) into resorufin (pink and fluorescent), their number correlates with the magnitude of dye reduction. Quantification of resofurin was performed on a Biotek Synergy HT (BioTek Instruments, Winooski, VT, USA) plate reader at 570 nm, with a reference wavelength of 620 nm. The production of nitric oxide was measured by the accumulation of nitrite in the culture supernatants, using a colorimetric reaction with the Griess reagent [65]. Briefly, 170 μL of culture supernatants were diluted with equal volumes of the Griess reagent [0.1% (*w/v*) *N*-(1-naphthyl)-ethylenediamine dihydrochloride and 1% (*w/v*) sulphanilamide containing 5% (*w/v*) H_3PO_4] and maintained for 30 min in the dark. The absorbance at 550 nm was measured on a Biotek Synergy HT plate reader. Culture medium was used as a blank and nitrite concentration (μM) was determined from a regression analysis using serial dilutions of sodium nitrite as standard. Experiments were carried out at least three times.

II.10.3. Antioxidant Capacity

Antioxidant activity was measured in the total lipid extract of *Gracilaria* sp. extracts by using DPPH methods. Free Radical Scavenging by the Use of the DPPH Radical is based on the neutralization of free radicals of DPPH by the extract antioxidants (275–277). Antioxidant assays was performed in a 96-well flat-bottom UV transparent microplate (BD Falcon TM, ref. 353261, well volume 370 µL).

Free Radical Scavenging by the Use of the DPPH Radical

For the $DPPH^{\bullet}$ assay, a stock solution of $DPPH^{\bullet}$ in ethanol (250 µM) was prepared and kept in the dark at room temperature. Three dilutions from the stock $DPPH^{\bullet}$ solution (between 10 and 300 µM) must also prepared in ethanol to determine the dilution of the $DPPH^{\bullet}$ stock solution necessary to obtain the $DPPH^{\bullet}$ concentration that provide an absorbance value of 0.9 at 517 nm. For $DPPH^{\bullet}$ assay, 150 µl of $DPPH^{\bullet}$ and 150 µl of ethanol was placed in each well and absorbance was performed at room temperature after 2 min of incubation, by using spectrophotometric detection in a UV-Vis spectrophotometer (Multiskan GO 1.00.38., Thermo Scientific) (275). Then, 150 µl of $DPPH^{\bullet}$ and 150 µl of ethanol of the $DPPH^{\bullet}$ solution providing an absorbance 0.9 was prepared and the stability of the radical upon reaction time is evaluated by measuring the absorbance at 517 nm every 5 min, during 120 min, at room temperature.

The percentage of $DPPH^{\bullet}$ radical remaining was calculated using the equation:

$$\%\ DPPH^{\bullet}_{Remaining} = (Abs_{\text{sample after incubation time}} / Abs_{\text{sample at the beginning of reaction}}) \times 100.$$

This solution was used for further experiments. For evaluation of radical species scavenging, 150 µL of Trolox standard solutions (between 5 and 75 µmol/L in ethanol), extracts of *Gracilaria* sp. (100, 500 and 1000 µg/mL in ethanol) were placed in each well, followed by addition of 150 µL of $DPPH^{\bullet}$ in ethanol. The $DPPH^{\bullet}$ scavenging activity of standards and samples was monitored at 517 nm every 5 min after the beginning of reaction during 120 min at room temperature. The microplate was automatically shaken for 5 s prior to each reading. For each sample, the experiment was performed in triplicate in three different days. For microplate $DPPH^{\bullet}$ 150 µl of Trolox standard solution or diluted

macroalgae extracts and 150 µl of DPPH• are placed in each well (275). The DPPH• scavenging capacity was monitored at 517nm during 120 min. The antioxidant activity of the tested samples expressed as percentage of inhibition of DPPH• radical was calculated (60 and 120 min) using the following equation:

$$\% \text{ inhibition} = ((Abs_{DPPH\bullet} - Abs_{sample})/Abs_{DPPH\bullet}) \times 100$$

The IC_{50} values (concentration of sample that induces a reduction of 50% in the initial DPPH• radical) obtained after 120 min of reaction were calculated by linear regression from the concentration of sample versus percentage of inhibition. This value was used to choose the range of concentration of lipid extracts to be evaluated in the anti-inflammatory assay.

II.11. Statistical Analysis

The experiments were done independently (at least two technical replicates of at least three different and independent experiments) and the results were expressed as the means ± SD. Data analysis was performed by using GraphPad Prism 5.0 for Windows (GraphPad Software, San Diego, CA, USA). Variation in the lipidome of macroalgae *Fucus vesiculosus* with season effect (section III.I.3) were obtained by *t*-test analysis of independent samples after test the normality (Shapiro-Wilk test) and homogeneity of variance (Levéne test) with results expressed by the changes of the relative abundance in the profile of molecular species of all classes. If the null hypothesis of Levene's Test was rejected then Welsh *t* test was performed; and applied non-parametric Mann-Whitney's U test. These preliminary results were obtained by multivariate analysis by using IBM SPSS Statistics for Windows, version 24 (IBM Corp., Armonk, N.Y., USA) and R: A language and environment for statistical computing. R (Foundation for Statistical Computing, Vienna, Austria) with a Package for Metabolomics Univariate and Multivariate Statistical - MUMA. Antiproliferative and anti-inflammatory bioassays were measured in quadruplicate and in three different and independent experiments. One-way analysis of variance (ANOVA) followed by Dunnett's multiple comparison tests was used to compare the treatment group to a single control group, after checking for assumptions. Results were expressed as mean ± SD. Statistical differences were calculated and represented with the

following symbols of significance level * $p < 0.05$, ** $p < 0.01$, *** $p < 0.001$, # $p < 0.05$, ### $p < 0.001$.

II.12. Nutritional Indexes

The nutritional quality of the lipids was assessed by considering atherogenic and thrombogenic indexes:

AI and TI indexes calculated by the method of Ulbricht and Southgate (278).

IA = (12:0 + 4 × 14:0 + 16:0) / (Σ MUFAs + Σ *n*-6 PUFAs + Σ *n*-3 PUFAs)

IT = (14:0 + 16:0 + 18:0) / (0.5 × Σ MUFAs + 0.5 × Σ *n*-6 PUFAs + 3 × Σ *n*-3 PUFAs + Σ *n*-3/*n*-6)

II.13. Standards and Reagents

HPLC grade chloroform, methyl tert-butyl ether (MTBE), and methanol (MeOH) were purchased from Fisher Scientific Ltd. (Loughborough, UK). All other reagents were purchased from major commercial sources. Milli-Q water (Synergy®, Millipore Corporation, Billerica, MA, USA) was used. TLC silica gel 60 glass plates (20 x 20 cm) with concentrating zone were purchased from Merck (Darmstadt, Germany). D-(+)-Glucose ≥ 99.5%, 6-Hydroxy-2,5,7,8-tetramethylchromane-2-carboxylic acid (Trolox) and 2,2-Diphenyl-1-picrylhydrazyl (DPPH$^{\bullet}$) were purchased from Sigma-Aldrich (St Louis, MO, USA), RPMI 1640 media from PAA (Pasching, Austria), Phenol-red-free RPMI 1640 medium, penicillin–streptomycin, TrypLE express and FBS were from Gibco Technologies (Paisley, UK), and Presto Blue was from Invitrogen.

Standards of polar lipid were purchased from Avanti® Polar Lipids, Inc. (Alabaster, USA): 1,2-diacyl-3-*O*-β-D-galactosyl-sn-glycerol (MGDG); 1,2-diacyl-3-*O*-(α-D-galactosyl1-6)-β-D-galactosyl-*sn*-glycerol (DGDG); sulfoquinovosyl diacylglycerol (SQDG); 1,2-dipalmitoyl-*sn*-glycero-3-*O*-4'-(*N*,*N*,*N*-trimethyl)-homoserine (DGTS); phospholipids internal standards 1,2-dimyristoyl-*sn*-glycero-3-phosphocholine (dMPC), 1-nonadecanoyl-2-hydroxy-*sn*-glycero-3-phosphocholine (LPC), 1,2-dimyristoyl-*sn*-glycero-3-phosphoethanolamine (dMPE), 1,2-dimyristoyl-*sn*-glycero-3-phosphate (dMPA), 1,2-dimyristoyl-*sn*-glycero-3-phospho-(1′-rac-glycerol) (dMPG), 1,2-dimyristoyl-*sn*-glycero-3-phospho-L-serine (dMPS) and 1,2-dipalmitoyl-*sn*-glycero-3-phospho-(1′-myo-inositol)

(dPPI). Methyl ester of fatty acids mixture was from Supelco 37 Component FAME Mix and Methyl heptadecanoate ≥ 99% was from Sigma. All standards used had a purity of ≥ 99% and were used without further purification.

CHAPTER III

RESULTS AND DISCUSSION

III.1. THE LIPIDOMIC APPROACH

III.1.1. The lipidome of Chlorophyta: *Codium tomentosum*

III.1.2. The lipidome of Rhodophyta:

III.1.2.1 The lipidome of *Gracilaria* sp.

III.1.2.2. The lipidome of *Porphyra dioica*

III.1.3. The lipidome of Ochrophyta: *Fucus vesiculosus*

III.2. BIOPROSPECTION OF POLAR LIPIDS

III.2.1. Anti-inflammatory activity on nitrite production in RAW 264.7 cells

III.2.2. Activity of lipid extracts o human cancer cell line viability

III.1. THE LIPIDOMIC APPROACH

III.1.1. The lipidome of Chlorophyta: *Codium tomentosum*

The data presented in the following work was published in:

Elisabete da Costa, Tânia Melo, Ana S.P. Moreira, Eliana Alves, Pedro Domingues, Ricardo Calado, Maria H. Abreu, Maria Rosário Domingues. **Decoding bioactive polar lipid profile of the macroalgae *Codium tomentosum* from a sustainable IMTA system using a lipidomic approach.** Algal Research (2015) 12, 388–397.

The lipidome of Chlorophyta: *Codium tomentosum*

Codium tomentosum is a marine green macroalgae (phylum Chlorophyta) of the family Codiaceae. It is commonly found on exposed rocks and/or deep rock pools on the lower seashore (279). This specimen is native to the North East of the Atlantic Ocean and is known to be an important source of compounds with bioactive properties such as sulfated galactans and pigments, among others, with antioxidant, antigenotoxic, anti-tumor, and hypoglycemic activities (8). Concerning lipids of *Codium*, a limited number of studies is currently available for the characterization of FA composition (143,280) and no studies on the profile of polar lipidome.

This study is the first report on the isolation and characterization of the polar lipids of *Codium tomentosum* from on land-based integrated multi-trophic aquaculture system (IMTA) by using a lipidomic-based approach employing hydrophilic interaction liquid chromatography–electrospray ionization mass spectrometry (HILIC–ESI-MS). As most of polar lipids have been reported to have nutritional and health benefits, the present study aims to decode the polar lipidome of *C. tomentosum* from IMTA fostering the bioprospection and their potential commercial applications in food, pharmaceutical and cosmetic industries.

III.1.1.1. Polar lipids from Codium tomentosum

The LC–MS analysis of the lipid extracts allowed the structural information of the lipidome of *C. tomentosum*, namely profile and the molecular species composition within the polar lipid belonging to GLs, PLs and betaine lipids. Structures of polar lipids were identified by high resolution MS and the detailed fragmentation obtained by ESI−MS/MS.

Glycolipids

Glycoglycerolipids occur widely in marine algae, in cyanobacteria and in higher plants. The basic structure of glycoglycerolipids is characterized by a 1,2-diacyl-*sn*-glycerol moiety with a mono- or oligosaccharide attached to the *sn*-3 position of the glycerol backbone [43]. Four groups of GLs were identified: SQDG, SQMG, MGDG, and DGDG.

Sulfoquinovosyl diacylglycerol (SQDG) and sulfoquinovosyl monoacylglycerol (SQMG)

The molecular species from 1,2-diacyl-3-*O*-(6-deoxy-6-sulfo-*α*-D-glucopyranosyl)-*sn*-glycerol (SQDG) were analyzed in the negative-ion mode and observed as $[M - H]^-$ ions (Fig. III.1 and Table III.1). The typical fragmentation under MS/MS of SQDGs is characterized by the presence of ions at *m/z* 225 corresponding to the sulfoquinovosyl group, confirming the polar head of these lipids, and the presence of ions formed due to the loss of fatty acyl chains, both as acid and keto derivatives (127,131,145). The carboxylate anions ($RCOO^-$) can also be detected. As an example, in Fig. III.2 it is shown the LC−MS/MS spectra of the SQDG molecular species observed as $[M - H]^-$ at *m/z* 737.4 identified as SQDG (28:0) (SQDG (12:0/16:0) and 14:0/14:0)) (Fig. III.2.A) and at *m/z* 833.4 identified as SQDG (35:1) (SQDG (19:1/16:0) and (17:0/18:1)) (Fig. III.2.B). Carboxylate anion at *m/z* 255.1 assigned as $RCOO^-$ of the FA 16:0, loss of $C_{11}H_{23}COOH$ at *m/z* 537.2 and loss of $C_{15}H_{31}COOH$ at *m/z* 481.1 confirm the presence of SQDG (12:0/16:0) and the loss of $C_{13}H_{27}COOH$ at *m/z* 509.2 confirm the presence of SQDG (14:0/14:0) (Fig. III.2.A). On the other hand, the carboxylate anions at *m/z* 255.1 (FA 16:0) and 295.1 (FA 19:1), product ions due to loss of $C_{18}H_{35}COOH$ (loss of FA 19:1) at *m/z* 537.2 and loss of $C_{15}H_{31}COOH$ at *m/z* 577.2 confirm the presence of SQDG 35:1 (SQDG (19:1/16:0)) (Fig. III.2.B). The SQDG (17:0/18:1) was confirmed by the loss of $C_{16}H_{33}COOH$ at *m/z* 563.2 (loss of FA 17:0) and of the loss of $C_{17}H_{33}COOH$ at *m/z* 551.2 (loss of FA 18:1) (Fig. III.2.B).

Based on the LC−MS and MS/MS analysis, several molecular species of SQDG were identified containing fatty acyl chains from 14:0 to 22:6, and the most abundant molecular species was found at *m/z* 793.5 assigned as SQDG (16:0/16:0). SQDGs species containing odd fatty acyl chains (C_{17} and C_{19}) were also identified. Monoacyl forms of diacylglycerolipids (SQMG) were detected in *C. tomentosum* for the first time, and firstly reported in the lipidome of *Codium* spp. (Supplementary Fig. S.1). The typical fragmentation of SQMGs by MS/MS reveals the presence of ions at *m/z* 224.8, as for SGDGs (Supplementary Fig. S.2) (127,131,145). Carboxylate anions ($RCOO^-$) could also be found. The most abundant species of SQMG was found at *m/z* 555.3, corresponding to SQMG (16:0) (Supplementary Fig. S.2) and at *m/z* 597.3 attributed to SQMG (19:0).

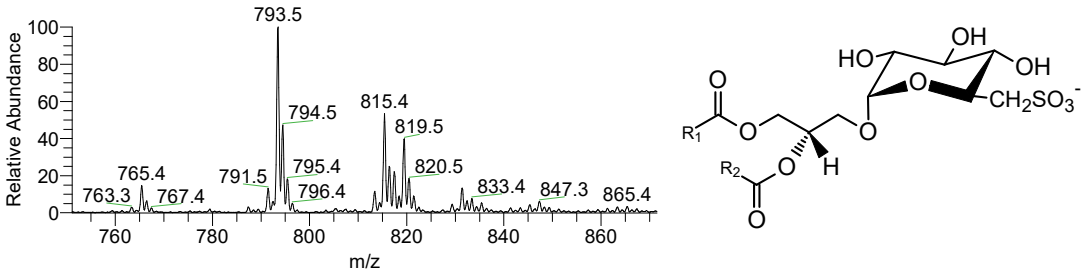

Figure III. 1. LC–MS spectrum of sulfoquinovosyl diacylglycerol (SQDG) observed by HILIC–ESI–MS as $[M - H]^-$ ions. A general structure is also represented.

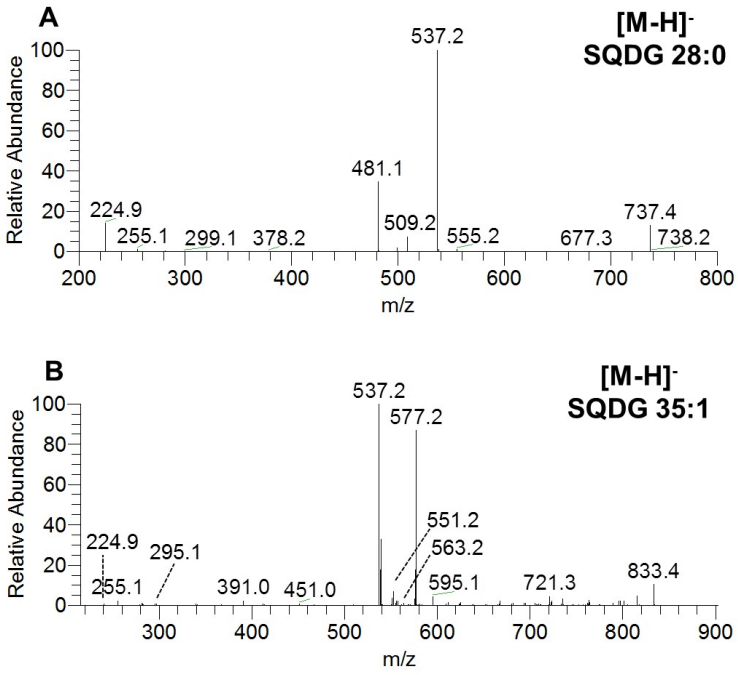

Figure III. 2. ESI–MS/MS spectra of the SQDG molecular species observed as $[M - H]^-$ at *m/z* 737.4 identified as SQDG (28:0) (SQDG (12:0/16:0) and (14:0/14:0)) (A), and at *m/z* 833.4 identified as SQDG (35:2) (SQDG (17:0/18:1) and (16:0/19:1)) (B).

Monogalactosyl diacylglycerol (MGDG)

The molecular species from monogalactosyl diacylglycerol (MGDG) were identified in the LC–MS in positive-ion mode as $[M + NH_4]^+$ ions (Fig. III.3). Confirmation of the structure was achieved by MS/MS analysis, that showed product ions resulting from the loss of NH_3, loss of hexose residue (-162 Da, -Hex_{res}) and hexose moiety (-180 Da, -Hex) (123,156,210,211). Product ions formed by combined loss of the one FA and the hexose yield a typical acylium ions plus 74 $(RCO + 74)^+$ confirm the FA composition. The MGDG

molecular species are indicated in the Figure III.3 and in the Table III.1 (210). The most abundant $[M + NH_4]^+$ ion was found at *m/z* 774.3 mainly corresponding to MGDG (18:1/16:0) and minor to MGDG (18:0/16:1), followed by the ion at *m/z* 796.3 assigned to MGDG (18:1/18:3) and MGDG (18:2/18:2). Low abundant $[M + Na]^+$ ions correspondent to all MGDG species were detected and the structures were confirmed by MS/MS as described in the literature and in the Section II.9 (123,145,156,210,211). In the Figure III.4 is shown as example the MS/MS spectrum of $[M + Na]^+$ ion MGDG (34:1) at *m/z* 779.7. The spectrum contains the ion at *m/z* 497.4 attributed to the loss of $C_{17}H_{33}COOH$ (FA 18:1) and the ion at *m/z* 523.4 due to the loss of $C_{15}H_{31}COOH$ (loss of FA 16:0). The ion at *m/z* 243, as described in the Section II.9, is attributed to the product ion galactosyl glycerol head group $[C_9H_{16}O_6 + Na]^+$.

MGDG molecular species identified contain in their composition fatty acyl chains from 16:0 to 20:5, including essential FA like oleic (18:1) and linolenic (18:3, ALA) and long fatty acyl chains eicosapentaenoic (20:5, EPA) bearing PUFAs.

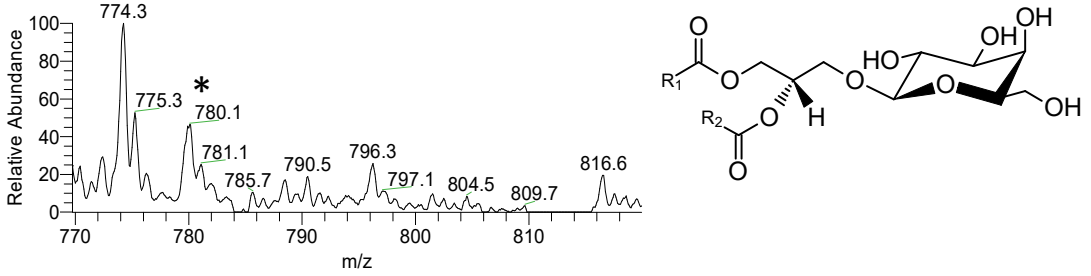

Figure III. 3. LC–MS spectrum of monogalactosyl diacylglycerol (MGDG) molecular species observed by HILIC–ESI–MS as $[M + NH_4]^+$ ions. *Eluent contamination. A general structure is also represented.

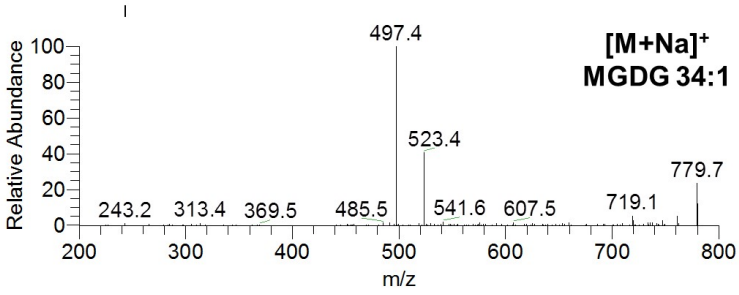

Figure III. 4. ESI–MS/MS spectrum of the ion $[M + Na]^+$ of MGDG (34:1) (MGDG (16:0/18:1) and (16:1/18:0)) at *m/z* 779.7.

Digalactosyl diacylglycerol (DGDG)

The molecular species from digalactosyl diacylglycerol (DGDG) were analyzed by LC−MS in positive-ion mode and the molecular species were identified as $[M + NH_4]^+$ ions. The MS/MS spectrum showed product ions formed due to the losses of the hexose moiety (-162 Da and -180 Da), loss of NH_3, and further loss of H_2O (123,156,210,211), similarly to observed for MGDG. The profile of the molecular species of DGDG, identified by LC−MS, is shown in the Table III.1 and in the Figure III.5. The most abundant ion was found at *m/z* 936.3 as $[M + NH_4]^+$ of DGDG (18:1/16:0) and DGDG (18:0/16:1). DGDG molecular species contain fatty acyl chains from C_{16} to C_{20} including PUFAs 18:3 and 20:5 FA and hydroxyl FA 18:2-OH and 18:3-OH. DGDG containing oxylipins precursors were reported in algae species (163,281,282).

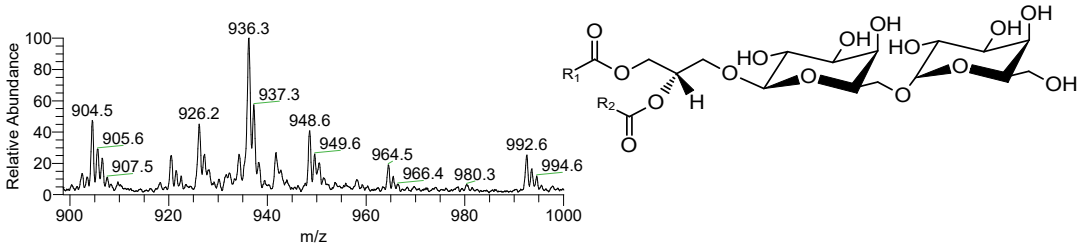

Figure III. 5. LC–MS spectrum of the digalactosyl diacylglycerol (DGDG) molecular species observed by HILIC−ESI−MS as $[M + NH_4]^+$ ions. A general structure is represented.

The confirmation of the proposed identification was obtained from the MS/MS analysis of $[M + Na]^+$ ions, as described in the literature (123,145,156,210,211). As an example, it is shown in Fig. III.6, the LC−MS/MS spectrum of the DGDG molecular species observed as $[M + Na]^+$ at *m/z* 927.7 identified as DGDG (33:1) ((15:0/18:1), (17:1/16:0) and (14:0/19:1)) (Fig. III.6.A) and DGDG (32:2-OH) (14:0/18:2-OH) (Fig. III.6.A).

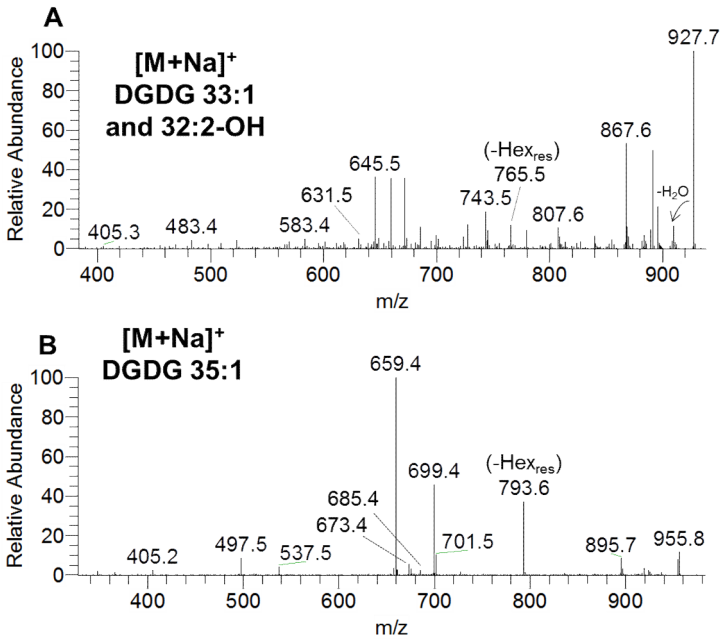

Figure III. 6. LC–MS/MS spectra of the DGDG molecular species observed as $[M + Na]^+$ at *m/z* 927.7 identified as DGDG (33:1) (DGDG (16:0/17:1)) and DGDG (32:2-OH) (DGDG (14:0/18:2-OH)) (A), and at *m/z* 955.8 identified as DGDG (35:1) (DGDG (16:0/19:1) and (17:0/18:1)) (B).

The presence of hydroxylated FA, as oxylipin, was inferred by the presence of the product ion due to loss of H_2O, that is absent in the MS/MS spectrum of the other DGDG as can be seen in Fig. III.6.B for DGDG (35:1), allowing to propose the presence of hydroxylated FAs. The ion at *m/z* 631.5 observed in the Fig. III.6.A, was attributed to the loss of $C_{17}H_{31}COO\text{-}OH$ (FA 18:2-OH) and the ion at *m/z* 699.5 was attributed to the loss of $C_{13}H_{27}COOH$ (loss of FA 14:0) (Fig. III.6.A), thus confirming the DGDG (14:0/18:2-OH). On the other hand, the ion at *m/z* 645.5 was attributed to the loss of $C_{17}H_{33}COOH$ (FA 18:1) and the ion at *m/z* 685.5 was attributed to loss of $C_{14}H_{29}COOH$ (FA 15:0) confirming the DGDG (15:0/18:1). Also, the ions at *m/z* 671.5 and the ion at *m/z* 658.5 were assigned by the loss of $C_{15}H_{31}COOH$ (FA 16:0) and $C_{16}H_{31}COOH$ (FA 17:1) confirming the presence of DGDG (16:0/17:1). The assignment of DGDG (14:0/19:1) due to the loss of $C_{13}H_{27}COOH$ (FA 14:0) at *m/z* 699.5 and $C_{18}H_{35}COOH$ (FA 19:1) at *m/z* 631.5 was also considered. The fragmentation under MS/MS of $[M + Na]^+$ ions of DGDGs showed the loss of one hexose residue (neutral loss of 162 Da) at *m/z* 765.5 (Fig. III.6.A) and at *m/z* 793.6 (Fig. III.6.B). In both spectra it is possible to see the ions at *m/z* 405.3 (Fig. III.6.A) and 405.2 (Fig. III.6.B) corresponding to the digalactosyl glycero head group $[C_{15}H_{26}O_{11} + Na]^+$. On the other hand, the DGDG 35:1 (19:1/16:0 and 17:0/18:1) (Fig. III.6.B) product

ions were observed at *m/z* 659.4 and 699.4 due to the loss of $C_{18}H_{35}COOH$ (loss of FA 19:1) and $C_{15}H_{31}COOH$ (loss of FA 16:0) respectively, and the product ions assigned at *m/z* 685.4 and 673.4 are due to the loss of $C_{16}H_{33}COOH$ (loss of FA 17:0) and to the loss of $C_{17}H_{33}COOH$ (loss of FA 18:1).

Table III. 1 Identification of MGDG and DGDG molecular species observed by HILIC–ESI–MS, as $[M + NH_4]^+$ ions and SQDG and SQMG molecular species observed as $[M - H]^-$ ions, with the assignment of the fatty acyl composition of each lipid molecular species, according to the interpretation of the correspondent MS/MS spectra

Galactolipids $[M + NH_4]^+$ ***m/z***	**Lipid Species (C:N)**	**Fatty Acyl Chain**	**Sulfolipids $[M - H]^-$** ***m/z***	**Lipid Species (C:N)**	**Fatty Acyls Chain**
Monogalactosyl diacylglycerol			Sulfoquinovosyl diacylglycerol		
772.3	MGDG (34:2)	18:2/16:0	737.4	SQDG (28:0)	14:0/14:0 and 12:0/16:0
774.3	**MGDG (34:1)**	18:1/16:0	765.4	SQDG (30:0)	14:0/16:0
776.3	MGDG (34:0)	18:0/16:0	791.5	SQDG (32:1)	16:0/16:1 and 14:0/18:2
790.5	MGDG (36:7)	18:3/18:4	**793.5**	SQDG **(32:0)**	**16:0/16:0 and 14:0/18:0**
792.3	MGDG (36:6)	18:3/18:3	813.4	SQDG (34:4)	18:4/16:0
794.3	MGDG (36:5)	18:2/18:3	**815.4**	SQDG **(34:3)**	**18:3/16:0**
796.3	MGDG (36:4)	18:2/18:2	817.5	SQDG (34:2)	18:2/16:0
800.3	MGDG (36:2)	18:0/18:2	819.5	SQDG (34:1)	18:1/16:0
804.5	MGDG (36:0)	18:0/18:0	831.4	SQDG (35:2)	19:2/16:0 and 17:0/18:2
816.6	MGDG (38:8)	18:3/20:5	833.4	SQDG (35:1)	19:1/16:0 and 17:0/18:1
Digalactosyl diacylglycerol			835.4	SQDG (35:0)	19:0/16:0 and 17:0/18:0
904.6	DGDG (32:3)	16:3/16:0	845.4	SQDG (36:2)	20:2/16:0
906.6	DGDG (32:2)	16:2/16:0	847.3	SQDG (36:1)	20:1/16:0
920.6	DGDG (32:3-OH)	14:0/18:3-OH and	865.4	SQDG (38:6)	22:6/16:0
	DGDG (33:2)	15:0/18:2 and 14:0/19:2	Sulfoquinovosyl monoacylglycerol		
	DGDG (32:2-OH)	14:0/18:2-OH and	549.3	SQMG (16:3)	
922.5	DGDG (33:1)	15:0/18:1 and 16:0/17:1 and 14:0/19:1	**555.3**	**SQMG (16:0)**	
926.2	DGDG (34:6)	16:3/18:3	567.3	SQMG (17:1)	
932.3	DGDG (34:3)	18:3/16:0	597.3	SQMG (19:0)	
936.3	**DGDG (34:1)**	18:1/16:0 and 18:0/16:1			
948.6	DGDG (35:2)	17:0/18:2 and 19:2/16:0			
950.5	DGDG (35:1)	17:0/18:1 and 19:1/16:0			
958.6	DGDG (36:4)	18:2/18:2			
964.5	DGDG (36:1)	18:0/18:1 and 20:0/16:1			
980.3	DGDG (38:7)	18:2/20:5			
992.6	DGDG (38:1)	18:1/20:0			

Bold *m/z* values correspond to the most abundant species detected in the LC-MS spectrum; C means the number of total carbon atoms and N represents total number of double bonds in the fatty acyl chains

Phospholipids

Phospholipids are characterized by the presence of a phosphate group at *sn*-3 position, which is further linked to a hydrophilic head group that classifies individual PL molecules. The major PLs identified in *C. tomentosum* are phosphatidylglycerols (PG), phosphatidylcholines (PC), phosphatidylinositols (PI), and phosphatidic acids (PA). The structural assignments were based on the study of the detailed fragmentation of PLs (138).

Phosphatidylglycerol (PG) and lyso PG

The classes of PG (Fig. III.7) and lyso PG (Supplementary Fig. S.3) were identified by LC–MS as $[M - H]^-$ ions. The LC−MS/MS spectra of PG showed ions formed due to the loss of fatty acyl chains both as acid and keto derivatives and the carboxylate anions of the fatty acyl chains (138,145,156,212). Ions corresponding to the neutral loss of 74 Da (loss of glycerol head group as an oxirane, $C_3H_6O_2$) and to the combined loss of 74 Da and the fatty acyl chain were also found (Fig. III.8). The most abundant PG molecular species was found at *m/z* 747.4 corresponding to PG (18:0/18:1). The second most abundant species was found at *m/z* 765.3 and corresponds to PG (16:1/20:5) and PG (18:3/18:3) (Table III.2, Fig.III.7). These species contain EPA and AA PUFAs and odd chain FA in their composition.

The LC−MS/MS spectrum of LPGs (Fig. III.8.B) showed ions formed due to the loss of 74 Da (loss of glycerol head group as an oxirane, $C_3H_6O_2$), ions at *m/z* 171 ($[C_3H_7O_2OPO_3H]^-$, glycerol phosphate), at *m/z* 153 (glycerol phosphate- H_2O), at *m/z* 227 ($[C_6H_{12}O_7P]^-$, loss of water from glycerophosphate glycerol) and the carboxylate anion of fatty acyl chain (145,212). Lipidomic analysis showed that the most abundant molecular species was LPG (16:0), at *m/z* 483.3, followed by LPG (18:1), LPG (19:0) and LPG (20:3) with $[M - H]^-$ ions at *m/z* 509.3, 525.3 and 533.3 respectively (Table III.2, Fig. S.3).

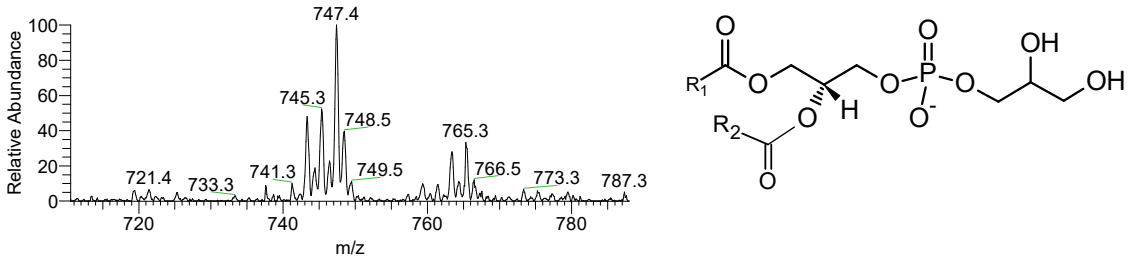

Figure III. 7. LC–MS spectrum of the phosphatidylglycerol (PG) observed by HILIC–ESI–MS as $[M - H]^-$ ions. A general structure is presented.

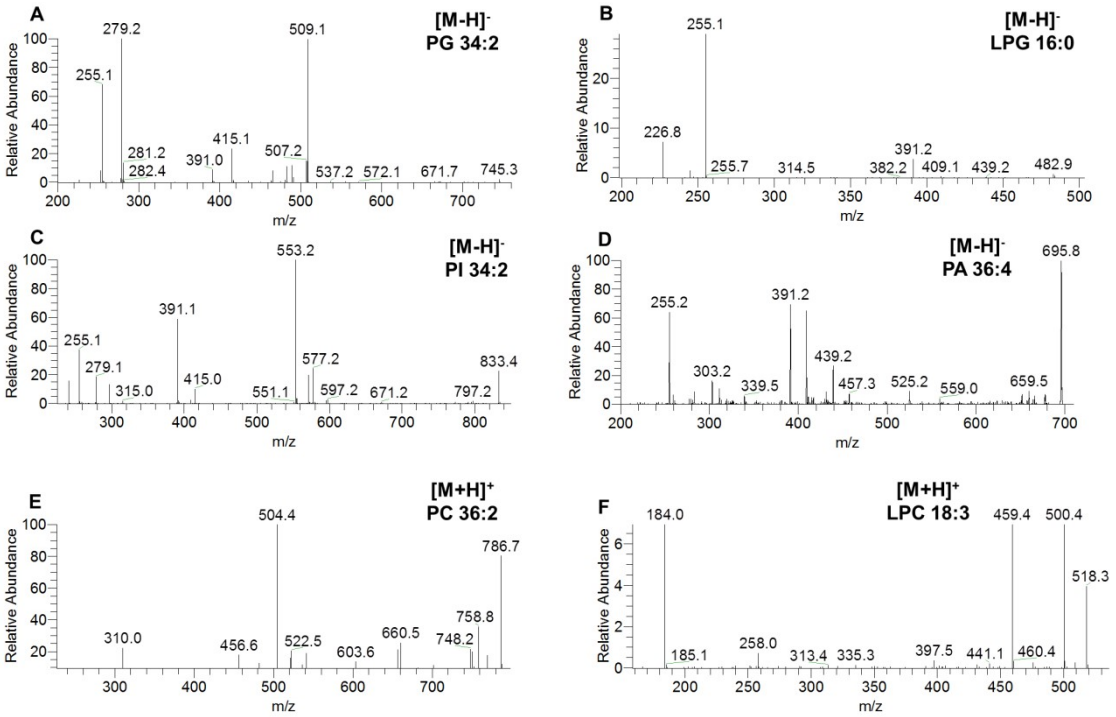

Figure III. 8. ESI–MS/MS spectra of the PG (34:2) (A), LPG (16:0) (B), PI (34:2) (C), PA (36:4) (D), PC (36:2) (E) and LPC (18:3) (F).

Phosphatidylcholine (PC) and lyso- PC

The classes of PC and lyso-PC were identified in positive-mode as $[M + H]^+$ ions (Fig.III.9 and Fig.III.8.E) and confirmed in the negative-ion mode as $[M + CH_3COO]^-$ ions. The LC−MS spectrum obtained in positive mode and the composition of the PC molecular identified, including the fatty acyl chain substitution, is presented in Table III.2. The classes PC and LPC also have a specific product ion of the polar head in the MS/MS spectra of $[M + H]^+$ ions, at *m/z* 184 ($H_2PO_4(CH_2)_2N^+(CH_3)_3$, phosphocholine) (138,145,156,215). The MS/MS spectra in negative-ion mode allowed the identification of the carboxylate anions ($RCOO^-$) of fatty acyl chains. Most abundant molecular species was found at *m/z* 756.5 and assigned as $[M + H]^+$ ions corresponding to PC (16:0/18:3) and PC (16:2/18:1). The second most abundant ions was found at *m/z* 782.5 for $[M + H]^+$ ions and correspond to PC (18:2/18:2) and PC (16:0/20:4). Several other species can be seen in Figure III.9 also bearing SFA, MUFAs, PUFAs namely AA, EPA and DHA.

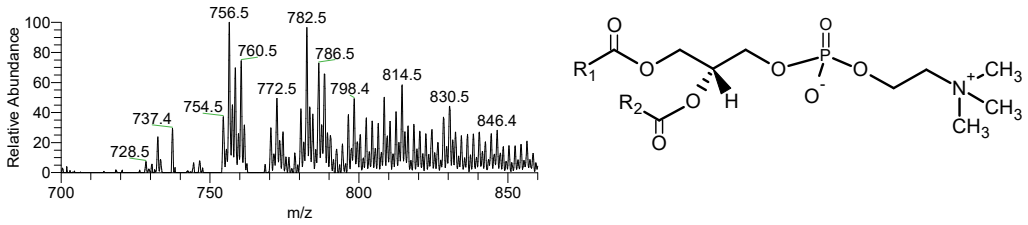

Figure III. 9. LC–MS spectrum of the phosphatidylcholine (PC) molecular species observed by HILIC-ESI-MS as $[M + H]^+$ ions. A general structure is shown.

The class of lyso-PCs were identified in positive-ion mode as $[M + H]^+$ ions, and the LC−MS spectrum obtained for the $[M + H]^+$ ions is presented in Table III.2, Figure S.4. The most abundant molecular species was found at *m/z* 496.4, corresponding to LPC (16:0), at *m/z* 518.4 corresponding to LPC (18:3) (Fig. III.8.F), and at *m/z* 522.4 that corresponds to LPC (18:1). Other species can be seen in Table III.2 also bearing PUFAs.

Phosphatidylinositol (PI)

The class of PI was observed in the MS spectra of the $[M - H]^-$ ions (Fig. III.10). The MS/MS spectra showed the product ion at *m/z* 241 corresponding to an inositol-1,2-cyclic phosphate anion and the product ions attributed to $[M - H - R_2CO_2H]^-$ and $[M - H - R_1CO_2H]^-$ arising from losses of the FA substituent as acids allowing to identify the structure of PI molecular species (Fig. III.8.C) (138,214).

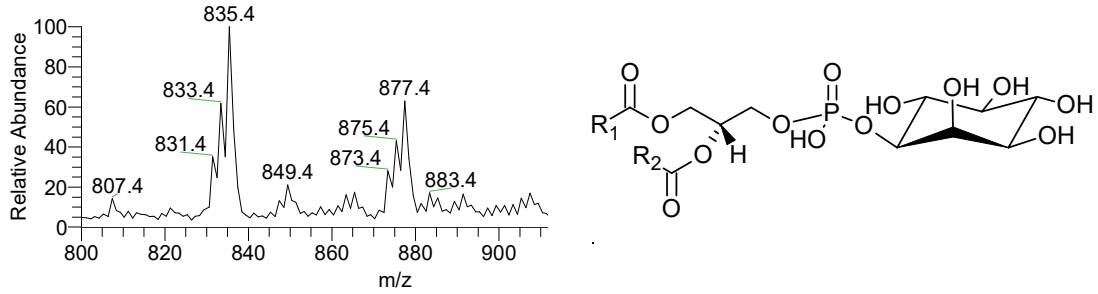

Figure III. 10. LC–MS spectrum and general structure of the phosphatidylinositol (PI) molecular species observed by HILIC−ESI−MS as $[M - H]^-$ ions.

The most abundant molecular species were found at *m/z* 835.4 and at *m/z* 833.4, corresponding to PI (16:0/18:1) and to PI (16:0/18:2). Other ions were found and correspond to PIs with fatty acyl chains varying from 16:0 to 19:0 and with PUFAs as 18:1, 18:2, 18:3, 20:4 and 22:6 (Table III.2, Fig. III.10).

Table III. 2. Identification of phospholipids molecular species observed by HILIC–ESI–MS, for PG, LPG, PA and PI as $[M - H]^-$ ions and for PC and LPC as $[M + H]^+$, with the assignment of the fatty acyl composition of each lipid molecular species, according to the interpretation of the correspondent MS/MS spectra

$[M-H]^-$	Lipid Species	Fatty acyl Chain	$[M+H]^+$	Lipid Species	Fatty Acyl Chain
m/z	(C:N)		*m/z*	(C:N)	
Phosphatidylglycerol			Lyso-phosphatidylcholine		
717.4	PG (32:2)	16:0/16:2 and 16:1/16:1	482.5	LPC (O-16:0a)	
719.4	PG (32:1)	16:0/16:1	494.4	LPC (16:1)	
721.4	PG (32:0)	16:0/16:0	**496.4**	**LPC (16:0)**	
733.3	PG (33:1)	16:0/17:1 and 16:1/17:0	516.4	LPC (18:4)	
741.3	PG (34:4)	16:1/18:3	518.4	LPC (18:3)	
743.3	PG (34:3)	16:0/18:3 and 16:1/18:2	520.4	LPC (18:2)	
745.3	PG (34:2)	16:0/18:2 and 16:1/18:1	522.4	LPC (18:1)	
747.4	**PG (34:1)**	**16:0/18:1 and 16:1/18:0**	524.4	LPC (18:0)	
759.4	PG (35:2)	17:0/18:2	536.6	LPC (O-18:1a)	
763.3	PG (35:0)	17:0/18:0 and 19:0:16:0	542.4	LPC (20:5)	
765.3	**PG (36:6)**	**16:1/20:5 and 18:3/18:3**	544.4	LPC (20:4)	
767.3	PG (36:5)	16:0/20:5 and 18:2/18:3	Phosphatidylcholine		
787.3	PG (37:2)	17:0/20:2 and 19:0/18:2	702.5	PC (30:2)	14:0/16:2
Lyso-phosphatidylglycerol			728.5	PC (32:3)	16:0/16:3 or 16:1/16:2
481.3	LPG (16:1)		730.6	PC (32:2)	16:0/16:2 or 16:1/16:1
483.3	**LPG (16:0)**		732.6	PC (32:1)	16:0/16:1 and 14:0/18:1
507.3	LPG (18:2)		734.6	PC (32:0)	16:0/16:0 and 14:0/18:0
509.3	LPG (18:1)		744.6	PC (O-34:2)	O-16:0a/18:2 or O-16:0e/18:1
523.3	LPG (19:1)		754.5	PC (34:4)	16:2/18:2
525.3	LPG (19:0)		**756.5**	**PC (34:3)**	**16:0/18:3 and 16:2/18:1**
533.3	LPG (20:3)		758.5	PC (34:2)	16:0/18:2 and 16:1/18:1
535.3	LPG (20:2)		760.5	PC (34:1)	16:0/18:1
Phosphatidic acid			762.5	PC (34:0)	16:0/18:0
665.2	PA (34:5)	16:1/18:4	770.5	PC (O-36:3)	O-18:0a/18:3 or O-18:1a/18:2
681.3	PA (O-36:4)	O-18:1a/18:3	772.5	PC (O-36:2)	O-18:0a/18:2 or O-18:1a/18:1
695.3	PA (36:4)	18:1/18:3 and 16:0/20:4	774.5	PC (O-36:1)	O-18:0a/18:1 or O-18:1a/18:0
697.3	PA (36:3)	18:1/18:2 and 18:0/18:3	780.5	PC (36:5)	16:0/20:5 and 18:2/18:3
701.3	PA (36:1)	18:0/18:1	**782.5**	**PC (36:4)**	**16:0/20:4 and 18:2/18:2**
719.4	PA (38:6)	18:3/20:3	784.4	PC (36:3)	16:0/20:3 and 18:0/18:3
721.4	PA (38:5)	18:0/20:5	786.5	PC (36:2)	16:0/20:2 and 18:0/18:2
Phosphatidylinositol			788.5	PC (36:1)	18:0/18:1
807.4	PI (32:1)	16:0/18:2	794.4	PC (O-38:5)	O-18:0a/20:5
831.4	PI (34:3)	16:0/18:3	796.4	PC (O-38:4)	O-18:0a/20:4
833.4	PI (34:2)	16:0/18:2	798.4	PC (O-38:3)	O-18:0a/20:3
835.4	**PI (34:1)**	**16:0/18:1**	800.4	PC (O-38:2)	O-18:0a/20:2
849.4	PI (35:1)	17:0/18:1	802.4	PC (O-38:1)	O-18:0a/20:1 and O-18:1a/20:0
861.4	PI (36:2)	18:0/18:2	804.4	PC (38:7)	18:2/20:5 and 18:3/20:4
873.4	PI (37:3)	19:0/18:3	806.4	PC (38:6)	18:2/20:4 and 18:3/20:3
875.4	PI (37:2) and (38:9)	19:0/18:2 and 18:4/20:5	808.4	PC (38:5)	18:2/20:3 and 18:3/20:2
877.4	PI (37:1) and (38:8)	19:0/18:1 and 18:3/20:5	810.4	PC (38:4)	18:2/20:2 and 18:3/20:1
883.3	PI (38:5)	18:0/20:5	812.5	PC (38:3)	18:1/20:2 and 18:3/20:0
907.4	PI (40:6)	18:0/22:6	814.5	PC (38:2)	18:0/20:2 and 18:2/20:0 and 16:0/22:2
			818.5	PC (38:0)	18:0/20:0 or 16:0/22:0
			822.5	PC (O-40:5)	O-18:0a/22:5 or O-18:Oe/22:4
			824.4	PC(O-40:4)	O-18:0a/22:4
			828.5	PC(O-40:2)	O-18:0a/22:2 or O-18:Oe/22:1
			830.5	PC(O-40:1)	O-18:0a/22:1
			834.4	PC (40:6)	20:2/20:4 and 20:3/20:3 and 18:0/22:6
			836.4	PC (40:5)	20:2/20:3 and 20:0/20:5
			840.4	PC (40:3)	20:0/20:3 or 20:1/20:2 or 18:3/22:0 or 18:1/22:2
			844.4	PC (40:1)	18:1/22:0
			846.4	PC (40:0)	20:0/20:0 and 18:0/22:0

Bold *m/z* values correspond to the most abundant species detected in the LC-MS spectrum; C means the number of total carbon atoms and N represents total number of double bonds in the fatty acyl chains

Phosphatidic acid (PA)

The class of PA was analyzed by LC−MS in negative-ion mode with the formation of $[M - H]^-$ ions (Supplementary Fig. S.5) (214). The major pathways leading to formation of the $[M - H - R_1CO_2H]^-$ and $[M - H - R_2CH{=}C{=}O]^-$ ions are via losses of the fatty acyl substituent as an acid or as a ketene derivative, respectively, for the $[M - H]^-$ ion of PA (Fig. III.10.D) (214). Several molecular species were identified by the LC − MS/MS analysis, including PA and PA-*O* species (Table III.2, Fig. S.5) also bearing PUFAs.

Betaine lipids

Betaine lipids (diacylglyceryl-*N,N,N*-trimethyl-homoserine, DGTS) are a class of acylglycerolipids that have a quaternary amine alcohol ether-linked to a diacylglycerol moiety, and are lacking in phosphorus. The LC−MS spectrum of DGTS (Fig. III.11) was obtained in positive-ion mode and the molecular species of DGTS were identified as $[M + H]^+$ ions (145,156,216).

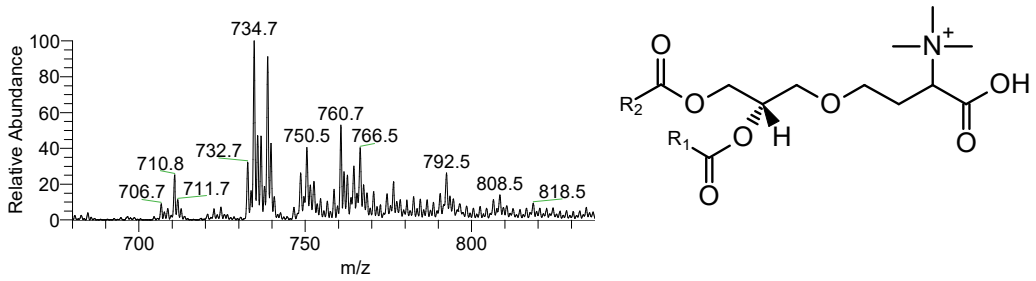

Figure III. 11. LC–MS spectrum of the diacylglyceryl-*N,N,N*-trimethyl-homoserine (DGTS) species, observed by HILIC–ESI–MS as $[M + H]^+$ ions. A general structure is presented.

The LC−MS analysis of DGTS is depicted in the Fig. III.11 and contains several molecular species found in the lipid extract of *C. tomentosum*. The MS/MS spectra of $[M + H]^+$ ions typically showed product ions at *m/z* 236 identified as $C_{10}H_{22}O_5N^+$ considered the diagnostic product ion of this class, resulting from the combined loss of both FA (Fig. III.12.A and B). The most abundant $[M + H]^+$ ion was found at *m/z* 734.7 mainly corresponding to DGTS (16:0/18:3) and minor ions to DGTS (16:1/18:2) and DGTS (14:0/20:3). The second most abundant ion was at *m/z* 740.7 and was attributed to DGTS (16:0/18:0) and DGTS (14:0/20:0) species (Fig. III.11, Table III.3). DGTS species also include 20:3, 20:5, and 22:6 FA.

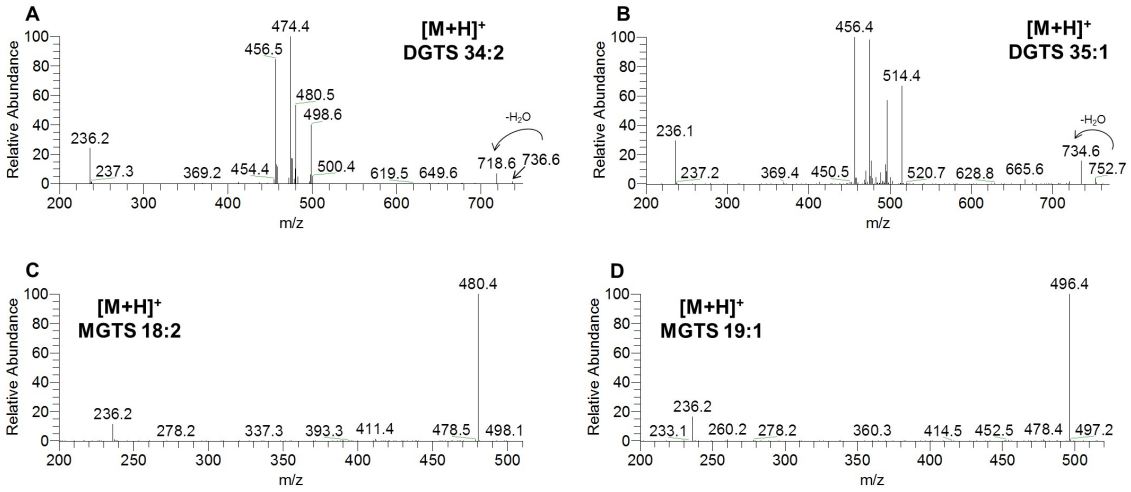

Figure III. 12. ESI–MS/MS spectra of the DGTS (34:2) (A), DGTS (35:1) (B), MGTS (18:2) (C) and MGTS (19:1) (D).

Monoacylglyceryl-*N*,*N*,*N*-trimethyl-homoserine lipids (MGTS) were identified in positive ion mode as $[M + H]^+$ ions (Supplementary Fig. S.6 and Table III.3). These species have not been reported for macroalgae but have already been identified in the green microalgae *Nannochloropsis salina* by using lipidomics (283). The MS/MS spectra of $[M + H]^+$ ions showed product ions at *m/z* 236, considered the diagnostic precursor ion of this class, corresponding to the product of cleavage of the unique FA (Fig. III.12.C and D) (216). Several MGTS were detected and the most abundant were at *m/z* 474.6, attributed to MGTS (16:0), at *m/z* 500.4 attributed to MGTS (18:1), at *m/z* 496.6 to MGTS (18:3) and at *m/z* 522.5 to MGTS (20:4) Supplementary (Fig. S.6).

Table III. 3. Identification of betaine molecular species observed by HILIC–ESI–MS, as $[M + H]^+$, for DGTS and MGTS, with the assignment of the fatty acyl composition of each lipid molecular species, according to the interpretation of the correspondent MS/MS spectra

$[M + H]^+$	Lipid Species	Fatty Acyls Chain	$[M + H]^+$	Lipid Species
m/z	(C:N)		*m/z*	(C:N)
Diacylglyceryl trimethyl-homoserine			Monoacylglyceryl trimethyl-homoserine	
680.7	DGTS (30:2)	14:0/16:2	446.5	MGTS (14:0)
682.7	DGTS (30:1)	14:0/16:1 and 16:0/14:1	470.5	MGTS (16:2)
706.7	DGTS (32:3)	16:0/16:3 and 16:1/16:2 and 14:0/18:3	472.5	MGTS (16:1)
710.7	DGTS (32:1)	14:0/18:1 and 16:0/16:1	**474.5**	**MGTS (16:0)**
732.5	DGTS (34:4)	14:0/20:4 and 16:0/18:4 and 16:1/18:3	494.6	MGTS (18:4)
734.7	**DGTS (34:3)**	**16:0/18:3 and 16:1/18:2 and 14:0/20:3**	**496.5**	**MGTS (18:3)**
736.7	DGTS (34:2)	16:0/18:2 and 16:1/18:1 and 14:0/20:2	498.5	MGTS (18:2)
738.7	DGTS (34:1)	16:0/18:1 and 16:1/18:0 and 14:0/20:1	500.6	MGTS (18:1)
740.7	DGTS (34:0)	16:0/18:0 and 14:0/20:0	512.5	MGTS (19:2)
748.6	DGTS (35:3)	15:0/20:3 and 16:3/19:0	514.5	MGTS (19:1)
750.6	DGTS (35:2)	15:0/20:2 and 16:0/19:2	516.4	MGTS (19:0)
752.6	DGTS (35:1)	16:1/19:0	520.5	MGTS (20:5)
760.6	DGTS (36:4)	18:1/18:3 and 18:0/18:4	522.5	MGTS (20:4)
764.6	DGTS (36:2)	18:1/18:1 and 16:0/20:2	524.5	MGTS (20:3)
766.5	DGTS (36:1)	16:0/20:1 and 16:1/20:0 and 18:0/18:1	528.5	MGTS (20:1)
776.5	DGTS (37:3)	18:3/19:0	554.3	MGTS (22:2)
784.5	DGTS (38:6)	18:1/20:5 and 18:3/20:3		
790.5	DGTS (38:3)	18:0/20:3		
792.5	DGTS (38:2)	18:0/20:2		
794.5	DGTS (38:1)	18:0/20:1		
808.5	DGTS (40:8)	18:2/22:6 and 20:4/20:4		
818.5	DGTS (40:3)	18:0/22:3		

Bold *m/z* values correspond to the most abundant species detected in the LC-MS spectrum; C means the number of total carbon atoms and N represents total number of double bonds in the fatty acyl chains

III.1.1.2. Fatty acid profile

Fatty acids are important components of lipids, being esterified to polar lipids. The identification and quantification of the FA profile of the polar lipidic extract of *C. tomentosum* was performed by GC–MS analysis of methyl esters of FA (Table III.4). The most abundant FA in this species was palmitic 16:0, palmitoleic 16:1, oleic 18:1(*n*-9) and

α-linolenic 18:3(*n*-3) acids. *C. tomentosum* contains others *n*-3 PUFAs like hexadecatrienoic acid 16:3(*n*-3), eicosatrienoic 20:3(*n*-3) and eicosapentaenoic acid 20:5(*n*-3). Odd FA like C_{15}, C_{17} and C_{19} were also identified. It was reported that green algae majorly contain C_{16} and C_{18} PUFAs (97,143).

Table III. 4. Fatty acid profile of total lipid extract from *Codium tomentosum*

Fatty Acyl Chain	**Mean (%)**	**±S. D.**
12:0	tr	
14:0	1.18	0.06
16:0	36.7	1.40
17:0	tr	
18:0	0.80	0.01
19:0	tr	
20:0	tr	
22:0	2.06	0.62
24:0	1.94	0.54
Σ SFA	**44.7**	
16:1*n*-7	2.30	0.68
18:1*n*-9$_{c+t}$	17.3	0.53
Σ MUFA	**19.6**	
16:2	1.52	0.04
16:3*n*-3	8.77	0.21
18:2*n*-6	6.04	0.09
18:3*n*-6	2.59	0.24
18:3*n*-3	13.9	0.48
18:4*n*-3	tr	
20:3*n*-3	0.62	0.04
20:4*n*-6	tr	
20:5*n*-3	2.46	0.09
22:6*n*-3	tr	
Σ PUFA	**35.9**	
Uns/Sat	1.24	
***n*-6/*n*-3**	0.33	

SFA, MUFA, PUFA, saturated, mono- unsaturated, and polyunsaturated fatty acids, respectively; Uns/Sat, unsaturation/saturation ratio. Means (%) and standard deviations (S.D.) were obtained from three replicates; tr., traces (content less than 0.1%)

The results herein presented are consistent with those found in the related literature for the *Codium* species (57,96,143,284) and with FA profile inferred by HILIC−ESI−MS analysis.

III.1.1.3. Discussion

In the present study, the molecular profile of polar lipids from *C. tomentosum* cultivated on land-based IMTA system was identified for the first time using the modern lipidomic approach based on HILIC–LC–MS and MS/MS. The results obtained culminated in the identification of two hundred and thirty-eight molecular species from twelve classes of polar glycolipids, phospholipids, and betaine lipids. No sphingolipids were found.

While LC−MS has been used with success in the characterization of the lipidome of plants and also of microalgae (40,123,156), only two studies have addressed the lipidome of macroalgae (*Chondrus crispus* (145) and *Ulva lactuca* (33,164)). Previous works on lipid composition of *Codium fragile* solely used TLC and GC−MS, pinpointing a restricted number of lipid classes without identifying the molecular species within each class nor detecting less abundant lipid classes (134,135). The results gathered in the present work allowed to unravel the detailed lipid composition giving a full picture at molecular level of polar lipids including GLs, PLs and betaine lipids. In the group of GLs, it were identified MGDG (10 molecular species) and DGDG (22 molecular species) bearing fatty acyl substitution from 16:0 to 20:5, and SQDG (20 molecular species) containing 14:0 to 22:6 FAs with most abundant species combined (16:0/16:0), (18:1/16:0) and (18:3/16:0) FAs. In fact, abundant 16:0 and 18:1 obtained by GC−MS in the FA profile is in accordance with the results reported for *Codium* sp. (91,143) and other green algae such as *Ulva fenestrata* (134). These reported results were based on analytical approaches such as separation of GLs by plate chromatography and further analysis of FA by GC−MS. In the class of DGDG, molecular species containing hydroxy-PUFAs were recently reported in algae species (163). Oxidized FAs, including hydroxylated FAs, are natural occurring metabolites than can be found in plants and other organisms (285). In plants and marine organisms, they can be mainly produced enzymatically by the action of lipoxygenases (286). They are involved in the defense mechanisms and are considered essential components of innate immunity mechanisms (163). The monoacyl sulfoquinovosyl lipids (SQMG or lyso SQDG) were identified, have never been reported in lipidome of *Codium* sp., and were scarcely reported in macroalgae. The major SQMG species detected in the lipid extract of *C. tomentosum* corresponds to SQMG 16:0. This class was found recently in spinach and reported to present an antitumoral effect (287).

Glycolipids are predominantly located in photosynthetic membranes (thylakoid and chloroplasts) (38). Their role is to provide energy and also serve as markers for cellular recognition (10,23,33). The SQDGs are acidic lipids important to maintain the anionic characteristics, thus preserving the structure and function of the thylakoid membranes. Glycolipids have high content in *n*-3 PUFA, being valuable products to be used in functional food, and in the pharmaceutical and cosmetic industries (10). The bioactive properties of SQDG (25,30), altogether with MGDG and DGDG (23,27) species, have been recently highlighted due to their anti-inflammatory activity, with SQDGs being known to display antiviral activity and help in the prevention of cancer (38).

Phospholipids from *C. tomentosum* were identified and distributed by PC (60 molecular species) and LPC (11 molecular species), PI (13 molecular species), PA (9 molecular species), PG (22 molecular species) and LPG (8 molecular species). The PLs in *C. tomentosum* include saturated FA species such as 16:0 and 18:0, unsaturated FA species such as 16:1, 18:1, 18:2, 18:3, 20:2 and 20:5, and PC and PI having 20:5 and 22:6 FA, respectively. The most abundant PC species were PC (16:0/18:1) and PC (18:2/18:2) plus (16:0/20:4). Lyso-PC and lyso-PG, with C_{18} and C_{20} unsaturated acyl chains were identified. Lyso-phospholipids were previously detected in *Ulva lactuca* (164) and *Chondrus crispus* by using LC−MS (145). It is likely that these molecules have not been detected before in macroalgae due to the lack of sensitivity of the approaches based on TLC and GC−MS methodologies commonly employed to screen the lipid profile of these organisms. Previous studies have identified PC, PS, and PE classes in *Codium fragile*, based on chromatographic plates (TLC) and GC−MS analyses, designed to screen for FA composition (97). Nonetheless, the confirmation of the corresponding PL species was not performed by MS and was only tentatively identified by comparison with standards (97). We did not identify PS and PE in the present study. By using TLC, PI and PS migrate closely and some confusion could occur. PS was recently found in *Ulva lactuca* by employing MS-based approach (164). Nevertheless, the identification was based on uncertain patterns of fragmentation and was not consistent with other well documented reference (138).

Phospholipids from algae are considered promising agents to be used in the cosmetic and pharmaceutical industries (28,288), have been described to be beneficial for cognitive functions, and to fight inflammatory diseases (32), also being known to display antiviral,

antibacterial and antitumor properties (116). Also, beneficial effects of PLs on blood and hepatic lipids and both cholesterol and TG levels were suggested (32). Marine PLs proved to have antivirus, antibacterial and antitumor properties (116).

Betaine lipids (DGTS) were identified in the lipidome of *C. tomentosum*. They are widely distributed in algae (36,150,216). By MS-based analysis of the lipidic extract, DGTS molecular species were identified (43 molecular species) and included saturated FA chains such as 14:0, 16:0, 18:0, 20:0 FA, and unsaturated 16:2, 16:3, 18:2, 18:3, 20:4, 20:5 and 22:6 FA species. Betaine lipids have never been recognized before in the genus *Codium*, but DGTS was identified in *Chondrus crispus* and *Ulva lactuca* by LC−MS and MS/MS approaches (145,164). Within betaine lipids, a new class was herein reported in the lipidome of *C. tomentosum* and never reported in macroalgae: the betaine lipids with one acyl chain, MGTS, corresponding to lyso betaine lipids (16 molecular species). No sphingolipids were detected in *C. tomentosum*, in agreement with reports suggesting them to be mainly present in red algae (67,147).

Lipid species bearing odd FAs such as FA 17:0 and 19:0 were identified in polar lipids classes including SQDG, SQMG, DGDG, PG, LPG and PI. The presence of odd numbered FAs is not very usual and could have been contributed by contaminants. However, they can also be part of the lipidome from macroalgae and these odd FAs have already been reported (135,143,284). Traces of C_{15}, C_{17}, and C_{19} have been reported in several published papers for *Codium* species. Fatty acids with odd number were identified esterified in lipid species of glycolipids from *Chondrus crispus*, namely C_{17} and C_{19} species for example in SQDG, PG, and DGTS by a LC−MS approach (145). Odd FAs esterified in SQDG were identified by LC−MS in the lipidome of microalgae *Nannochloropsis oculata* (40) and in SQDG and PG molecular species of *Skeletonema* sp. (160).

Polar lipids in *C. tomentosum* contain PUFAs of the *n*-3 series such 18:3 and 20:5 and as 16:3, mainly provided by GLs and betaine lipids, suggesting the capability of *Codium tomentosum* for synthesize larger PUFAs. Since the human body has a limited ability to convert linolenic acid into the longer-chain *n*-3 FA EPA and DHA, *C. tomentosum* produced in aquaculture under controlled conditions may be a marine source of this essential PUFAs important to health improvement by preventing pathologic conditions such as cancer, cardiovascular, inflammatory and autoimmune diseases (10,95,132).

III.1.2. The lipidome of Rhodophyta

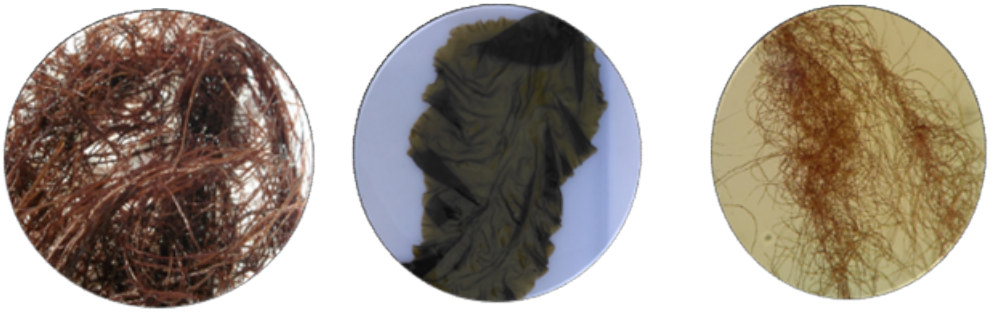

III.1.2.1. The lipidome of *Gracilaria* sp.

Gracilaria sp.*

The data contained this section was published in:

Elisabete da Costa, Tânia Melo, Ana S. P. Moreira, Carina Bernardo, Luisa Helguero, Isabel Ferreira, Maria Teresa Cruz, Andreia M. Rego, Pedro Domingues, Ricardo Calado, Maria H. Abreu and Maria Rosário Domingues, ***Valorization of Lipids from Gracilaria sp. through Lipidomics and Decoding of Antiproliferative and Anti-Inflammatory Activity*****.** Marine Drugs (2017) 15(3), 62.

The lipidome of *Gracilaria* sp.

Gracilaria spp. is one of the world's most cultivated and valuable seaweeds (49,93). Traditionally, its economic importance comes from the phycolloid industry, being the main source of agar (289). Among *Gracilaria* taxonomy, *Gracilaria* sp. thrives in Ria de Aveiro lagoon, Portugal, and is a cosmopolitan in its occurrence (49). Only recently this taxonomic classification was confirmed by Saunders (2009) (58); until then, this species was misidentified as *G. verrucosa and G. bursa-pastoris*. To our best knowledge, there is no studies about characterization of polar lipids profile of these species from aquaculture, neither from the Portuguese coastline (10,203). The present investigation is the first report on the characterization of the lipidome of the edible red seaweed *Gracilaria* sp., cultivated in an integrated multi-trophic aquaculture system by using advanced mass-spectrometry techniques such as hydrophilic interaction liquid chromatography-electrospray ionization mass spectrometry (HILIC−ESI−MS) approach. Lipid extracts from *Gracilaria* sp. are promising phytochemicals with anti-oxidant, anti-inflammatory and antitumor activities, as will be described.

III.1.2.1.1. Polar lipids from *Gracilaria* sp.

The lipid extracts of *Gracilaria* sp. obtained by using methanol/chloroform extraction accounted for about 3000 ± 600 mg/kg dry mass. This lipid extract was mainly composed of glycolipids (1980 ± 148 mg/kg of biomass) and phospholipids (165 ± 53 mg/kg of biomass), and the remaining lipid extract corresponded to betaine lipids and others (Table III.5).

Table III. 5. Composition of lipid extracts of *Gracilaria* sp.

Composition	Mean	SD
Lipids (mg/kg biomass)	3000	600
Glycolipids (mg/kg biomass)	1980	148
Phospholipids (mg/kg biomass)	165	52.7
Betaines and others [1]	855	-

[1]Betaines and others were determined by the difference of lipid content and the sum of content of glycolipids and phospholipids.
Means (%) and standard deviations (S.D.) were obtained from three replicates

The polar lipidome profile of *Gracilaria´*s was determined by HILIC–ESI–MS, and it allowed the identification of glycolipids, phospholipids and betaine lipids. Overall, the lipidome of *Gracilaria* sp. comprised one hundred and forty-seven molecular species.

Glycolipids

The glycolipids identified were monogalactosyl diacylglycerol (MGDG) and digalactosyl diacylglycerol (DGDG), identified in the LC–MS spectra in positive mode as $[M + NH_4]^+$ ions, and sulfoquinovosyl diacylglycerol (SQDG) and sulfoquinovosyl monoacylglycerol (SQMG)**,** identified as negative $[M - H]^-$ ions. Detailed structure of MGDG and DGDG molecular species was also accomplished as $[M + Na]^+$ ions by using ESI-MS/MS after solid phase extraction (SPE) fractionation of lipid extract (fraction 3 rich in glycolipids). Overall, thirty-four molecular species were identified (Fig. III.13) and are described in Table III.6.

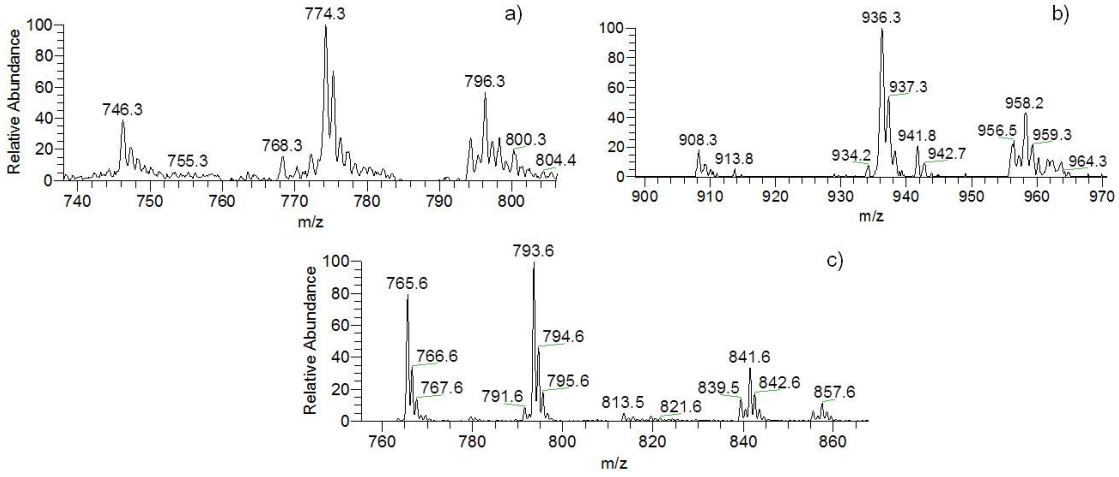

Figure III. 13 LC–MS spectra of the GLs classes a) monogalactosyl diacylglyceride (MGDG) and b) digalactosyl diacylglyceride (DGDG) observed by HILIC–ESI–MS as $[M + NH_4]^+$ ions, and c) sulfoquinovosyl diacylglyceride (SQDG) observed as $[M - H]^-$ ions.

Monogalactosyl diacylglycerol and digalactosyl diacylglycerol

Galactolipids included nine MGDG molecular species and ten DGDG molecular species (Table III.6, Figure III.13 a)). The most abundant MGDG molecular species were found at *m/z* 774.3 and 796.3 $[M + NH_4]^+$, corresponding to MGDG (18:1/16:0) and to MGDG (20:4/16:0), with a minor contribution from MGDG (18:2/18:2). Other MGDG molecular species identified contained in their composition 14-, 16-, and 18-carbon saturated fatty

acids (SFAs) and monounsaturated fatty acids (MUFAs) and 18:2, 20:4, and 20:5 polyunsaturated fatty acyl (PUFAs) moieties (Table III.6). Regarding DGDGs, the most abundant molecular species were identified as $[M + NH_4]^+$ ions at *m/z* 936.3, corresponding to DGDG (18:1/16:0), followed by DGDG (20:4/16:0) with minor contribution of DGDG (18:2/18:2) at *m/z* 958.2. Moreover, other DGDG molecular species were identified containing 14-, 16-, 18-, and 20-carbon fatty acids (FAs) such as 20:4 and 20:5 PUFAs.

Table III. 6. Identification of MGDG and DGDG molecular species observed by HILIC–ESI–MS as $[M + NH_4]^+$ ions and SQDG and SQMG molecular species observed as $[M - H]^-$ ions in *Gracilaria* sp.

$[M + NH_4]^+$	**Lipid Species**	**Fatty Acyl Chains**
m/z	(C:N)	
	Monogalactosyl diacylglycerol	
746.3	MGDG (32:1)	16:1/16:0 and 14:0/18:1
748.3	MGDG (32:0)	16:0/16:0 and 14:0/18:0
774.3	MGDG (34:1)	**18:1/16:0**
776.3	MGDG (34:0)	18:0/16:0
794.3	MGDG (36:5)	20:5/16:0
796.3	MGDG (36:4)	**20:4/16:0 and 18:2/18:2**
	Digalactosyl diacylglycerol	
908.3	DGDG (32:1)	16:1/16:0 and 14:0/18:1
910.3	DGDG (32:0)	16:0/16:0 and 14:0/18:0
934.3	DGDG (34:2)	18:2/16:0 and 18:1/16:1
936.3	DGDG (34:1)	**18:1/16:0**
956.3	DGDG (36:5)	20:5/16:0
958.3	DGDG (36:4)	**20:4/16:0 and 18:2/18:2**
$[M - H]^-$	**Lipid Species**	**Fatty Acyl Chains**
	Sulfoquinovosyl diacylglycerol	
763.6	SQDG (30:1)	14:0/16:1
765.6	SQDG (30:0)	**14:0/16:0**
791.6	SQDG (32:1)	16:1/16:0 and 14:0/18:2
793.6	SQDG (32:0)	**16:0/16:0 and 14:0/18:0**
813.6	SQDG (34:4)	18:4/16:0
817.6	SQDG (34:2)	18:2/16:0
819.6	SQDG (34:1)	18:1/16:0
839.6	SQDG (36:5)	20:5/16:0
841.6	SQDG (36:4)	**20:4/16:0**
857.6	SQDG (36:4-OH)	20:4-OH/16:0
	Sulfoquinovosyl monoacylglycerol	
527.4	SQMG (14:0)	
553.4	SQMG (16:1)	
555.4	SQMG (16:0)	

Bold *m/z* values correspond to the most abundant species detected in the LC-MS spectrum; C means the number of total carbon atoms and N represents total number of double bonds in the fatty acyl chains

Sulfolipids

The SQDG molecular species were analyzed in the negative-ion mode and observed as $[M-H]^-$ ions (Fig. III.13.c). The most abundant species were attributed to SQDG (14:0/16:0), SQDG (16:0/16:0) and SQDG (16:0/20:4), observed as $[M - H]^-$ ions at *m/z* 765.5, 793.5, and 841.6, respectively. The fatty acyl signature of SQDGs included 14-, 16-, 18-carbon SFAs and MUFAs and 18- and 20-carbon PUFAs ((Table III.6, Fig. III.13 c). Three SQMGs were identified, namely SQMG (14:0), SQMG (16:0), and SQMG (16:1). SQMGs were never before reported in the lipidome of macroalgae from the genus *Gracilaria*. Glycolipids have already been identified for members of the Rhodophyta (red seaweeds), namely in the genus *Gracilaria*, however, the majority of published works only identified a few species of glycolipids, either by using offline TLC-MS (134,181,290) or selected solvent extraction and MS analysis (33,224). More recently, a detailed profile of *Chondrus crispus* was reported using LC−MS and MS/MS (145).

Phospholipids

The lipidome of *Gracilaria* sp. hold eighty-seven molecular species of phospholipids (PLs) within eight classes, namely phosphatidylglycerol (PG) and lyso-PG (LPG), phosphatidylcholine (PC) and lyso-PC (LPC), phosphatidylethanolamine (PE), phosphatidylinositol (PI), inositol phosphoceramide (IPC) and phosphatidic acid (PA). PC is a main component of extraplastidial membranes, while PG is found in chloroplastic membranes (15).

Phosphatidylcholine and lyso-PC

About thirty-nine PCs were identified by LC–MS as $[M + H]^+$ and confirmed in the negative-ion mode as $[M + CH_3COO]^-$ ions (Fig. III.14.a)). The most abundant ions were observed at *m/z* 760.6 and at *m/z* 782.6, respectively attributed to PC (16:0/18:1) and to PC (16:0/20:4) with a minor contribution of PC (18:2/18:2). Other PC molecular species were identified and contained 14- to 22-carbon fatty acids. Lyso-PC consisted of eight molecular species (Table III.7, Fig III.14. b) and the most abundant was LPC (20:4), observed at *m/z* 544.4. All molecular species identified are described in Table III.7.

Phosphatidylglycerol

Thirteen PGs and four lyso-PGs species were identified by LC–MS as $[M - H]^-$ ions (Table III.7, Figure III.14 c). The most abundant ion was observed at *m/z* 769.4, mainly corresponding to PG (16:0/20:4), with a minor contribution from PG (18:2/18:2). The prominent lyso-PG at *m/z* 483.3 was LPG (16:0) (Fig. III.14 d), Table III.7).

Phosphatidylethanolamine

The class of PE contained eight molecular species, identified as $[M + H]^+$ (Table III.7, Fig. III.14. f). The most abundant ion was observed at *m/z* 716.4 and identified as PE (16:1/18:1) and PE (16:0/18:2). Other PEs were observed at *m/z* 742.3 and 744.3 (Fig. III.14. e), attributed to the PE (18:1/18:2) and PE (18:1/18:1)**.**

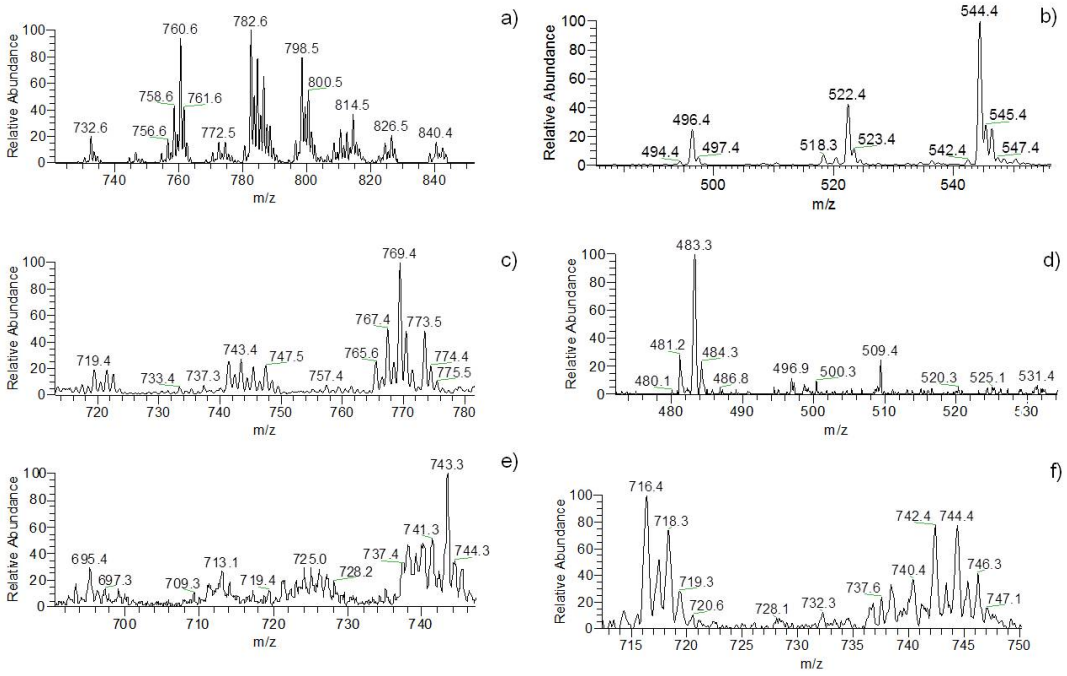

Figure III. 14. LC−MS spectra of the classes a) phosphatidylcholine (PC) and b) lyso phosphatidylcholine (LPC) observed as $[M + H]^+$ ions; c) phosphatidylglycerol (PG) and d) lyso phosphatidylglycerol (LPG) observed as $[M - H]^-$ ions; e) phosphatidic acid (PA) observed as $[M - H]^-$ ions and f) phosphatidylethanolamine (PE) observed as $[M + H]^+$ ions.

Phosphatidylinositol

The class of PI was observed as $[M - H]^-$ ions at *m/z* 833.5 and 835.5 and attributed to PI (16:1/18:1) and PI (16:0/18:1), respectively.

Phosphatidic acid

Eight PAs were identified (Table III.7, Fig. III.14. e), with the most abundant species identified as PA (20:4/20:4) at *m/z* 743.3, while the other PA molecular species were esterified to 16:0, 18:1, 18:2, 18:3, 20:3, 20:4, and 20:5 FAs.

Table III.7. Identification of phospholipid molecular species observed by HILIC–ESI–MS, as $[M + H]^+$ ions for PC, LPC, and PE and as $[M - H]^-$ ions for PG, LPG, PI, PA, and IPC in *Gracilaria* sp.

$[M + H]^+$	**Lipid Species**	**Fatty Acyls Chain**
m/z	**(C:N)**	
	Phosphatidylcholine	
732.6	PC (32:1)	16:0/16:1 and 14:0/18:1
734.6	PC (32:0)	16:0/16:0 and 14:0/18:0
754.6	PC (34:4)	14:0/20:4 and 16:2/18:2
756.6	PC (34:3)	16:0/18:3 and 14:0/20:3
758.6	PC (34:2)	16:0/18:2 and 16:2/18:1
760.6	PC (34:1)	**16:0/18:1**
762.6	PC (34:0)	16:0/18:0
780.6	PC (36:5)	16:0/20:5 and 18:2/18:3
782.6	PC (36:4)	**16:0/20:4 and 18:2/18:2**
784.6	PC (36:3)	16:0/20:3 and 18:1/18:2
786.6	PC (36:2)	18:0/18:2 and 18:1/18:1
788.6	PC (36:1)	18:0/18:1
798.5	PC (37:3)	16:0/21:3 and 18:1/19:2
804.5	PC (38:7)	18:3/20:4 and 18:2/20:5
806.5	PC (38:6)	18:2/20:4 and 18:1/20:5
808.5	PC (38:5)	18:1/20:4 and 18:2/20:3
810.5	PC (38:4)	18:1/20:3 and 16:0/22:4
812.5	PC (38:3)	18:0/20:3 and 18:1/20:2
814.5	PC (38:2)	16:0/22:2 and 18:1/20:1
818.5	PC (38:0)	18:0/20:0 and 16:0/22:0
840.4	PC (40:3)	18:1/22:2
844.4	PC (40:1)	18:1/22:0
	Lyso-phosphatidylcholine	
494.4	LPC (16:1)	
496.4	LPC (16:0)	
518.4	LPC (18:3)	
520.4	LPC (18:2)	
522.4	LPC (18:1)	
524.4	LPC (18:0)	
542.4	LPC (20:5)	
544.4	**LPC (20:4)**	
	Phosphatidylethanolamine	
716.4	PE (34:2)	**16:1/18:1 and 16:0/18:2**
718.3	PE (34:1)	16:1/18:0 and 16:0/18:1
740.4	PE (36:4)	18:2/18:2
742.4	PE (36:3)	18:1/18:2
744.4	PE (36:2)	18:1/18:1
746.3	PE (36:1)	18:0/18:1
$[M - H]^-$	**Lipid Species**	**Fatty Acyl Chains**
	Phosphatidylglycerol	

717.4	PG (32:2)	16:1/16:1 and 16:0/16:2
719.4	PG (32:1)	16:0/16:1
721.4	PG (32:0)	16:0/16:0
741.4	PG (34:4)	16:0/18:4
743.5	PG (34:3)	16:0/18:3
745.5	PG (34:2)	16:1/18:1
747.5	PG (34:1)	16:0/18:1 and 16:1/18:0
767.5	PG (36:5)	16:0/20:5
769.4	PG (36:4)	**16:0/20:4 and 18:2/18:2**
773.5	PG (36:2)	18:1/18:1
	Lyso-phosphatidylglycerol	
481.3	LPG (16:1)	
483.3	**LPG (16:0)**	
509.3	LPG (18:1)	
531.3	LPG (20:4)	
	Phosphatidylinositol	
833.5	PI (34:2)	16:1/18:1
835.5	PI (34:1)	16:0/18:1
	Phosphatidic acid	
693.4	PA (36:5)	16:0/20:5
695.4	PA (36:4)	16:0/20:4
717.4	PA (38:7)	18:3/20:4
719.4	PA (38:6)	18:2/20:4
721.4	PA (38:5)	18:1/20:4
741.3	PA (40:9)	20:4/20:5
743.3	PA (40:8)	**20:4/20:4**
745.3	PA (40:7)	20:3/20:4
	Inositol phosphoceramide	
810.5	IPC (*t*35:0)	***t*18:0/17:0**
908.6	IPC (*t*42:0)	*t*18:0/24:0
920.6	IPC (*t*42:2-OH)	***t*18:1/24:1-OH**
922.6	IPC (*t*42:1-OH)	*t*18:0/24:1-OH
924.6	IPC (*t*42:0-OH)	*t*18:0/24:0-OH

Bold *m/z* values correspond to the most abundant species detected in the LC-MS spectrum; C means the number of total carbon atoms and N represents number of double bonds in the fatty acyl chains

Inositol phosphoceramide (IPC)

Five molecular species were assigned as IPCs (Fig. III.15. a), Table III.7) and the most abundant ones were IPC (*t*18:0/17:0), observed at *m/z* 810.5, and IPC (*t*18:1/24:1-OH), observed at *m/z* 920.6 (Fig. III.15. b). LC–MS/MS spectrum of the $[M - H]^-$ ions of IPCs, as exemplified for IPC at *m/z* 920.6, showed the typical fragmentation pathways of IPCs such as the losses of 162 Da and 180 Da, due to elimination of inositol, the product ion at *m/z* 538.3 resulting from the loss of hydroxy-fatty acyl chains, and the product ion at *m/z* 259.0 that corresponded to an inositol monophosphate anion. IPCs identified in lipid extract of *Gracilaria* sp. are considered an important biomarker of Rhodophyta taxonomy, in accordance with what was already reported for *Chondrus crispus* using a lipidomic approach (145). IPCs are required to maintain membrane properties such as viscosity and

electrical charge and participate in the control of enzymatic activity or act as membrane anchors for some proteins [44].

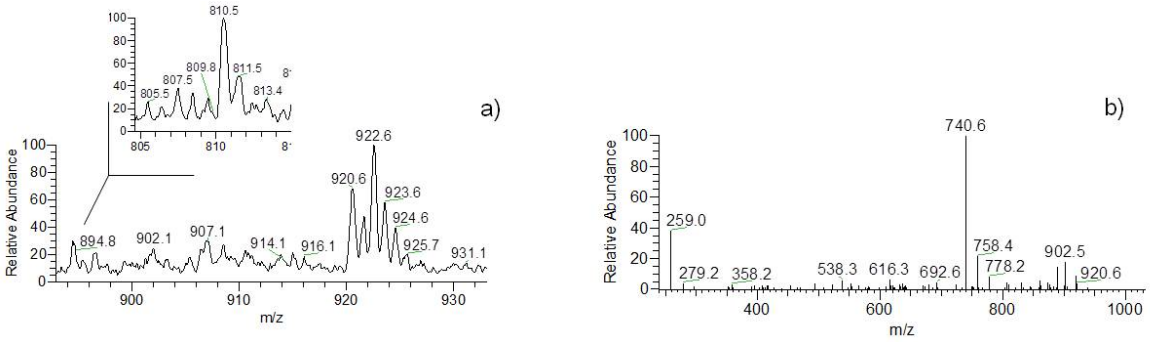

Figure III. 15. a) LC–MS spectrum of inositol phosphoceramide (IPC) observed by HILIC–ESI–MS as $[M - H]^-$. ions; b) LC−MS/MS spectrum of $[M - H]^-$ ions of IPC at *m/z* 920.6 (IPC (*t*18:1/24:1-OH).

Betaine lipids

Twenty-one DGTS and five MGTS molecular species were identified by LC−MS and MS/MS as $[M + H]^+$ ions (Fig. III.16 and Table III.8). The most abundant DGTS species was found at *m/z* 710.7, corresponding to DGTS (16:0/16:1), with a minor contribution from DGTS (14:0/18:1) species, followed by DGTS (18:1/18:1) observed at *m/z* 764.8. Overall, DGTSs combine distinctive molecular species bearing different combinations of FAs, ranging between 14- and 20-carbon FAs, as reported on Table III.8. MGTSs comprised MGTS (14:0), MGTS (16:1), MGTS (16:0), MGTS (18:2), and MGTS (18:1) species, identified at *m/z* 446.5, 472.5, 474.5, 498.6, and 500.6, respectively.

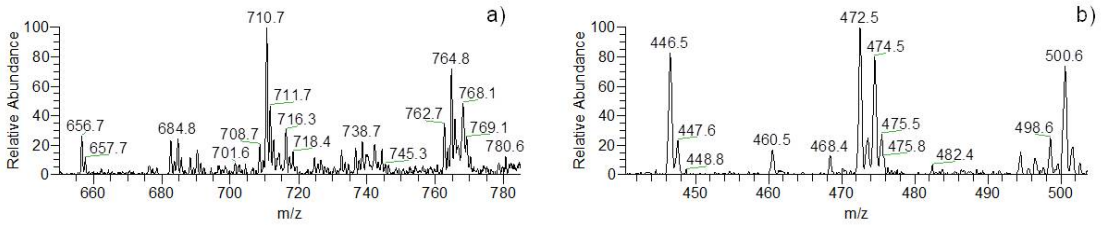

Figure III. 16. LC–MS spectra of a) diacylglyceryl-*N*,*N*,*N*-trimethyl-homoserine species (DGTS) and b) monoacylglyceryl-*N,N,N*-trimethylhomoserine (MGTS), observed by HILIC–ESI–MS as $[M + H]^+$ ions.

Table III. 8. Identification of betaine molecular species observed by HILIC–ESI–MS as $[M + H]^+$ ions of DGTS and MGTS in *Gracilaria* sp.

$[M + H]^+$	Lipid Species	Fatty Acyls Chain
m/z	**(C:N)**	
Diacylglyceryl trimethyl-homoserine		
656.7	DGTS (28:0)	14:0/14:0
682.7	DGTS (30:1)	14:0/16:1
684.8	DGTS (30:0)	14:0/16:0
708.7	DGTS (32:2)	16:1/16:1 and 14:0/18:2
710.7	DGTS (32:1)	**16:0/16:1 and 14:0/18:1**
712.7	DGTS (32:0)	16:0/16:0 and 14:0/18:0
732.7	DGTS (34:4)	16:2/18:2 and 14:0/20:4
734.7	DGTS (34:3)	16:1/18:2
736.7	DGTS (34:2)	16:0/18:2 and 16:1/18:1
738.7	DGTS (34:1)	16:0/18:1 and 16:1/18:0
740.7	DGTS (34:0)	16:0/18:0 and 14:0/20:0
760.6	DGTS (36:4)	16:0/20:4
764.8	DGTS (36:2)	**18:1/18:1**
766.8	DGTS (36:1)	18:0/18:1
Monoacylglyceryl trimethyl-homoserine		
446.5	MGTS (14:0)	
472.5	MGTS (16:1)	
474.5	MGTS (16:0)	
498.6	MGTS (18:2)	
500.6	MGTS (18:1)	

Bold *m/z* values correspond to the most abundant species detected in the LC-MS spectrum; C means the number of total carbon atoms and N represents number of double bonds in the fatty acyl chains

III.1.2.1.2. Fatty acid profile

The fatty acid profile of the lipid extract was characterized by GC−MS analysis of fatty acid methyl esters (FAMEs). The profile of fatty acids included 14:0, 16:0, 18:0, 18:1(*n*-9), 18:2(*n*-6), 20:4(*n*-6), and 20:5(*n*-3), among which 16:0 (48.5 ± 1.1%), 18:1(*n*-9) (14.4 ± 0.38%), and 20:4(*n*-6) (13.6 ± 0.46%) were the most abundant (Table III.9). Overall, SFA accounted for 57.5% of the total FA identified, followed by MUFA (18.3%) and PUFA (18.4%). The fatty acids identified by GC−MS were esterified to polar lipids of *Gracilaria* sp., as assigned by LC−MS and MS/MS analysis.

The *n*-6/*n*-3 ratio determined for our *Gracilaria* sp. sample was 3.69. The World Health Organization (WHO) recommends an optimal balance intake of *n*-6 PUFAs and *n*-3 PUFAs to prevent chronic diseases and that this balance should be maintained with an adequate daily dosage of *n*-6 PUFAs (5%–8% of daily energy intake) and *n*-3 PUFAs (1%

– 2% of daily energy intake, World Health Organization, 2003). With this recommendation in mind, it is possible to estimate that a suitable *n*-6/*n*-3 ratio is less than 5. Also, some authors reported that a ratio of *n*-6/*n*-3 less than 4 is adequate in the prevention of several diseases such as cardiovascular (291), autoimmune (292), and inflammatory diseases (292), and cancer (236). These findings support the advantage of the use of *Gracilaria* sp. as a source of *n*-6 and *n*-3 for human consumption.

Table III. 9. Fatty acid profile of lipids from *Gracilaria* sp. determined by GC–MS analysis of fatty acid methyl esters (FAMEs)

Fatty Acyl Chain	**Mean (%)**	**± S. D.**
14:0	5.25	0.58
16:0	48.5	1.26
18:0	2.85	1.29
24:0	0.95	0.12
Σ SFA	**43.5**	
14:1*n*-5	0.41	0.01
16:1*n*-7	3.49	0.29
18:1*n*-9$_{c+t}$	14.4	0.42
Σ MUFA	**18.3**	
18:2*n*-6	0.88	0.08
20:4*n*-6	13.6	0.50
20:5*n*-3	3.92	0.17
Σ PUFA	**18.4**	
Uns/Sat	0.64	
***n*-6/*n*-3**	3.69	

SFA, MUFA, PUFA, saturated, mono- unsaturated, and polyunsaturated fatty acids, respectively; Uns/Sat, unsaturation/saturation ratio. Means (%) and standard deviations (S.D.) were obtained from three replicates (content less than 0.1% not shown)

III.1.2.1.3. Photosynthetic Pigments

Chlorophyll and pheophytin derivatives were identified in the lipid extracts by LC–MS in positive-ion mode as $[M + H]^+$ ions (Supplementary Fig. S.7, Table III.10) (104,145,293). The LC–MS/MS spectra of chlorophyll derivatives showed product ions formed due to the neutral losses of 278 Da (loss of phytyl side chain as an alkene, $[M – C_{20}H_{38}]^+$), 310 Da (loss of 278 plus 32, which means loss of phytyl plus 32 Da) and 338 (loss of 278 plus 60 Da). In the case of pheophytin derivatives, the LC–MS/MS spectra showed ions formed by the losses of 278 Da and 338 (loss of 278 plus 60, which means loss of phytyl plus $HCOOCH_3$).

Pheophytin derivatives such as pheophorbide were found at *m/z* 593.5 and 607.4. The identification of these molecular species corroborates the reports of previous studies (104,145,261,293,294). As shown in Table III.10 the extract of *Gracilaria* sp. *contains* chlorophyll a, 15-OH-lactone chlorophyll, pheophytin a, pheophytin d, hydroxypheophytin and pheophorbide a and b. Table III.11 refers to the proximate composition of pigments in the methanolic extract.

Table III. 10. UV and MS spectral data of chlorophylls and their derivatives extracted from *Gracilaria* sp.

$[M+H]^+$	λ_{max} (reported)	**Species**
m/z		
593.5	409	Pheophorbide a
607.4	409	Pheophorbide b
609.4		Chlorophyl derivative
871.8	408, 506, 536, 608, 666	Pheophytin a
873.8	408, 506, 536, 608, 666	Pheophytin d
887.6	408, 504, 534, 610, 666	Hydroxypheophytin a
893.5	430,618,664	Chlorophyll a
903.6		15-hydroxypheophytin a lactone

Table III. 11. Pigments content on the methanolic extract of *Gracilaria* sp. IMTA cultured.

Methanolic extract	
Pigments (µg g^{-1} biomass)	
Chl a	267
Carotenoids	15.3

III.1.2.2. The lipidome of *Porphyra dioica*

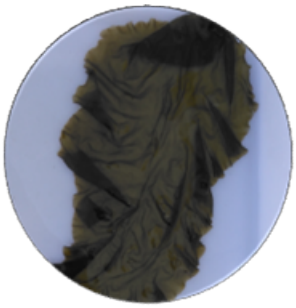

Porphyra dioica: blade

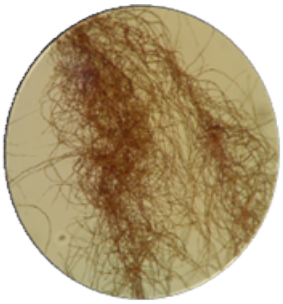

Porphyra dioica: conchocelis

This section is part of the manuscript submitted for publication on “Molecules” (by invitation):

Elisabete da Costa, Vitor Azevedo, Tânia Melo, Andreia M. Rego, Pedro Domingues, Dmitry V. Evtuguin, Ricardo Calado, Maria H. Abreu and Maria Rosário Domingues, ***High-Resolution Lipidomics of the Early Life Stages of the red seaweed*** **Porphyra dioica,** on "Phytochemicals: Biosynthesis, Metabolism and Biological Activities", Molecules (2018, IF 2.861). Gentle invitation of Prof. Dr. Marcello Iriti (Milan State University, Italy).

The lipidome of *Porphyra dioica*

Porphyra spp. (Bangiales, Rhodophyta) are commercially important macroalgae produced and traditionally consumed in Asia for nutrition and with recognized human health benefits (61,62). In Western countries the consumption of *Porphyra* (Nori) is increasing, mainly due to the "sushi" trend but also for being considered as part of the super foods list with health promotion claims. The increasing demand prompted by a spreading consumption habits, the need of high-quality biomass, and locally sourced food, has been promoting the aquaculture crops of genus *Porphyra*, among is *Porphyra dioica* (J. Brodie & L. M. Irvine, 1997-World Register of Marine Species) (63). This species is native to the Atlantic and its cultivation started in the late 90´ in collaboration between Portugal and North American researchers (295). At present, the first steps in its commercial production is realized by ALGAplus Lda, where the full life cycle of the species is completed, with continuous organic production of conchocelis and blades, in a land-based IMTA system (60,295).

Porphyra dioica has a unique trimorphic life history and two of the stages were analyzed in the present work: the blade and conchocelis phases (65,66). Blades are the gametophyte phase of *Porphyra* spp., being the most commercially relevant stage and used mainly for nutrition and other high value biotechnological applications (1,21). *Porphyra* species are also a source of diverse metabolites such as peptides, sulfated polysaccharides (296), or valuable lipids such as *n*-3 and *n*-6 PUFAs (297).

Lipids from macroalgae are mainly composed of polar lipids that are a source of esterified FA (18). Some studies suggested that they have a vast array of biological activities (23,30,181). Polar lipids from *Porphyra* sp. were reported to display anti-inflammatory properties by downregulation of LPS-induced pro-inflammatory responses in human macrophages through inhibition of IL-6 and IL-8 production (23,224) and antitumoral activities such as telomerase-inhibition effect (298). However, there is still a gap in the knowledge of its lipidome and related health benefits. The early-stage filaments of *Porphyra,* conchocelis, are already used in cosmetics but not routinely consumed for food, are at present being surveyed by researchers, as it can be a potential source of PUFAs namely 20:5(*n*-3) FA (299,300). Nowadays, it can be vegetatively propagated in controlled

conditions, with the advantages of exhibiting a fast growth and controlled cost production of standardized biomass (61,206,299). In fact, and similarly to microalgae (1,301), conchocelis can be used to produce biomass enriched in target compounds such as lipids with nutritional and biological added-value and for distinct applications (62,296,298,302,303). In Asia, conchocelis (from *Pyropia* spp.) was typically cultivated on oyster shells (62). However, for the first time in the case of *Porphyra dioica*, the Portuguese farmer partners of this study were able to overcome that need and developped an easier processes, with the potential for outdoor cultivation of conchocelis (60).

Lipids from macroalgae are considered a source of valuable compounds for food and pharma and have been bioprospected worldwide (6). Glycolipids anchor potential health benefits to be used for food and feed and for biotechnological applications (23,86,304). Phospholipids have a superior nutritional source of *n*-3 PUFAs for food industries, but are also good for pharmaceutical applications due to the beneficial impact on the central nervous system and their recognized antitumoral effects (32,116,288). These molecules are also used as vehicles or carriers in dermatologic delivery systems and skin moisturizing products in the cosmetics industry (32).

The lack of knowledge on the lipidome of *Porphyra*, at molecular level, has encourage us to identify and characterize the polar lipid profile of the conchocelis phase (indoor nursery) and young blades (outdoor cultures) of *Porphyra dioica* (*P. dioica*) from in land-based IMTA system. To achieve this unprecedented characterization, we have used hydrophilic interaction chromatography coupled to Q–Exactive high resolution−mass spectrometry instrument (LC−MS). This approach will allow to unveil the composition of these distinct life stages of *Porphyra dioica* and contribute to a better understanding on the lipid dynamics along the life cycle of this alga. Moreover, this study will also provide valuable clues on the potential bioactive properties and nutritional value, as source of *n*-3 and *n*-6 FA, for the different life stages of this macroalgae fostering the integral valorization of *Porphyra dioica* as food, feed or other high end biotechnological applications.

III.1.2.2.1. Polar lipids from *Porphyra dioica*

The lipid extracts of the two life stages of *P. dioica* analyzed in the present study accounted for about 8.60 ± 1.20 g/kg dry biomass of blade and 10.8 ± 0.90 g/kg dry

biomass of conchocelis. These results are in accordance with those previously reported for *Porphyra* spp. in other studies, which ranged between 2.5 - 10.3 g/kg of biomass (305,306).

The profile of polar lipids from the extracts of blade and conchocelis eluted in HILIC−LC−MS is represented in Figure III.17. Differences between chromatograms of both stages were reflected on peak abundance eluted at 5 minutes in positive mode (Fig. III.17. B and C) and at 2, 5 and 19 minutes in the negative mode (Fig. III.18, B´and C´), slight higher in the analysis of the lipidome from conchocelis and particularly attributed to the elution of phospholipids after the comparison with standards profile. However, based on LC–MS analysis, we found the same classes of polar lipids in both life cycle stages: glycolipids, betaines and PL, although with some different profile mainly observed in PLs category.

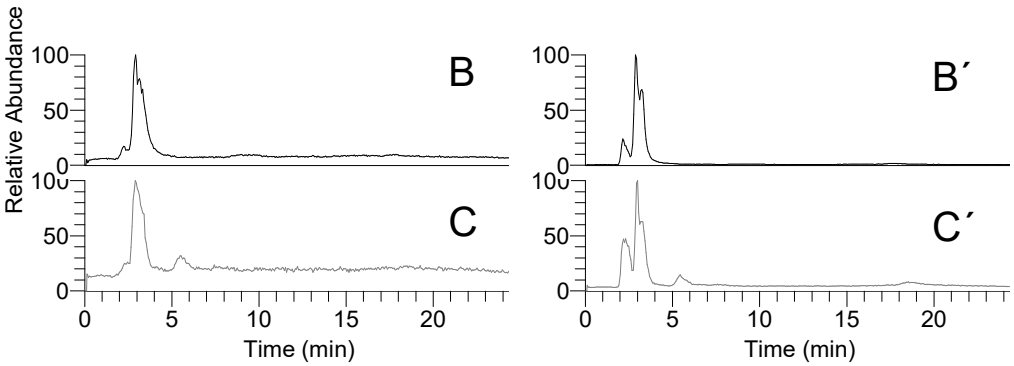

Figure III. 17. LC–MS chromatograms of *Porphyra dioica* blade (B) and conchocelis (C) stages observed by HILIC–MS, acquired in the positive mode and blade (B´) and conchocelis (C´) acquired in the negative mode.

The analysis of the MS data & mass accuracy and the MS/MS spectra from the lipid extracts of *P. dioica* blade and conchocelis stages provided the detailed structural information to identify the different lipid classes at molecular level in each life cycle stage. The analysis of lipid classes allowed the identification of glycolipids (GLs), phospholipids (PLs), and betaine lipids *in P. dioica* lipid extracts will be detailed.

Glycolipids

The analysis of total lipid extracts allowed the identification of galactolipids and sulfolipids (Table III.12, Fig. III.18). MGDG and DGDG were identified by LC–MS as $[M + NH_4]^+$ ions (Fig. III.18.a-b), Table III.12). GLs are important membrane lipids located in

photosynthetic membranes (thylakoid and chloroplast membranes) (15,134). MGDG and DGDG were identified by LC–MS as $[M + NH_4]^+$ ions. MGDG included five and six molecular species and DGDG contained four molecular species assigned in blade and conchocelis lipidome, respectively. Both life stages contained the abundant MGDG (20:5/16:0) at *m/z* 794.6. The MGDG (20:4/16:0) and MGDG (18:1/16:0) (*m/z* 796.6 and *m/z* 774.6, respectively) were also abundant in conchocelis extracts and a source of eicosapolyenoic acid 20:4(*n*-6). MGDG (18:1/18:0) at *m/z* 802.6 was not observed in blade lipidome. The most abundant DGDG in both stages was DGDG (20:5/16:0) at *m/z* 956.6. In the case of conchocelis the second most abundant molecular species was the DGDG (18:1/16:0) at *m/z* 936.7, matching with results observed in the MGDG class. The remaining molecular species included 18:2 FA, a precursor of omega-pathway (114,163).

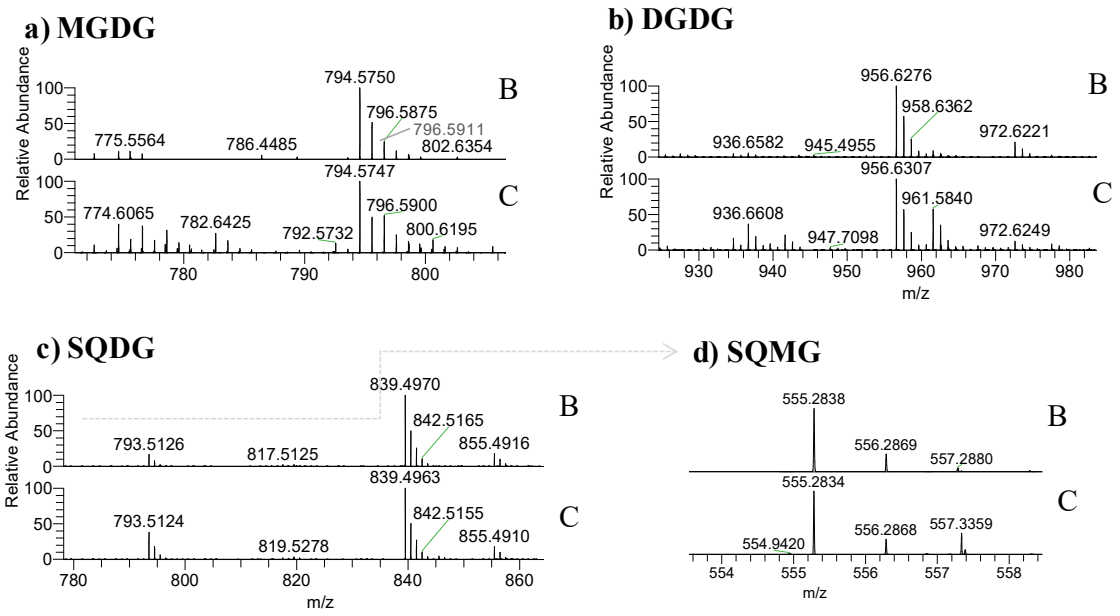

Figure III. 18. LC–MS spectra of glycolipids from *Porphyra dioica* blade (B) and conchocelis (C) stages: a) MGDG and b) DGDG observed by HILIC–LC–MS as $[M + NH_4]^+$ ions, c) SQDG and d) SQMG observed as $[M - H]^-$ ions.

The anionic sulfolipids SQDG and SQMG were identified in both stages as $[M - H]^-$ ions. Overall, four SQDGs were identified and were common in both stages. SQDG (20:5/16:0) at *m/z* 839.5 was the most abundant. Other molecular species combining 16:0 plus 18:2, 20:4 and 20:5 FA were observed. Only one SQMG (16:0), a lyso-SQDG, was identified in the lipidome of blades and conchocelis (*m/z* 555.3). Sulfolipids have a

functional role in the "plastid membrane mosaic" that relies particularly in signaling and coordinating between chloroplast lipids and cytosolic partners (122).

Table III. 12. Identification of glycolipid molecular species observed by HILIC–LC–MS in *Porphyra dioica* blade and conchocelis, MGDG and DGDG molecular species were identified as $[M + NH_4]^+$ ions and SQDG and SQMG as $[M - H]^-$ ions

Galactolipids $[M + NH_4]^+$		**Fatty acyl composition**	
m/z Theoretical	**(C:N)**	**Blade**	**Conchocelis**
Monogalactosyl diacylglycerol			
772.594	MGDG (34:2)	18:2/16:0	18:2/16:0
774.609	MGDG (34:1)	18:1/16:0	**18:1/16:0**
794.578	MGDG (36:5)	**20:5/16:0**	**20:5/16:0**
796.594	MGDG (36:4)	20:4/16:0	**20:4/16:0**
800.624	MGDG (36:2)	18:0/18:2	18:2/18:0
802.641	MGDG (36:1)	----------	18:1/18:0
Digalactosyl diacylglycerol			
934.647	DGDG (34:2)	18:2/16:0	18:2/16:0
936.662	DGDG (34:1)	18:1/16:0	**18:1/16:0**
956.631	DGDG (36:5)	**20:5/16:0**	**20:5/16:0**
972.626	DGDG (36:5-OH)	20:5-OH/16:0	20:5-OH/16:0
Sulfolipids $[M - H]^-$		**Fatty acyl composition**	
m/z Theoretical	**(C:N)**	**Blade**	**Conchocelis**
Sulfoquinovosyl monoacylglycerol			
555.284	SQMG 16:0	**16:0**	**16:0**
Sulfoquinovosyl diacylglycerol			
793.514	SQDG (32:0)	16:0/16:0	16:0/16:0
817.514	SQDG (34:2)	18:2/16:0	18:2/16:0
839.498	SQDG (36:5)	**20:5/16:0**	**20:5/16:0**
855.493	SQDG (36:5-OH)	20:5-OH/16:0	20:5-OH/16:0

Numbers in parentheses (C:N) indicate the number of carbon atoms (C) and number of double bonds (N) in the fatty acid side chains. Bold represents the abundant molecular species

Phospholipids

The PLs classes identified in *Porphyra dioica* were phosphatidic acid (PA), phosphatidylglycerol (PG), lyso-PG (LPG), phosphatidylcholine (PC), lyso-PC (LPC), phosphatidylethanolamine (PE), lyso-PE (LPE), phosphatidylinositol (PI), lyso-PI (LPI), and inositol phosphoceramide lipids (IPC) (Figure III.19, Table III.13).

Phosphatidylcholine and lyso - PC

Twenty-seven PCs were identified in blade stage and seventeen PCs in conchocelis stage by LC−MS as $[M + H]^+$ (Table III.13, Fig. III.19. a) and confirmed in the negative-ion mode as $[M + CH_3COO]^-$ ions. The most abundant PC was common to both stages and attributed to PC (18:1/18:1) at *m/z* 786.6, with minor contribution of PC (18:0/18:2). The second prominent PC in the lipidome of blades was PC (16:0/20:3) at *m/z* 784.6, with minor contribution of PC (18:1/18:2), while in the lipidome of conchocelis the second most representative was PC (18:1/20:4) at *m/z* 808.6. However, the blade stage was also distinguishable from conchocelis, not only by the number of PC identified, but also by the profile of molecular species, as can be seen in Figure 19. a). Particularly, the blade stage included molecular species combining the fatty acyl 14:0/18:1, 16:0/16:1, 16:0/18:0, 18:0/18:1, 18:0/20:3, and 18:3/20:4 plus 18:2/20:5 that were absent on the lipidome of conchocelis, contributing to a slightly higher number of PCs on blades. Some of these molecular species present in blades included the important 18:3 and 20:5(*n*-3) FA and 16:0 FA related to chloroplastic biosynthesis of lipids. Moreover, both stages have molecular species with the 20:3 FA that along with 18:3 FA are precursor of the *n*-3 and *n*-6 pathway. Both stages have also lyso-PC, similarly as described for *Porphyra haitanensis* (307), as well as other Rhodophyta (145,308). Five LPC molecular species were identified in blade and two LPC assigned conchocelis with most abundant LPC (16:0), observed at *m/z* 496.3 (Table III.13, Fig. III.19. b).

Phosphatidylethanolamine and lyso-PE

PEs and lyso-PE were identified as $[M - H]^-$ ions (Table III.13, Fig. III.19. c). Eleven PEs were identified in the lipidome of blades while thirteen PEs were found in conchocelis. Herein, it was observed a large differentiation between the profile of molecular species of PE between stages (Figure 3c). The most abundant species found in the blade was PE (16:0/20:4) at *m/z* 738.5, that was not assigned in the profile of conchocelis. Nevertheless, PE (16:0/16:1) and PE (16:1/18:1) were the most abundant in conchocelis stage (*m/z* 688.5 and 714.5). In common, both stages included the molecular species with acyl composition $C_{14\text{-}16}/C_{14\text{-}20}$, while their differentiation was based on the higher number of PEs combining C_{18}/C_{18} moieties, absent in the lipidome of the blade stage (e.g., PE (18:0/18:1)). Meanwhile, PE (20:4/20/4) was only identified in the lipidome

of the blade. Three lyso-PEs were identified on both stages (Table III.13, Fig. III.19. d), however LPE 16:0 at *m/z* 452.3 was the most abundant molecular species on the blade, while LPE 16:1 and LPE 18:1 (*m/z* 450.3 and 478.3) were higher on conchocelis. The non-photosynthetic class PE can be a precursor of PC and play very important roles in the maintenance of shape and curvature of cell membranes; these features are important to membrane fusion and the molecular folding of some membrane proteins, as well as to establish protein-lipid conjugates in biological pathways (15,309).

Phosphatidylglycerol and lyso-PG

Phosphatidylglycerol (PG) and lyso-PG (LPG) classes were identified as $[M - H]^-$ ions. Twenty PGs were identified in the blade, while twenty-seven PGs assigned conchocelis (Table III.13, Fig. III.19. e). In the lipidome of conchocelis, the most abundant PG was at *m/z* 719.5 corresponding to PG (16:1/16:0) with minor contribution of PG (14:0/18:1), followed by PG (18:0/18:1) at *m/z* 775.5, with minor contribution of PG (16:0/20:1). It is worth highlighting that PG (18:0/18:1) at *m/z* 775.5, was the most abundant in the blade stage and that PG (16:0/20:5) at *m/z* 767.5 with minor contribution of PG (16:1/20:4) was also relevant in the PG profile of this life stage of *P. dioica*. Overall, both stages contained molecular species of PG that incorporated C_{16} with C_{14} - C_{22} and C_{18} with C_{14} - C_{22} of saturated, MUFA and PUFA with a distinct relative abundance profile of molecular species. PG is involved in the formation of chloroplasts and directly related to the biosynthesis of SQDG (18,310). The profile of PG from the conchocelis stage was differentiated by molecular species that incorporate more four molecular species. Three lyso-PG are present in both stages, and the most abundant in blade corresponded to LPG (16:0), while both LPG (16:0) and LPG (18:1) are abundant in the lipidome of conchocelis (Table III.13, Fig. III.19. f).

Phosphatidic acid

The class PA was identified in negative-mode as $[M - H]^-$ ions and seventeen molecular species were identified in the lipidome of the blade, while only six were detected in conchocelis (Table III.19, Fig III. 19 g). The most abundant PA observed in the blade was PA (16:0/20:1) at *m/z* 701.5, while the second most abundant was recorded at m/z 693.4 and corresponded to PA (16:0/20:5). The predominant PA in the conchocelis lipidome was detected at *m/z* 671.5 and assigned to PA (16:0/18:2) and at *m/z* 645.4 corresponding to PA

(16:0/16:1) plus PA (14:0/18:1). The profile of molecular species of PA in the lipidome of both stages included distinct combinations between 16:0 and 16- to 20-carbon chains FA. The number of molecular species is significantly higher in the blade stage and the profile of molecular species is contrasting between both stages.

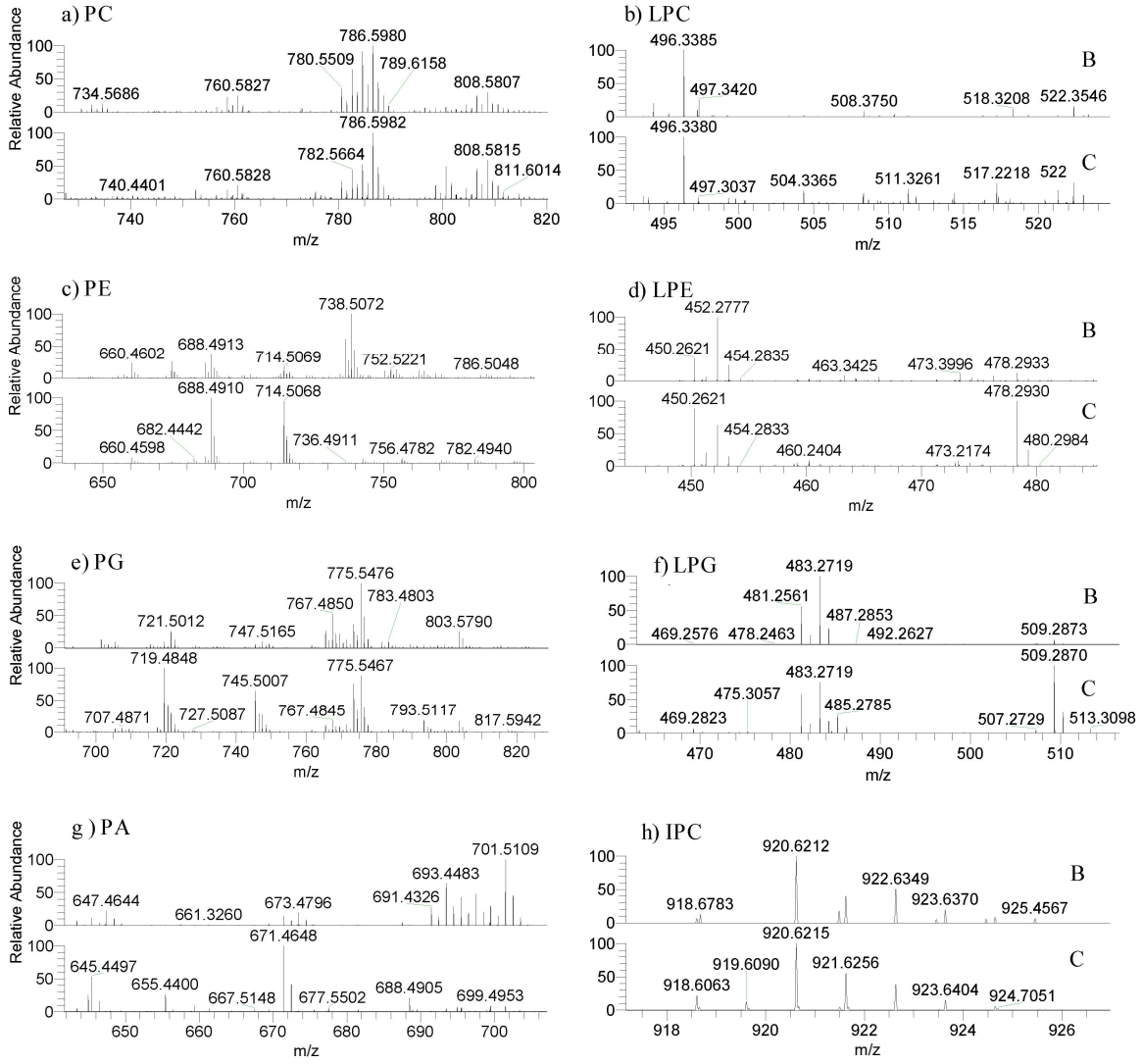

Figure III. 19. LC–MS spectra of phospholipids from *Porphyra dioica* blade (B) and conchocelis (C) stages: a) PC, b) LPC observed by HILIC–LC–MS as $[M + H]^+$ ions and c) PE, d) LPE, e) PG, f) LPG, g) PA, and (h) IPC observed as $[M - H]^-$ ions.

Table III. 13. Identification of phospholipid molecular species observed by HILIC–LC–MS in *Porphyra dioica* blade and conchocelis, PC and LPC as $[M + H]^+$ ions and PE, LPE, PG, LPG, PA, PI, and IPC as $[M – H]^-$ ions

$[M + H]^+$		**Fatty Acyls Chain**	
m/z Theoretical	**(C:N)**	**Blade**	**Conchocelis**
		Phosphatidylcholine	
732.554	PC (32:1)	16:0/16:1 and 14:0/18:1	----------
734.569	PC (32:0)	16:0/16:0 and 14:0/18:0	16:0/16:0
752.523	PC (34:5)	----------	14:0/20:5
754.538	PC (34:4)	14:0/20:4 and 16:2/18:2	14:0/20:4 and 16:2/18:2
756.554	PC (34:3)	16:0/18:3 and 14:0/20:3	16:1/18:2
758.569	PC (34:2)	16:0/18:2 and 16:1/18:1	16:0/18:2 and 16:1/18:1
760.585	PC (34:1)	16:0/18:1	16:0/18:1
762.601	PC (34:0)	16:0/18:0	----------
780.554	PC (36:5)	16:0/20:5 and 16:1/20:4	16:0/20:5
782.569	PC (36:4)	**16:0/20:4**	16:0/20:4
784.585	PC (36:3)	**16:0/20:3 and 18:1/18:2**	16:0/20:3 and 18:1/18:2
786.601	PC (36:2)	**18:1/18:1 and 18:0/18:2**	**18:1/18:1 and 18:0/18:2**
788.616	PC (36:1)	18:0/18:1	----------
804.554	PC (38:7)	18:3/20:4 and 18:2/20:5	----------
806.569	PC (38:6)	18:2/20:4 and 18:1/20:5	18:1/20:5
808.585	PC (38:5)	18:1/20:4	**18:1/20:4**
810.601	PC (38:4)	18:1/20:3	18:1/20:3
812.616	PC (38:3)	18:0/20:3	----------
		Lyso-phosphatidylcholine	
494.339	LPC (16:1)	LPC (16:1)	----------_
496.323	LPC (16:0)	**LPC (16:0)**	**LPC (16:0)**
518.321	LPC (18:3)	LPC (18:3)	----------
522.355	LPC (18:1)	LPC (18:1)	LPC (18:1)
524.370	LPC (18:0)	LPC (18:0)	----------
$[M – H]^-$		**Fatty Acyls Chain**	
m/z Theoretical	**(C:N)**	**Blade**	**Conchocelis**
		Phosphatidylethanolamine	
660.460	PE (30:1)	14:0/16:1	14:0/16:1
662.477	PE (30:0)	14:0/16:0	14:0/16:0
686.477	PE (32:2)	16:1/16:1	16:1/16:1
688.492	PE (32:1)	**16:0/16:1**	**16:0/16:1**
712.492	PE (34:3)	16:0/18:3 and 16:1/18:2	16:0/18:3 and 16:1/18:2
714.508	PE (34:2)	16:1/18:1	**16:1/18:1**
716.524	PE (34:1)	16:0/18:1	16:0/18:1
736.492	PE (36:5)	16:0/20:5	16:0/20:5
738.508	PE (36:4)	**16:0/20:4**	----------
740.524	PE (36:3)	----------	18:0/18:3
742.539	PE (36:2)	----------	18:1/18:1 and 18:0/18:2
744.555	PE (36:1)	----------	18:0/18:1
786.508	PE (40:8)	20:4/20:4	----------
		Lyso-Phosphatidylethanolamine	
450.263	LPE (16:1)	LPE (16:1)	**LPE (16:1)**
452.278	LPE (16:0)	**LPE (16:0)**	LPE (16:0)

478.294	LPE (18:1)	LPE (18:1)	**LPE (18:1)**
		Phosphatidylglycerol	
691.456	PG (30:1)	----------	14:0/16:1
717.471	PG (32:2)	----------	16:0/16:2 and 16:1/16:1
719.487	PG (32:1)	16:1/16:0 and (14:0/18:1)	**16:1/16:0 and 14:0/18:1**
721.502	PG (32:0)	16:0/16:0 and 14:0/18:0	16:0/16:0 and 14:0/18:0
745.503	PG (34:2)	----------	**16:1/18:1 and 16:0/18:2**
747.518	PG (34:1)	16:0/18:1 and 18:0/16:1	16:0/18:1 and 18:0/16:1
749.534	PG (34:0)	----------	16:0/18:0
765.471	PG (36:6)	16:1/20:5 and 18:3/18:3	16:1/20:5 and 18:3/18:3
767.487	PG (36:5)	**16:0/20:5 and 16:1/20:4**	16:0/20:5 and 16:1/20:4
769.503	PG (36:4)	16:0/20:4 and 18:1/18:3 and 18:2/18:2	16:0/20:4 and 18:1/18:3 and 18:2/18:2
771.518	PG (36:3)	18:1/18:2 and 16:0/20:3	18:1/18:2 and 16:0/20:3
773.534	PG (36:2)	18:1/18:1 and 16:0/20:2	**18:1/18:1 and 16:0/20:2**
775.549	PG (36:1)	**18:0/18:1**	**18:0/18:1 and 16:0/20:1**
801.565	PG (38:2)	16:0/22:2	16:0/22:2
803.580	PG (38:1)	16:0/22:1	16:0/22:1
		Lyso-phosphatidylglycerol	
481.257	LPG (16:1)	LPG (16:1)	LPG (16:1)
483.273	LPG (16:0)	**LPG (16:0)**	**LPG (16:0)**
509.289	LPG (18:1)	LPG (18:1)	**LPG (18:1)**
		Phosphatidic acid	
643.434	PA (32:2)	14:0/18:2 and 16:1/16:1	----------
645.450	PA (32:1)	14:0/18:1 and 16:0/16:1	14:0/18:1 and 16:0/16:1
647.466	PA (32:1)	16:0/16:0	----------
669.450	PA (34:3)	16:0/18:3 and 16:1/18:2 14:0/20:3	----------
671.465	PA (34:2)	16:0/18:2	**16:0/18:2**
673.481	PA (34:1)	16:1/18:0 and 16:0/18:1	----------
691.434	PA (36:6)	16:1/20:5	----------
693.450	PA (36:5)	16:0/20:5	----------
695.466	PA (36:4)	16:0/20:4	16:0/20:4
697.481	PA (36:3)	16:0/20:3	----------
699.497	PA (36:2)	16:0/20:2	16:0/20:2
701.513	PA (36:1)	**16:0/20:1**	16:0/20:1
		Phosphatidylinositol	
831.503	PI (34:3)	----------	16:0/18:3
833.519	PI (34:2)	**16:0/18:2 and 16:1/18:1**	**16:0/18:2 and 16:1/18:1**
835.534	PI (34:1)	16:0/18:1	16:0/18:1
883.534	PI (38:5)	----------	18:0/20:5
		Inositol phosphoceramide	
918.681	IPC (d44:1)	d18:1/26:0	----------
920.623	IPC (t42:2-OH)	**t18:1/24:1-OH**	t18:1/24:1-OH
922.639	IPC (t42:1-OH)	t18:0/24:1-OH	t18:0/24:1-OH
924.654	IPC (t42:0-OH)	t18:0/24:0-OH	t18:0/24:0-OH

Numbers in parentheses (C:N) indicate the number of carbon atoms (C) and double bonds (N) in the fatty acid side chains

Phosphatidylinositol

Phosphatidylinositol (PI) molecular species were identified in negative-mode as $[M - H]^-$ ions: three PIs were identified in the blade and five PIs were verified in conchocelis lipidome (Table III.13). Both stages included PI (16:0/18:2) with contribution of PI (16:1/18:1) at *m/z* 833.5 and PI (16:0/18:1) at *m/z* 835.5. Other molecular species of PI that fingerprinted the lipidome of conchocelis included *n*-3 FA: PI (16:0/18:3) and PI (18:0/20:5). It is known that PI are present in low abundance in the pool of PLs or display a transient occurrence in polar lipids metabolism, although they play important regulatory roles (311).

Inositol phosphoceramide

Inositol phosphoceramides (IPC) were identified as $[M - H]^-$ ions and found in both development stages were identified in *Porphyra dioica* as $[M - H]^-$ ions, in both life stages studied. Four molecular species were detected in the blade and three in conchocelis (Table III.13, Fig. III.19. h). The most abundant IPC in blades was observed at *m/z* 920.6 (IPC (t42:2-OH), and the molecular species IPC (d18:1/26:0) was not present in the lipidome of conchocelis. Other molecular species included phytosphingosine t18:0 as the long-chain base and C_{24} as the fatty acid component. It is important highlight that IPCs were reported for the first time for the Rhodophyta in *Gracilaria verrucosa* (312), latter also being reported for *Chondrus crispus* and *Gracilaria* sp. (145,308) being considered a putative biomarker of this phylum.

Betaine lipids

The analysis of total lipid extract provided the identification of betaine lipids diacylglyceryl-*N,N,N*-trimethyl-homoserine DGTS, identified as $[M + H]^+$ ions. A total of six molecular species were identified in conchocelis phase but only three were identified in blade samples (Fig. III.20 and Table III.14). The most abundant molecular species in conchocelis corresponded to DGTS (16:0/16:1) at *m/z* 710.6, with minor contributions of DGTS (14:0/18:1). These molecular species were also identified in the blade lipidome, that included other DGTSs combining 14:0, 16:0, 16:1 and 18:2 FA, but not eicosapolyenoic 20:4 and 20:5 FA.

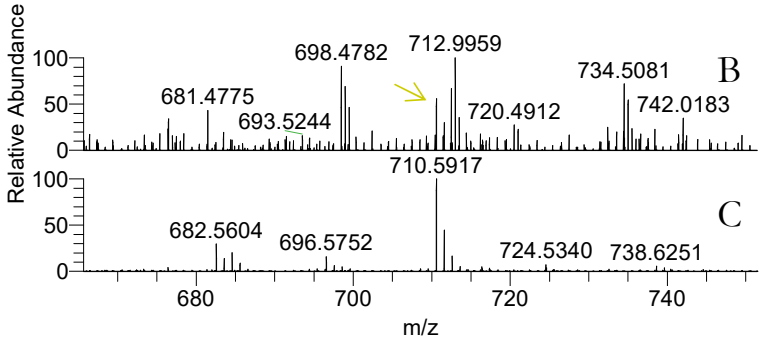

Figure III. 20. LC–MS spectra of betaine lipids from *Porphyra dioica* blade (B) and conchocelis (C) stages: DGTS observed by HILIC–LC–MS as $[M + H]^+$ ions.

Table III. 14. Identification of betaine molecular species observed by HILIC–LC–MS in *Porphyra dioica* blade and conchocelis, DGTS as $[M + H]^+$

$[M + H]^+$		Fatty acyl composition	
m/z *Theoretical*	**(C:N)**	**Blade**	**Conchocelis**
		Betaine lipids	
682.562	DGTS (30:1)	----------	14:0/16:1
684.578	DGTS (30:0)	----------	14:0/16:0
710.593	DGTS (32:1)	**16:0/16:1 and 14:0/18:1**	**16:0/16:1 and 14:0/18:1**
736.609	DGTS (34:2)	16:0/18:2	16:0/18:2
738.625	DGTS (34:1)	----------	16:0/18:1

Numbers in parentheses (C:N) indicate the number of carbon atoms (C) and double bonds (N) in the fatty acid side chains

III.1.2.2.2. Fatty acids profile

The fatty acid profile of the lipid extracts was obtained for the two phases. Fifteen different fatty acids were identified in *P. dioica* blade and conchocelis stages (Table III.15). Among these were 14:0 (myristic acid), 15:0 (pentadecanoic acid), 16:0 (palmitic acid), 16:1 (palmitoleic acid), 18:0 (stearic acid), 18:1(*n*-9) (oleic acid), 18:1(*n*-7) (vaccenic acid), 18:2(*n*-6) (linoleic acid), 20:1(*n*-9) (eicosenoic acid), 20:2(*n*-6) (eicosadienoic acid), 20:3(*n*-6) (dihomo-gama linolenic acid), 20:4(*n*-6) (eicosatetraenoic acid or arachidonic acid, AA), 20:5(*n*-3) (eicosapentaenoic acid, EPA), 22:1(*n*-9) (docosenoic acid). Both life stages displayed the same composition in terms of FAs, but differed in the content of some of the fatty acids identified. The blade phase was characterized by higher amounts of SFA (47.2%) mainly due to the high content of 16:0 (44.4 ± 1.06%); and higher amount of eicosapentaenoic acid 20:5(*n*-3) (24.9 ± 1.51%). In comparison, conchocelis contained a higher amount of MUFA and PUFA, and was richer in arachidonic acid 20:4(*n*-6) (21.2 ± 0.79%), but also contained a high amount of 20:5(*n*-3) (15.5 ± 2.00%). *Porphyra dioica* contained alpha-linolenic acid 18:3(*n*-3) in low amounts, an important precursor of 20:5(*n*-3).

Comparing with available literature, *Porphyra* sp. (adult stages) typically display high concentrations of 20:5(*n*-3), with 20:4(*n*-6) being the second most abundant PUFA (306,313,314). The percentage of 20:5(*n*-3) commonly ranges from 20 up to 50 % of the total pool of FA (224,306,315). This feature highlights the particular potential for *Porphyra* spp. as a commercial supply of *n*-3 EPA, assuming that sufficient biomass can be provided sustainably, such as in the case of cultivation in aquaculture systems (34,292,313).

Table III. 15. Fatty acids profile of polar lipids from blade and conchocelis stages of *Porphyra dioica* determined by GC–MS analysis of fatty acid methyl esters (FAMEs)

	Blade		**Conchocelis**	
Fatty acids	**Mean (%)**	**±SD**	**Mean**	**±SD**
14:0	0.42	0.01	0.65	0.14
15:0	0.95	0.04	0.97	0.15
16:0	**44.4**	1.06	**22.9**	2.76
18:0	1.36	0.06	1.49	0.19
Σ SFA	**47.2**		**26.1**	
16:1*n*-7	1.92	0.03	6.09	0.76
18:1*n*-9	9.29	1.27	10.5	0.81
18:1*n*-7	2.13	0.16	8.31	0.22
20:1*n*-9	2.87	0.17	2.40	0.11
22:1*n*-9	0.18	0.01	0.14	0.06
Σ MUFA	**16.4**		**27.4**	
18:2*n*-6	3.37	0.57	4.43	0.11
18:3*n*-3	0.00	0.00	0.36	0.06
20:2*n*-6	0.85	0.13	0.77	0.01
20:3*n*-6	1.74	0.28	4.21	0.01
20:4*n*-6	5.58	0.51	**21.2**	0.79
20:5*n*-3	**24.9**	1.51	**15.5**	2.00
Σ PUFA	**36.4**		**46.5**	
***n*-6/*n*-3**	**0.46**		**1.93**	
IA*	1.10		0.35	
IT*	0.52		0.32	

*IA-Index of atherogenicity; IT-Index of thrombogenicity; Means (%) and standard deviations (S.D.) were obtained from three replicates (content less than 0.1% not shown)

The conchocelis stage displayed a higher content of 20:4(*n*-6) rather than 20:5(*n*-3), in agreement with literature (206,299,315). Both FA are within ranges previously reported: 23% up to 45% of 20:4(*n*-6) FA and 5% up to 26 % of 20:5(*n*-5) (315). Highest PUFA and MUFA, and lowest SFA contents were found in conchocelis phase, but the relative

percentage of 20:5(*n*-3) of blade stage was higher than in conchocelis. It must be highlighted that *n*-3 FA have important roles on regulatory pathways controlling inflammatory responses (316,317). Consistent with this, many studies support that supplementation in nutrition with EPA contribute to reduce the risk of acute inflammatory response (71,318). General benefit to human health through anti-inflammatory actions can be achieved by reinforcing diet with EPA of somewhere between 1.35 and 2.7 g EPA per day (319).

The balance *n*-6/*n*-3 PUFA ratio in both life stages was calculated as 0.46 for blades and 1.93 for conchocelis. Overall, the *n*-6/*n*-3 ratio was less than 2 in both stages, and below the upper limit reported for *Porphyra* spp. (1.2% up to 9%) or other seaweeds (299,306). This ratio in *P. dioica* is within the range recommend as beneficial (< 4) to reduce chronic diseases (96,291,297,320). This feature enhances its valorization for consumption in human diet, as well as other potential application for this species biomass (299), since lipids provided by diet are recognized to promote health and complement therapies (278,297,318,319).

Atherogenic and thrombogenic indexes (IA and IT) allow to estimate the effects of dietary FA on human health and on coronary diseases, such in atheroma and/or thrombus formation (278). The ratio between saturated thrombogenic FA and the sum of anti-thrombogenic MUFA and PUFA were estimated for both *P. dioica* life stages studied and are presented in (Table III.15). Both IA and IT were higher in the blade stage (1.10 and 0.52 respectively) than in conchocelis (0.35 and 0.32 respectively), but lower than reported for some Rhodophyta and even Ochrophyta and Chlorophyta macroalgae (278,321). The IT values obtained in this study were similar to those of other products which consumption is considered to be beneficial for the prevention of chronic diseases, namely olive oil (0.32), chicken (0.95) and milk-based products (2.1). Altogether, based on the FA profile, both *Porphyra dioica* blade and conchocelis are valuable in what concerns lipid composition for food, as a food additive, for nutraceutical purposes or for inclusion in the formulation of highly unsaturated low-fat diets. Overall, they can help to prevent diseases by improving the thrombogenic and atherogenic potential and thus allow the development of healthier lipid formulations.

III.1.2.3. Discussion on the lipidome of Rhodophyta

The lipid extracts of *Gracilaria* sp. yielded about 3.00 ± 0.60 g/kg of dry biomass while lipid extracts of *Porphyra dioica* sp. accounted for about 8.60 ± 1.20 g/kg dry biomass of blade and 10.8 ± 0.90 g/kg dry biomass of conchocelis. These results are in accordance with previous reports, *Gracilaria* sp. has low lipid content within expected range 0.60 - 3 g/kg of dry biomass (67,267,322). The total content of lipids from *Porphyra* sp. reported ranged between 2.5 - 10.3 g/kg of dry biomass (305,306), pinpointing that season and life cycle effects influence lipid yield. Lipid content from *P. dioica* was higher compared to *Gracilaria* and in accordance with literature (313).

The molecular profile of polar lipids from *Gracilaria* sp. and *P. dioica,* cultivated on-land based IMTA system, were established for the first time by using modern lipidomic approaches based on HILIC–LC–MS and MS/MS. *Gracilaria* sp. contained 147 molecular species distributed by MGDG, DGDG, SQDG, SQMG, phospholipids PC and lyso- PC, PG and lyso- PG, PI, PA, PE, and IPC plus betaine lipids such as DGTS and MGTS (Fig. III.21), while both stages of *Porphyra dioca* contained 110 and 100 molecular species on the lipidome of blade – B and conchocelis – C, respectively, and contained LPE not found in *Gracilari*a. However, the lipidome of *Gracilaria* sp. contained MGTS and higher number of molecular species of DGTS while *P. dioica* stages contained high number of PE, PG, and PA (Fig. III. 21).

Porphyra dioica contained a lower number of molecular species of GLs, particularly in the SQDG class, than *Gracilaria* sp. or other reported Rhodophyta such as *Chondrus crispus* (145). These features deserve to be more explored by the analysis of other Rhodophyta to evaluate if these dissimilarities could be due to genetic evolutionary reasons and taxonomic variation. MS-based approach is an important tool for discrimination between families from the same phylum.

Glycolipids from *Gracilaria* sp. mostly included molecular species with acyl composition 16:0 FA combined to C_{14}, C_{16}, C_{18}, and C_{20} FA while GLs combining 16:0 with C_{18} and C_{20} FA, were assigned in *Porphyra* macroalgae. Both specimens contained GLs with 20:4(*n-6*) and 20:5(*n-3*) FA. By using distinct MS-approaches (159,308) and NMR-approaches (181), it was reported that GLs from Rhodophyta (e.g., *Chondrus crispus, Palmaria palmata*, *Porphyra* sp., among others) contained a range of molecular species combining eicosapolyenoic acids such as 20:4(*n*-6) and 20:5(*n*-3). However, herein

this work it were found in same extent in both MGDG and DGDG, contrary to reported by using other analytical techniques (134). Both stages of *P. dioica* contained a lower number of molecular species of SQDG class than other Rhodophyta already screened by using the same lipidomics analytical strategy, such as *Gracilaria* sp. or reported *Chondrus crispus* (145) and may constitute a putative biomarker for intra-taxonomic differentiation.

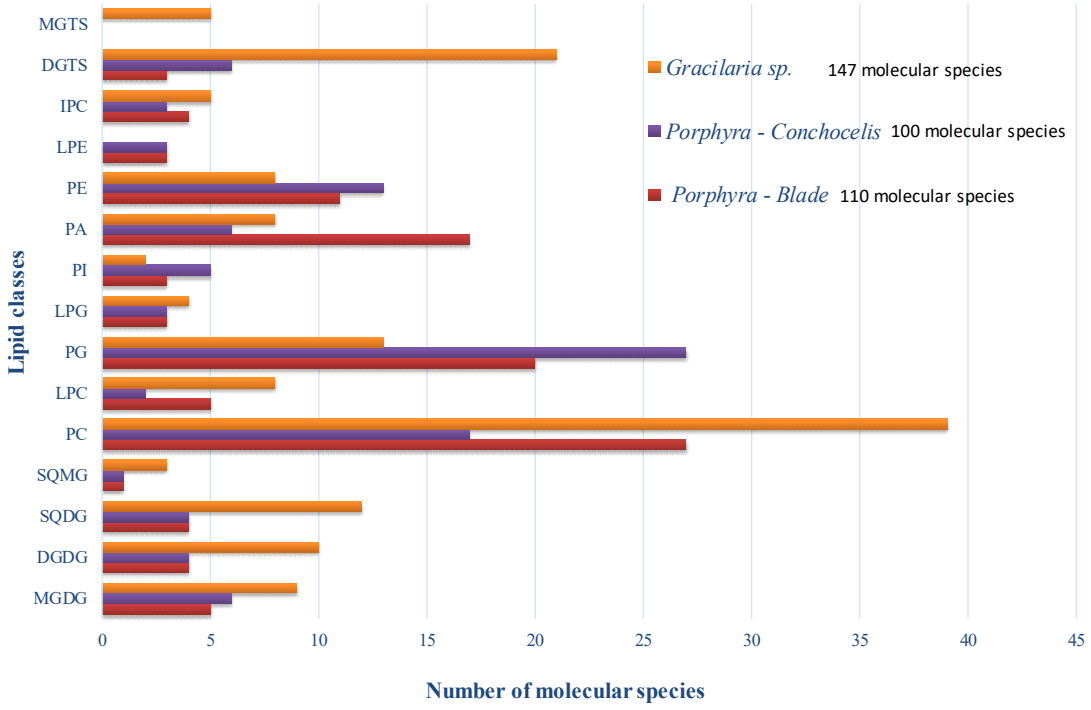

Figure III. 21. Number of molecular species identified in the lipidome of *Gracilaria* sp., *Porphyra dioica* – blade and conchocelis phases.

No great changes were observed in the profile of GLs from *P. dioica* comparing between both life cycle stages, showing a similar profile of the majority of GLs. Since GLs are found in chloroplast, during the development stages, the formation of chloroplasts, structural rearrangement and development of plastid structure occurs but seems to preserve the profile. A particular feature was observed within GLs, MGDG and DGDG class from conchocelis rather contained relevant molecular species combining 18:1 and 16:0, reported to confer less flexibility to membrane (323). Moreover, the predominance of molecular species that include desaturated acyl chains within the chloroplast membrane lipids, as noted here namely in blade stage, are more associated to the increase of membrane fluidity and more developed-stadiums.

In fact, GLs bearing *n*-3 PUFA were reported with biological activities as antibacterial, antitumor, and antiviral activities, enhancing the pharmacological potential of these compounds (23,71). MGDG (20:4/16:0), MGDG (20:5/16:0), SQDG (20:5/14:0) are recognized by their inhibitory effects as anti-inflammatory and antitumoral activity (132,181,308). Altogether these structures provide important cues related to the potential bioactive properties of both lipid extracts and GLs from *P. dioica* and also as an important source of *n*-3 and *n*-6 FA, envisaging the valorization of these macroalgae.

The phospholipids (PLs) identified in the lipidome of both Rhodophyta *Gracilaria* sp. and both stages of *P. dioica* included PC, LPC, PG, LPG, PA, PE, and PI. The PLs from *Gracilaria* mainly included C_{14}, C_{16}, C_{18}, $C_{20,}$ and C_{22} while *P. dioica* included PLs with C_{14}-C_{20} FAs. The fatty acyl composition of PLs was distinguished from GLs by the predominance of molecular species that combine C_{18} and C_{20}. A plethora of molecular species from distinct classes of PLs fingerprint both stages from *P. dioica*. PLs such as PC, LPC and PA contained a variety of molecular species in blade while PG and PE contained a high number of molecular species in the lipidome of conchocelis. Overall, dissimilarities of the phospholipidome were observed between stages due to the number of molecular species, composition and profile of molecular species, suggesting some change in the metabolism of this important biological membranes lipids across the development stages. PC, PE, PG, and PI are related to the formation of new cells and organelles and thus contribute to the variation on the profiles of molecular species between stages (167). The quantity and composition of PLs is regulated in a way that enables membranes for maintaining their structure and function in spite of their developmental and environmental changes (167,324,325). Early-stages contain less developed chloroplast than more developed stages (113,324). Comparing with the lipidome of *Gracilaria*, *P. dioica* contained higher number of molecular species from the class of PE and contained LPE that, altogether, may suggest that these classes are putative candidates in the intra-taxonomic differentiation of Rhodophyta, which deserve to be explored. Interestingly, distinct lyso-phospholipids from PC, PG, and PE were found in the lipidomes of these macroalgae, suggesting that phospholipases can be activated to a greater extent than galactolipases (307).

The industrial application of PLs is a new area in food industry, mainly as an ingredient for food fortification. PLs may serve important functions within the functional food

segment: (a) emulsifying properties, (b) supplementation of *n*-3 FAs such as 20:5(*n*-3), (c) better bioavailability of PUFA, and (d) beneficial nutritional effects of the PLs themselves (288). PLs in diet act as natural emulsifiers, facilitating the digestion and absorption of fatty acids, cholesterol and other lipophilic nutrients [21]. Furthermore, emulsions of marine PL can be used as effective carriers of *n*-3 PUFA-rich oil as they could be incorporated easily into aqueous and emulsified foods. Besides the nutraceutical relevance, there is also a growing interest to use PLs from macroalgae in the cosmetic and pharmaceutical industries, not only as emulsifiers but also considering their described health benefits (30,224,308,326). The *n*-6 and *n*-3 PUFA incorporated into PLs classes have been reported with important biological functions, namely to alleviate senescence, to be beneficial for cognitive functions or to prevent inflammatory diseases (32). Anti-inflammatory effect of PLs rich-extracts was attributed to PUFA composition and to polar head groups, namely molecular species such as PG (20:5/16:0), PG (20:5/16:1), and PC (20:5/20:5) (181). Choline from the headgroup of PC was considered to play important roles in the stimulation of the production of acetylcholine with beneficial impact on the central nervous system (32). Thus, macroalgae or isolated PLs used as functional food or ingredients afford diverse health benefits.

Betaine lipids from *Gracilaria* comprised DGTS and MGTS and include C_{14}, C_{16}, C_{18}, and C_{20} FA, particularly the 20:4(*n*-6) FA. Regarding betaine lipids from *P. dioica*, few molecular species from DGTS assigned in the lipidome of blade and of conchocelis. Betaine lipids can be considered a biomarker to discriminate between Rhodophyta. Otherwise, by using TLC-based approaches, Kunzler reported that DGTS was detected in small amounts in the orders Gigartinales, Rhodymeniales and Ceramiales, and not in Bangiales, the order of *Porphyra* (153). This suggest that, at least in some red algal species, the biosynthetic pathway for betaine lipids is operating, although these classes do not contribute substantially to polar lipids as occurs in Chlorophyta (36,150,327). Betaine lipids are naturally occurring lipids not found in higher plants, but are quite widely distributed in algae (149,150). They are components of extraplastidial membranes and of the outer membrane of chloroplasts (150), are involved in the transfer of fatty acids from the cytoplasm to the chloroplast, and may contribute as marker for signaling during environmental and nutrition depleted conditions (36,151). They can replace phospholipids under conditions of phosphorous limitation being correlated with the phospholipids PC and

PE to substitute PLs membrane constituent and/or an intermediate in cellular lipid metabolism (153). This are novel-lipids not well explored in macroalgae, several gaps remain in the field of structural characterization, metabolic pathways, bioactivity and, thus, potential further applications. Amphiphilic character of betaines is similar to those from PC, suggesting some relation to biological role and bioactivity, however all these properties are an unexplored field.

The set of FA from *Gracilaria* sp. and *Porphyra dioica* mainly comprised C_{14}, C_{16}, C_{18}, and C_{20}, FA, particularly 14:0, 16:0, 18:1, 18:2*(n*-6*)*, 20:4(*n*-6) and 20:5(*n*-3) species, esterified to polar lipids. *Gracilaria* sp. contained high abundant 16:0, 18:1 FA and 20:4(*n*-6) FA. *Porphyra dioica* was found to contain high content 20:5(*n*-3) PUFA in blade stage and 20:4(*n*-6) followed by 20:5(*n*-3) in conchocelis phase. Blade phase of *P. dioica* account for high concentrations of 20:5(*n*-3), with 20:4(*n*-6) as the second most abundant PUFA in accordance with literature (306,313,314). Depending on season effect and other abiotic factors, the percentage of 20:5(*n*-3) ranges from 20% - 50% (224,306,315). This feature highlights the particular potential for red species as a source of this *n*-3, suitable as commercial source of PUFA, assuming that sufficient biomass can be provided sustainably (e.g., aquaculture system) (34,292,313). In the conchocelis stage, 20:4(*n*-6) content was higher than 20:5(*n*-3), in agreement with literature (206,299,315). Both FA are within reported range: 23% up to 45% of 20:4(*n*-6) FA and 5% up to 26% of 20:5(*n*-5) (315). Highest content of PUFA and MUFA, and lowest of SFA, was found in conchocelis phase, but the relative percentage of 20:5(*n*-3) of blade stage was higher than in conchocelis. The *n*-3 FA have important roles on regulatory pathways controlling inflammatory responses (316,317). Consistent with this, many studies support that supplementation in nutrition with EPA contribute to reduce the risk of acute inflammatory response (71,318). General benefit to human health through anti-inflammatory actions can be achieved by reinforcing diet with EPA of somewhere between 1.35 and 2.7 g EPA per day (319).

The balance *n*-6/*n*-3 PUFAs ratio it was found as 0.47 in blade stage and a higher value of 1.93 was obtained in the conchocelis stage, *n*-6/*n*-3 ratio was less than 2 in both stages. *Gracilaria* sp. has the highest value (3.69) but below reported for other macroalgae (299,306). A balanced ratio *n*-6/*n*-3 of less than 4 is in agreement with intake ratios recommended by WHO (292), enhancing the valorization of genus *Gracilaria* and *Porphyra* as food item for human consumption with beneficial contribution to reduce

chronic diseases, with ratio assigned to be less than four (96,291,297,320). Dietary factors of lipids can promote or protect against the development of cardiovascular disease that usually involve atherosclerosis or thrombosis events (278,328,329). The ratio between saturated thrombogenic FA and the sum of anti-thrombogenic MUFA and PUFA estimated for *Porphyra* stages was much lower than those reported for Rhodophyta and even Ochrophyta and Chlorophyta macroalgae (321). The IA and IT values observed in the results of the present study were in some order of reported for the most of the macroalgae (278). Macroalgae possess great amounts of protective PUFA of the *n*-6 and *n*-3 series and MUFA linked with the slow down intra-arterial occlusion and platelet aggregation, preventing disease (330). Indeed, IT values obtained herein were similar to the values for products which consumption is considered beneficial to health and for the prevention of chronic diseases, such as olive oil (0.32), and much lower than chicken (0.95) and milk-based products (2.1). These results for the IA and IT are important to prevent the emergence of heart diseases by diet. Indeed, the highest PUFAs and MUFA, and lowest SFA contents were found in conchocelis phase, however higher contents of 20:5(*n*-3) where found in blade stage. Thus, altogether, *Gracilaria* sp., *Porphyra dioica* blade, and *Porphyra dioica* conchocelis stages are valuable in what concerns polar lipid composition. Their intrinsic nutritional value is useful for food, or food additive, and for inclusion in the formulation of highly unsaturated low-fat diets, with particular emphasis in both stages of macroalgae *Porphyra dioica*. Moreover, same molecular species may be functional to prevent diseases and thus in the development of healthier lipid formulations for pharma.

III.1.3. The lipidome of Ochrophyta:

Fucus vesiculosus

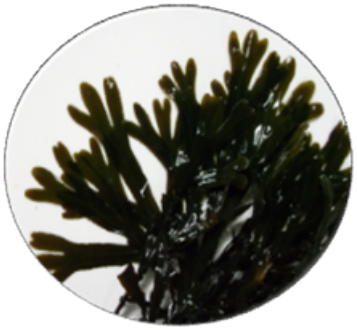

The lipidome of *Fucus vesiculosus*

The brown macroalgae *Fucus vesiculosus* (family Fucaceae, order Fucales), is a native species in the Atlantic cost of Portugal, and thrives in Ria de Aveiro. This macroalgae was widely used as fertilizer and feed for animal and also as a source of sulphated fucan for industrial exploitation (13). As other macroalgae, *Fucus* sp. is considered a potential source of food and *n*-3 fatty acids with nutritional value and/or pharmaceutical applications (314). Lipids have recognized beneficial effects on human health (1,331) but are modeled by environmental factors (330,332). In aquaculture systems such as IMTA, the manipulation of factors such as pH, salinity, light and nutrients may minimize drastic effects due to seasonal variations, or even modulate the plasticity of lipids and furthermore adjust composition to enhance the production of target compounds and standard biomass. Brown macroalgae are considered important sources of lipids, such as *n*-3 and *n*-6 with optimal *n*-6/*n*-3 ratio between of 1.5 - 3 (313,330,333). However, beside the fatty acids profile of *Fucus vesiculosus* (*F. vesiculosus*), the composition of lipids at molecular level, as others brown macroalgae, is not well documented. It encourages us to study the detailed composition of the polar lipidome of *F. vesiculosus*. Due to the considerable interest in understanding metabolism of polar lipids relying on season effects, the polar lipids profile of *F. vesiculosus* collected on mid-winter and end-spring from a land based IMTA in the west coast of Portugal is studied for the first time. It was performed by using high resolution HILIC–LC–MS & MS/MS. This will contribute to the elucidate the lipidome of *F. vesiculosus* and the role of season effect towards lipids.

III.1.3.1. Polar lipids from Fucus vesiculosus

The total lipid extracts from *Fucus vesiculosus* were extracted by using methanol/chloroform system, and *F. vesiculosus* collected on mid-winter (February) accounted for about 9.13 ± 0.91 g/kg dry biomass while the one obtained from end-spring (May) accounted for 4.10 ± 0.36 g/kg dry biomass. The elution profile of polar lipids in the extracts from both seasons was obtained by LC–MS and is represented in Figure III.22. Variations in the profile between seasons were observed at 2 up to 3 minutes within both

ionization modes and at 16 minutes in the positive mode of acquisition (Fig. III.22. A and C).

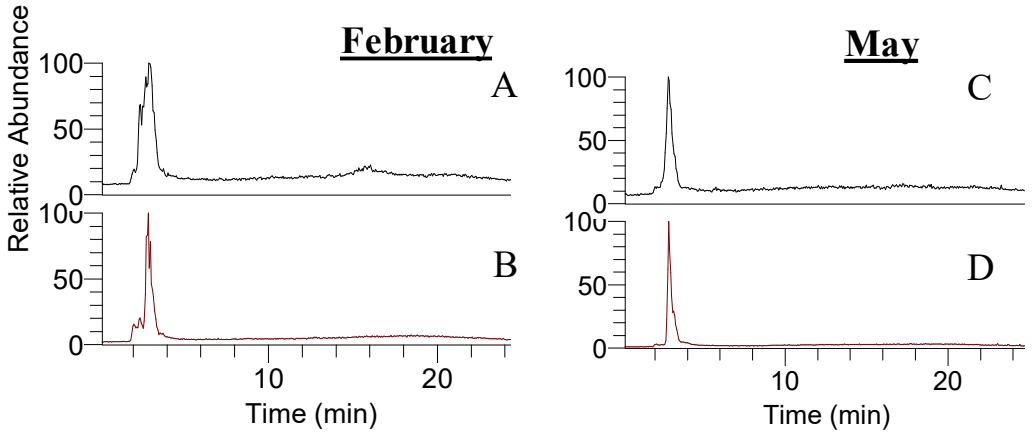

Figure III. 22.. LC–MS chromatograms of lipid extracts obtained from *Fucus vesiculosus* collected on February (mid-winter) and acquired on positive mode (A) and negative mode (B) and collected on May (end-spring) on positive mode (C) and negative mode (D).

The MS raw data was pre-processed by using the software package MZmine 2 with mass tolerance of 5 ppm. Based on mass accuracy and on detailed structural information inferred by MS/MS spectra, the lipid classes and molecular species assigned on the lipidome of *F. vesiculosus* from different seasons were identified. Data integration and statistical analyses allowed the comparison between the profile of molecular species of all classes from *F. vesiculosus* in both seasons and variation in the lipidome was expressed by the changes of the relative abundance. These are preliminary results about the lipidome of *F. vesiculosus* extracts that deserve to be explored in the future.

The polar lipid profile of *F. vesiculosus* was identified for the first time and it were identified glycolipids, phospholipids, and betaine lipids distributed by seventeen classes with a total of 181 molecular species. The same classes and lipid species were detected in the lipidome of *F. vesiculosus* collected in both seasons, showing variation in their relative abundance profile within each class, as will be described.

Identification of the glycolipids´ profile of* Fucus vesiculosus *and their variation with season effect

Seventy-two molecular species of glycolipids were detected and were distributed within sulfolipids and galactolipids categories. Galactolipids from *F. vesiculosus* (both seasons) were identified by LC–MS as $[M + NH_4]^+$ ions (Fig. III.23. a-b and e-f), Table III.16) and included 25 MGDG molecular species and 27 DGDG molecular species. In both seasons, the most abundant was MGDG (38:8) attributed to MGDG (20:5/18:3) at *m/z* 816.6 with minor contribution from MGDG (20:4/18:4). The lipidome of *F. vesiculosus* collected on winter (February) also contained the abundant MGDG (38:9) attributed to MGDG (20:5/18:4) at *m/z* 814.5 and MGDG (36:7) attributed to MGDG (18:3/18:4) at *m/z* 790.5.

The lipidome of *F. vesiculosus* from spring (May) season contained the abundant MGDG (38:7) at *m/z* 818.6 due to MGDG (20:5/18:2) with slight contribution from MGDG (20:4/18:3) and the abundant MGDG (38:6) at *m/z* 820.6 due to MGDG (20:4/18:2). Significant alterations were observed comparing the glicolipidomes of *F. vesiculosus* from spring versus winter (February) (Fig. III.24. a). Statistically analysis revealed significant increase of MGDG (32:3), MGDG (32:4), MGDG (34:4), MGDG (36:5), MGDG (38:5), MGDG (38:6), MGDG (38:7) ($p < 0.001$); MGDG (36:4) ($p < 0.01$); and MGDG (32:1) ($p < 0.05$) and combine C_{16}, C_{18} and C_{20} FA in spring season. In the glycolipidome of winter *F. vesiculosus*, it was observed a significant increase of MGDG (36:6), MGDG (36:7), MGDG (36:8), MGDG (38:8), and MGDG (38:9) ($p < 0.001$); MGDG (34:2) ($p < 0.01$); MGDG (36:2) ($p < 0.05$) with high contribution from molecular species combining 18:3 and 18:4 and 20:5 FA to differentiate the lipidome of winter macroalgae.

In both seasons, most abundant DGDG (38:8) at *m/z* 978.6 was attributed to DGDG (20:5/18:3) plus DGDG (20:4/18:4). Significant alterations were observed comparing the lipidome of *F. vesiculosus* from spring versus winter (Fig. III.24. b), with statistically significant increase of relative abundance of DGDG (36:4), DGDG (36:5), DGDG (38:4), DGDG (38:5), DGDG (38:6), DGDG (38:7) ($p < 0.001$) in spring season, most of them related to molecular species combining C_{16}, C_{18} and C_{20} FA among are molecular species combining 20:4 and 20:5 FA with 18:1 and 18:2 FA.

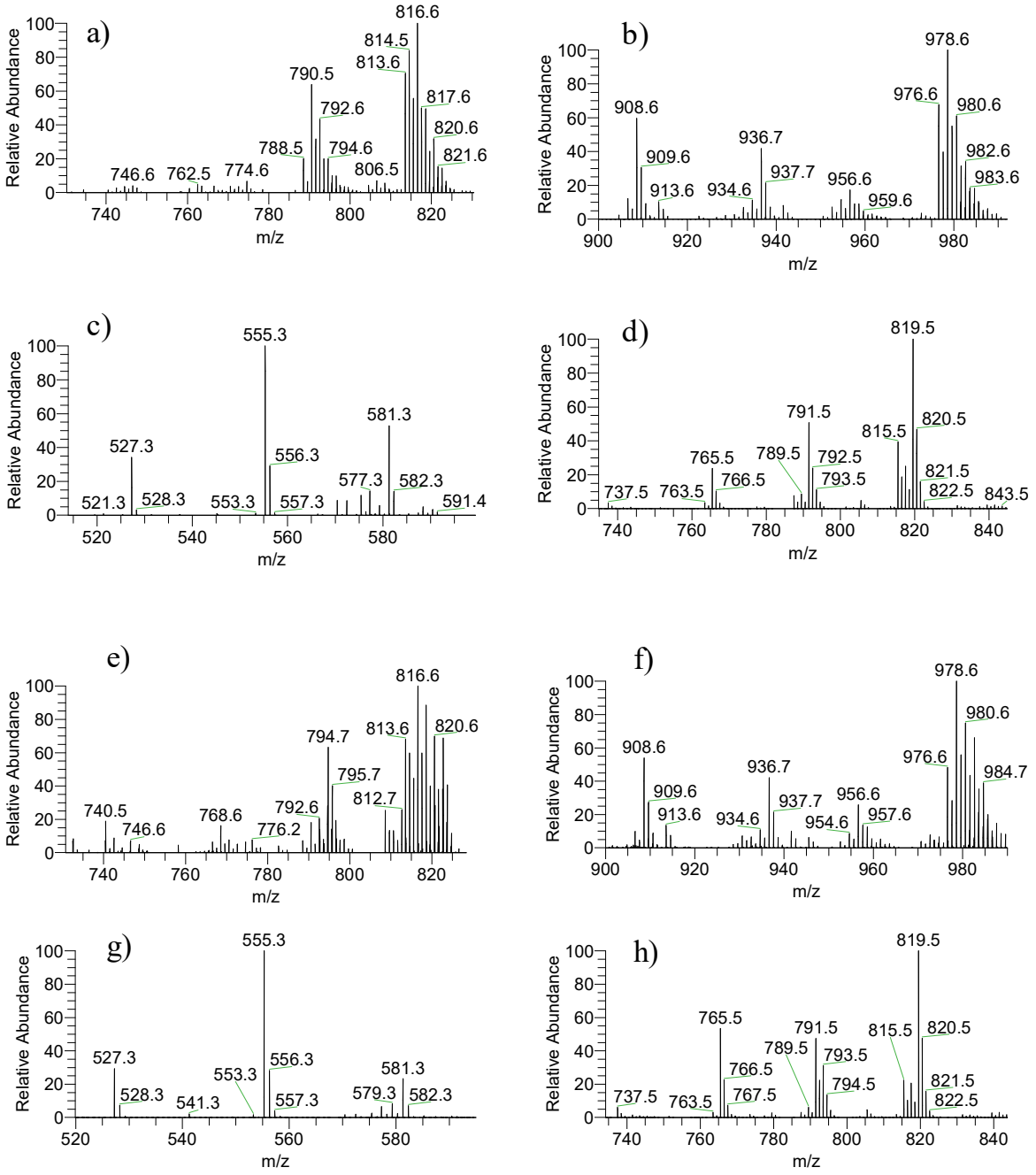

Figure III. 23. LC–MS spectra of glycolipids from *Fucus vesiculosus* collected in February (mid-winter) and May (end-spring) observed by LC–MS, respectively a) and e) MGDG, b) and f) DGDG molecular species were identified as $[M + NH_4]^+$ ions, c) and g) SQMG and d) and h) SQDG identified as $[M - H]^-$ ions.

Significant increase of DGDG in the lipidome of winter *F. vesiculosus* was reflected on DGDG (32:1), DGDG (32:2), DGDG (32:3), DGDG (34:2), DGDG (36:6), DGDG (36:7), DGDG (38:8) and DGDG (38:9) ($p < 0.001$); DGDG (34:1) and DGDG (36:2) ($p < 0.01$), among molecular species majorly contributing to the differentiation include PUFA such as 16:3, 18:2, 18:3 and 18:4 FA.

Sulfolipids SQDG were analysed by LC–MS as $[M - H]^-$ ions (Fig. III.23. c-d and g-h), Table III.16) and 14 molecular species of SQDG plus six molecular species of SQMG were identified. In both seasons, most abundant SQDG (34:1) was attributed to SQDG (18:1/16:0) at *m/z* 819.5 and a second prominent molecular species SQDG (32:1) at *m/z* 791.5 identified as SQDG (18:1/14:0). The lipidome of *F. vesiculosus* from spring contained the abundant SQDG (30:0) at *m/z* 765.5 identified as SQDG (16:0/14:0). Significant alterations were observed comparing spring versus winter lipidomes (Fig. III.24. c) and significant increase was observed in spring at SQDG (28:0), SQDG (30:0) and SQDG (32:1) ($p < 0.001$), SQDG (30:1) and SQDG (32:0) ($p < 0.01$), and SQDG (36:4) and SQDG (36:5) ($p < 0.05$). Most significant increase included SQDG with SFA such as 14:0, 16:0 and 18:0 while the major contribution in the differentiation of spring lipidome was reflected by the increase of SQDG (30:0). Significant increase was observed in winter season at SQDG (32:1), SQDG (32:2), SQDG (32:3), SQDG (34:1), SQDG (34:2), SQDG (34:3) ($p < 0.001$); and SQDG (30:1) ($p < 0.01$), with molecular species including 18:1, 18:2, and 18:3 FA.

Lyso-sulfolipids (SQMG) were identified in the lipidome from both seasons, with the most abundant SQMG (16:0) at *m/z* 555.3. Lyso-sulfolipids included the C_{14} and C_{16} SFA and C_{18} FA. Significant alterations were observed comparing spring versus winter lipidomes (Fig. III.24 d) with significant increase of SQMG (16:1) ($p < 0.001$); SQMG (16:0) and SQMG (18:2) ($p < 0.01$); and SQMG (14:0). ($p < 0.05$). Otherwise, significant increase of SQMG (18:1) and SQMG (18:3) was observed in the lipidome of *F. vesiculosus* from winter.

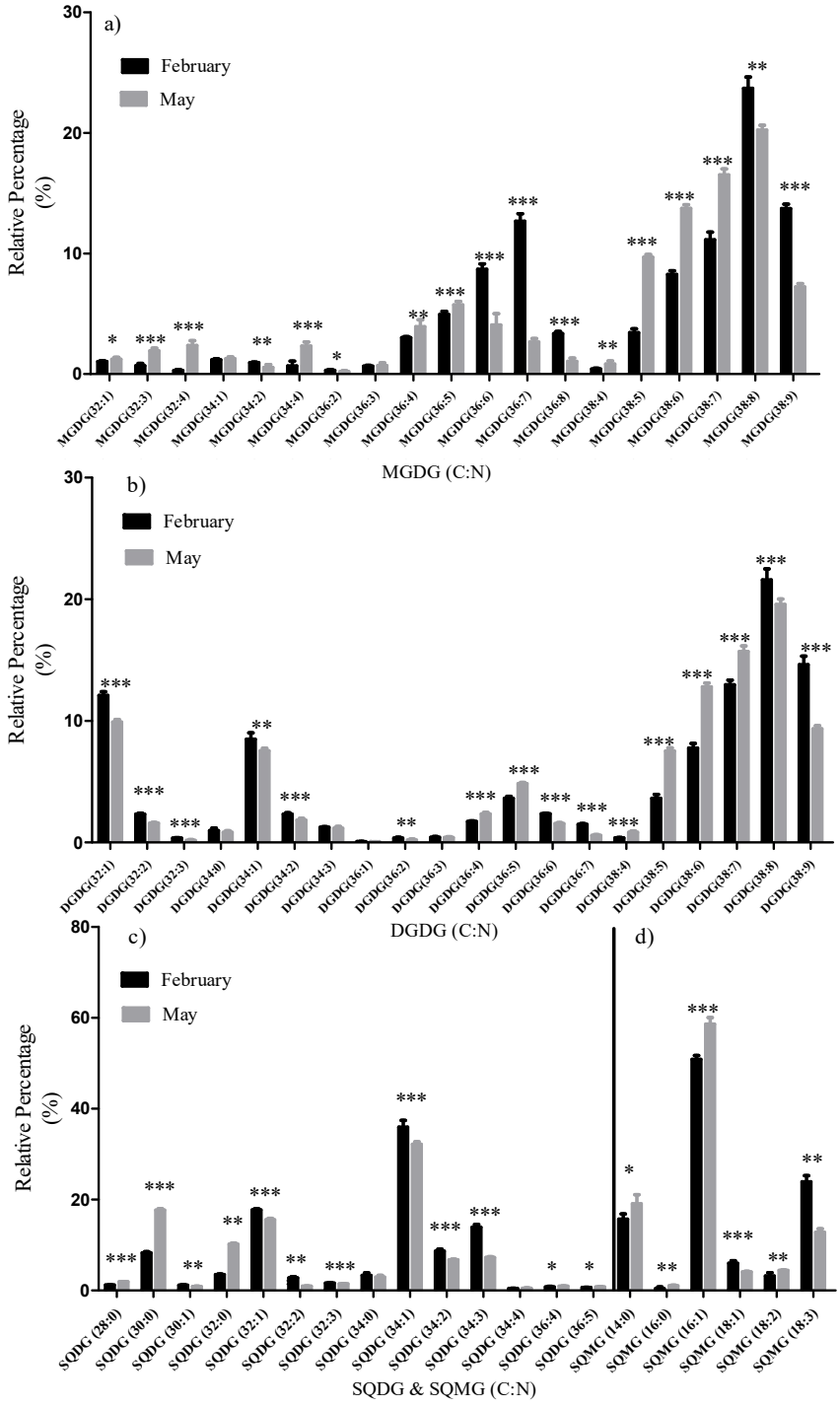

Figure III. 24. Percentage of a) MGDG, b) DGDG and c) SQDG plus d) SQMG molecular species identified after LC–MS and MS/MS. The results are expressed as percentage obtained by dividing the ratio between peak areas of each molecular species and internal standards and the total of all ratios. Values are means ± standard deviation of the duplicate of three independent experiments. (***, significantly different $p < 0.001$; **, significantly different $p < 0.01$, * significantly different $p < 0.05$). February refers to *Fucus vesiculosus* collected in mid-winter. May refers to *Fucus vesiculosus* collected in end-spring.

Table III. 16. Identification of glycolipids observed by HILIC–LC–MS in *Fucus vesiculosus*. MGDG and DGDG molecular species were identified as $[M + NH_4]^+$ ions, SQDG and SQMG as $[M – H]^-$ ions

Galactolipids $[M + NH_4]^+$	**Mass accuracy < 5 ppm**	
Observed *m/z*	**Lipid species (C:N)**	**Fatty acyl chain**
	Monogalactosyl diacylglycerol	
740.5309	MGDG (32:4)	16:0/16:4
742.5479	MGDG (32:3)	16:0/16:3 and 14:1/18:2
746.5765	MGDG (32:1)	14:0/18:1 and 16:0/16:1
768.5621	MGDG (34:4)	18:4/16:0 and 16:1/18:3
772.5935	MGDG (34:2)	18:2/16:0 and 16:1/18:1
774.6074	MGDG (34:1)	18:1/16:0
788.5307	MGDG (36:8)	18:4/18:4
790.5459	MGDG (36:7)	18:3/18:4
792.5614	MGDG (36:6)	18:3/18:3
794.5772	MGDG (36:5)	18:2/18:3 and 20:5/16:0
796.5929	MGDG (36:4)	20:4/16:0 and 18:2/18:2
814.5546	MGDG (38:9)	20:5/18:4
816.5608	MGDG (38:8)	20:5/18:3 and 20:4/18:4
818.5766	MGDG (38:7)	20:5/18:2 and 20:4/18:3
820.5926	MGDG (38:6)	20:4/18:2
822.6073	MGDG (38:5)	20:4/18:1
824.6235	MGDG (38:4)	20:4/18:0
	Digalactosyl diacylglycerol	
904.5992	DGDG (32:3)	16:0/16:3
906.6148	DGDG (32:2)	14:0/18:2
908.6305	DGDG (32:1)	14:0/18:1 and 16:0/16:1
932.6305	DGDG (34:3)	18:3/16:0
934.6461	DGDG (34:2)	18:2/16:0 and 18:1/16:1
936.6618	DGDG (34:1)	18:1/16:0
938.6780	DGDG (34:0)	18:0/16:0
952.5992	DGDG (36:7)	18:3/18:4
954.6148	DGDG (36:6)	18:3/18:3
956.6305	DGDG (36:5)	20:5/16:0 and 18:2/18:3
958.6461	DGDG (36:4)	20:4/16:0 and 18:2/18:2
960.6623	DGDG (36:3)	18:1/18:2
962.6780	DGDG (36:2)	18:1/18:1
964.6936	DGDG (36:1)	18:1/18:0
976.5992	DGDG (38:9)	20:5/18:4
978.6148	DGDG (38:8)	20:5/18:3 and 20:4/18:4
980.6305	DGDG (38:7)	20:4/18:3 and 20:5/18:2
982.6461	DGDG (38:6)	20:4/18:2 and 20:5/18:1

984.6623	DGDG (38:5)	20:4/18:1
986.6780	DGDG (38:4)	20:4/18:0
Sulfolipids [M − H]$^-$		**Mass accuracy < 5 ppm**
Observed *m/z*	**Lipid species (C:N)**	**Fatty acyl chain**
	Sulfoquinovosyl monoacylglycerol	
527.2525	SQMG (14:0)	
553.2688	SQMG (16:1)	
555.2838	SQMG (16:0)	
577.2678	SQMG (18:3)	
579.2839	SQMG (18:2)	
581.3000	SQMG (18:1)	
	Sulfoquinovosyl diacylglycerol	
737.4510	SQDG (28:0)	14:0/14:0
763.4666	SQDG (30:1)	16:0/14:1
765.4823	SQDG (30:0)	16:0/14:0
787.4666	SQDG (32:3)	18:3/14:0
789.4666	SQDG (32:2)	18:2/14:0
791.4979	SQDG (32:1)	18:1/14:0
793.5136	SQDG (32:0)	18:0/14:0
813.4823	SQDG (34:4)	18:3/16:1
815.4979	SQDG (34:3)	18:3/16:0
817.5136	SQDG (34:2)	18:2/16:0
819.5292	SQDG (34:1)	18:1/16:0
821.5449	SQDG (34:0)	18:0/16:0
839.4979	SQDG (36:5)	20:5/16:0
841.5136	SQDG (36:4)	20:4/16:0

Numbers in parentheses (C:N) indicate the number of carbon atoms (C) and double bonds (N) in the fatty acid side chains. Bold represents the abundant molecular species

Identification of the phospholipids´ profile of **Fucus vesiculosus** *and their variation with season effect*

Phospholipids in the lipid extract of *Fucus vesiculosus* from both seasons were identified by LC–MS and distributed by nine classes of PLs such as phosphatidylcholine (PC) and lyso-PC, phosphatidylglycerol (PG) and lyso-PG, phosphatidylinositol (PI) and lyso-PI, phosphatidylethanolamine (PE) and lyso-PE, and phosphatic acid (PA) (Figure III.25, Table III.17).

Phosphatidylcholine and lyso-PC

The PC and lyso-PC (LPC) were identified as $[M + H]^+$ ions. Seven PCs were seen in the lipidome of macroalgae from both seasons with most abundant at *m/z* 784.6 attributed

to PC (36:3). Other molecular species are described in Table III.17. Significant alterations were observed comparing the lipidomes of *F. vesiculosus* from spring versus winter (Fig. III.27. a). Statistically significant increase of PC (36:2) ($p < 0.001$) was observed in spring season. In winter, it was observed a significant increase of PC (36:5) ($p < 0.001$) and of PC (38:6) ($p < 0.01$). Three LPC were detected (Table III.17, Fig. III.26. b) and the most abundant was LPC (16:0), observed at *m/z* 496.3 in winter while LPC (18:1) was the most abundant in spring. Comparing spring versus winter lipidomes, there was a significant increase of aforementioned molecular species ($p < 0.001$) and decrease of LPC (16:1) ($p < 0.05$).

Phosphatidylglycerol and lyso-PG

The classes PG and lyso-PG were identified as $[M - H]^-$ ions. Sixteen PGs were identified and PG (34:4) at *m/z* 741.4, attributed to PG (16:1/18:3) while the lipidome of *F. vesiculosus* from winter contained the abundant at *m/z* 743.5 attributed to PG (16:0/18:3) and in the spring, it contained the abundant at *m/z* 773.5 attributed to PG (18:1/18:1). The other molecular species are described in Table III.17. Significant alterations were observed comparing lipidomes from spring versus winter macroalgae (Fig. III.25. c). Significant increase of PG (32:1), PG (34:1), PG (36:2) plus PG (36:4) ($p < 0.001$); PG (32:2) ($p < 0.01$), and PG (34:0) ($p < 0.05$) was observed in spring. These molecular species are mainly composed by 16:0 and 18:0 SFA and C_{18} MUFA. Regarding the winter lipidome, there was a significant increase of PG (34:3), identified as PG (16:0/18:3) and PG (34:4), identified as PG (16:1/18:3) ($p < 0.001$). Three LPG were observed in the lipidome from both seasons, being the most abundant the LPG (16:0) and the LPG (16:1), at *m/z* 483.3 and 481.3, respectively. It was observed a significant increase of LPG (16:0) ($p < 0.01$) and decrease of the LPG (16:1) ($p < 0.001$) comparing spring versus winter seasons (Fig. III.25. d).

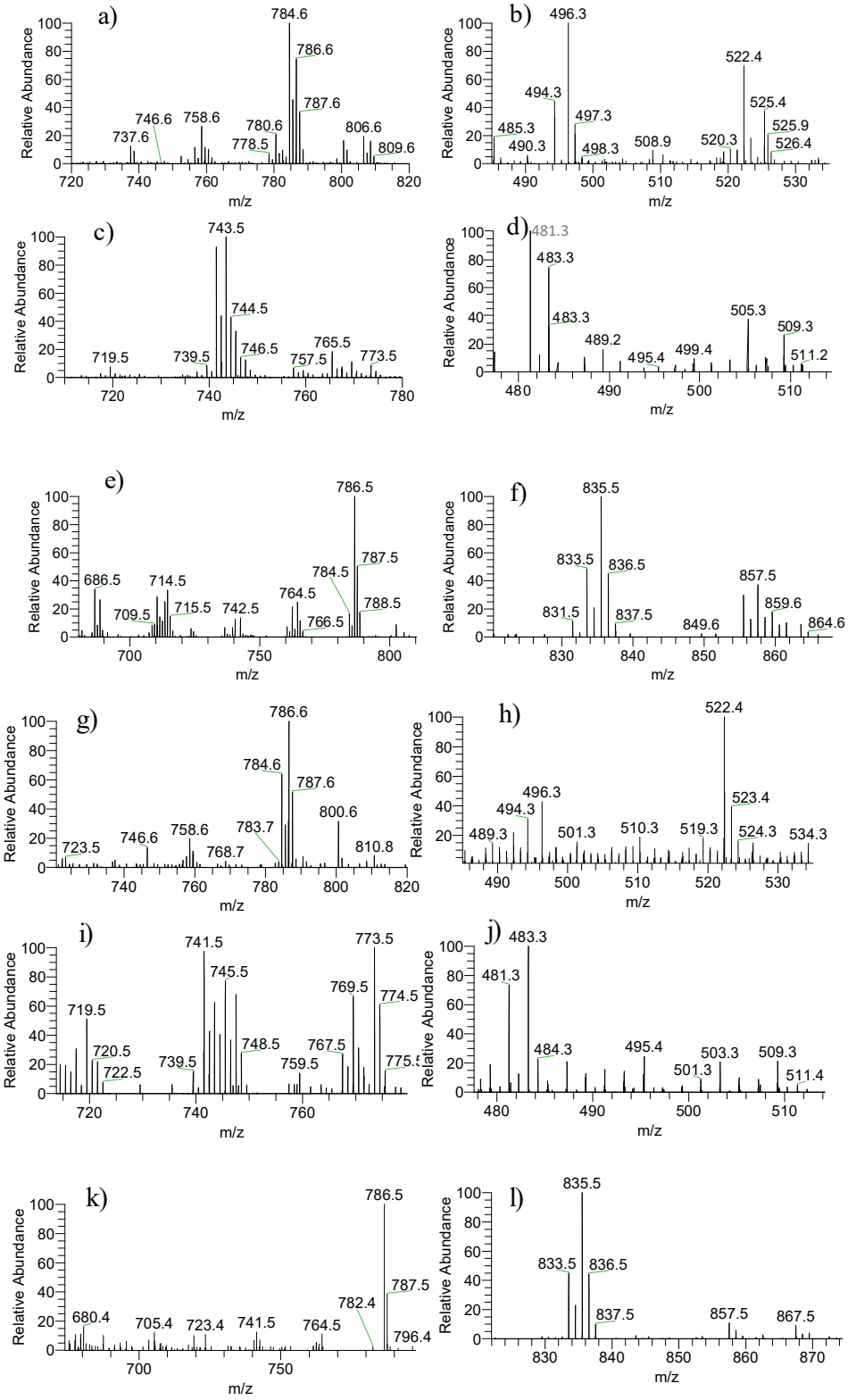

Figure III. 25. LC–MS spectra of phospholipids from *Fucus vesiculosus* collected in February (mid-winter) and May (end-spring) observed by LC–MS, respectively a) and g) PC, b) and h) LPC as $[M + H]^+$ ions; c) and i) PG, d) and j) LPG, e) and k) PE, f) and l) PI as $[M - H]^-$ ions.

Table III. 17. Identification of phospholipid molecular species observed by HILIC–LC–MS in *Fucus vesiculosus*, PC and LPC as $[M + H]^+$ ions; PG, LPG, PI, LPI, PE, LPE, and PA, were identified as $[M - H]^-$ ions

Phospholipids $[M + H]^+$	**Mass accuracy < 5 ppm**	
Observed *m/z*	**Lipid species (C:N)**	**Fatty acyl chain**
	Phosphatidylcholine	
758.5689	PC (34:2)	*
760.5835	PC (34:1)	*
780.5530	PC (36:5)	*
784.5850	PC (36:3)	*
786.6005	PC (36:2)	*
806.5683	PC (38:6)	*
808.5831	PC (38:5)	*
	Lyso-phosphatidylcholine	
496.3392	LPC (16:0)	
494.3241	LPC (16:1)	
522.3556	LPC (18:1)	
Phospholipids $[M - H]^-$		**Mass accuracy < 5 ppm**
Observed *m/z*	**Lipid species (C:N)**	**Fatty acyl chain**
	Phosphatidylglycerol	
717.4710	PG (32:2)	16:0/16:2 and 16:1/16:1
719.4868	PG (32:1)	16:1/16:0 and 14:0/18:1
721.5033	PG (32:0)	16:0/16:0 and 14:0/18:0
741.4713	PG (34:4)	16:1/18:3
743.4862	PG (34:3)	16:0/18:3 and 16:1/18:2
745.5018	PG (34:2)	16:0/18:2
747.5183	PG (34:1)	18:0/16:1
749.5335	PG (34:0)	16:0/18:0
769.5017	PG (36:4)	16:0/20:4 and 18:2/18:2
771.5160	PG (36:3)	18:1/18:2
773.5333	PG (36:2)	18:1/18:1
	Lyso-phosphatidylglycerol	
481.2569	LPG (16:1)	
483.2733	LPG (16:0)	
509.2887	LPG (18:1)	
	Phosphatidylinositol	
833.5175	PI (34:2)	16:0/18:2
835.5339	PI (34:1)	16:0/18:1
837.5491	PI (34:0)	16:0/18:0
855.5041	PI (36:5)	18:4/18:4
857.5196	PI (36:4)	16:0/20:4
859.5352	PI (36:3)	18:0/18:3
861.5505	PI (36:2)	18:0/18:2

863.5674	PI (36:1)	18:0/18:1
	Lyso-Phosphatidylinositol	
597.3060	LPI(18:1)	
	Phosphatidylethanolamine	
686.4758	PE (32:2)	14:0/18:2
688.4923	PE (32:1)	14:0/18:1
714.5067	PE (34:2)	16:0/18:2
716.5227	PE (34:1)	16:0/18:1
762.5073	PE (38:6)	18:2/20:4
764.5232	PE (38:5)	18:1/20:4
784.4918	PE (40:9)	20:4/20:5
786.5076	PE (40:8)	20:4/20:4
788.5218	PE (40:7)	20:4/20:3
	Lyso-Phosphatidylethanolamine	
498.2613	LPE (20:5)	
500.2779	LPE (20:4)	
	Phosphatidic acid	
619.4330	PA (30:0)	14:0/16:0
645.4507	PA (32:1)	14:0/18:1
665.4184	PA (34:5)	14:0/20:5

Numbers in parentheses (C:N) indicate the number of carbon atoms (C) and double bonds (N) in the fatty acid side chains; * molecular species were identified by mass accuracy and by MS/MS by the product ion at *m/z* 184 of $[M + H]^+$ ions

Phosphatidylinositol

The class of PI was identified in negative-mode as $[M - H]^-$ ions and eight molecular species were identified in the lipidome of macroalgae from mid-winter (February) and seven were assigned in the lipidome from end-spring (May). The lipidome from both seasons was characterized by the abundant PI (34:1) at *m/z* 835.5, PI (16:0/18:1), followed by PI (34:2) at *m/z* 833.5 as PI (16:0/18:2). Others molecular species are described in Table III.17. Differences were observed after comparison between lipidomes of *F. vesiculosus* from spring versus winter (Fig. III.26. e). In the lipidome of spring, there was a significant increase of PI (34:1) and PI (34:2) ($p < 0.001$) that were composed by 16:0 and 18:1 or 18:2 FA, respectively; in the winter lipidome there was increase of PI (34:0), PI (36:1), PI (36:2), PI (36:3), and PI (36:4) ($p < 0.001$) plus PI (36:5) ($p < 0.01$) with some of these molecular species including 18:3, 18:4 and 20:4 PUFA. Only one LPI was identified at *m/z* 597.3 as LPI (18:1) that was more abundant in the lipidome of spring season (data not shown).

Phosphatidylethanolamine and lyso-PE

The classes of PE and lyso-PE were identified as $[M - H]^-$ ions. Nine PEs were identified in the lipidome from both seasons, with the most abundant PE (40:8) at *m/z* 786.5 attributed to PE (20:4/20:4). All molecular species are described in Table III.17. Significant alterations were observed comparing lipidome of *F. vesiculosus* from spring versus winter (Fig. III.25. f) and significant increase was found in PE (32:1), PE (32:2), and PE (34:2) ($p < 0.001$) from spring season while significant increase of PE (38:5) and PE (40:8) ($p < 0.001$); PE (38:6), PE (40:7), and PE (40:9) ($p < 0.05$) was observed in the lipidome from winter season. Moreover, two LPE were identified at *m/z* 498.3 and 500.3 corresponding to LPE (20:4) (the most abundant LPE in both seasons) and LPE (20:5). Comparing the lipidomes of spring versus winter, a statistically significant increase occurs with the LPE (20:4) and the contrary was observed with LPE (20:5) (Fig. III.25. f).

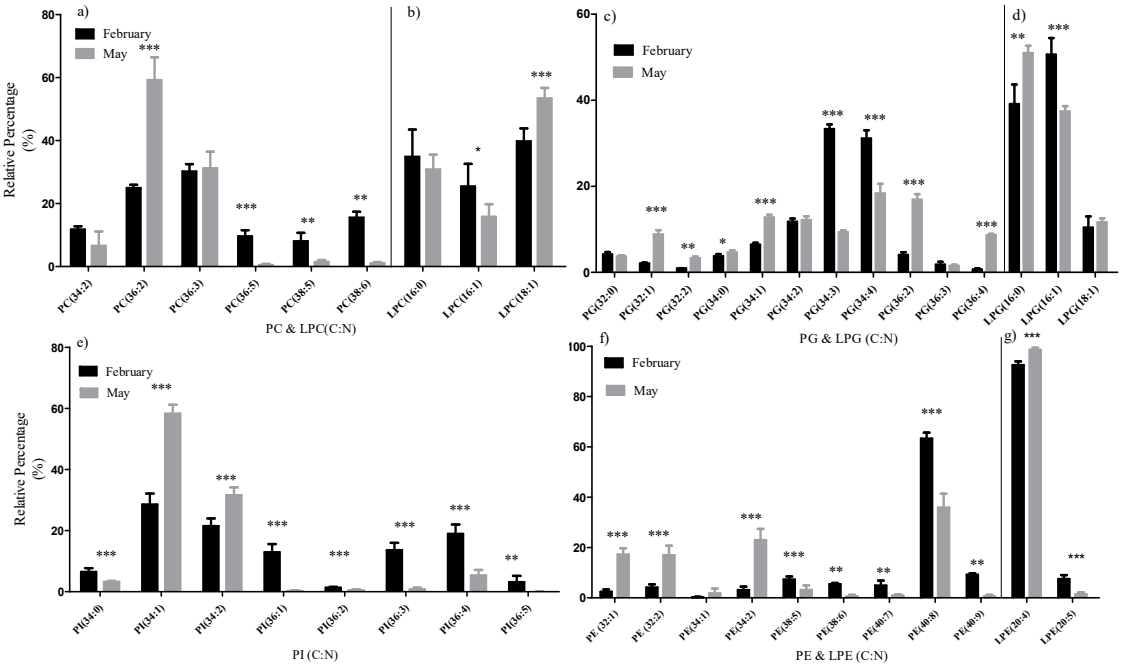

Figure III. 26. Percentage of a) PC, b) LPC and c) PG plus d) LPG, e) PI, f) PE and g) LPE, molecular species identified after LC–MS, MZ mine software and MS/MS analysis. The results are expressed as percentage obtained by dividing the ratio between peak areas of each molecular species and internal standards and the total of all ratios. Values are means ± standard deviation of the duplicate of three independent experiments. (***, significantly different $p < 0.001$; **, significantly different $p < 0.01$, * significantly different $p < 0.05$). February refers to *Fucus vesiculosus* collected in mid-winter. May refers to *Fucus vesiculosus* collected in end-spring.

Phosphatidic acid

PAs were identified in negative-mode as $[M - H]^-$ ions and three PAs were identified in the lipidomes of *F. vesiculosus* from both seasons. Significant alterations were observed comparing lipidomes from spring versus winter macroalgae (Supplementary Fig. S.8.) and significant increase was found at PA (30:0) as PA (14:0/16:0) and this was the abundant molecular species in the lipidome of macroalgae from spring. Most abundant PA (32:1) characterized the lipidome from winter and was attributed to PA (14:0/18:1), that also contribute to the statistically decrease observed comparing spring versus winter macroalgae.

Identification of the betaine lipids´ profile of* Fucus vesiculosus *and their variation with season effect

The analysis of total lipid extract provided the identification of betaine lipids diacylglyceryl-*N,N,N*-trimethyl-homoserine (DGTS), monoacylglyceryl-*N,N,N*-trimethyl-homoserine (MGTS), diacylglyceryl hydroxymethyltrimethyl-β-alanine (DGTA) and monoacylglyceryl hydroxymethyltrimethyl-β-alanine (MGTA) that were identified as $[M + H]^+$ ions (Fig. III.27. a-h), Table III.18, Supplementary Fig. S.9). In both seasons, it was identified sixteen DGTS, seven MGTS, twenty-one DGTA and twelve MGTA. Regarding DGTS, in both seasons, most abundant DGTS was DGTS (32:1) observed at *m/z* 710.6 attributed to DGTS (14:0/18:1) and DGTS (16:0/16:1). Significant alterations were observed comparing lipidomes of macroalgae from spring versus winter (Fig. III.28.a) and significant increase was observed at DGTS (32:0), DGTS (32:1), DGTS (36:2), and DGTS (36:3) ($p < 0.001$), molecular species that combine 16:0, 16:1, 18:1, 18:2, and 18:3 FA. Significant increase of DGTS in the lipidome of *F. vesiculosus* from winter was attributed to DGTS (32:2), DGTS (32:3), DGTS (34:2) and DGTS (34:3) ($p < 0.001$); DGTS (34:1) ($p < 0.01$); and DGTS (32:4) ($p < 0.05$), molecular species combining 16:0 FA and C_{16} and C_{18} PUFA. All molecular species are described in Table III.18.

Betaine lipids were identified by using LC–MS, MS/MS and mass accuracy approaches as $[M + H]^+$ ions. The class of DGTA was for the first time identified at molecular level in *Fucus vesiculosus* and in macroalgae; and MGTA was identified for the first time in the lipidome of macroalgae (Fig. III.27. e-f), Table III. 18). These classes have different

elution profile in the chromatogram (LC–MS), with DGTS and MGTS eluting within 6 - 8 minutes while DGTA and MGTA eluted within 16 - 20 minutes (Supplementary Fig. S.9).

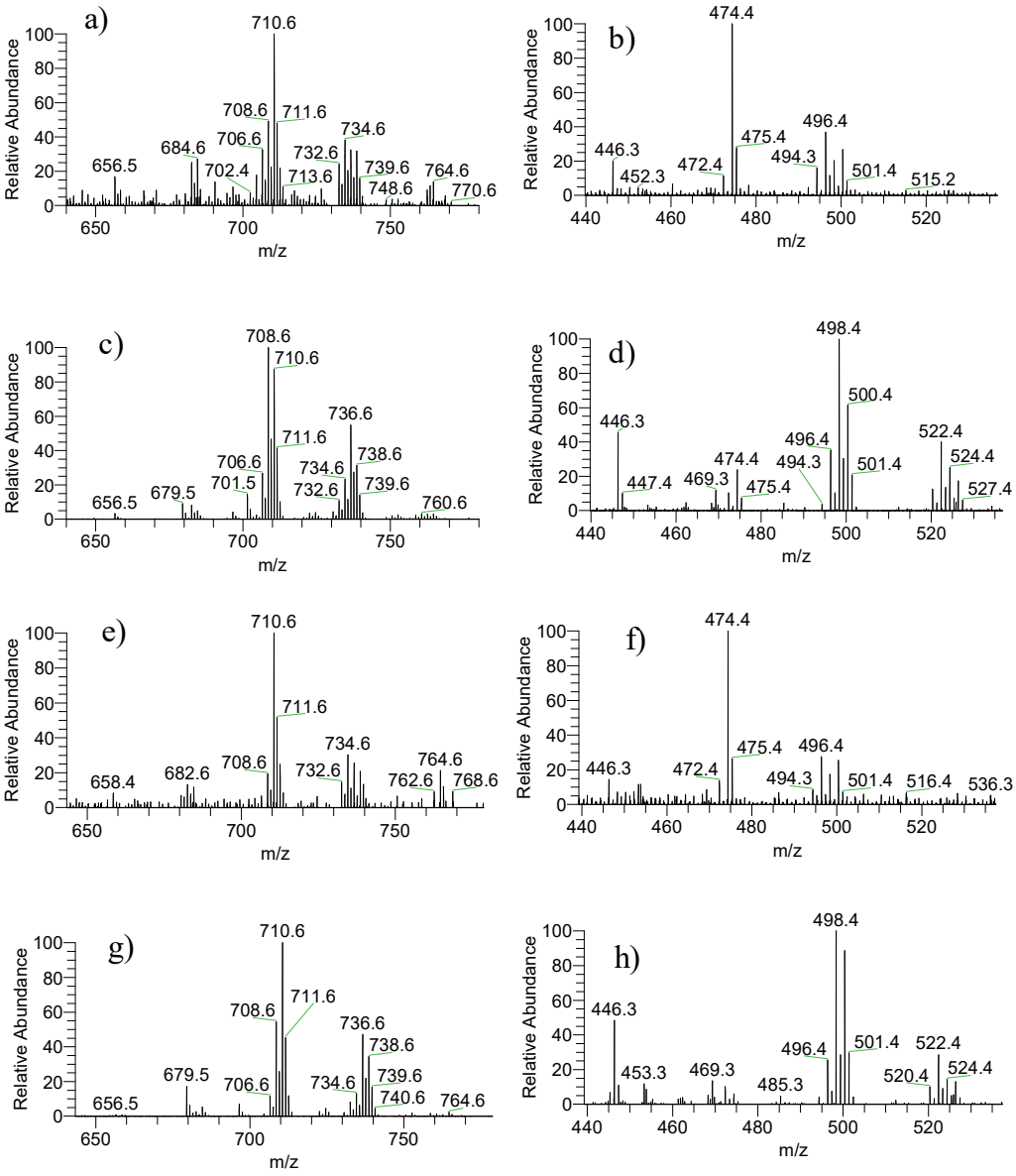

Figure III. 27. LC–MS spectra of betaine lipids from *Fucus vesiculosus* collected in February (mid-winter) and May (end-spring) observed by LC-MS, respectively a) and e) DGTS, b) and f) MGTS, c) and g) DGTA, e) and h) MGTA as $[M + H]^+$ ions.

Moreover, the structural identification of each class was supported by MS/MS and the fragmentation pattern analysis by polar head assigned at the characteristic *m/z* 236 and the assignment of product ions that result from the loss of fatty acyl (Supplementary Fig. S.9). DGTA was distinguished from the structural isomer DGTS by the higher abundance of the

molecular ion and much lower abundance of the product ions representing the polar head and the loss of fatty acyl. These features were described by Roche et al (2010) that studied sodiated adducts of DGTS and DGTA of Chlorarachniophyta (216). The most abundant DGTA observed in the lipidome of *F. vesiculosus* from winter was attributed to DGTA (32:2) at *m/z* 708.6 as DGTA (14:0/18:2) and DGTA (16:0/16:2), and to DGTA (32:1) at *m/z* 710.6 and DGTA (34:2), that was also the most abundant DGTA in spring season. Significant alterations were observed comparing lipidomes of *F. vesiculosus* from spring versus winter (Fig. III.28. c) and significant increase was observed for DGTA (28:0), DGTA (30:0), DGTA (32:1), and DGTA (34:1) ($p < 0.001$); and DGTA (32:0) ($p < 0.01$), with molecular species including SFA and MUFA. Moreover, significant increase observed in the lipidome of macroalgae from winter was attributed to DGTA (32:2), DGTA (32:3), DGTA (34:2), DGTA (34:4), DGTA (36:3), and DGTA (36:4) ($p < 0.001$); and DGTA (30:1), DGTA (32:4), and DGTA (34:3) ($p < 0.01$), molecular species that include C_{16}, C_{18}, and C_{20} PUFAs.

The molecular species MGTA (18:2), observed at *m/z* 498.4, was the most abundant and was common in the lipidome from both seasons, while spring *F. vesiculosus* also contained the MGTA (18:1) at *m/z* 500.4. Considering the variation on the lipidome of *F. vesiculosus* from spring, it was inferred by the significant increase of MGTA (18:1), MGTA (18:2), and MGTA (18:4) ($p < 0.001$), while significant increase in the lipidome from winter was inferred by the MGTA (16:0), MGTA (18:3), MGTA (20:2), MGTA (20:3), MGTA (20:4), and MGTA (20:5).

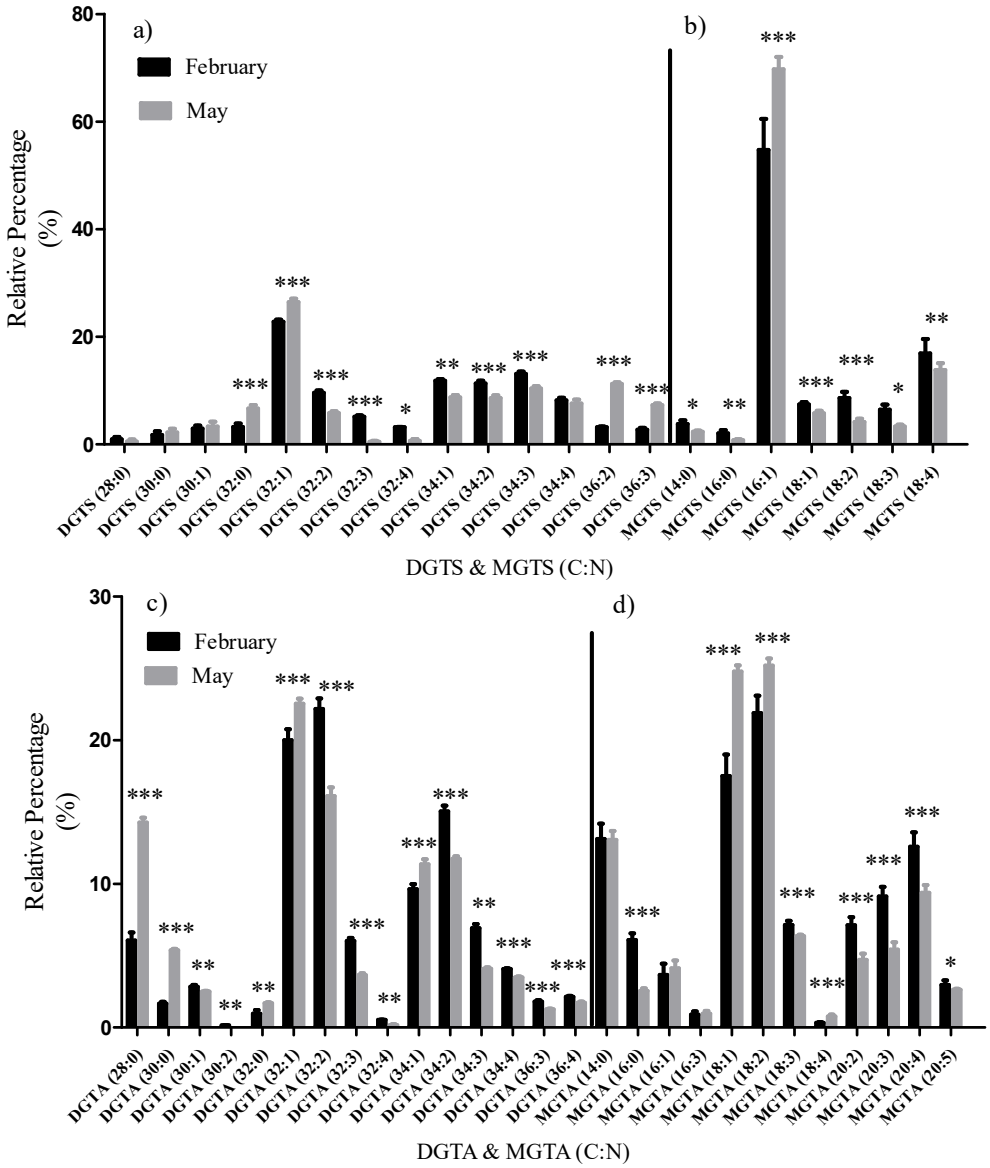

Figure III. 28. Percentage of a) DGTS, b) MGTS and c) DGTA plus d) SQMG molecular species identified after LC–MS, and MS/MS analysis. The results are expressed as percentage obtained by dividing the ratio between peak areas of each molecular species and internal standards and the total of all ratios. Values are means ± standard deviation of the duplicate of three independent experiments. (***, significantly different $p < 0.001$; **, significantly different $p < 0.01$, * significantly different $p < 0.05$). February refers to *Fucus vesiculosus* collected in mid-winter. May refers to *Fucus vesiculosus* collected in end-spring.

Table III. 18. Identification of betaine molecular species observed by HILIC–LC–MS in *Fucus vesiculosus.* DGTS, MGTS, DGTA, and MGTA are identified as $[M + H]^+$ ions

Betaine lipids $[M + H]^+$	**Mass accuracy < 5 ppm**	
Observed *m/z*	**Lipid species (C:N)**	**Fatty acyl chain**
Diacylglyceryl trimethyl-homoserine (DGTS)		
656.5465	DGTS (28:0)	14:0/14:0
682.5622	DGTS (30:1)	14:0/16:1
684.5778	DGTS (30:0)	14:0/16:0
704.5465	DGTS (32:4)	16:1/16:3
706.5622	DGTS (32:3)	14:0/18:3 and 16:0/16:3
708.5778	DGTS (32:2)	16:0/16:2
710.5935	DGTS (32:1)	14:0/18:1 and 16:0/16:1
712.6091	DGTS (32:0)	16:0/16:0
732.5778	DGTS (34:4)	16:0/18:4
734.5935	DGTS (34:3)	16:0/18:3
736.6091	DGTS (34:2)	16:0/18:2
738.6248	DGTS (34:1)	16:0/18:1
762.6248	DGTS (36:3)	18:0/18:3
764.6404	DGTS (36:2)	18:0/18:2
Monoacylglyceryl trimethyl-homoserine (MGTS)		
446.3470	MGTS (14:0)	
472.3632	MGTS (16:1)	
474.3792	MGTS (16:0)	
494.3477	MGTS (18:4)	
496.3634	MGTS (18:3)	
498.3796	MGTS (18:2)	
500.3943	MGTS (18:1)	
Diacylglyceryl hydroxymethyl-trimethyl-β-alanine (DGTA)		
656.5465	DGTA (28:0)	14:0/14:0
680.5465	DGTA (30:2)	14:0/16:2
682.5622	DGTA (30:1)	14:0/16:1
684.5778	DGTA (30:0)	14:0/16:0
704.5465	DGTA (32:4)	16:1/16:3
706.5622	DGTA (32:3)	14:0/18:3 and 16:0/16:3
708.5778	DGTA (32:2)	14:0/18:2 and 16:0/16:2
710.5935	DGTA (32:1)	14:0/18:1 and 16:0/16:1
712.6091	DGTA (32:0)	14:0/18:0 and 16:0/16:0
732.5778	DGTA (34:4)	14:0/20:4
734.5935	DGTA (34:3)	14:0/20:3 and 16:0/18:3
736.6091	DGTA (34:2)	14:0/20:2 and 16:0/18:2
738.6248	DGTA (34:1)	16:0/18:1
760.6091	DGTA (36:4)	16:0/20:4
762.6248	DGTA (36:3)	16:0/20:3

Monoacylglyceryl hydroxymethyl-trimethyl-β-alanine (MGTA)	
446.3481	MGTA (14:0)
468.3308	MGTA (16:3)
472.3632	MGTA (16:1)
474.3799	MGTA (16:0)
494.3472	MGTA (18:4)
496.3632	MGTA (18:3)
498.3784	MGTA (18:2)
500.3942	MGTA (18:1)
520.3642	MGTA (20:5)
522.3795	MGTA (20:4)
524.3957	MGTA (20:3)
526.4109	MGTA (20:2)

Numbers in parentheses (C:N) indicate the number of carbon atoms (C) and double bonds (N) in the fatty acid side chains

III.1.3.2. Fatty acids profile

The fatty acid methyl esters (FAMEs) profile of the lipid extracts from February (mid-winter) and May (end-spring) *Fucus vesiculosus* included twenty different fatty acids (Table III.19). The fatty acids were 14:0, 15:0, 16:0, 16:1, 16:2(*n*-6), 16:3(*n*-3), 18:0, 18:1(*n*-9), 18:2(*n*-6), 18:3(*n*-6), 18:3(*n*-3), 18:4(*n*-3), 20:0, 20:1(*n*-9), 20:2(*n*-6), 20:3(*n*-6), 20:4(*n*-6), 20:5(*n*-3), 22:0, and 24:0.

The lipidome of macroalgae from both seasons had similar composition in FAs, but showed significant differences in the content of some of the FAs. *Fucus vesiculosus* was characterized by high amounts of the 18:1(*n*-9) FA (25.3 ± 0.69% and 28.1 ± 1.44%, respectively) and 16:0 (17.2 ± 1.98% and 20.8 ± 2.12% in winter and spring seasons, respectively). However, both seasons *F. vesiculosus* also contained 20:4(*n*-6) (10.7 ± 0.96% and 13.5 ± 1.81%, respectively), 18:2(*n*-6) (8.78 ± 0.22% and 6.62 ± 0.49%, respectively), 18:3(*n*-3) (7.13 ± 0.58% and 3.92 ± 0.34%, respectively) and 20:5(*n*-3) (6.69 ± 0.94% and 4.75 ± 0.47%, respectively). In winter, *F. vesiculosus* was characterized by high amounts of PUFAs (40.5%), followed by SFA (32.2%) and MUFA (27.3%), meanwhile in spring season it mainly contained SFA (36.1%), followed by PUFAs (33.9%) and MUFAs (29.9%). Significant alterations were observed comparing FA profile of *F. vesiculosus* from spring versus winter (Fig. III.29) and significant increase was observed for FA 18:0 ($p < 0.001$), 18:1(*n*-9), 20:4(*n*-6) ($p < 0.01$), 16:0 and 20:0 ($p < 0.05$). In the winter season, there was a significant increase of the FA 16:2(*n*-6), 18:2(*n*-6) ($p < 0.001$), 14:0, 18:3(*n*-3), 18:4(*n*-3) and 20:1(*n*-9) $p < 0.01$, 16:1(*n*-7), and 20:5(*n*-3) FA ($p <$

0.05). Among these, the content of 18:0 was much higher in spring (6.09 ± 0.43%) than in winter (1.64 ± 0.25 %), and 18:3(*n*-3) was much lower in spring (3.92 ± 0.34%) than in winter (7.13 ± 0.58%).

Table III. 19. Fatty acid profile of *Fucus vesiculosus* collected in February (mid-winter) and May (end-spring), determined by GC–MS analysis of fatty acid methyl esters (FAMEs)

	February		May	
Fatty acids	**Mean (%)**	**±SD**	**Mean (%)**	**±SD**
14:0	10.9	1.08	6.58	1.48
15:0	0.54	0.05	0.49	0.05
16:0	17.2	1.98	20.8	2.12
18:0	1.64	0.25	6.09	0.43
20:0	0.35	0.11	0.59	0.14
22:0	0.50	0.07	0.65	0.25
24:0	1.11	0.23	0.90	0.22
Σ SFA	**32.2**		**36.1**	
16:1*n*-7	1.55	0.05	1.41	0.10
18:1*n*-9	25.3	0.69	28.1	1.44
20:1*n*-9	0.49	0.04	0.34	0.07
Σ MUFA	**27.3**		**29.9**	
16:2*n*-6	0.37	0.02	0.15	0.03
16:3*n*-3	0.12	0.03	0.21	0.06
18:2*n*-6	8.78	0.22	6.62	0.49
18:3*n*-6	0.89	0.41	0.70	0.11
18:3*n*-3	7.13	0.58	3.92	0.34
18:4*n*-3	4.35	0.51	2.71	0.19
20:2*n*-6	0.71	0.04	0.70	0.15
20:3*n*-6	0.71	0.09	0.70	0.17
20:4*n*-6	10.7	0.96	13.5	1.81
20:5*n*-3	6.69	0.94	4.75	0.47
Σ PUFA	**40.5**		**33.9**	
AA/EPA	1.60		2.85	
Σ *n*-6/**Σ** *n*-3	1.15		1.86	
Σ C_{16}/**Σ** C_{18}	0.40		0.47	

AA – Arachidonic acid; EPA – Eicosapentaenoic acid; Means (%) and standard deviations (S.D.) were obtained from three replicates (content less than 0.1% not shown)

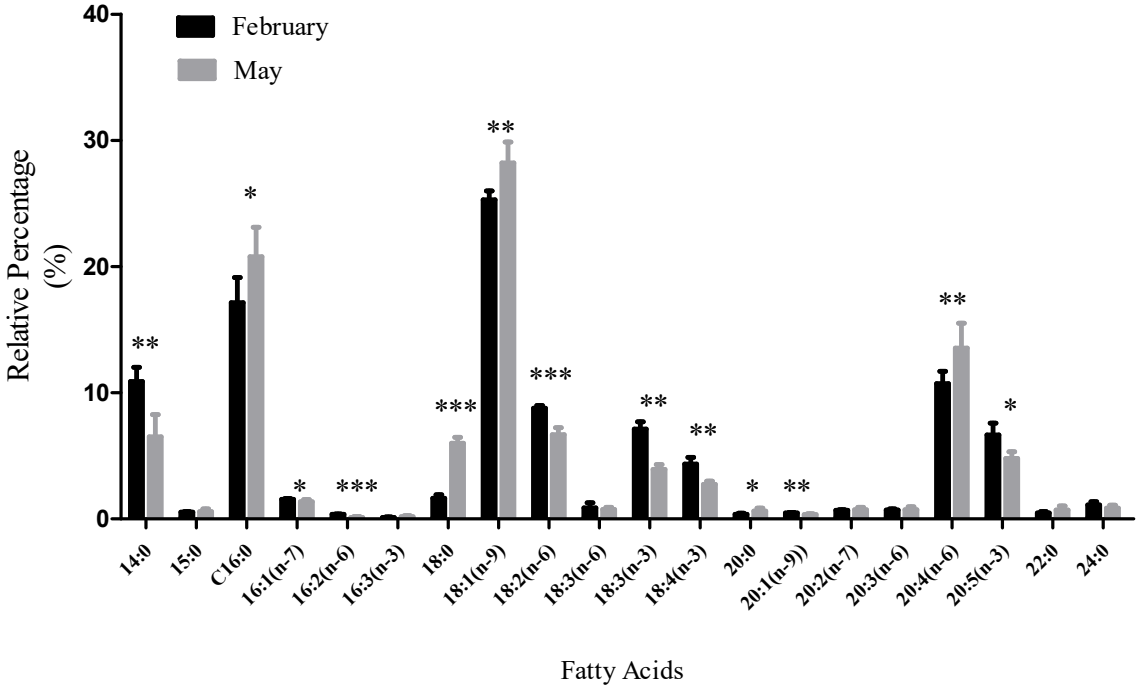

Figure III. 29. Percentage of FAMEs expressed by the ratio between each FAME and the total of all individual areas. Values are means ± standard deviation of the duplicate of three independent experiments. (***, significantly different $p < 0.001$; **, significantly different $p < 0.01$, * significantly different $p < 0.05$). February refers to *Fucus vesiculosus* collected in mid-winter. May refers to *Fucus vesiculosus* collected in end-spring.

These aforementioned contents are reflected on *n*-6/*n*-3 PUFAs ratio that was 1.15 in winter season and 1.86 in spring season. AA/EPA ratio was higher in spring season (2.85) than in winter season (1.60), and same trend was observed for the content of MUFA and SFA, while the highest content of PUFA was obtained in the lipidome of winter *F. vesiculosus*.

III.1.3.3 Discussion

The lipids extracted from mid-winter *Fucus vesiculosus* accounted for 9.13 ± 0.91 g/kg of dry biomass and end-spring biomass accounted for 4.10 ± 0.36 g/kg of dry biomass. These amounts are in agreement with previous published works, obtained in analogous seasons and adult stages and accumulation of lipids in winter is known to be related with membrane-forming, energy storage roles of lipids and the decrease of lipid content in spring may be due to the energy loss on sporogenesis (310,330,334).

The lipidome of *F. vesiculosus* was established for the first time by using LC–MS, mass accuracy & MS/MS. In both season samples, seventy-two glycolipids, fifty-three phospholipids, and fifty-six betaine lipids were identified. Among these it was identified the MDGD, DGDG, SQDG, PC, PG, PI, PE, and DGTA also previously described in the order of Fucales and other brown alga (150,335). The classes SQMG, lyso-PC, lyso-PG, lyso-PI, lyso-PE, phosphatic acid (PA); betaine lipids DGTS, MGTS, and MGTA were identified in the lipidome of *F vesiculosus* never reported before (36,335). Most probably, the nonappearance of these classes in previous published work can be due to the use of low sensitive analytical techniques such as off-line TLC. In what concern betaine lipids, both DGTA and the structural isomer DGTS were identified. DGTA is reported as a typical class of brown macroalgae, while DGTS was mainly attributed to assign green and, more recently found in red macroalgae (36,136). Otherwise, it was reported that some Ochrophyta like genus *Fucus* did not contain DGTS structural isomers (150,154,335). DGTS and MGTS were herein found in Fucales, contrary to previous published information. The full differentiation of these isomers was possible herein by using HILIC–MS, that allowed the elution of both isomers at different retention times, and MS/MS & mass accuracy to confirm the identity of DGTA and DGTS based on the fragmentation pattern (154). Roche & Leblond identified both isomers in the lipidome of microalgae as sodiated adducts, with a previous separation of both classes by off-line TLC (216). It has been suggested that the presence of DGTA within brown macroalgae is an indicative for the differentiation inter-taxonomy, that its corroborate with our results (336).

At molecular level, the lipidome of *Fucus vesiculosus* can be characterized by the high number of GLs including PUFA highlighting the presence of MGDG and DGDG molecular species that include 20:4, 20:5 with 18:3 and 18:4. SQDG preferably combined SFA and a minor number of species included 20:4 and 20:5 FA. These species showed variation with season, with the ones with PUFA increasing in winter, probably due to the lower temperature characteristic from this season. Also, there is a tendency of the increase of the abundance of polar lipids molecular species with C_{18} while a partial decrease of C_{20}, as was already been reported for the FA profile (97). Some glycolipid esterified to 18:2, 18:3, 18:4, 20:4 and 20:5 FA from brown algae have been reported with activity against tumors (27,67,94,97), namely some SQDG and DGDG were found to induce apoptosis of the human colon carcinoma Caco-2 cell (223).

The PLs from brown macroalgae molecular species had a varied composition including 14:0, 16:0, C_{18} and C_{20} FA. PG is a plastidial lipid and contained a major number of molecular species that include the C_{16} combined with C_{18} FA type such as 18:3 FA and, in less extent, C_{20} PUFA. Among PLs, PE class major include PUFAs such as 20:3, suggested as brown macroalgae´s biomarker of PLs (97,335). The role of PE carrying on more unsaturated lipid PLs deserves to be more explored, suggesting the greatest importance of this extra-plastidial class as a source of 20:4 and 20:5 PUFA. The composition of PLs was found to be dependent on season effect. The classes PC, PG, PI and PE of macroalgae from the winter season showed the increasing in the relative abundance of several molecular species that contained PUFAs preferably 18:3 and 18:4, while molecular species combining MUFAs such as 18:1 and as 18:2 substantially decreased, and with PE contributing to the increase of 20:4 and 20:5 pool in winter season.

Betaine lipids classes commonly combined 14:0 and 16:0 with C_{18} FA, however DGTS and MGTS are differentiated by including C_{16} and C_{18} PUFA while DGTA and MGTA preferably included C_{18} and C_{20} FA such as 20:4 and 20:3 FA. The season effect was also reflected in betaine lipids such as DGTS and MGTS, by the increase of molecular species C_{16} and unsaturated C_{18} in winter season while DGTA and MGTA was major reflected by the statistically increase of molecular species with PUFA such as 16:3, 18:3, and 20:3. Spring season effects was more reflected in the increase of molecular species combining SFA and MUFA.

In the lipidome of macroalgae, it was identified a new class, MGTA, never reported in algae, and showed the increase of C_{18} PUFA in winter season. Thus, overall, with season effect it is suggested a great variation in the content of total lipids and a shift between SFA and PUFA, mainly reflected by the increase of C_{18} and C_{20} PUFA by major contributions of GLs related to C_{18} and C_{20} (*n*-3) type while in PLs was generally more reflected on 18:2(*n*-6) and 18:3(*n*-3) and C_{20} pool inferred by the contribution of PE class to while betaine lipids contributed to the increase of C_{16}, C_{18} (*n*-3), and DGTA plus MGTA particular contribution to the variation of C_{20} PUFA namely 20:3(*n*-6) and 20:4(*n*-6) FA.

Fucus vesiculosus contained abundant 14:0, 16:0, 18:1(*n*-9) and 20:4(*n*-6) FA, in accordance with literature (335,337). The variation in the lipidome with season effect was particularly reflected by the increase of C_{18}-PUFA and of *n*-3 FA in *F. vesiculosus* from

winter season, and consequently, total PUFA content in winter is higher than MUFA and SFA. Lipidome from spring season was characterized by high SFA content (36.1%).

To maintain cell membrane fluidity, adaptive changes allow macroalgae to adjust to environmental conditions (85,338). It is known that major adaptation of metabolic function at low temperatures to maintain membrane fluidity is by changing membrane lipid desaturation to control the melting point and thus respond to environment temperature (339). These changes are directly reflected on the *n*-6/*n*-3 PUFA ratio that was lower in winter season, and lower than reported to genus *Fucus* (297). In fact, temperature seems to have major effects in the composition and profile of polar lipids from brown macroalgae to adapt according season (97,120). Altogether, Fucales from winter season have major features to be used for food or feed diet as a source of lipids with nutritional value and as potential source of bioactive lipids fostering their smart valorization.

III.2. BIOPROSPECTION OF POLAR LIPIDS

The data contained this section was published:

Elisabete da Costa, Tânia Melo, Ana S. P. Moreira, Carina Bernardo, Luisa Helguero, Isabel Ferreira, Maria Teresa Cruz, Andreia M. Rego, Pedro Domingues, Ricardo Calado, Maria H. Abreu and Maria Rosário Domingues, ***Valorization of Lipids from Gracilaria sp. through Lipidomics and Decoding of Antiproliferative and Anti-Inflammatory Activity*.** Marine Drugs (2017) 15(3), 62.

Bioprospection of polar lipids

Macroalgae are consumed all over the world and are recognized as a source of nutrients and bioactive compounds. Macroalgae and macroalgae-based products are continuously reaching the markets and are associated with health claims and beneficial effects in maintenance of health and preventing aging associated disease (28,181). New products containing anti-inflammatory compounds are gathering the attention of food and pharma industries to treat and prevent these chronic and inflammatory diseases. Polar lipids from macroalgae are considered high value novel-lipids with health beneficial effects such as anti-inflammatory and antitumoral, with potential applications in nutraceutical, cosmetics and pharmaceutical industries (1,23,28).

III.2.1. Anti-inflammatory activity on nitrite production in RAW 264.7 cells

III.2.1.1 Introduction

Inflammation is a pathological condition and the first response of the immune system to infection or irritation in which highly reactive species are produced. Inflammation activated by lipopolysaccharide (LPS) release various pro- and anti-inflammatory mediators. Among them, NO a free radical produced from L-arginine by nitric oxide synthases (NOS) play key roles in this process (316,340,341). NF-κB is one of the most important transcription factors involved in the transactivation of genes related to the regulation of inflammatory responses (341) and in response to LPS, it controls expression of genes for iNOS (Fig.III.30).

The anti-inflammatory effects of lipids have been related to the inhibition of certain inflammation mediators such as inducible forms of NOS (341), important pro-inflammatory enzymes. Nitric oxide – NO - is a small diffusible molecule responsible for vasodilatation, neurotransmission and inflammation. Expression of inducible NOS (iNOS) catalyzes the formation of large amounts of NO that plays a key role in the pathogenesis of a variety of inflammatory diseases. Therefore, the level of NO induced by iNOS may reflect the degree of inflammation and provides an indicator to assess inflammatory

processes. The use of macrophage cell lines exposed to the bacterial cell-wall component lipopolysacharide (LPS) is a common *in vitro* procedure for anti-inflammatory capacity evaluation (234). In murine macrophage RAW 264.7 cells, LPS stimulation alone allows nuclear translocation of the transcription factor to activate the expression of iNOS and its protein synthesis, with a corresponding increase in NO production. This cell system is often used as model for drug screening with anti-inflammatory properties and the subsequent evaluation of potential inhibitors against iNOS and NO production.

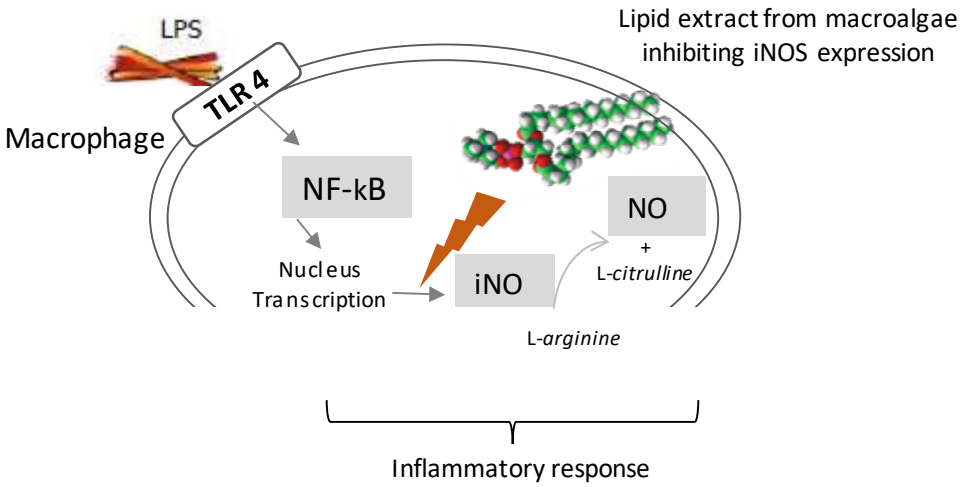

Figure III. 30. Representation of the inhibitory effect on NO production by lipid extracts in macrophages. LPS stimulation induces NF-kB that induce the nucleus translocation and production of iNOS through the activation of iNOS gene in the nucleus. iNOS produces NO and L-citrulline through the precursor L-arginine. NO is released to the extracellular medium. LPS – lipopolysaccharide; TLR4 – toll like receptor 4; NF-kB –nuclear factor kappa; iNOS – inducible nitric oxide synthase.

Polar lipids and FA isolated from algae have been reported as iNOS inhibitors. In addition, most of the inhibitory activity of these compounds towards NO production has been demonstrated to occur by the inhibition of the expression of iNOS (316,342). Lopes *et al*, 2014 were able to isolate two species of MGDG from *Fucus spiralis* that expressed the capacity to reduce NO release in a dose-dependent manner (27). Banskota et al. (30) evaluated the anti-inflammatory activity of isolated fractions of lipid extracts-rich in galactolipids from *Chondrus crispus,* that exibit inhibitory activity against lipopolysaccharide (LPS) inducible nitric oxide synthase (iNOS) production in murine RAW264.7 cells.

However, a better understand of lipid structures and correspondent action on the treatment of inflammatory diseases still represents a scientific challenge for further advances in the resolution of pathologies. Thus, the ability of lipid extracts from *Gracilaria* sp. to reduce the NO production in the extracellular medium of LPS-stimulated macrophages was evaluated. The Griess reaction, a spectrophotometric determination for nitrite, was carried out to quantify the nitrite levels in the conditioned medium of RAW 264.7 cells treated with LPS.

III.2.1.2 Results

The anti-inflammatory activity of the lipid extract of *Gracilaria* sp. was assessed based on its ability to inhibit nitric oxide (NO) production in RAW 264.7 macrophages stimulated with LPS. Previously, anti-oxidant activity of the extract was assessed by DPPH bioassay for a range of concentration between 50 and 500 µg/mL and it was obtained a IC_{50} of 250 µg/mL of ethanol. For a range of concentrations between 25 and 100 µg/mL, the lipid extract did not compromise the cellular viability of macrophages (Figure III.31.A).

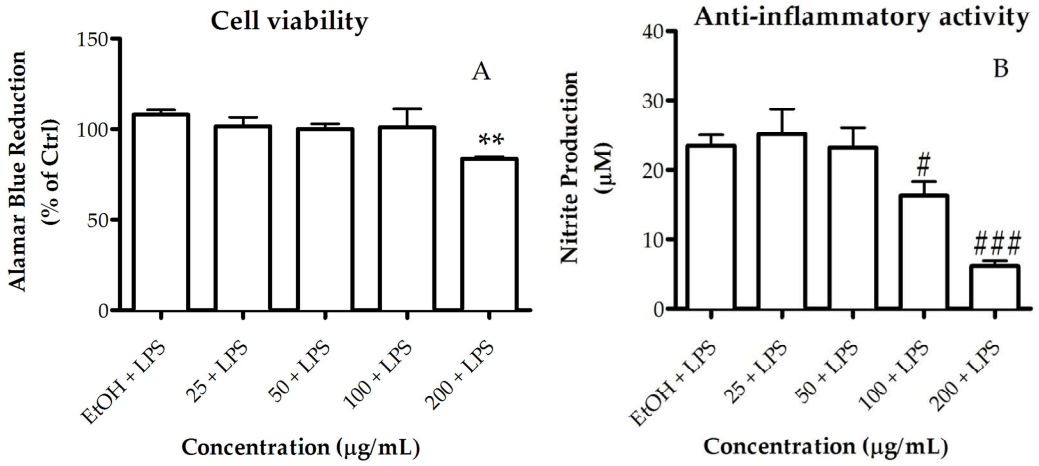

Figure III. 31. Cell viability and anti-inflammatory activity of *Gracilaria* sp. lipid extract. (**A**) Assessment of metabolically active cells was performed using a resazurin bioassay. Results are expressed as a percentage of resazurin reduction relative to the control (Ctrl). (**B**) Anti-inflammatory activity was measured as inhibition of NO production, quantified by the Griess assay. Nitrite concentration was determined from a sodium nitrite standard curve and the results are expressed as concentration (µM) of nitrite in a culture medium. Each value represents the mean ± SD from at least three independent experiments (** $p < 0.01$ compared to Ctrl; # $p < 0.05$, ### $p < 0.001$ compared to ethanol (EtOH, vehicle) plus lipopolysaccharide (LPS)).

The extract showed a dose-dependent NO inhibition of 35% attained at the concentration of 100 μg/mL (Figure III.31.B). Therefore, the concentration exhibiting anti-inflammatory activity also presented a safety profile to macrophages (Figure III.31.A). Meanwhile, at lower concentrations (≤ 50 μg/mL), the extract had no significant inhibitory effect.

Previous works have reported that polar lipid rich in PUFA may be beneficial for inflammatory diseases (23,30,32,181). Moreover, inflammation effect was more related to the omega-families of FA and, particularly, with the increasing ratio of *n*-6 to *n*-3. In fact, eicosanoids derived from *n*-6 PUFAs (such as 20:4(*n*-6)) have pro-inflammatory and immunoactive functions, while eicosanoids derived from *n*-3 PUFAs (20:5(*n*-3)) have anti-inflammatory properties (343). However, these FA showed less inhibitory effect when compared with polar lipids and it was suggested that the activity was rather related to the entire polar lipid structure (344). Accordingly, polar lipids isolated from red algae have demonstrated strong anti-inflammatory activity, even higher when compared with pure 20:5(*n*-3) FA isolated from the same extracts (181), suggesting that the polar lipid itself may contribute to the anti-inflammatory activity. In the cases of *Chondrus crispus* and *Palmaria palmata* the polar lipids such as glycolipids and phospholipids showed NO inhibitory activity through downregulation of inducible nitric oxide synthase (iNOS) (30,181). Moreover, extracts rich in glycolipids bearing high proportions of PUFA, isolated from the red macroalgae *Palmaria palmata*, *Porphyra dioica*, and *Chondrus crispus*, downregulated LPS-induced pro-inflammatory responses in human macrophages through the inhibition of IL-6 and IL-8 production, thus inferring their potential anti-inflammatory activity (224). Therefore, as for other red macroalgae, the lipid extract from *Gracilaria* sp. proved to have effective anti-inflammatory activity.

III.2.2. Activity of Lipid Extract on Human Cancer Cell Viability

III.2.2.1. Introduction

Cancer incidences are increasing and therefore instant effective therapies are needed to control these malignant diseases (236). Cancer is one of the most common and serious disease, and there are six properties that make cells capable of cancerous growth; they are not under the control of signals that regulate cell proliferation, they are resistant to apoptosis, they overcome the limitations on proliferation by avoiding replicative senescence and evading differentiation, they are genetically unstable, are able to invade surrounding tissues and are capable of metastasis (345,346). The cancerous tumor develops when cancer cells overcome replicative cell senescence and become "immortalized" *i.e*. continue dividing indefinitely (237) and instead of stopping, they continue to grow and divide. Chemotherapy is usually the first line treatment to cure cancers and a group of drugs are used to kill or inhibit the growth of cancer cells (238). The research in anticancer activities of non-toxic biological macromolecules as alternative to chemotherapy drugs emerges (236,238).

Macroalgae consumption and health benefits are considered potential source of anticancer drugs, functional foods and pharmacological products (5). In the current scenario, pharmaceutical companies are gaining much interest into compounds isolated from marine algae for drug development, for example lipids (71,223,347,348). Marine algae are considered a potential source of natural bioactive substances and there has now emerged a great interest towards isolating and identifying compounds and constituents from algae (236,237,240,241). Recent research on polar lipids isolated from macroalgae revealed that these can promote growth-inhibiting effects on distinct human adenocarcinoma, malignant melanoma and human hepatocellular carcinoma, as well as inhibiting DNA polymerases (132,349). Lipid-based agents are therefore emerging molecules in therapeutics aimed to regulate inflammatory pathways or even impair downstream tumorigenic processes that promote the proliferation of cancer cells (287,350). Among the polar classes, glycolipids dominated the research and were found to induce apoptosis of the human colon carcinoma Caco-2 cell (223) or inhibit the grow of human hepatocellular carcinoma cell line (HepG2) (132). Algal phospholipids showed high

anticancer activity against breast (MCF-7) and liver human (HepG2) cancer cells and highly inhibition of MCF-7 cell line growth.

The biological properties of polar lipids are closely related to chemical composition, but it is nevertheless difficult to determine exactly which compounds are responsible for the bioactivity (188). The modulating effects of macroalgae extracts and their bioactive components on oxidative stress and on oxidative stress-related diseases and cancers need to be more investigated (3,137).

In the process of identifying potential anticancer agents, they are tested for cytotoxic activity against a panel of standard cancer cell lines, estimating the dose required to inhibit the growth of each cell line (236). Bladder cancer is one of most common urological malignancy in the world, with transitional cell carcinoma being the most prevalent type (~90%) of bladder cancer (351) while breast cancer is a complex heterogeneous disease and one of the leading causes of death among women (316,348,352). Red macroalgae studied so far, exhibited strong potential against various cancer cells without producing toxicity. Thus, in this work, antiproliferative effect of *Gracilaria* sp. lipid extract in two human cancer cell lines of breast cancer - T-47D and bladder cancer – 5637 was assessed by using a colorimetric Presto blue assay, aiming to contribute for developing potential anticancer drugs from red macroalgae.

III.2.2.2 Results

The growth inhibitory effect induced by the lipid extract on cancer cells is shown in Figure III.32. A lipid extract of *Gracilaria* sp. reduced cell viability in both cell lines in a dose-dependent manner at concentration range of 10 up to 20 μg/mL ($p < 0.001$), with a calculated half-maximal inhibitory concentration (IC_{50}) of 12.2 μg/mL and 12.9 μg/mL for T-47D (Figure III.32.A) and 5637 (Figure III.32.B) cancer cells, respectively.

The anti-tumor effects of polar lipids were previously reported as affecting angiogenesis and solid tumor growth via inhibition of replicative DNA polymerase activities (236,287). Extracts rich in glycolipids isolated from distinct macroalgae inhibited the growth of a human hepatocellular carcinoma cell line (HepG2) (IC_{50} of 126 μg/mL) (132) and were found to induce apoptosis of human colon carcinoma Caco-2 cells when associated with sodium butyrate (223). Otherwise, SQDG isolated from *Gigartina tenella* inhibited DNA

polymerase α, DNA polymerase β, and HIV-reverse transcriptase type 1 or downregulated *Tie2* gene expression in tumors (241,350).

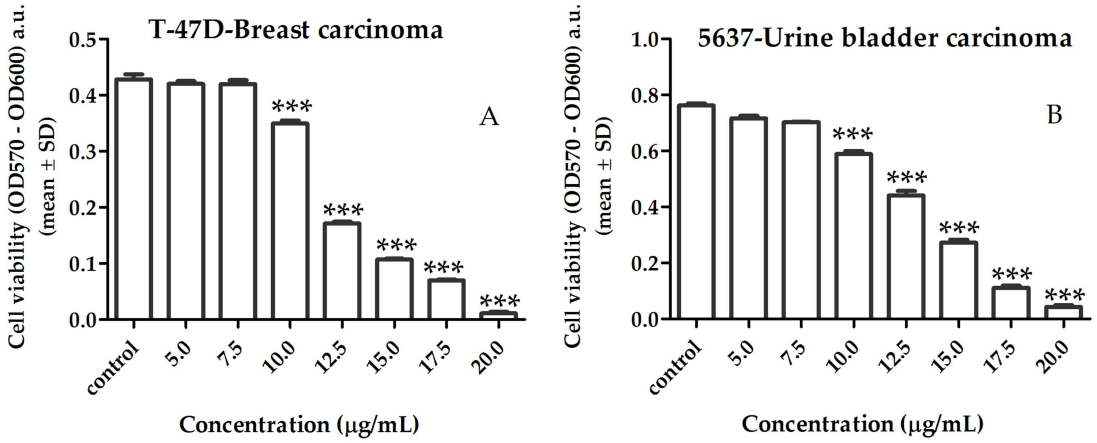

Figure III. 32. Effect of lipid extracts of *Gracilaria* sp. on T-47D breast (**A**) and 5637 bladder (**B**) cancer cell lines, after 96 h incubation. Results are shown as mean ± SD of three independent determinations (*** $p < 0.001$, compared to control). OD: optical density; a.u.: arbitrary units.

It has been hypothesized that the biological properties of glycolipids such as SQDG are closely related to the sugar moiety and the presence of PUFA chains.

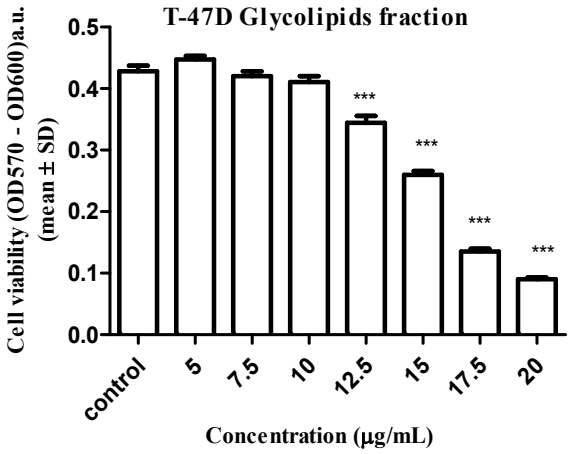

Figure III. 33. Effect of glycolipid rich extracts of *Gracilaria* sp. on T-47D breast cancer cell lines, after 96 h incubation. Results are shown as mean ± SD of three independent determinations (*** $p < 0.001$, compared to control). OD: optical density; a.u.: arbitrary units.

Thus, we further isolated the glycolipids-rich extract of *Gracilaria* sp. total lipid extract and the glycolipids-rich extract of *Gracilaria* sp. effect was tested to evaluate cell viability in T-47D cell lines in a dose-dependent manner at concentration range of 5 to 20

μg/mL ($p < 0.001$), with a calculated half-maximal inhibitory concentration (IC_{50}) of 17.5 μg/mL for T-47D, of the same order than the obtained with total lipid extract (Fig. III. 33).

III.2.3. Discussion

Lipid extract from *Gracilaria* sp. showed antiproliferative and anti-inflammatory activity. However, it was not possible to determine exactly which lipid components are responsible for these bioactivities. Even in the literature, the majority of studies have also addressed biological activities of lipid extracts rather than pure lipid molecules that hampers the determination of a relationship between structure and bioactivity. This is due to the fact that the isolation of a pure lipid molecule is very difficult and even pure lipid standards are not available for several lipid classes. Some authors have put some effort into this issue, scarcely addressed for the lipid extracts from macroalgae, and isolated enriched extracts in some classes of lipids to further test their bioactivity. Having this in mind, we also have also isolated a glycolipids-rich extract from total lipid extract and tested antiproliferative effect on T-47D cell line. The results of the measured IC_{50} (12.2 μg/mL – total extract and 17.5 μg/mL – GLs-rich extract) were of the same order, slightly minor in the total lipid extract. These results may infer the potential role of glycolipids on the antiproliferative effect of the total lipid extract.

Ohta et al. [17] reported that SQDG (20:5/16:0), isolated from red macroalgae *Gigartina tenella*, was a potent inhibitor of eukaryotic DNA polymerases [17]. Tsai et al. also reported that enriched extract with SQDG isolated from red macroalgae, with high levels of PUFAs such as 20:4(*n*-6) FA and 20:5(*n*-3) FA, inhibited the growth of human hepatocellular carcinoma cell line (HepG2), rather than enriched extracts with MGDG or DGDG [16]. This research group has also showed that the sulfolipids isolated from macroalgae exhibited higher inhibitory effect than sulfolipids isolated from spinach, previously reported as inhibitors of DNA polymerases and of the proliferation of human cervix carcinoma (HeLa) [22]. The aforementioned SQDG-enriched extracts displayed strong inhibitory effects and contained SQDG (20:5/16:0) [17] or contained SQDG assembling PUFAs [16], which are also found in the extract of *Gracilaria* sp. analyzed within this work. Thus, SQDG (18:2/16:0), SQDG (18:4/16:0), SQDG (20:4/16:0), and SQDG (20:5/16:0), identified in the extract of *Gracilaria* sp., can contribute to the observed antiproliferative effects.

In what concern anti-inflammatory activities, Banskota et al. reported that the extracts rich in MGDG and DGDG isolated from red macroalgae *Chondrus crispus* inhibited NO production through downregulation of iNOS [21]. The enriched extract contained MGDG (20:5/20:5), MGDG (20:5/20:4), MGDG (18:4/16:0), MGDG (20:4/16:0), and MGDG (20:5/16:0) and the respective DGDG analogues. Interestingly, the majority of these molecular species were also found in the extract of *Gracilaria* sp. analyzed in the present work. Moreover, the same group of researchers isolated MGDG, DGDG, SQDG, PC, and PG molecular species from the lipid extract of *Palmaria palmata* and all the polar lipids showed NO inhibitory activity [20]. The isolated polar lipids identified were MGDG (20:5/20:5), MGDG (20:5/16:0), DGDG (20:5/20:5), DGDG (20:5/14:0), DGDG (20:5/16:0), SQDG (20:5/14:0), PG (20:5/16:0), PG (20:5/16:1) and PC (20:5/20:5). All the molecular species contained 20:5(*n*-3) FA, and showed higher activity than the free FA 20:5(*n*-3), suggesting that the entire polar lipid structure (e.g., sulfolipid, phospholipid, or galactolipids) is essential for the extension of NO inhibition. Aside from the PC, the reported glycolipids and PG were also found in the lipidome of *Gracilaria* sp. Thus, the presence of these glycolipids and PGs in the lipid extract of *Gracilaria* sp. can contribute to the observed anti-inflammatory properties.

Lipid extracts (~80% polar lipids and 66% of glycolipids) from *Gracilaria* sp. cultivated on land-based IMTA were screened for bioactivity and collectively shown to be a natural source of bioactive lipids with antiproliferative and anti-inflammatory activities. The presence of these bioactive polar lipids in *Gracilaria* sp. promotes its consumption as a functional food for the prevention of various diseases and give insights for further biotechnological applications of this macroalgae. Using land-based culture of macroalgae may present a sustainable solution towards the production of large volumes of biomass displaying replicable bioactive properties. In the future, it is expected that marine macroalgae lipids will become part of the target bioactive compound to exploit for drug discovery, and marine algae incorporation as functional food may provide a natural source of health promoting benefits against disease. The presence of several polar lipids with recognized bioactive polar lipids in *Gracilaria* sp. can be related to the bioactivity observed in this work. However, more studies are needed to understand the structural/bioactivity relation of macroalgal polar lipids, and extracts rich in glycolipids, which deserve to be explored.

CHAPTER IV

CONCLUSIONS

Conclusions

The work developed during this Ph.D. aimed to characterize the polar lipidome from selected macroalgae, obtained from sustainable aquaculture practices and representative of the Chlorophyta, Rhodophyta, and Ochrophyta phyla, as well as to evaluate possible bioactive properties of selected polar lipid extracts.

The characterization of the polar lipid profile from macroalgae *Codium tomentosum* (Chlorophyta), *Gracilaria* sp. and *Porphyra dioica* (Rhodophyta), *and Fucus vesiculosus* (Ochrophyta) was accomplished at molecular level by using advanced lipidomic-approaches based on HILIC–LC–MS/MS. With the results obtained, it was possible to identify the complex and diverse lipidome of macroalgae from the three phyla that was related to different categories of glycolipids, phospholipids and betaine lipids. Among these, several classes such as MGDG, DGDG, SQDG, SQMG, PG, LPG, PC, LPC, PI, PA, and DGTS were identified in all specimens. Meanwhile, MGTS and MGTA were identified for the first time in macroalgae.

In addition, inter-taxonomic differentiation may be suggested by some lipid classes detected in specific phylum such as the case of IPC identified in Rhodophyta, PE identified in Rhodophyta and Ochrophyta, MGTS identified in Chlorophyta, Ochrophyta and in the Rhodophyta *Gracilaria* sp., LPE was identified in Ochrophyta and in the Rhodophyta *Porphyra dioica* while LPI, DGTA, and MGTA were only identified in Ochrophyta.

Depending on the phylum, different profiles of polar lipids were observed, based on the number of molecular species and in fatty acyl composition. Chlorophyta are clearly marked by having an important number of molecular species of glycolipids in the MGDG and DGDG groups that include species with C_{16}, C_{18}, and C_{20} PUFA from *n*-3 type and a high number of the betaine lipids DGTS and MGTS.

Rhodophyta are distinguished by the presence of a low number of molecular species of MGDG and DGDG that however include molecular species with *n*-3 FA such as 20:5(*n*-3) and *n*-6 FA such as 20:4(*n*-6). Within PLs, Rhodophyta is particularly assigned by PE and its molecular species that include saturated and monounsaturated C_{16} and C_{18} FA and by the

high number of PC that in higher extent combined C_{18} with C_{20} FA. Low number of betaine lipids assigned Rhodophyta. A characteristic feature of polar lipid from red macroalgae is the presence of the class IPC, a putative biomarker specific to the Rhodophyta phylum.

The intra-taxonomic differentiation in Rhodophyta was also achieved between genus *Gracilaria* and *Porphyra*. A lower number of molecular species in SQMG and betaine lipid classes and a higher number of molecular species in PE class assigned the lipidome of *Porphyra dioica*. The LPE class only assigned the lipidome of *Porphyra dioica* while MGTS only assigned the lipidome of *Gracilaria* sp.. Altogether, these features support the putative differentiation between the red algae. Regarding composition, the molecular species particularly include C_{20} PUFA that was mainly inferred by GLs and PLs such as PC and PG, and PE in the case of *Porphyra dioica*, supporting the nutritional benefits of this macroalgae suitable to be consumed as functional food.

Within Rhodophyta, the lipidomic profile of two different life cycle stages of *Porphyra dioica* was established. The differences between the stages was mainly reflected on the phospholipidome, particularly PE and PG highlighted on the lipidome of the sporophyte and PC and PA on the lipidome of gametophyte, while glycolipids seem to be preserved. Otherwise, the profile of GLs and PLs is characterized by the presence of diverse molecular lipids that include C_{20} FA-type from *n*-3 and *n*-6 families, a similar feature aforementioned within Rhodophyta.

Ochrophyta are particularly differentiated by the high number of MGDG and DGDG that include C_{18} FA-family such as 18:3 and 18:4(*n*-3), and the C_{20} FA-family such as 20:4(*n*-6) and 20:5(*n*-3) PUFA. Comparing with Chlorophyta and Rhodophyta, Ochrophyta are mainly differentiated by the high number of molecular species identified in betaine lipid classes that exclusively include DGTA and MGTA (reported for the first time in macroalgae). The season effect in Ochrophyta was evaluated by MS-based approaches that allowed to identify the increase of number of molecular species with *n*-3 PUFA from C_{18} family such as 18:3, 18:4 and from C_{20} such as 20:5 in winter season, mainly supplied by GLs and betaine lipid classes. Its low ratio *n*-6/*n*-3 makes *Fucus vesiculosus* a good functional food for human nutrition and feed.

By using MS-based approaches, results gathered within this Ph.D. work, in the identification of the lipid signature of macroalgae from different origins, genus and phyla, different growth cycles and seasons, will certainly contribute to further investigation about their role in biosynthesis, in lipid metabolism, and for bioprospection.

Polar lipids containing *n*-3 and *n*-6 PUFA seems to have important roles in human health. Total lipid extracts and extracts rich in glycolipids from *Gracilaria* sp. demonstrated antiproliferative effect and anti-inflammatory properties. These properties suggest that macroalgae can be valuable not only for food and feed, but also for pharmaceutical and cosmetical, fostering new biological and biotechnological applications.

The profile of lipids can be standardized by obtaining algae biomass produced in IMTA systems and lipidomics can act as fast and reliable tool to aid producers optimizing culture protocols based on the identification of the target bioactive trait and/or responsible lipid compound. The accurate knowledge on the value of the polar lipid fraction of macroalgae and the ability to "naturally" manipulate its content is a key point in the context of biorefinery.

All macroalgae studied may be considered an interesting cash-crop for food stuffs, but mostly as a functional ingredient for feed and food, due to their high nutritional value and a complex range of health benefits for human life. Rhodophyta, Ochrophyta, and Chlorophyta are a source of promising lipids with potential biological activities associated to different molecular species, namely from glycolipids and phospholipids, to be used both in the development of functional foods or additives with anti-inflammatory and antitumor effects. Overall, based on the lipidome profile, the results obtained within this work contribute to the smart and integral valorization of macroalgae cultivated on land-based IMTA systems.

CHAPTER V

REFERENCES

References

1. Stengel DB, Connan S, Popper ZA. Algal chemodiversity and bioactivity: sources of natural variability and implications for commercial application. Biotechnol Adv. 2011; 29(5):483–501.
2. Verpoorte R, Crommelin D, Danhof M, Gilissen LJWJ, Schuitmaker H, van der Greef J, et al. Commentary: "A systems view on the future of medicine: inspiration from Chinese medicine?". J Ethnopharmacol. 2009; 121(3):479–481.
3. Faulkner DJ. Marine natural products. Nat Prod Rep. 2001; 18(1):1–49.
4. Ibañez E, Cifuentes A. Benefits of using algae as natural sources of functional ingredients. J Sci Food Agric. 2013; 93(4):703–709.
5. Holdt SL, Kraan S. Bioactive compounds in seaweed: Functional food applications and legislation. J Appl Phycol. 2011; 23(3):543–597.
6. Leal MC, Munro MHG, Blunt JW, Puga J, Jesus B, Calado R, et al. Biogeography and biodiscovery hotspots of macroalgal marine natural products. Nat Prod Rep. 2013; 30(11):1380–1390.
7. Guedes AC, Amaro HM, Malcata FX. Microalgae as sources of carotenoids. Mar Drugs. 2011; 9(4):625–644.
8. Costa LS, Fidelis GP, Cordeiro SL, Oliveira RM, Sabry DA, Câmara RBG, et al. Biological activities of sulfated polysaccharides from tropical seaweeds. Biomed Pharmacother. 2010; 64(1):21–28.
9. Cardoso S, Carvalho L, Silva P, Rodrigues M, Pereira O, Pereira L. Bioproducts from Seaweeds: A Review with Special Focus on the Iberian Peninsula. Curr Org Chem. 2014; 18(7):896–917.
10. Mattos BB, Romanos MT V., Souza LM De, Sassaki G, Barreto-Bergter E. Glycolipids from macroalgae: potential biomolecules for marine biotechnology? Rev Bras Farmacogn. 2011; 21(2):244–247.
11. Shahidi F. Nutraceuticals and functional foods: Whole versus processed foods. Trends Food Sci Technol. 2009; 20(9):376–387.
12. Mayer AMS, Rodríguez AD, Berlinck RGS, Fusetani N. Marine pharmacology in 2007-8: Marine compounds with antibacterial, anticoagulant, antifungal, anti-inflammatory, antimalarial, antiprotozoal, antituberculosis, and antiviral activities; affecting the immune and nervous system, and other miscellaneous mechanisms of action. Comp Biochem Physiol C Toxicol Pharmacol. 2011; 153(2):191–222.
13. Smit AJ. Medicinal and pharmaceutical uses of seaweed natural products : A review. J Appl Phycol. 2004; 245–262.
14. Thompson GA. Lipids and membrane function in green algae. Biochim Biophys Acta - Lipids Lipid Metab. 1996;1302(1):17–45.
15. Guschina IA, Harwood JL. Lipids and lipid metabolism in eukaryotic algae. Prog Lipid Res. 2006; 45(2):160–186.
16. Harwood J. Membrane Lipids in Algae. In Siegenthaler P-A, Murata N (Eds.), Lipids in Photosynthesis: Structure, Function and Genetics, 1998; 53-64. Advances in Photosynthesis and Respiration, vol. 6. Springer, Dordrecht.

17. Nishida I, Murata N. Chilling sensitivity in plants and cyanobacteria: The crucial contribution of membrane lipids. Annu Rev Plant Physiol Plant Mol Biol. 1996;47(1):541–568.

18. Harwood JL, Guschina IA. The versatility of algae and their lipid metabolism. Biochimie. 2009; 91(6):679–684.

19. Stirk WA., Reinecke DL, van Staden J. Seasonal variation in antifungal, antibacterial and acetylcholinesterase activity in seven South African seaweeds. J Appl Phycol. 2007; 19(3):271–276.

20. Kadam SU, Tiwari BK, O'Donnell CP. Application of novel extraction technologies for bioactives from marine algae. J Agric Food Chem. 2013; 61(20):4667–4675.

21. Stabili L, Acquaviva MI, Biandolino F, Cavallo RA, De Pascali SA, Fanizzi FP, et al. The lipidic extract of the seaweed *Gracilariopsis longissima* (Rhodophyta, Gracilariales): a potential resource for biotechnological purposes? N Biotechnol. 2012; 29(3):443–450.

22. El Baz FK, El-Baroty GS, Ibrahim AE, Abd El Baky. Cytotoxicity, Antioxidants and Antimicrobial Activities of Lipids Extracted from Some Marine Algae. J Aquac Res Dev. 2014; 5(7):284.

23. Plouguerné E, da Gama BAP, Pereira RC, Barreto-Bergter E. Glycolipids from seaweeds and their potential biotechnological applications. Front Cell Infect Microbiol. 2014; 4:1–3.

24. Bayir H, Fadeel B, Palladino MJ, Witasp E, Kurnikov I V, Tyurina YY, et al. Apoptotic interactions of cyctochrome c: Redox flirting with anionic phospholipids within and outside of mitochondria. Biochim Biophys Acta-Bioenergetics. 2006; 1757(5–6):648–659.

25. Plouguerné E, De Souza LM, Sassaki GL, Cavalcanti JF, Romanos MT V, da Gama BAP, et al. Antiviral Sulfoquinovosyldiacylglycerols (SQDGs) from the Brazilian brown seaweed *Sargassum vulgare*. Mar Drugs. 2013; 11(11):4628–4640.

26. Bruno A, Rossi C, Marcolongo G, Di Lena A, Venzo A, Berrie CP, et al. Selective *in vivo* anti-inflammatory action of the galactolipid monogalactosyldiacylglycerol. Eur J Pharmacol. 2005; 524(1–3):159–168.

27. Lopes G, Daletos G, Proksch P, Andrade PB, Valentão P. Anti-inflammatory potential of monogalactosyl diacylglycerols and a monoacylglycerol from the edible brown seaweed *Fucus spiralis* Linnaeus. Mar Drugs. 2014; 12(3):1406–18.

28. Küllenberg D, Taylor L a, Schneider M, Massing U. Health effects of dietary phospholipids. Lipids Health Dis. 2012; 11(1):1–16.

29. Gupta S, Abu-Ghannam N, Scannell AGM. Growth and kinetics *of Lactobacillus plantarum* in the fermentation of edible Irish brown seaweeds. Food Bioprod Process. 2011; 89(4):346–355.

30. Banskota AH, Stefanova R, Sperker S, Lall S, Craigie JS, Hafting JT. Lipids isolated from the cultivated red alga *Chondrus crispus* inhibit nitric oxide production. J Appl Phycol. 2014; 26(3):1565–1571.

31. Abreu MH, Pereira R, Sassi J-F. Marine Algae and the Global Food Industry. In Pereira L, Magalhaes J (Eds), Marine Algae - Biodiversity, Taxonomy, Environmental Assessment, and Biotechnology, 2014; 300-319. CRC Press.

32. Burri L, Hoem N, Banni S, Berge K. Marine omega-3 phospholipids: metabolism and biological activities. Int J Mol Sci. 2012; 13(11):15401–15419.

33. Ragonese C, Tedone L, Beccaria M, Torre G, Cichello F, Cacciola F, et al. Characterisation of lipid fraction of marine macroalgae by means of chromatography techniques coupled to mass spectrometry. Food Chem. 2014; 145:932–40.

34. Kumari P, Reddy CRK, Jha B. Comparative evaluation and selection of a method for lipid and fatty acid extraction from macroalgae. Anal Biochem. 2011; 415(2):134–44.

35. Ibañez E, Herrero M, Mendiola JA, Castro-puyana M. Marine Bioactive Compounds. In Hayes M (ed.), 2012; 55-99. Boston, MA: Springer US.

36. Dembitsky VM. Betaine ether-linked glycerolipids. Prog Lipid Res. 1996; 35(1):1–51.

37. Jones J, Manning S, Montoya M, Keller K, Poenie M. Extraction of algal lipids and their analysis by HPLC and mass spectrometry. J Am Oil Chem Soc. 2012; 1371–1381.

38. Hölzl G, Dörmann P. Structure and function of glycoglycerolipids in plants and bacteria. Prog Lipid Res. 2007; 46(5):225–243.

39. Herrero M, Simo C, Cifuentes A. FOODOMICS: MS-based strategies in modern food science and nutrition. Mass Spectrom Rev. 2012; 31:49–69.

40. He H, Rodgers RP, Marshall AG, Hsu CS. Algae polar lipids characterized by online liquid chromatography coupled with hybrid linear quadrupole ion trap/Fourier transform ion cyclotron resonance mass spectrometry. energy&fuels. 2011; 25(10):4770–4775.

41. Cajka T, Fiehn O. Comprehensive analysis of lipids in biological systems by liquid chromatography-mass spectrometry. Trends Analyt Chem. 2014; 61:192–206.

42. Goulitquer S, Potin P, Tonon T. Mass spectrometry-based metabolomics to elucidate functions in marine organisms and ecosystems. Marine drugs. 2012; 10:849-880.

43. Wenk MR. Lipidomics: New tools and applications. Cell. 2010; 143(6):888–895.

44. Xu J, Chen D, Yan X, Chen J, Zhou C. Global characterization of the photosynthetic glycerolipids from a marine diatom *Stephanodiscus* sp. by ultra performance liquid chromatography coupled with electrospray ionization-quadrupole-time of flight mass spectrometry. Anal Chim Acta. 2010; 663(1):60–68.

45. Yao L, Gerde JA, Lee S-L, Wang T, Harrata KA. Microalgae lipid characterization. J Agric Food Chem. 2015; 63(6):1773–1787.

46. Li JWH, Vederas JC. Drug discovery and natural products: End of era or an endless frontier? Biomed. Khim. 2011; 57(2):148–60.

47. Dionísio G, Rosa R, Leal MC, Cruz S, Brandão C, Calado G, et al. Beauties and beasts: A portrait of sea slugs aquaculture. Aquaculture. 2013; 408–409.

48. Ridler N, Wowchuk M, Robinson B, Barrington K, Chopin T, Robinson S, et al. Integrated MultiTrophic Aquaculture (IMTA): a potential strategic choice for farmers. Aquac Econ Manag. 2007; 11(1):99–110.

49. Abreu MH, Pereira R, Yarish C, Buschmann AH, Sousa-Pinto I. IMTA with *Gracilaria vermiculophylla*: Productivity and nutrient removal performance of the seaweed in a land-based pilot scale system. Aquaculture. 2011; 312(1–4):77–87.

50. Raven JA, Hurd CL. Ecophysiology of photosynthesis in macroalgae. Photosynth Res. 2012; 113(1–3):105–25.

51. Dumay J, Morançais M, Munier M, Le Guillard C, Fleurence J. Phycoerythrins: Valuable Proteinic Pigments in Red Seaweeds. In Nathalie Bourgougnon (Ed.), Sea Plants. Advances in Botanical Research, 2014:321-343. Advances in Botanical Research; vol. 71. Elsevier.

52. Pereira DM, Valentão P, Andrade PB. Marine natural pigments: Chemistry, distribution and analysis. Dye Pigment. 2014; 111:124–134.

53. Heydarizadeh P, Poirier I, Loizeau D, Ulmann L, Mimouni V, Schoefs B, et al. Plastids of marine phytoplankton produce bioactive pigments and lipids. Mar Drugs. 2013; 11(9):3425–3471.

54. Adl SM, Simpson AGB, Lane CE, Lukeš J, Bass D, Bowser SS, et al. The revised classification of eukaryotes. J Eukaryot Microbiol. 2012; 59(5):429–493.

55. Guiry MD & Guiry GM. AlgaeBase. World-wide electronic publication: http: //www.algaebase.org/about/. Ireland (Accessed on 20th January 2014).

56. Wang L, Wang X, Wu H, Liu R. Overview on biological activities and molecular characteristics of sulfated polysaccharides from marine green algae in recent years. Mar Drugs. 2014; 12(9):4984–5020.

57. Valentão P, Trindade P, Gomes D, Guedes de Pinho P, Mouga T, Andrade PB. *Codium tomentosum* and *Plocamium cartilagineum*: Chemistry and antioxidant potential. Food Chem. 2010; 119(4):1359–1368.

58. Francavilla M, Franchi M, Monteleone M, Caroppo C. The red seaweed *Gracilaria gracilis* as a multi products source. Mar Drugs. 2013; 11(10):3754–3776.

59. Pereira L. As Algas Marinhas e Respectivas Utilidades As Algas Marinhas e Respectivas Utilidades. University of Coimbra. Available from: ww.uc.pt/seaweeds.

60. Pereira R, Sousa-Pinto I, Yarish C. Field and culture studies of the life history of *Porphyra dioica* (Bangiales, Rhodophyta) from Portugal. Phycologia. 2004;43(6):756–67.

61. Sahoo S, Tang X, YArish C. *Porphyra* – the economic seaweed as a new experimental system. Curr Sci. 2002; 83(11):1313-1316.

62. Blouin NA, Brodie JA, Grossman AC, Xu P, Brawley SH. Porphyra: A marine crop shaped by stress. Trends Plant Sci. 2011; 16(1):29–37.

63. WoRMS Editorial Board (2017). World Register of Marine Species. Available from http://www.marinespecies.org at VLIZ. (Accessed on 20th January 2017).

64. Pereira R, Kraemer G, Yarish C, Sousa-Pinto I. Nitrogen uptake by gametophytes of *Porphyra dioica* (Bangiales, Rhodophyta) under controlled-culture conditions. Eur J Phycol. 2008; 43(1):107–118.

65. Drew KM. Studies in the Bangioideae. Ann Bot. 1954; 18(2):183–216.

66. Candia A, Lindstrom S, Reyes E. *Porphyra* sp. (Bangiales, Rhodophyta): Reproduction and life form. Hydrobiologia-April. 1999;1,@1999;@3:115–9.

67. Khotimchenko S V. Lipids from marine alga *Gracilaria verrucosa*. Chem Nat Compd. 2005; 41(3):230–2.

68. de Almeida CLF, Falcão HDS, Lima GRDM, Montenegro CDA, Lira NS, de Athayde-Filho PF, et al. Bioactivities from marine algae of the genus *Gracilaria*. Int J Mol Sci. 2011; 12(7):4550–4573.

69. Veena CK, Josephine A, Preetha SP, Varalakshmi P. Beneficial role of sulfated polysaccharides from edible seaweed *Fucus vesiculosus* in experimental hyperoxaluria. Food Chem. 2007; 100(4):1552–1559.

70. Peinado I, Girón J, Koutsidis G, Ames JM. Chemical composition, antioxidant activity and sensory evaluation of five different species of brown edible seaweeds. Food Res Int. 2014; 66:36–44.

71. Lordan S, Ross RP, Stanton C. Marine bioactives as functional food ingredients: potential to reduce the incidence of chronic diseases. Mar Drugs. 2011; 9(6):1056–100.

72. European Commission. Report on the blue growth strategy: Towards more sustainable growth and jobs in the blue economy. SWD/2017/128 Final. 2017;1–62. (Available from: https://ec.europa.eu/maritimeaffairs/sites/maritimeaffairs/)

73. Pereira L. Algae, Uses in agriculture, gastronomy and food industry. Litoral de Viana do

Castelo. 2010.

74. Paiva L, Lima E, Patarra RF, Neto AI, Baptista J. Edible Azorean macroalgae as source of rich nutrients with impact on human health. Food Chem. 2014; 164:128–35.

75. Anaëlle T, Serrano Leon E, Laurent V, Elena I, Mendiola JA, Stéphane C, et al. Green improved processes to extract bioactive phenolic compounds from brown macroalgae using *Sargassum muticum* as model. Talanta. 2013; 104:44–52.

76. Joana Gil-Chávez G, Villa JA, Fernando Ayala-Zavala J, Basilio Heredia J, Sepulveda D, Yahia EM, et al. Technologies for extraction and production of bioactive compounds to be used as nutraceuticals and food ingredients: an overview. Compr Rev Food Sci Food Saf. 2013; 12:5–23.

77. Silva AMS AA. Chemical study and biological activity evaluation of two azorean macroalgae: *Ulva rigida* and *Gelidium microdon*. Oceanogr. 2013; 1(1):1–7.

78. Domínguez H. Part I: Structure and occurrence of the major algal components. In Functional ingredients from algae for foods and nutraceuticals. 2013: 23-251. Woodhead Publishing Series in Food and Science, Technology and Nutrition.

79. Aníbal J, Madeira HT, Carvalho LF, Esteves E, Veiga-Pires C, Rocha C. Macroalgae mitigation potential for fish aquaculture effluents: an approach coupling nitrogen uptake and metabolic pathways using *Ulva rigida* and *Enteromorpha clathrata*. Environ Sci Pollut Res Int. 2013; 21(23):13324-13334.

80. Kadam SU, Prabhasankar P. Marine foods as functional ingredients in bakery and pasta products. Food Res Int. 2010; 43(8):1975–1980.

81. Anastas PT, Kirchhoff MM. Origins, current status, and future challenges of green chemistry. Acc Chem Res. 2002; 35(9):686–694.

82. Kang YH, Shin JA, Kim MS, Chung IK. A preliminary study of the bioremediation potential of *Codium fragile* applied to seaweed integrated multi-trophic aquaculture (IMTA) during the summer. J Appl Phycol. 2008; 20(2):183–90.

83. Neori A. Essential role of seaweed cultivation in integrated multi-trophic aquaculture farms for global expansion of mariculture: an analysis. J Appl Phycol. 2007; 20(5):567–570.

84. Duarte CM, Holmer M, Olsen Y, Soto D, Marbà N, Guiu J, et al. Will the Oceans Help Feed Humanity? Bioscience. 2009; 59(11):967–976.

85. Guschina IA, Harwood JL. Algal Lipids and Effect of the Environment on their Biochemistry. In Arts MT, Brett MT, Kainz M (Eds), Lipids in Aquatic Ecosystems. 2009:1-24. Springer Dordrecht Heidelberg London.

86. Bhakuni DS, Rawat DS. Bioactive Metabolites of Marine Algae, Fungi and Bacteria. In: Bioactive Marine Natural Products. 2005:1–19.Springer Anamaya.

87. Paul-André S, Murata N, Harwood J. Membrane lipids in algae. Lipids Photosynth Struct Funct Genet. 2004; 6:53–64.

88. Fernandis AZ, Wenk MR. Membrane lipids as signaling molecules. Curr Opin Lipidol. 2007; 18(2):121–8.

89. Chen H, Zhou D, Luo G, Zhang S, Chen J. Macroalgae for biofuels production: Progress and perspectives. Renew Sustain Energy Rev. 2015; 47:427–37.

90. Ramadan MF, Mohamed M, Asker S, Ibrahim ZK. Functional Bioactive Compounds and Biological Activities of Spirulina platensis Lipids. 1996; 26(3):211–22.

91. Khotimchenko SV., Vaskovsky YE, Titlyanova TV, Vaskovsky VE. Fatty acids of marine algae from the Pacific Coast of North California. Bot Mar. 2002; 45(1):17–22.

92. Larsen R, Eilertsen K-E, Elvevoll EO. Health benefits of marine foods and ingredients. Biotechnol Adv. 2011; 29(5):508–518.

93. Gupta S, Abu-Ghannam N. Recent developments in the application of seaweeds or seaweed extracts as a means for enhancing the safety and quality attributes of foods. Innov Food Sci Emerg Technol. 2011; 12(4):600–609.

94. Gupta S, Abu-Ghannam N. Bioactive potential and possible health effects of edible brown seaweeds. Trends Food Sci Technol. 2011; 22(6):315–26.

95. Kumari P, Kumar M, Gupta V, Reddy CRK, Jha B. Tropical marine macroalgae as potential sources of nutritionally important PUFAs. Food Chem. 2010; 120(3):749–757.

96. Pereira H, Barreira LL, Figueiredo F, Custódio LL, Vizetto-Duarte C, Polo C, et al. Polyunsaturated Fatty acids of marine macroalgae: potential for nutritional and pharmaceutical applications. Mar Drugs. 2012; 10(9):1920–1935.

97. Sanina NM, Goncharova SN, Kostetsky EY. Fatty acid composition of individual polar lipid classes from marine macrophytes. Phytochemistry. 2004; 65(6):721–730.

98. Sánchez-Machado DI, López-Hernández J, Paseiro-Losada P, López-Cervantes J. An HPLC method for the quantification of sterols in edible seaweeds. Biomed Chromatogr. 2004; 18(3):183–90.

99. Lopes G, Sousa C, Bernardo J, Andrade PB, Valentão P, Ferreres F, et al. Sterol profiles in 18 macroalgae of the Portuguese Coast. J Phycol. 2011; 47(5):1210–1218.

100. Kendel M, Couzinet-Mossion A, Viau M, Fleurence J, Barnathan G, Wielgosz-Collin G. Seasonal composition of lipids, fatty acids, and sterols in the edible red alga *Grateloupia turuturu*. J Appl Phycol. 2012; 25(2):425–32.

101. Cardozo KHM, Guaratini T, Barros MP, Falcão VR, Tonon AP, Lopes NP, et al. Metabolites from algae with economical impact. Comp Biochem Physiol C Toxicol Pharmacol. 2007; 146(1):60–78.

102. Mohamed S, Hashim SN, Rahman HA. Seaweeds: A sustainable functional food for complementary and alternative therapy. Trends Food Sci Technol. 2012; 23(2):83–96.

103. Pangestuti R, Kim S-K. Biological activities and health benefit effects of natural pigments derived from marine algae. J Funct Foods. 2011; 3(4):255–266.

104. Milenković SM, Zvezdanović JB, Anđelković TD. The identification of chlorophyll and its derivatives in the pigment mixtures: HPLC-chromatography , visible and mass spectroscopy studies. Adv Technol. 2012; 1(1):16–24.

105. Michalak I, Chojnacka K. Algal extracts: Technology and advances. Eng Life Sci. 2014;1–32.

106. Guedes A. C, Gião MS, Matias A, Nunes AVM, Pintado ME, Duarte CMM, et al. Supercritical fluid extraction of carotenoids and chlorophylls a, b and c, from a wild strain of *Scenedesmus obliquus* for use in food processing. J Food Eng. 2013; 116(2):478–82.

107. Hosikian A, Lim S, Halim R, Danquah MK. Chlorophyll Extraction from Microalgae: A Review on the process engineering aspects. Int J Chem Eng.2010; 1–11.

108. Amorim-Carrilho KT, Cepeda A, Fente C, Regal P. Review of methods for analysis of carotenoids. TrAC Trends Anal Chem. 2014; 56:49–73.

109. Kim H, Lee M. Potential utilization of seaweed as nutraceuticals anti-oxidant activity. 2010; 149–63.

110. Plaza M, Herrero M, Alejandro Cifuentes A, Ibáñez E. Innovative natural functional ingredients from microalgae. J Agric Food Chem. 2009; 57(16):7159–70.

111. Chu W. biotechn application. IeJSME. 2012; 6(126):24–37.

112. Cian RE, Caballero MS, Sabbag N, González RJ, Drago SR. Bio-accessibility of bioactive compounds (ACE inhibitors and antioxidants) from extruded maize products added with a red seaweed Porphyra columbina. LWT - Food Sci Technol. 2014; 55(1):51–58.

113. Boudière L, Michaud M, Petroutsos D, Rébeillé F, Falconet D, Bastien O, et al. Glycerolipids in photosynthesis: Composition, synthesis and trafficking. Biochim Biophys Acta - Bioenerg. 2014; 1837(4):470–480.

114. Khozin-Goldberg I, Cohen Z. Unraveling algal lipid metabolism: Recent advances in gene identification. Biochimie. 2011; 93(1):91–100.

115. Baba M, Shiraiwa Y. Biosynthesis of lipids and hydrocarbons in algae, In: Dubinsky Z (Ed.), Photosynthesis. 2013; 13. InTech

116. Abd HH, Baky E, Baz FK El, Baroty GS El, Asker MMS, Ibrahim EA, et al. Phospholipids of some marine macroalgae : Identification , antivirus , anticancer and antimicrobial bioactivities. Der Pharma Chemica.2014;6(5):370–382.

117. Meneses P, Navarro JN, Glonek T, College C, Avenue SE, Me P. Algal phospholipids by ^{31}P NMR comparing isopropanol pretretatment with simpe chloroform/methanol extraction. Int J Biochem. 1993; 25(6):903–910.

118. Fereidoon S, Wanasundara PKJPD. Extraction and analysis of lipids. In Akoh C, Min DB (Eds), Food Lipids: Chemistry, Nutrition, and Biotechnology, Third ed. 2008; 128-49. Marcel Dekker: New York and Basel

119. Petroutsos D, Amiar S, Abida H, Dolch L-J, Bastien O, Rébeillé F, et al. Evolution of galactoglycerolipid biosynthetic pathways--from cyanobacteria to primary plastids and from primary to secondary plastids. Prog Lipid Res. 2014; 54:68–85.

120. Nelson MM, Phleger CF, Nichols PD. Seasonal lipid composition in macroalgae of the Northeastern Pacific Ocean. Bot Mar. 2002; 45(1):58–65.

121. Murata N, Higashi S-I, Fujimura Y. Glycerolipids in various preparations of Photosystem II from spinach chloroplasts. Biochim Biophys Acta - Bioenerg. 1990; 1019(3):261–268.

122. Wang Z, Benning C. Chloroplast lipid synthesis and lipid trafficking through ER–plastid membrane contact sites. Biochem Soc Trans. 2012; 40(2):457–463.

123. Lu N, Wei D, Chen F, Yang S-T. Lipidomic profiling and discovery of lipid biomarkers in snow alga *Chlamydomonas nivalis* under salt stress. Eur J Lipid Sci Technol. 2012; 114(3):253–265.

124. Lu N, Wei D, Chen F, Yang S-T. Lipidomic profiling reveals lipid regulation in the snow alga *Chlamydomonas nivalis* in response to nitrate or phosphate deprivation. Process Biochem. 2013; 48(4):605–613.

125. Reshef V, Mizrachi E, Maretzki T, Silberstein C, Loya S, Hizi A, et al. New acylated sulfoglycolipids and digalactolipids and related known glycolipids from cyanobacteria with a potential to inhibit the reverse transcriptase of HIV-1. J Nat Prod. 1997; 60(12):1251–1260.

126. Gustafson KR, Cardellina JH, Fuller RW, Weislow OS, Kiser RF, Snader KM, et al. AIDS-antiviral sulfolipids from cyanobacteria (blue-green algae). J Natl Cancer Inst. 1989; 81(16):1254–1258.

127. El Baz FK, El Baroty GS, Abd El Baky HH, Abd El-Salam OI, Ibrahim EA. Structural characterization and biological activity of sulfolipids from selected marine algae. Grasas y Aceites. 2013; 64:561–571.

128. Lee AG. Membrane lipids: It's only a phase. Curr Biol. 2000; 10:377–80.

129. Li H, Yan X, Xu J, Zhou C. Precise identification of photosynthetic glycerolipids in microalga *Tetraselmis chuii* by UPLC-ESI-Q-TOF-MS. Sci China, Ser C Life Sci. 2008; 51(12):1101–7.

130. Wang Z, Benning C. *Arabidopsis thaliana* polar glycerolipid profiling by thin layer chromatography (TLC) coupled with gas-liquid chromatography (GLC). J Vis Exp. 2011; (49):2–7.

131. Naumann I, Darsow KH, Walter C, Lange HA, Buchholz R. Identification of sulfoglycolipids from the alga *Porphyridium purpureum* by matrix-assisted laser desorption / ionisation quadrupole ion trap time-of-flight mass spectrometry. Rappid Commun Mass Spectrom. 2007; 3185–3192.

132. Tsai C, Pan BS. Identification of sulfoglycolipid bioactivities and characteristic fatty acids of marine macroalgae. JAFC. 2012; 60:8404−8410.

133. Benning C. Biosynthesis and function of the sulfolipid sulfoquinovosyl diacylglicerol. Annu Rev Plant Physiol Plant Mol Biol. 1998; 49:53–75.

134. Khotimchenko S V. Distribution of glyceroglycolipids in marine algae and grasses. Chem Nat Compd. 2002; 38(3):186–191.

135. Vaskovsky VE, Khotimchenko S V., Svetlana K, Bangmei X, Hefang L. Polar lipids and fatty acids of some marine macrophytes from Yellow Sea. Phytochemistry. 1996; 42(5):1347–1356.

136. Dembitsky VM, Rozentsvet OA, Pechenkina EE. Glycolipids, phospholipids and fatty acids of brown algae species. Phytochemistry. 1990; 29(11):3417–3421.

137. Lee J-C, Hou M-F, Huang H-W, Chang F-R, Yeh C-C, Tang J-Y, et al. Marine algal natural products with anti-oxidative, anti-inflammatory, and anti-cancer properties. Cancer Cell Int. 2013; 13(1):55.

138. Pulfer M, Murphy RC. Electrospray mass spectrometry of phospholipids. Mass Spectrom Rev. 2003; 22(5):332–364.

139. Mühlroth A, Li K, Røkke G, Winge P, Olsen Y, Hohmann-Marriott MF, et al. Pathways of lipid metabolism in marine algae, co-expression network, bottlenecks and candidate genes for enhanced production of EPA and DHA in species of Chromista. Mar Drugs. 2013; 11(11):4662–4697.

140. D'Arrigo P, Servi S. Synthesis of lysophospholipids. Molecules. 2010; 15(3):1354–1377.

141. Farooqui A., Horrocks LA, Farooqui T. Glycerophospholipids in brain: their metabolism, incorporation into membranes, functions, and involvement in neurological disorders. Chem Phys Lipids. 2000; 106(1):1–29.

142. Li J, Wang X, Zhang T, Wang C, Huang Z, Luo X, et al. A review on phospholipids and their main applications in drug delivery systems. Asian J Pharm Sci. 2014; 10(2):81–98.

143. Dembitsky VM, Řezanková H, Řezanka T, Hanuš LO. Variability of the fatty acids of the marine green algae belonging to the genus *Codium*. Biochem Syst Ecol. 2003; 31(10):1125–1145.

144. Thomson PG, Wright SW, Bolch CJS, Nichols PD, Skerratt JH, McMinn A. Antarctic distribution, pigment and lipid composition, and molecular identification of the brine Dinoflagellate *Polarella Glacialis* (Dinophyceae). J Phycol. 2004; 40(5):867–873.

145. Melo T, Alves E, Azevedo V, Martins AS, Neves B, Domingues P, et al. Lipidomics as a new approach for the bioprospecting of marine macroalgae — Unraveling the polar lipid and fatty acid composition of *Chondrus crispus*. Algal Res. 2015; 8:181–191.

146. Khotimchenko S V., Yakovleva IM. Lipid composition of the red alga *Tichocarpus crinitus*

exposed to different levels of photon irradiance. Phytochemistry. 2005; 66(1):73–79.

147. Khotimchenko S V., Vaskovsky VE. An Inositol-containing sphingolipid from the red Alga *Gracilaria verrucosa*. Russ J Bioorganic Chem. 2004; 30(2):168–171.

148. Pettitt TR, Jones AL, Harwood JL. Lipids of the marine red algae, *Chondrus crispus* and Polysiphonia lanosa. Phytochemistry. 1989;28(2):399–405.

149. Dembitsky VM. Betaine ether-linked glycerolipids: Chemistry and biology. Vol. 35, Progress in Lipid Research. 1996; 35:1–51.

150. Sato N. Betaine Lipids. Bot Mag Tokyo. 1992; 1(3):185–97.

151. Li S, Xu J, Chen JJ, Chen JJ, Zhou C, Yan X. The major lipid changes of some important diet microalgae during the entire growth phase. Aquaculture. 2014; 428–429:104–110.

152. Benning C, Huang Z-H, Gage D. Accumulation of a novel glycolipid and a betaine lipid in cells of *Rhodobacter sphaeroides* grown under phosphate limitation. Arch Biochem Biophys. 1995; 317(1):103–11.

153. Kunzler K, Eichenberger W. Betaine lipids and zwitterionic phospholipids in plants and fungi. Phytochemistry. 1997; 46(5):883–92.

154. Cañavate JP, Armada I, R'ios JL, Hachero-Cruzado I, Canãvate JP, Armada I, et al. Exploring occurrence and molecular diversity of betaine lipids across taxonomy of marine microalgae. Phytochemistry. 2016; 124:68–78.

155. Gurr MI, Harwood JL, Frayn KN, Murphy DJ, Michell RH. Roles of Lipids in Cellular Structures. In Lipids: Biochemistry, Biotechnology and Health. Sixth ed. 2016; 187-227. Wiley-Blackwell.

156. Okazaki Y, Kamide Y, Hirai MY, Saito K. Plant lipidomics based on hydrophilic interaction chromatography coupled to ion trap time-of-flight mass spectrometry. Metabolomics. 2013; 9(1):121–131.

157. Nakamura Y. Phosphate starvation and membrane lipid remodeling in seed plants. Prog Lipid Res. 2013; 52(1):43–50.

158. Millar AA, Smith MA, Kunst L. All fatty acids are not equal: Discrimination in plant membrane lipids.Trends in Plant Science. 2000; 5:95–101.

159. da Costa E, Melo T, Moreira ASP, Alves E, Domingues P, Calado R, et al. Decoding bioactive polar lipid profile of the macroalgae *Codium tomentosum* from a sustainable IMTA system using a lipidomic approach. Algal Res. 2015; 12:388-397.

160. Yan X, Chen D, Xu J, Zhou C. Profiles of photosynthetic glycerolipids in three strains of *Skeletonema* determined by UPLC-Q-TOF-MS. J Appl Phycol. 2011; 23(2):271–282.

161. Dormann P, Benning C. Galactolipids rule in seed plants. Trends Plant Sci. 2002; 7(3):112–118.

162. Hamner RM. Seasonality of the invasive seaweed *Gracilaria vermiculophylla* along the southeastern coast of North Carolina. 2006; 122(2):49–55.

163. Kumari P, Reddy R, Jha B. Quantification of selected endogenous hydroxy-oxylipins from tropical marine macroalgae. Mar Biotechnol. 2014; 16(1):74–87.

164. Kumari P, Kumar M, Reddy CRKRK, Jha B. Nitrate and phosphate regimes induced lipidomic and biochemical changes in the intertidal macroalga *Ulva lactuca* (Ulvophyceae, Chlorophyta). Plant Cell Physiol. 2014; 55(1):52–63.

165. Kumari P, Kumar M, Reddy CRK, Jha B. Algal lipids, fatty acids and sterols. In Dominguez H. (Ed), Functional Ingredients from Algae for Foods and Nutraceuticals. Functional ingredients from algae for foods and nutraceuticals. 2013: 87-134. Woodhead

Publishing Series in Food and Science, Technology and Nutrition.

166. Kim S-H, Liu K-H, Lee S-Y, Hong S-J, Cho B-K, Lee H, et al. Effects of light intensity and nitrogen starvation on glycerolipid, glycerophospholipid, and carotenoid composition in *Dunaliella tertiolecta* culture. PLoS One. 2013; 8(9):e72415.

167. Khotimchenko S V. Variations in lipid composition among different developmental stages of *Gracilaria verrucosa* (Rhodophyta). Bot Mar. 2006; 49(1):34–38.

168. Floreto EAT, Teshima S. The fatty acid composition of seaweed exposed to different levels of light intensity and salinity. Bot Mar. 1998; 41(5):467–481.

169. Ivanova P, Milne S, Myers D, Brown H. Lipidomics: a mass spectrometry based systems level analysis of cellular lipids. Curr Opin Chem Biol. 2009; 13(5–6):526–531.

170. Bou Khalil M, Hou W, Zhou H, Elisma F, Swayne LA, Blanchard AP, et al. Lipidomics era: accomplishments and challenges. Mass Spectrom Rev. 2010; 29(6):877–929.

171. Alves E, Melo T, Simões C, Faustino MAF, Tomé JPC, Neves MGPMS, et al. Photodynamic oxidation of *Staphylococcus warneri* membrane phospholipids: new insights based on lipidomics. Rapid Commun Mass Spectrom. 2013; 27(14):1607–1618.

172. Santinha DR, Marques DR, Maciel EA, Simões CSO, Rosa S, Neves BM, et al. Profiling changes triggered during maturation of dendritic cells: a lipidomic approach. Anal Bioanal Chem. 2012; 403(2):457–471.

173. Dória ML, Cotrim CZ, Simões C, Macedo B, Domingues P, Domingues MR, et al. Lipidomic analysis of phospholipids from human mammary epithelial and breast cancer cell lines. J Cell Physiol. 2013;228(2):457–468.

174. Simões C, Domingues P, Ferreira R, Amado F, Duarte JA, Vitorino R, et al. Remodeling of liver phospholipidomic profile in streptozotocin-induced diabetic rats. Arch Biochem Biophys. 2013; 538(2):95–102.

175. Liengprayoon S, Sriroth K, Dubreucq E, Vaysse L. Glycolipid composition of *Hevea brasiliensis* latex. Phytochemistry. 2011; 72(14–15):1902–1913.

176. Cheong WF, Wenk MR, Shui G. Comprehensive analysis of lipid composition in crude palm oil using multiple lipidomic approaches. J Genet Genomics. 2014; 41(5):293–304.

177. Zianni R, Bianco G, Lelario F, Losito I, Palmisano F, Cataldi TRI. Fatty acid neutral losses observed in tandem mass spectrometry with collision-induced dissociation allows regiochemical assignment of sulfoquinovosyl-diacylglycerols. J Mass Spectrom. 2013; 48(2):205–215.

178. Basconcillo LS, Zaheer R, Finan TM, McCarry BE. A shotgun lipidomics approach in *Sinorhizobium meliloti* as a tool in functional genomics. J Lipid Res. 2009; 50(6):1120–1132.

179. Popendorf KJ, Fredricks HF, Van Mooy B a S. Molecular ion-independent quantification of polar glycerolipid classes in marine plankton using triple quadrupole MS. Lipids. 2013; 48(2):185–195.

180. Rezanka T, Nedbalová L, Procházková L, Sigler K, Tomá R, Rezanka T, et al. Lipidomic profiling of snow algae by ESI-MS and silver-LC / APCI-MS. Phytochemistry. 2014; 100:1–9.

181. Banskota AH, Stefanova R, Sperker S, Lall SP, Craigie JS, Hafting JT, et al. Polar lipids from the marine macroalga *Palmaria palmata* inhibit lipopolysaccharide-induced nitric oxide production in RAW264.7 macrophage cells. Phytochemistry. 2014; 101:101–108.

182. Bligh EG, Dyer WJ. A rappid method of total lipid extraction and purification. Can J Biochem Physiol. 1959; 37(8):911–917.

183. Folch J, Lees M, Sloane Stanley GH. A simple method for the isolation and purification of total lipides from animal tissues. J Biol Chem. 1957; 226:497–509.

184. Matyash V, Liebisch G, Kurzchalia T V., Shevchenko A, Schwudke D. Lipid extraction by methyl-tert-butyl ether for high-throughput lipidomics. J Lipid Res [Internet]. 2008; 49(5):1137–1146.

185. de Souza LM, Müller-Santos M, Iacomini M, Gorin PAJ, Sassaki GL. Positive and negative tandem mass spectrometric fingerprints of lipids from the halophilic *Archaea Haloarcula marismortui*. J Lipid Res. 2009; 50(7):1363–1373.

186. Herrero M, Ibáñez E. Green processes and sustainability: An overview on the extraction of high added-value products from seaweeds and microalgae. J Supercrit Fluids. 2014; 96:211-216

187. Herrero M, Cifuentes A, Ibanez E. Sub- and supercritical fluid extraction of functional ingredients from different natural sources: Plants, food-by-products, algae and microalgae:A review. Food Chem. 2006; 98(1):136–148.

188. Li Y, Ghasemi Naghdi F, Garg S, Adarme-Vega TC, Thurecht KJ, Ghafor WA, et al. A comparative study: the impact of different lipid extraction methods on current microalgal lipid research. Microb Cell Fact. 2014; 13(1):14.

189. Iqbal J, Theegala C. Optimizing a continuous flow lipid extraction system (CFLES) used for extracting microalgal lipids. GCB Bioenergy. 2013; 5(3):327–337.

190. Zhuang Y, Guo J, Chen L, Li D, Liu J, Ye N. Microwave-assisted direct liquefaction of *Ulva prolifera* for bio-oil production by acid catalysis. Bioresour Technol [Internet]. 2012 Jul [cited 2014 Sep 5];116:133–139.

191. Dejoye Tanzi C, Abert Vian M, Chemat F. New procedure for extraction of algal lipids from wet biomass: a green clean and scalable process. Bioresour Technol. 2013; 134:271–275.

192. Mustafa A, Turner C. Pressurized liquid extraction as a green approach in food and herbal plants extraction: A review. Anal Chim Acta. 2011; 703(1):8–18.

193. Carabias-Martínez R, Rodríguez-Gonzalo E, Revilla-Ruiz P, Hernández-Méndez J. Pressurized liquid extraction in the analysis of food and biological samples. J Chromatogr A. 2005; 1089:1–17.

194. Dettmer K, Aronov PA, Hammock BD. Mass spectrometry-based metabolomics. Mass Spectrom Rev. 2007; 26:51–78.

195. Yan X, Li H, Xu J, Zhou C. Analysis of phospholipids in microalga *Nitzschia closterium* by UPLC-Q-TOF-MS. Chinese J Oceanol Limnol. 2010; 28(1):106–112.

196. Ejsing CS, Moehring T, Bahr U, Duchoslav E, Karas M, Simons K, et al. Collision-induced dissociation pathways of yeast sphingolipids and their molecular profiling in total lipid extracts: a study by quadrupole TOF and linear ion trap-orbitrap mass spectrometry. J Mass Spectrom. 2006; 41(3):372–389.

197. Hummel J, Segu S, Li Y, Irgang S, Jueppner J, Giavalisco P. Ultra performance liquid chromatography and high resolution mass spectrometry for the analysis of plant lipids. Front Plant Sci. 2011; 2:1–17.

198. Wuhrer M, de Boer AR, Deelder AM. Structural glycomics using hydrophilic interaction chromatography (HILIC) with mass spectrometry. Mass Spectrom Rev. 2009; 28(2):192–206.

199. Buszewski B, Noga S. Hydrophilic interaction liquid chromatography (HILIC) – A powerful separation technique. Anal Bioanal Chem. 2012; 402(1):231–47.

200. Chao Z, Ping H, Qiong-Lin L, Yi-Ming W, Guo-An L. Recent advances in lipidomics. Chinese J Anal Chem. 2009; 37(9):1390–1396.

201. Oradu SA, Cooks RG. Multistep mass spectrometry methodology for direct characterization of polar lipids in green microalgae using paper spray ionization. Anal Chem. 2012; 84(24):10576–10585.

202. de Souza LM, Sassaki GL, Romanos MTV, Barreto-Bergter E. Structural characterization and anti-HSV-1 and HSV-2 activity of glycolipids from the marine algae *Osmundaria obtusiloba* isolated from Southeastern Brazilian coast. Mar Drugs 2012; 10(4):918–931.

203. Al-Fadhli A, Wahidulla S, D'Souza L. Glycolipids from the red alga *Chondria armata* (Kutz.) Okamura. Glycobiology. 2006;16:902–915.

204. Kim YH, Kim EH, Lee C, Kim MH, Rho J-R. Two new monogalactosyl diacylglycerols from brown alga *Sargassum thunbergii*. Lipids. 2007; 42(4):395–399.

205. Kendel M, Wielgosz-collin G, Bertrand S, Roussakis C, Bourgougnon N, Bedoux G. Lipid composition,f acids and sterols in the seaweeds *Ulva armoricana*, and *Solieria chordalis* from Brittany (France): An analysis from nutritional, chemotaxonomic, and antiproliferative activity perspectives. Mar. Drugs. 2015; 13(9):5606–5628.

206. Wang X, Zhao P, Luo Q, Yan X, Xu J, Chen J, et al. Metabolite changes during the life history of *Porphyra haitanensis*. Plant Biol. 2015; 17(3):660–666.

207. Ma A-C, Chen Z, Wang T, Song N, Yan Q, Fang Y, et al. Isolation of the molecular species of monogalactosyldiacylglycerols from brown edible seaweed *Sargassum horneri* and their inhibitory effects on triglyceride accumulation in 3T3-L1 Adipocytes. J Agric Food Chem. 2014; 62:11157–11162.

208. Myers DS, Ivanova PT, Milne SB, Brown HA. Quantitative analysis of glycerophospholipids by LC – MS : Acquisition , data handling , and interpretation. Biochim Biophys Acta. 2011; 1811(11):748–757.

209. Da Costa E, Silva J, Mendonça SHS, Abreu MHMH, Domingues MR, Mendonça SH, et al. Lipidomic approaches towards deciphering glycolipids from microalgae as a reservoir of bioactive lipids. Mar Drugs. 2016; 14(5):1–27.

210. Tatituri RV V., Brenner MB, Turk J, Hsu F-F. Structural elucidation of diglycosyl diacylglycerol and monoglycosyl diacylglycerol from *Streptococcus pneumoniae* by multiple-stage ninear ion-trap mass spectrometry with electrospray ionization. J Mass Spectrom. 2013; 47(1):115–123.

211. Kim YH, Choi J-S, Yoo JS, Park Y-M, Kim MS. Structural identification of glycerolipid molecular species isolated from *Cyanobacterium Synechocystis* sp. PCC 6803 using fast atom bombardment Tandem Mass Spectrometry. Anal Biochem. 1999; 267(2):260–270.

212. Hsu F-F, Turk J. Studies on phosphatidylglycerol with triple quadrupole tandem mass spectrometry with electrospray ionization: Fragmentation processes and structural characterization. J Am Soc Mass Spectrom. 2001; 12(9):1036–1043.

213. Hsu F-F, Turk J. Studies on phosphatidylserine by tandem quadrupole and multiple stage quadrupole ion-trap mass spectrometry with electrospray ionization: structural characterization and the fragmentation processes. J Am Soc Mass Spectrom. 2005; 16(9):1510–1522.

214. Hsu F-F, Turk J. Electrospray ionization with low-energy collisionally activated dissociation Tandem mass spectrometry of glycerophospholipids: Mechanisms of fragmentation and structural characterization. J Chromatogr B. Analyt Technol Biomed Life Sci. 2009; 877:2673–2695.

215. Hsu FF, Turk J. Electrospray ionization/tandem quadrupole mass spectrometric studies on

phosphatidylcholines: the fragmentation processes. J Am Soc Mass Spectrom. 2003; 14(4):352–363.

216. Roche SA, Leblond JD. Betaine lipids in chlorarachniophytes. Phycol Res. 2010; 58(4):298–305.

217. Kumari P, Bijo AJ, Mantri VA, Reddy CRK, Jha B. Fatty acid profiling of tropical marine macroalgae: an analysis from chemotaxonomic and nutritional perspectives. Phytochemistry. 2013; 86:44–56.

218. Banskota A., Gallant P, Stefanova R, Melanson R, O'Leary SJ. B. Monogalactosyldiacylglycerols, potent nitric oxide inhibitors from the marine microalga *Tetraselmis chui*. Nat Prod Res. 2012;37–41.

219. Chang HW, Jang KH, Lee D, Kang HR, Kim T-Y, Lee BH, et al. Monoglycerides from the brown alga *Sargassum sagamianum*: Isolation, synthesis, and biological activity. Bioorg Med Chem Lett. 2008 Jun 15; 18(12):3589–3592.

220. Harvey AL. Medicines from nature : are natural products still relevant to drug discovery ? TiPS. 1999; 20(5):196–198.

221. Dudonné S, Vitrac X, Coutière P, Woillez M, Mérillon J-M. Comparative study of antioxidant properties and total phenolic content of 30 plant extracts of industrial interest using DPPH, ABTS, FRAP, SOD, and ORAC assays. J Agric Food Chem. 2009; 57(5):1768–1774.

222. Sangha JS, Fan D, Banskota AH, Stefanova R, Khan W, Hafting J, et al. Bioactive components of the edible strain of red alga, *Chondrus crispus*, enhance oxidative stress tolerance in *Caenorhabditis elegans*. J Funct Foods. 2013; 5(3):1180–1190.

223. Hossain Z, Kurihara H, Hosokawa M, Takahashi K. Growth inhibition and induction of differentiation and apoptosis mediated by sodium butyrate in Caco-2 cells with algal glycolipids. Vitr Cell Dev Biol. 2005; 41(5):154–159.

224. Robertson RC, Guihéneuf F, Bahar B, Schmid M, Stengel DB, Fitzgerald GF, et al. The anti-Inflammatory effect of algae-derived lipid extracts on lipopolysaccharide (LPS)-Stimulated Human THP-1 Macrophages. Mar Drugs. 2015; 13(8):5402–5424.

225. Arunkumar K, Rengasamy R. The antibacterial compound sulphoglycerolipid 1-0 palmitoyl- 3-0 (6 -sulphoquinovopyranosyl) -glycerol from *Sargassum wightii* Greville (Phaeophyceae). Bot Mar. 2005; 48:441–445.

226. Stabili L, Acquaviva MI, Biandolino F, Cavallo RA, De Pascali SA, Fanizzi FP, et al. Biotechnological potential of the seaweed *Cladophora rupestris* (Chlorophyta, Cladophorales) lipidic extract. N Biotechnol. 2014; 31(5):436–444.

227. Magalhães LM, Segundo M a, Reis S, Lima JLFC. Methodological aspects about *in vitro* evaluation of antioxidant properties. Anal Chim Acta. 2008; 613(1):1–19.

228. Ban J, Tan L, Lim YY. Critical analysis of current methods for assessing the *in vitro* antioxidant and antibacterial activity of plant extracts. 2015; 172:814–822.

229. Zubia M, Robledo D, Freile-Pelegrin Y. Antioxidant activities in tropical marine macroalgae from the Yucatan Peninsula, Mexico. J Appl Phycol. 2007; 19(5):449–458.

230. Andrade PB, Barbosa M, Matos RP, Lopes G, Vinholes J, Mouga T, et al. Valuable compounds in macroalgae extracts. Food Chem. 2013; 138(2–3):1819–1828.

231. Melo JVML-F, Carvalho; AFFU, Freitas; SM, M.M. V. Antibacterial activity of extracts of six macroalgae from the northeaster brazilian coast. Brazilian J Microbiol. 2002; 33:311–313.

232. Bergé JP, Debiton E, Dumay J, Durand P, Barthomeuf C. In vitro anti-inflammatory and

anti-proliferative activity of sulfolipids from the red *alga Porphyridium cruentum*. J Agric Food Chem. 2002; 50(21):6227–6232.

233. Shu M-H, Appleton D, Zandi K, AbuBakar S. Anti-inflammatory, gastroprotective and anti-ulcerogenic effects of red algae *Gracilaria changii* (Gracilariales, Rhodophyta) extract. BMC Complement Altern Med. 2013; 13:61.
234. Ricciardolo FLM, Sterk PJ, Gaston B, Folkerts G. Nitric oxide in health and disease of the respiratory system. Physiol Rev. 2004; 84(3):731–765.
235. Moncada S. Nitric oxide: discovery and impact on clinical medicine. J R Soc Med. 1999; 92(4):164–169.
236. Murray M, Hraiki A, Bebawy M, Pazderka C, Rawling T. Anti-tumor activities of lipids and lipid analogues and their development as potential anticancer drugs. Pharmacol Ther. 2015; 150:109–128.
237. Sharif N, Munir N, Saleem F, Aslam F, Naz S. Prolific Anticancer Bioactivity of Algal Extracts (Review). Am J Drug Deliv Ther. 2014; ISSN 2349-7211.
238. Nobili S, Lippi D, Witort E, Donnini M, Bausi L, Mini E, et al. Natural compounds for cancer treatment and prevention. Pharmacol Res. 2009; 59(6):365–378.
239. da Rocha, Adriana B da Rocha, Rafael M Lopes GS. Natural products in anticancer therapy. Curr Opin Pharmacol. 2001; 1(4):364–369.
240. Yuan Y V, Walsh NA. Antioxidant and antiproliferative activities of extracts from a variety of edible seaweeds. Food Chem Toxicol. 2006; 44(7):1144–1150.
241. Zhang J, Li C, Yu G, Guan H. Total synthesis and structure-activity relationship of glycoglycerolipids from marine organisms. Mar Drugs. 2014; 12(6):3634–3659.
242. Mendes M, Pereira R, Sousa Pinto I, Carvalho APP, Gomes AMM, Pinto S, et al. Antimicrobial activity and lipid profile of seaweed extracts from the North Portuguese Coast. Int Food Res J. 2013; 20(6):3337–3345.
243. Cowan MM. Plant Products as Antimicrobial Agents. Clin Microbiol Rev [Internet]. 1999;12(4):564–82. Available from: http://cmr.asm.org/content/12/4/564.short
244. Guiry MD, The Seaweed Site: information on marine algae. Available from http://www.seaweed.ie/ (Accessed on 16th March 2017).
245. McHugh DJ. A Guide to the Seaweed Industry. In Fisheries and Aquaculture Departmen 2003. FAO FISHERIES TECHNICAL PAPER 441, Rome.
246. Steriti A, Rossi R, Concas A, Cao G. A novel cell disruption technique to enhance lipid extraction from microalgae. Bioresour Technol. 2014 ;164:70–77.
247. Ranjan A, Patil C, Moholkar VS. Mechanistic Assessment of Microalgal Lipid Extraction. Ind Eng Chem Res. 2010; (59):2979–2985.
248. Carrapiso AI, García C. Development in Lipid Analysis : Some new extraction techniques and *in situ* transesterification. 2000; 35(11):1167–1177.
249. Lee J-Y, Yoo C, Jun S-Y, Ahn C-Y, Oh H-M. Comparison of several methods for effective lipid extraction from microalgae. Bioresour Technol. 2010; 101(1):75-77.
250. Fuchs B, Süß R, Teuber K, Eibisch M, Schiller J. Lipid analysis by thin-layer chromatography-A review of the current state. J Chromatogr A. 2011; 1218(19):2754–2774
251. Fuchs B, Bresler K, Schiller J. Oxidative changes of lipids monitored by MALDI MS. Chem. and Phys. Lipids. 2011; 164:782–795.
252. Larsen K, Thygesen MB, Guillaumie F, Willats WGT, Jensen KJ. Solid-phase chemical tools for glycobiology. Carbohydr Res. 2006; 341(10):1209–1234.

253. Henry M, SPE Tecnhology – Principles and practical consequences. In Simpson N. (Ed.), Solid-Phase Extraction Principles, Techniques, and Applications. Acta Chem Scand. 2000:125–179. Marcel Dekker, Inc. USA.

254. Simpson N, Martha W. Introduction to solid-phase extraction. In Simpson N. (Ed.), Solid-Phase Extraction: Principles, Techniques, and Applications. 2000:1–17. Marcel Dekker, Inc. USA.

255. Hennion MC. Solid-phase extraction: method development, sorbents, and coupling with liquid chromatography. J Chromatogr A. 1999; 856(1–2):3–54.

256. Ruiz-Gutiérrez V, Pérez-Camino MC. Update on solid-phase extraction for the analysis of lipid classes and related compounds. J Chromatogr A. 2000; 885(1–2):321–341.

257. Kim HY, Salem NJ. Separation of lipid classes by solid phase extraction. J Lipid Res. 1990; 31(12):2285-2289.

258. Balasubramanian RK, Yen Doan TT, Obbard JP. Factors affecting cellular lipid extraction from marine microalgae. Chem Eng J. 2013; 215–216:929–936.

259. Leblond JD, Dahmen JL, Seipelt RL, Elrod-Erickson MJ, Kincaid R, Howard JC, et al. Lipid Composition of Chlorarachniophytes (Chlorarachniophyceae) From the Genera Bigelowiella, Gymnochlora, and Lotharella. J Phycol. 2005; 41(2):311–321.

260. Schmid KM, Bates PD, Larson T, Markham JE, Debono A, Samuels L, et al. Methods and protocols for arabidopsis lipid analysis. In Li-Beisson Y, Shorrosh B, Beisson F, Andersson M, Arondel V, et al (Eds). Acyl lipid metabolism. The Arabidopsis Book. 2013; (8),1–65. American Society of Plant Biologists: Rockville, MD, USA.

261. Torres PB, Chow F, Furlan CM, Mandelli F, Mercadante A, Santos DYAC Dos. Standardization of a protocol to extract and analyze chlorophyll a and carotenoids in *Gracilaria tenuistipitata* Var. Liui. Zhang and Xia (Rhodophyta). Brazilian J Oceanogr. 2014; 62(1):57–63.

262. Lichtenthaler H, Wellburn A. Determinations of total carotenoids and chlorophylls b of leaf extracts in different solvents. Biochem Soc Trans [Internet]. 1983; 11:591–592.

263. Henriques M, Silva A, Rocha J. Extraction and quantification of pigments from a marine microalga: a simple and reproducible method. Commun Curr Res Educ Top Trends Appl Microbiol. 2007;586–593.

264. Koch A. K, Kappeli O, Fiechter A., Reiser J. Hydrocarbon assimilation and biosurfactant production in *Pseudomonas aeruginosa mutants*. J Bacteriol. 1991; 173(13):4212–4219.

265. Bell BM, Daniels DGH, Fearn T, Stewart BA. Lipid compositions, baking qualities and other characteristics of wheat varieties grown in the U.K. J Cereal Sci. 1987; 5(3):277–286.

266. Bartlett EM, Lewis DH. Spectrophotometric determination of phosphate esters in the presence and absence of orthophosphate. Anal Biochem. 1970; 36:159–67.

267. Rodrigues D, Freitas AC, Pereira L, Rocha-Santos TAP, Vasconcelos MW, Roriz M, et al. Chemical composition of red, brown and green macroalgae from Buarcos bay in Central West Coast of Portugal. Food Chem. 2015; 183:197–207.

268. Isca VMS, Seca AML, Pinto DCG a, Silva H, Silva AMS. Lipophilic profile of the edible halophyte *Salicornia ramosissima*. Food Chem. 2014; 165:330–336.

269. Quehenberger O, Armando AM, Dennis E a. High sensitivity quantitative lipidomics analysis of fatty acids in biological samples by gas chromatography-mass spectrometry. Biochim Biophys Acta. 2011; 1811(11):648–56.

270. Bourre J-M. Dietary omega-3 fatty acids for women. Biomed Pharmacother. 2007;61(2–3):105–112.

271. Pluskal T, Castillo S, Villar-Briones A, Orešič M. MZmine 2: Modular framework for processing, visualizing, and analyzing mass spectrometry- based molecular profile data. BMC Bioinformatics. 2010; 11:395

272. Cabral C, Poças J, Gonçalves MJ, Cavaleiro C, Cruz MT, Salgueiro L. *Ridolfia segetum* (L.) Moris (Apiaceae) from Portugal: A source of safe antioxidant and anti-inflammatory essential oil. Ind Crops Prod. 2015; 65:56–61.

273. Valente J, Zuzarte M, Gonçalves MJ, Lopes MC, Cavaleiro C, Salgueiro L, et al. Antifungal, antioxidant and anti-inflammatory activities of *Oenanthe crocata* L. essential oil. Food Chem Toxicol. 2013; 62:349–354

274. Green LC, Wagner DA, Glogowski J, Skipper PL, Wishnok JS, Tannenbaum SR. Analysis of nitrate, nitrite, and [15N]nitrate in biological fluids. Anal Biochem. 1982; 126(1):131–8.

275. Tournour HH, Segundo MA, Magalhães LM, Barreiros L, Queiroz J, Cunha LM. Valorization of grape pomace: extraction of bioactive phenolics with antioxidant properties. Ind Crops Prod. 2015; 74:397–406.

276. Miliauskas G, Venskutonis PR, van Beek TA. Screening of radical scavenging activity of some medicinal and aromatic plant extracts., Food Chemistry. 2004; (85): 231–237.

277. Price J a, Sanny CG, Shevlin D. Application of manual assessment of oxygen radical absorbent capacity (ORAC) for use in high throughput assay of "total" antioxidant activity of drugs and natural products. J Pharmacol Toxicol Methods. 2006; 54(1):56–61.

278. Ulbricht TLV, Southgate DAT. Coronary heart disease: seven dietary factors. The Lancet. 1991; 338(8773):985–992.

279. Pereira L. MACOI - Portuguese Seaweeds Web site. Available from http: //macoi.ci.uc.pt/. (Accessed on 9th October 2016).

280. Goecke F, Hernández V, Bittner M, González M. Fatty acid composition of three species of *Codium* (Bryopsidales , Chlorophyta) in Chile. Rev Biol Mar Oceanogr. 2010;45:325–330.

281. Bouarab K, Adas F, Gaquerel E, Kloareg B, Salau J, Potin P, et al. The Innate immunity of a marine red alga involves oxylipins from both the eicosanoid and octadecanoid Pathways. 2004;135:1838–1848.

282. Rempt M, Weinberger F, Grosser K, Pohnert G. Conserved and species-specific oxylipin pathways in the wound-activated chemical defense of the noninvasive red alga Gracilaria chilensis and the invasive *Gracilaria vermiculophylla*. Beilstein J Org Chem. 2012; 8:283–289.

283. Bartley ML, Boeing WJ, Corcoran A a., Holguin FO, Schaub T. Effects of salinity on growth and lipid accumulation of biofuel microalga *Nannochloropsis salina* and invading organisms. Biomass and Bioenergy. 2013; 54:83–88.

284. Xu X, Tran VH, Kraft JG, Beardall J. Fatty acids of six *Codium* species from southeast. Phytochemistry. 1998; 48(8):1335–1339.

285. Göbel C, Feussner I. Methods for the analysis of oxylipins in plants. Phytochemistry. 2009; 70(13-14):1485–1503.

286. Blée E. Impact of phyto-oxylipins in plant defense. Trends Plant Sci. 2002; 7(7):315–322.

287. Maeda N, Kokai Y, Ohtani S, Sahara H, Hada T, Ishimaru C, et al. Anti-tumor effects of the glycolipids fraction from spinach which inhibited DNA polymerase activity. Nutr Cancer. 2007;57(2):216–223.

288. Lu FSH, Nielsen NS, Baron CP, Jacobsen C. Marine phospholipids: The current understanding of their oxidation mechanisms and potential uses for food fortification. Crit Rev Food Sci Nutr. 2017; 57(10):2057–2070.

289. Francavilla M, Pineda A, Lin CSK, Franchi M, Trotta P, Romero A a, et al. Natural porous agar materials from macroalgae. Carbohydr Polym. 2013; 92(2):1555–1560.

290. Pettitt TR, Harwood JL. Alterations in lipid metabolism caused by illumination of the marine red algae *Chondrus crispus* and *Polysiphonia lanosa*. Phytochemistry. 1989; 28(12):3295–3300.

291. Simopoulos AP. The importance of the omega-6/omega-3 fatty acid ratio in cardiovascular disease and other chronic diseases. Exp Biol Med (Maywood). 2008; 233(6):674–688.

292. Simopoulos A. The importance of the ratio of omega-6/omega-3 essential fatty acids. Biomed Pharmacother. 2002; 56(8):365–379.

293. Kao TH, Chen CJ, Chen BH. An improved high performance liquid chromatography-photodiode array detection-atmospheric pressure chemical ionization-mass spectrometry method for determination of chlorophylls and their derivatives in freeze-dried and hot-air-dried *Rhinacanthus nasutus*. Talanta. 2011; 86:349–355.

294. Vencl F V, Gomez NE, Ploss K, Boland W. The chlorophyll catabolite, pheophorbide a, confers predation resistance in a larval tortoise beetle shield defense. J Chem Ecol. 2009; 35(3):281–288.

295. Pereira R, Kraemer G, Yarish C, Sousa-Pinto I. Nitrogen uptae by gametophytes of *Porphyra dioica* (Bangiales, Rhodophyta) under controlled-culture conditions. Eur J Phycol. 2008; 43(1):107–118.

296. Zhang W, Gao JT, Zhang YC, Qin S. Optimization of conditions for cell cultivation of *Porphyra haitanensis* conchocelis in a bubble-column bioreactor. World J Microbiol Biotechnol. 2006; 22(7):655–60.

297. Van Ginneken VJT, Helsper JPFG, de Visser W, Van Keulen H, Brandenburg WA. Polyunsaturated fatty acids in various macroalgal species from North Atlantic and tropical seas. Lipids Health Dis. 2011; 10(1):104.

298. Eitsuka T, Nakagawa K, Igarashi M, Miyazawa T. Telomerase inhibition by sulfoquinovosyldiacylglycerol from edible purple laver (*Porphyra yezoensis*). Cancer Lett. 2004; 212(1):15–20.

299. Chen CY, Chou HN. Screening of red algae filaments as a potential alternative source of eicosapentaenoic acid. Mar Biotechnol. 2002; 4(2):189–192.

300. Xiaolei F, Guangce W, Demao L, Pu X, Songdong S. Study on early-stage development of conchospore in *Porphyra yezoensis* Ueda. Aquaculture. 2008; 278(1–4):143–149.

301. Spolaore P, Joannis-Cassan C, Duran E, Isambert A. Commercial applications of microalgae. J Biosci Bioeng. 2006; 101(2):87–96.

302. Soler-Vila A, Coughlan S, Guiry MD, Kraan S. The red alga *Porphyra dioica* as a fish-feed ingredient for rainbow trout (*Oncorhynchus mykiss*): effects on growth, feed efficiency, and carcass composition. J Appl Phycol. 2009; 21(5):617–624.

303. Wells, M.L., Potin, P., Craigie, J.S. et al. Algae as nutritional and functional food sources: revisiting our understanding. J Appl Phycol (2017) 29: 949.

304. Wu D, Fujio M, Wong CH. Glycolipids as immunostimulating agents. Bioorganic and Medicinal Chemistry. 2008; 16:1073–1083.

305. Cian RE, Fajardo MA, Alaiz M, Vioque J, González RJ, Drago SR. Chemical composition, nutritional and antioxidant properties of the red edible seaweed *Porphyra columbina*. Int J Food Sci Nutr. 2014; 65(3):299–305.

306. Sánchez-Machado DI, López-Cervantes J, López-Hernández J, Paseiro-Losada P. Fatty acids, total lipid, protein and ash contents of processed edible seaweeds. Food Chem. 2004;

85(3):439–44.

307. Wang X, Su X, Luo Q, Xu J, Chen J, Yan X, et al. Profiles of glycerolipids in *Pyropia haitanensis* and their changes responding to agaro-oligosaccharides. J Appl Phycol. 2014; 26(6):1–8.

308. Da Costa E, Melo T, Moreira ASPA, Bernardo C, Helguero L, Ferreira I, et al. Valorization of Lipids from Gracilaria sp. through Lipidomics and Decoding of Antiproliferative and Anti-Inflammatory Activity. Mar Drugs. 2017; 15(3):62.

309. Birner R, Bürgermeister M, Schneiter R, Daum G. Roles of phosphatidylethanolamine and of its several biosynthetic pathways in *Saccharomyces cerevisiae*. Mol Biol Cell. 2001; 12(4):997–1007.

310. Gerasimenko NI, Busarova NG, Moiseenko OP. Age-dependent changes in the content of lipids, fatty acids, and pigments in brown alga *Costaria costata*. Russ J Plant Physiol. 2010; 57(1):62–68.

311. Mueller-Roeber B. Inositol phospholipid metabolism in *Arabidopsis* characterized and putative isoforms of inositol phospholipid kinase and phosphoinositide-specific phospholipase C. Plant Physiol. 2002; 130(1):22–46.

312. Khotimchenko S V. Lipids from the marine alga Gracilaria verrucosa. Chem Nat Compd. 2005; 41(3):285–288.

313. Schmid M, Guihéneuf F, Stengel DB. Fatty acid contents and profiles of 16 macroalgae collected from the Irish Coast at two seasons. J Appl Phycol. 2014; 26(1):451–63.

314. Fleurence J, Gutbier G, Mabeau S, Leray C. Fatty acids from 11 marine macroalgae of the French Brittany coast. J Appl Phycol. 1994; 6(5–6):527–532.

315. Luo Q, Zhu Z, Zhu Z, Yang R, Qian F, Chen H, et al. Different responses to heat shock stress revealed heteromorphic adaptation strategy of *Pyropia haitanensis* (Bangiales, Rhodophyta). PLoS One. 2014; 9(4):e94354.

316. Calder PC, Albers R, Antoine J-M, Blum S, Ferns GA, Folkerts G, et al. Inflammatory disease processes and interactions with nutrition. Br J Nutr. 2009; 101:2-14.

317. Calder PC. Omega-3 polyunsaturated fatty acids and inflammatory processes: nutrition or pharmacology? Br J Clin Pharmacol. 2013; 75(3):645–62.

318. De Roos B, Mavrommatis Y, Brouwer IA. Long-chain *n*-3 polyunsaturated fatty acids: New insights into mechanisms relating to inflammation and coronary heart disease. Br J Pharmacol. 2009; 158(2):413–428.

319. Calder PC. Omega-3 fatty acids and inflammatory processes: from molecules to man. Biochem Soc Trans. 2017; 45(5):1–11.

320. Simopoulos AP. Essential fatty acids in health and chronic disease. Am J Clin Nutr. 1999; 70(3):560-569.

321. Kumar M, Kumari P, Trivedi N, Shukla MK, Gupta V, Reddy CRK, et al. Minerals, PUFAs and antioxidant properties of some tropical seaweeds from Saurashtra coast of India. J Appl Phycol. 2010; 23(5):797–810.

322. Tabarsa M, Rezaei M, Ramezanpour Z, Waaland JR. Chemical compositions of the marine algae *Gracilaria salicornia* (Rhodophyta) and *Ulva lactuca* (Chlorophyta) as a potential food source. J Sci Food Agric. 2012; 92(12):2500–2506.

323. Whitman CE, Travis RL. Phospholipid composition of a plasma membrane-enriched fraction from developing soybean roots. Plant Physiol. 1985;7 9(2):494–498.

324. Paul-André S, Norio M, Joyard J, Maréchal E, Miège C, Block M, et al. Structure,

Distribution and biosynthesis of glycerolipids from higher plant chloroplasts. Lipids Photosynth Struct Funct Genet. 2004; 6:21–52.

325. Levchenko E V. Carbon Metabolism Transitions during the Development of Marine Macroalga *Gracilaria verrucosa*. Russ J Plant Physiol. 2003; 50(1):68–71.

326. McMillin JB, Dowhan W. Cardiolipin and apoptosis. Biochim Biophys Acta-Molecular Cell Biol Lipids. 2002; 1585(2–3):97–107.

327. Kato M, Sakai M, Adachi K, Ikemoto H, Sano H, Laboratories S, et al. Distribution of betaine lipids in marine algae. Phytochemistry. 1996; 42(5):1341–1345.

328. Alabdulkarim B, Bakeet ZAN, Arzoo S. Role of some functional lipids in preventing diseases and promoting health. J King Saud Univ - Sci. 2012; 24(4):319–329.

329. Bowen KJ, Harris WS, Kris-Etherton PM. Omega-3 Fatty Acids and Cardiovascular Disease: Are There Benefits? Curr Treat Options Cardiovasc Med. 2016; 18(11):69.

330. Gerasimenko N, Logvinov S. Seasonal composition of lipids, fatty acids pigments in the brown alga Sargassum pallidum: The potential for health. Open J Mar Sci. 2016; 6(4):498–523.

331. Hamed I, Özogul F, Özogul Y, Regenstein JM. Marine Bioactive Compounds and Their Health Benefits: A Review. Compr Rev Food Sci Food Saf. 2015; 14(4):446–465.

332. Juneja A, Ceballos RM, Murthy GS. Effects of environmental factors and nutrient availability on the biochemical composition of algae for biofuels production: A review. Energies. 2013; 6(9):4607–4638.

333. Marinho GS, Holdt SL, Jacobsen C, Angelidaki I. Lipids and composition of fFatty acids of *Saccharina latissima* cultivated year-round in Integrated Multi-Trophic Aquaculture. Mar Drugs. 2015 ;13:4357–74.

334. Nomura M, Kamogawa H, Susanto E, Kawagoe C, Yasui H, Saga N, et al. Seasonal variations of total lipids, fatty acid composition, and fucoxanthin contents of *Sargassum horneri* (Turner) and *Cystoseira hakodatensis* (Yendo) from the northern seashore of Japan. J Appl Phycol. 2013; 25(4):1159–1169.

335. Jones AL, Harwood JL. Lipid composition of the brown algae *Fucus vesiculosus* and *Ascophyllum nodosum*. Phytochemistry. 1992;3 1(10):3397–3403.

336. Vieler A, Wilhelm C, Goss R, Süß R, Schiller J. The lipid composition of the unicellular green alga *Chlamydomonas reinhardtii* and the diatom *Cyclotella meneghiniana* investigated by MALDI-TOF MS and TLC. Chem Phys Lipids. 2007; 150(2):143–155.

337. Khotimchenko S. . FAtty acids of brown algae from the russian far east. Phytochemistry. 1998;49(8):2363–9.

338. Harwood JL. Lipid metabolism in the Red Marine Algae Chondrus Crispus and Polysinphonza Lanosa as modified by temperature. Phytochemistry. 1989;28(8):1–6.

339. Morgan-Kiss RM, Priscu JC, Pocock T, Gudynaite-Savitch L, Huner NPA. Adaptation and acclimation of photosynthetic microorganisms to permanently cold environments. Microbiol Mol Biol Rev. 2006; 70(1):222–252.

340. Nishio K, Horie M, Akazawa Y, Shichiri M, Iwahashi H, Hagihara Y, et al. Attenuation of lipopolysaccharide (LPS)-induced cytotoxicity by tocopherols and tocotrienols. Redox Biol. 2013; 1(1):97–103.

341. Sherwood ER, Toliver-Kinsky T. Mechanisms of the inflammatory response. est Pract Res Clin Anaesthesiol. 2004; 18:385–405.

342. Calder PC. Marine omega-3 fatty acids and inflammatory processes: Effects, mechanisms

and clinical relevance. Biochim Biophys Acta. 2014; 1851(4):469–484.

343. Calder PC, Grimble RF. Polyunsaturated fatty acids, inflammation and immunity. Eur J Clin Nutr. 2002;56(3):14–19.

344. Banskota AH, Stefanova R, Gallant P, McGinn PJ. Mono- and digalactosyl diacylglycerols: Potent nitric oxide inhibitors from the marine microalga *Nannochloropsis granulata*. J Appl Phycol. 2013; 25(2):349–57.

345. Bertram JS. The molecular biology of cancer. Mol Aspects Med. 2000; 21:167–223.

346. Eroles P, Bosch A, Alejandro Pérez-Fidalgo J, Lluch A. Molecular biology in breast cancer: Intrinsic subtypes and signaling pathways. Cancer Treat. Rev. 2012; 38:698–707.

347. Andrianasolo EH, Haramaty L, Vardi A, White E, Lutz R, Falkowski P. Apoptosis-inducing galactolipids from a cultured marine diatom, *Phaeodactylum tricornutum*. J Nat Prod. 2008;7:1197–1201.

348. Hussain E, Wang L-J, Jiang B, Riaz S, Buttd GY, Shi D-Y. Components of brown seaweeds are potential candidate for cancer therapy - a review. SC Adv.2016;6:12592-12610

349. Hanashima S, Mizushina Y, Yamazaki T, Ohta K, Takahashi S, Sahara H, et al. Synthesis of sulfoquinovosylacylglycerols, inhibitors of eukaryotic DNA polymerase alpha and beta. Bioorganic Med Chem. 2001; 9(2):367–376.

350. Ohta K, Mizushina Y, Hirata N, Takemura M, Sugawara F, Matsukage A, et al. Sulfoquinovosyldiacylglycerol, KM043, a new potent inhibitor of eukaryotic DNA polymerases and HIV-reverse transcriptase type 1 from a marine red alga, *Gigartina tenella*. Chem Pharm Bull. 1998; 46(4):684–696.

351. Konno S. Effect of various natural products on growth of bladder cancer cells : Two promising mushroom extracts. 2007; 12(1):63–8.

352. Coussens LM, Werb Z. Inflammation and cancer. 2010; 420(6917):860–867.

Supplementary information

Supplementary material of Chapter III.1

Appendix A. Supplementary material of Chapter III.1.1

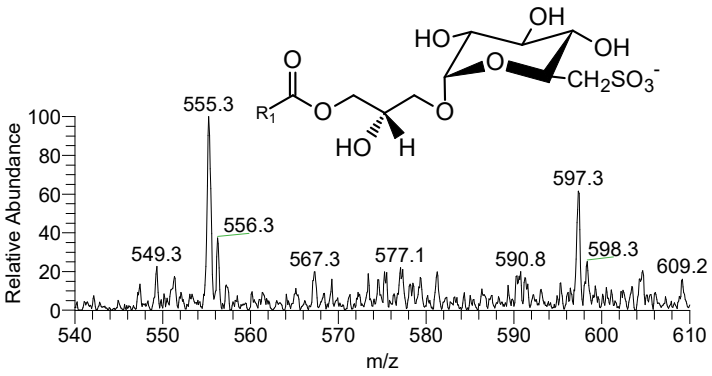

Sulfolipids [M - H]⁻ *m/z*	Lipid Species (C:N)
549.3	SQMG (16:3)
555.3	**SQMG (16:0)**
567.3	SQMG (17:1)
597.3	SQMG (19:0)

Figure S. 1. LC–MS spectrum of the sulfoquinovosyl monoacylglycerol (SQMG) molecular species observed by HILIC–ESI–MS as $[M - H]^-$ ions. Bold *m/z* values correspond to the most abundant species detected in the LC−MS spectrum. (C means number of carbon atoms and N represents the number of double bonds in the fatty acyl side chains). A general structure is also represented.

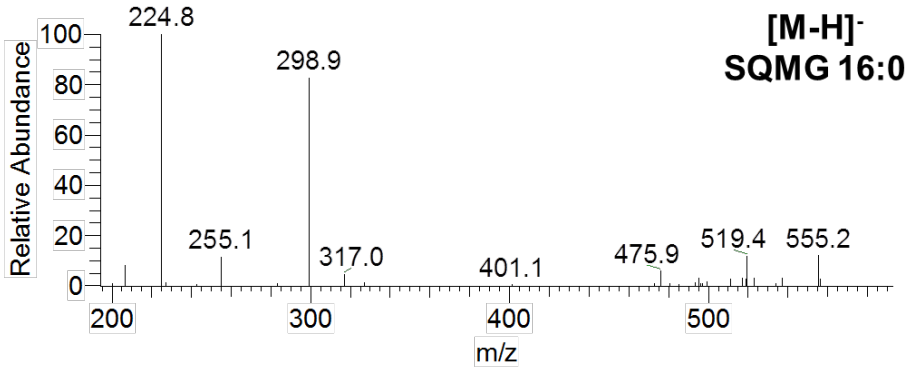

Figure S. 2. ESI–MS/MS spectrum of the ion $[M - H]^-$ of SQMG 16:0 at *m/z* 555.2 (A).

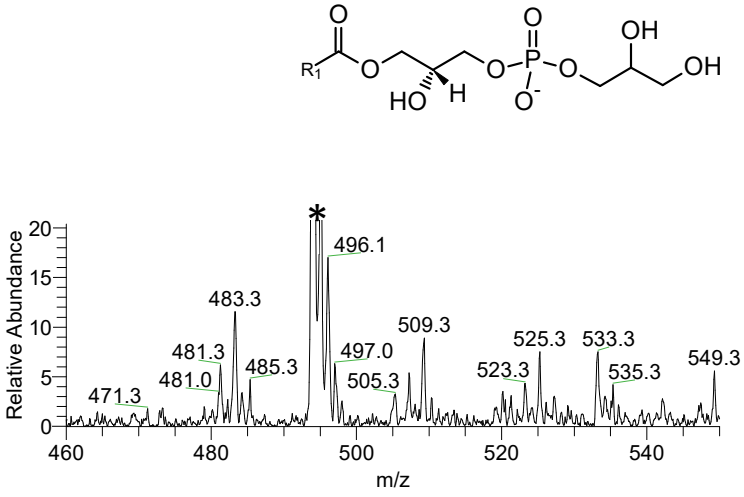

[M - H]⁻ *m/z*	Lipid Species (C:N)
Lyso phosphatidylglycerol	
481.3	LPG (16:1)
483.3	**LPG (16:0)**
507.3	LPG (18:2)
509.3	LPG (18:1)
523.3	LPG (19:1)
525.3	LPG (19:0)
533.3	LPG (20:3)
535.3	LPG (20:2)

Figure S. 3. LC–MS spectrum of the lyso phosphatidylglycerol (LPG) molecular species observed by HILIC−ESI−MS as $[M - H]^-$ ions. Bold *m/z* values correspond to the most abundant species detected in the LC–MS spectrum. (C means number of carbon atoms and N represents the number of double bonds in the fatty acyl side chains). *Eluent contamination. A general structure is also represented.

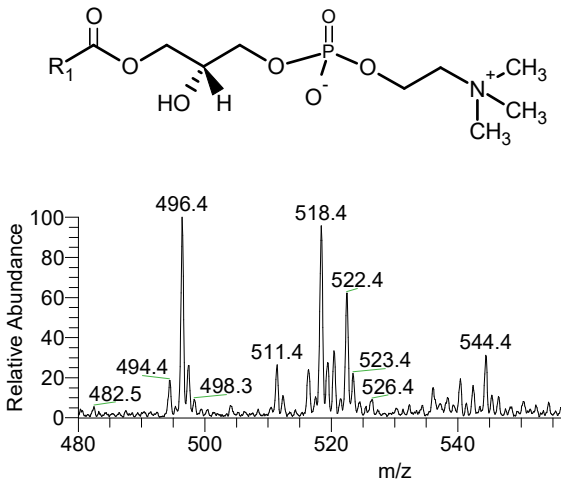

[M + H]⁺ *m/z*	Lipid Species (C:N)
Lyso phosphatidylcholine	
482.5	LPC (O-16:0a)
494.4	LPC (16:1)
496.4	**LPC (16:0)**
516.4	LPC (18:4)
518.4	**LPC (18:3)**
520.4	LPC (18:2)
522.4	LPC (18:1)
524.4	LPC (18:0)
536.6	LPC (O-18:1a)
542.4	LPC (20:5)
544.4	LPC 20:4

Figure S. 4. LC–MS spectrum of the lyso phosphatidylcholine (LPC) molecular species. The table includes the molecular species observed by HILIC–ESI–MS as $[M + H]^+$ ions. Bold *m/z* values correspond to the most abundant species detected in the LC-MS spectrum. (C means number of carbon atoms and N represents the number of double bonds in the fatty acyl side chains). A general structure is also represented.

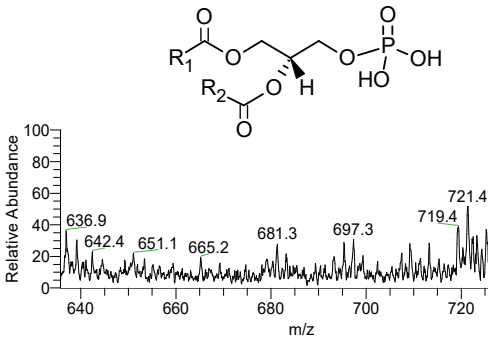

$[M-H]^-$	Lipid Species	Fatty acyl Chain
m/z	(C:N)	
Phosphatidic acid		
665.2	PA (34:5)	16:1/18:4
681.3	PA (O-36:4)	O-18:1a/18:3
695.3	PA (36:4)	18:1/18:3 and 16:0/20:4
697.3	PA (36:3)	18:1/18:2 and 18:0/18:3
701.3	PA (36:1)	18:0/18:1
719.4	PA (38:6)	18:3/20:3
721.4	PA (38:5)	18:0/20:5

Figure S. 5. LC–MS spectrum of the phosphatidic acid (PA) molecular species. The table includes the molecular species, observed by HILIC-ESI-MS, as $[M-H]^-$ ions. (C means number of carbon atoms and N represents the number of double bonds in the fatty acyl side chains). A general structure is also represented.

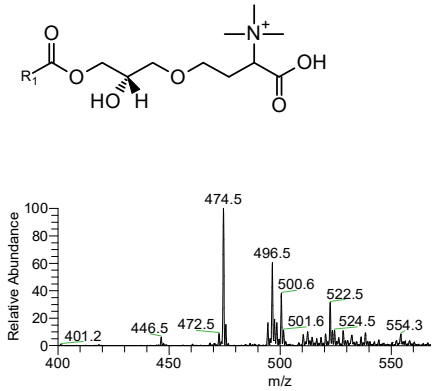

$[M+H]^+$	Lipid Species	$[M+H]^+$	Lipid Species
m/z	(C:N)	*m/z*	(C:N)
Monoacylglyceryl trimethyl-homoserine			
446.5	MGTS (14:0)	512.5	MGTS (19:2)
470.5	MGTS (16:2)	514.5	MGTS (19:1)
472.5	MGTS (16:1)	516.4	MGTS (19:0)
474.5	**MGTS (16:0)**	520.5	MGTS (20:5)
494.6	MGTS (18:4)	522.5	MGTS (20:4)
496.5	**MGTS (18:3)**	524.5	MGTS (20:3)
498.5	MGTS (18:2)	528.5	MGTS (20:1)
500.6	MGTS (18:1)	554.3	MGTS (22:2)

Figure S. 6. LC−MS spectrum of the monoacylglyceryl-*N,N,N*-trimethylhomoserine (MGTS) molecular species. The table includes the molecular species observed by HILIC−ESI−MS, as $[M+H]^+$. Bold *m/z* values correspond to most abundant species detected in the LC-MS spectrum. (C means number of carbon atoms and N represents the number of double bonds in the fatty acyl side chains). A general structure is also represented.

Appendix B. Supplementary material of Chapter III.1.2

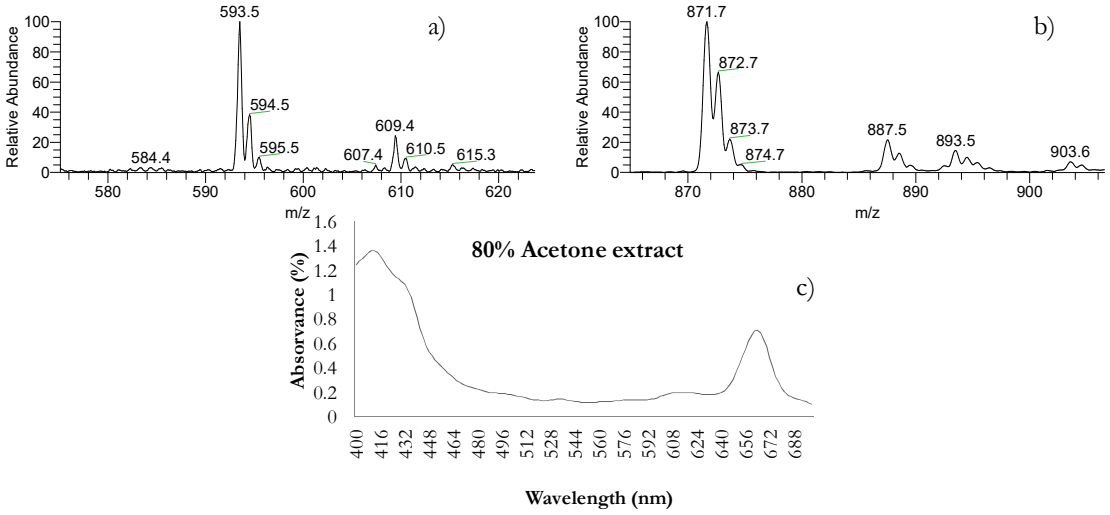

Figure S. 7. LC–MS spectrum of the pigments species in the total extract of *Gracilaria sp.*as $[M + H]^+$ ions and UV spectrum.

Table S. 1. Molecular species observed by HILIC−ESI−MS with the assignment of the total fatty acyl composition of each lipid molecular species, according to the analyses performed by mass accuracy (error < 5 ppm) using the Xcalibur software, exact mass calculator - http://www.sisweb.com/referenc/tools/exactmass.htm, and lipid maps tools - http://www.lipidmaps.org/tools/. C means number of carbon atoms and N represents the number of double bonds in the fatty acyl side chains

Porphyra dioica	Mass error (ppm, ≤ 5 ppm)			
Glycolipids	***m/z* theoretical**	**Blade**	**Conchocelis**	**Identification**
Sulfolipids [M - H]$^-$				
C25 H47 O11 S	555.2839	-0.7010	0.3110	SQMG 16:0
C41 H77 O12 S	793.5136	-1.0770	-0.3210	SQDG (32:0)
C43 H77 O12 S	817.5136	-1.1560	1.9510	SQDG (34:2)
C45 H75 O12 S	839.4979	-1.5180	-0.7920	SQDG (36:5)
C45H75O13S	855.4928	-1.5190	-0.2680	SQDG (36:5-OH)
Galactolipids [M + NH$_4$]$^+$				
C43H82O10N	772.5939	-3.2540	-4.6650	MGDG (34:2)
C43H84O10N	774.6095	-2.4190	-3.8910	MGDG (34:1)
C45H80NO10	794.5782	-4.0575	-4.4351	MGDG (36:5)
C45H82NO10	796.5939	-2.6410	-2.7920	MGDG (36:4)
C45H86NO10	800.6240	-4.9206	-4.8712	MGDG (36:2)
C45H88NO10	802.6408	----------	-4.9140	MGDG (36:1)
C49 H92 O15 N	934.6467	-3.4210	-2.2650	DGDG (34:2)
C49 H94 O15 N	936.6618	-3.8435	-2.6660	DGDG (34:1)
C51 H90 O15 N	956.6310	-3.6054	-0.3648	DGDG (36:5)
C51H90O16 N	972.6260	-3.9728	-1.0939	DGDG (36:5-OH)
Phospholipids	***m/z* theoretical**	**Blade**	**Conchocelis**	**Identification**
Phosphatidylcholine [M + H]$^+$				
C40H79O8NP	732.5538	-3.2762	----------	PC (32:1)
C42H73O8NP	734.5695	-1.6336	-2.5866	PC (32:0)
C42H75O8NP	752.5225	----------	-2.6577	PC (34:5)
C42H77O8NP	754.5382	-1.7229	-3.1808	PC (34:4)
C42H79O8NP	756.5538	-3.0401	-2.7758	PC (34:3)
C42H81O8NP	758.5695	-3.4275	-2.7684	PC (34:2)
C42H83O8NP	760.5851	-3.4184	-2.6296	PC (34:1)
C44H75O8NP	762.6008	-4.1962	----------	PC (34:0)
C44H79O8NP	780.5538	-3.7153	-4.0997	PC (36:5)
C44H81O8NP	782.5695	-3.7058	-3.9613	PC (36:4)
C44H83O8NP	784.5851	-3.5688	-2.6766	PC (36:3)
C44H85O8NP	786.6008	-3.5596	-3.3054	PC (36:2)
C44H87O8NP	788.6164	-4.8186	----------	PC (36:1)
C46H79O8NP	804.5538	-4.8474	----------	PC (38:7)

C46H81O8NP	806.5695	-4.9593		-4.4634	PC (38:6)
C46H83O8NP	808.5851	-4.9469		-4.4522	PC (38:5)
C46H85O8NP	810.6008	-2.4673		-4.9346	PC (38:4)
C46H87O8NP	812.6164	-4.4302	----------		PC (38:3)
Lyso-Phosphatidylcholine [M + H]$^+$					
C24H49NO7P	494.3241	-2.4276	----------		LPC (16:1)
C24H51NO7P	496.3398	-2.6192		-3.6266	LPC (16:0)
C26H49NO7P	518.3241	-4.6303	----------		LPC (18:3)
C26H53NO7P	522.3554	-2.1059		-0.5743	LPC (18:1)
C26H55NO7P	524.3711	-1.7163	----------		LPC (18:0)

Phospholipids	*m/z* theoretical	Blade	Conchocelis		Identification
Lyso-Phosphatidylglycerol [M-H]$^-$					
C22H42O9P	481.2572	-2.0779		-1.4545	LPG (16:1)
C22H44O9P	483.2728	-5.8179		-1.2467	LPG (16:0)
C24H46O9P	509.2885	-2.3562		-1.7672	LPG (18:1)
Phosphatidylglycerol [M-H]$^-$					
C36H68O10P	691.4556	----------		-0.0782	PG (30:1)
C38H70O10P	717.4712	----------		-2.0964	PG (32:2)
C38H72O10P	719.4869	-2.8551		-1.6042	PG (32:1)
C38H74O10P	721.5025	-2.6393		-2.6393	PG (32:0)
C40H74O10P	745.5025	-2.6884		-1.4812	PG (34:2)
C40H76O10P	747.5182	-2.3468		-2.3468	PG (34:1)
C40H78O10P	749.5338	----------		-4.9422	PG (34:0)
C42H70O10P	765.4712	-2.8794		-1.9649	PG (36:6)
C42H72O10P	767.4869	-3.1977		-1.8947	PG (36:5)
C42H74O10P	769.5025	-4.2940		-2.8645	PG (36:4)
C42H76O10P	771.5182	-2.7923		-2.1442	PG (36:3)
C42H78O10P	773.5338	-2.5912		-2.0741	PG (36:2)
C42H80O10P	775.5495	-3.1648		-2.3911	PG (36:1)
C44H82O10P	801.5651	-4.1170		-0.9980	PG (38:2)
C44H84O10P	803.5802	-1.6178		-1.3689	PG (38:1)
Phosphatidic acid [M-H]$^-$					
C35H64O8P	643.4344	-4.2346	----------		PA (32:2)
C35H66O8P	645.4501	0.9687		-0.8904	PA (32:1)
C35H68O8P	647.4657	-0.9680	----------		PA (32:0)
C37H66O8P	669.4501	2.5771	----------		PA (34:3)
C37H68O8P	671.4652	-0.1191		-0.8638	PA (34:2)
C37H70O8P	673.4814	-1.4475	----------		PA (34:1)
C39H64O8P	691.4344	-1.9158	----------		PA (36:6)
C39H66O8P	693.4501	-2.1267	----------		PA (36:5)
C39H68O8P	695.4652	-1.1216		3.6235	PA(36:2)
C39H70O8P	697.4814	-1.4337	----------		PA (36:3)
C39H72O8P	699.4970	-1.5726		-2.1444	PA (36:2)

C39H74O8P	701.5127	-1.4255		-1.8531	PA (36:1)
Phosphatidylethanolamine [M-H]$^-$					
C35H67O8NP	660.4610	1.5538		-4.3512	PE (30:1)
C35H69O8NP	662.4766	2.9830		-3.8097	PE (30:0)
C37H69O8NP	686.4766	-1.4914		-0.9088	PE (32:2)
C37H71O8NP	688.4923	-1.4145		-1.8503	PE (32:1)
C39H71O8NP	712.4923	-2.0687		-2.7704	PE (34:3)
C39H73O8NP	714.5079	-0.5934		-1.5731	PE (34:2)
C39H75O8NP	716.5236	1.1527		4.9209	PE (34:1)
C41H71O8NP	736.4923	-1.0508		-1.7297	PE (36:5)
C41H73O8NP	738.5079	-0.9803	----------		PE (36:4)
C41H75O8NP	740.5236	----------		-2.1256	PE (36:3)
C41H77O8NP	742.5392	----------		-2.0525	PE (36:2)
C41H79O8NP	744.5549	----------		2.3179	PE (36:1)
C45H73O8NP	786.5079	2.7667	----------		PE (40:8)
Lyso-Phosphatidylethanolamine [M-H]$^-$					
C21H41NO7P	450.2626	-1.3326		0.8884	LPE (16:1)
C21H43NO7P	452.2782	-1.1055		-0.4422	LPE (16:0)
C23H45NO7P	478.2939	-1.6726		-1.8817	LPE (18:1)
Phosphatidylinositol [M-H]$^-$					
C43H76O13P	831.5029	----------		-4.2070	PI (34:3)
C43H78O13P	833.5185	-4.3769		-4.2569	PI (34:2)
C43H80O13P	835.5342	-2.1523		1.1989	PI (34:1)
C47H80O13P	883.5342	----------		-3.5067	PI (38:5)
Inositephosphoceramide [M-H]$^-$					
C50H97NO11P	918.6805	-2.3947	----------		IPC (d44:1)
C48H99NO11P	920.6228	-1.3111		-1.4197	IPC (t42:2-OH)
C48H93NO13P	922.6385	-3.8553		-4.1804	IPC (t42:1-OH)
C48H95NO13P	924.6541	0.7495		1.7228	IPC (t42:0-OH)

Betaine lipids [M + H]$^+$	***m/z* theoretical**	**Blade**	**Conchocelis**	**Identification**
C40H76O7N	682.5622	----------	-2.606	DGTS (30:1)
C40H78O7N	684.5778	----------	-4.571	DGTS (30:0)
C42H80NO7	710.5935	-4.755	-2.504	DGTS (32:1)
C44H82O7N	736.6091	-3.703	-3.568	DGTS (34:2)
C44H84O7N	738.6248	----------	0.406	DGTS (34:1)

$$error\ (ppm) = ((m/z\ experimental - m/z\ library)\ \times 1E6)/(m/z\ experimental)$$

Appendix C. Supplementary material of Chapter III.1.3

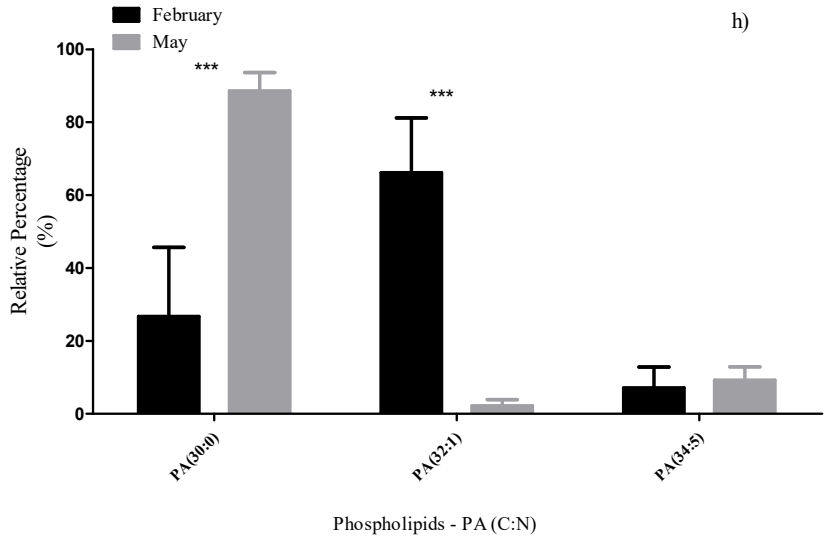

Figure S. 8. Percentage of PA molecular species identified after LC–MS, and MS/MS analysis. The results were expressed as percentage contained by dividing the ratio between peak areas of each molecular species and internal standards and the total of all ratios. Values are means ± standard deviation of the duplicate of three independent experiments. (***, significantly different $p < 0.001$; **, significantly different $p < 0.01$, * significantly different $p < 0.05$).

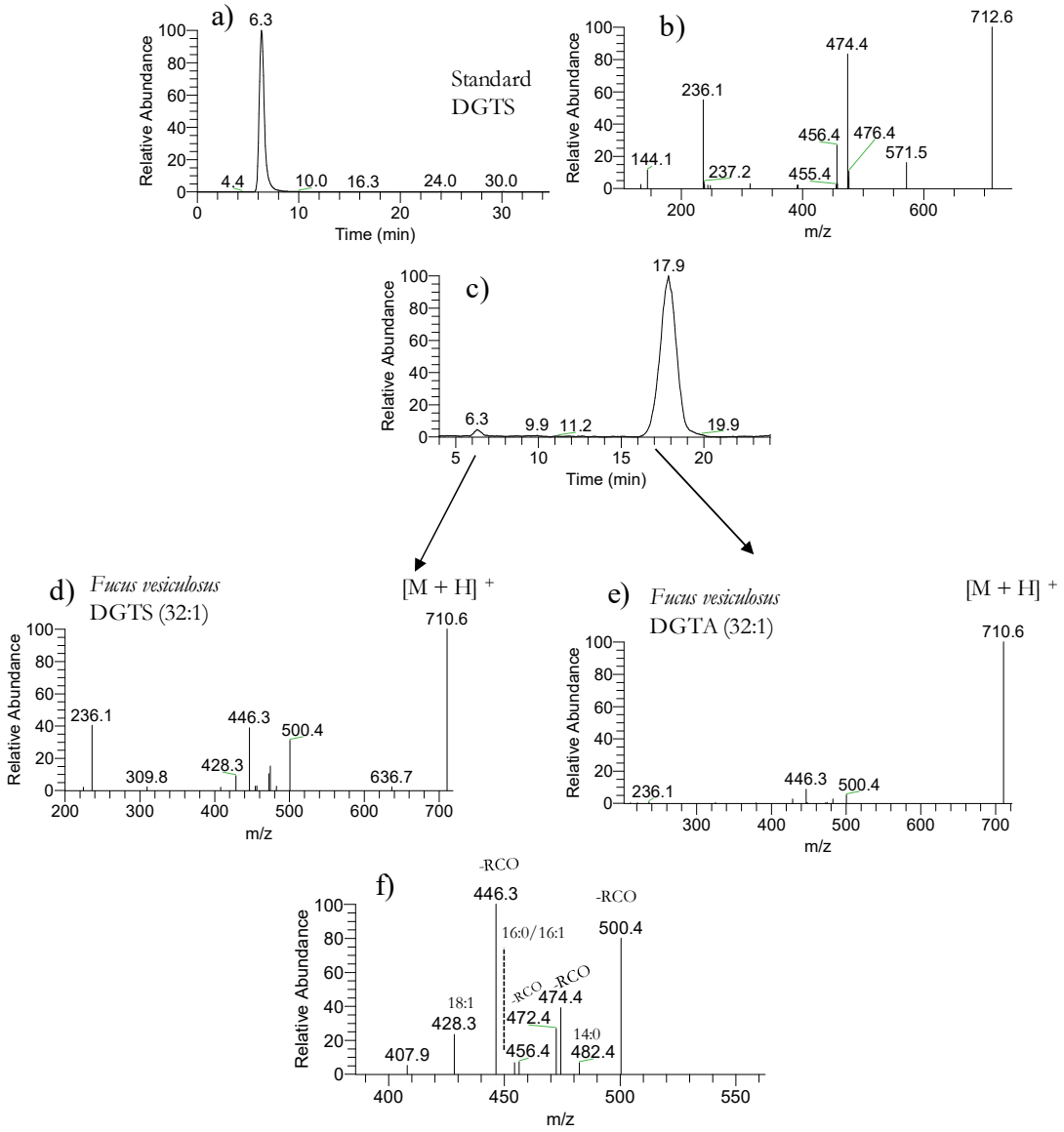

Figure S. 9. LC chromatogram and MS/MS spectra of the betaine molecular species as standard a) and b), respectively. The Figure b) includes the fragmentation of the ion at *m/z* 712.6 as $[M + H]^+$. LC chromatogram c); MS/MS spectrum of the ion at *m/z* 710.6 as $[M + H]^+$ identified in the extract of *Fucus vesiculosus* corresponding to the DGTS d) and MS/MS spectrum of the ion at *m/z* 710.6 as $[M + H]^+$ identified in the extract of *Fucus vesiculosus* corresponding to betaine class DGTA e). The figure f) includes the range of *m/z* between 375 and 550 and was extracted from spectrum e) representing product ions that allow the identification of the fatty acyl composition of $[M + H]^+$ ion at *m/z* 712.6 attributed to DGTA (16:0/16:1) and DGTA (14:0/18:1).

Appendix D. Supplementary resume table of the identification of polar lipids

Table S. 2. Molecular species identification observed by HILIC–ESI–MS as $[M + NH_4]^+$, as $[M + H]^+$, and as $[M - H]^-$ ions, with the assignment of the fatty acyl composition of each lipid molecular species, according to the interpretation of the corresponding MS/MS spectra. (C means number of carbon atoms and N represents the number of double bonds in the fatty acyl side chains)

Ionization	***m/z***	**Molecular species (C:N)**	
$[M + NH_4]^+$	910.3	DGDG (32:0)	16:0/16:0 and 14:0/18:0
$[M + NH_4]^+$	908.6305	DGDG (32:1)	14:0/18:1 and 16:0/16:1
$[M + NH_4]^+$	906.6148	DGDG (32:2)	14:0/18:2
$[M + NH_4]^+$	922.5	DGDG (32:2-OH)	14:0/18:2-OH
$[M + NH_4]^+$	904.5992	DGDG (32:3)	16:0/16:3
$[M + NH_4]^+$	920.6	DGDG (32:3-OH)	14:0/18:3-OH
$[M + NH_4]^+$	922.5	DGDG (33:1)	15:0/18:1 and 16:0/17:1 and 14:0/19:1
$[M + NH_4]^+$	920.6	DGDG (33:2)	15:0/18:2 and 14:0/19:2
$[M + NH_4]^+$	938.678	DGDG (34:0)	18:0/16:0
$[M + NH_4]^+$	936.6618	DGDG (34:1)	18:1/16:0 and 18:0/16:1
$[M + NH_4]^+$	934.6461	DGDG (34:2)	18:2/16:0 and 18:1/16:1
$[M + NH_4]^+$	932.6305	DGDG (34:3)	18:3/16:0
$[M + NH_4]^+$	926.2	DGDG (34:6)	16:3/18:3
$[M + NH_4]^+$	950.5	DGDG (35:1)	17:0/18:1 and 19:1/16:0
$[M + NH_4]^+$	948.6	DGDG (35:2)	17:0/18:2 and 19:2/16:0
$[M + NH_4]^+$	964.6936	DGDG (36:1)	18:1/18:0
$[M + NH_4]^+$	962.678	DGDG (36:2)	18:1/18:1
$[M + NH_4]^+$	960.6623	DGDG (36:3)	18:1/18:2
$[M + NH_4]^+$	958.6461	DGDG (36:4)	20:4/16:0 and 18:2/18:2
$[M + NH_4]^+$	956.6305	DGDG (36:5)	20:5/16:0 and 18:2/18:3
$[M + NH_4]^+$	972.626	DGDG (36:5-OH)	20:5-OH/16:0
$[M + NH_4]^+$	954.6148	DGDG (36:6)	18:3/18:3
$[M + NH_4]^+$	952.5992	DGDG (36:7)	18:3/18:4
$[M + NH_4]^+$	992.6	DGDG (38:1)	18:1/20:0
$[M + NH_4]^+$	986.678	DGDG (38:4)	20:4/18:0
$[M + NH_4]^+$	984.6623	DGDG (38:5)	20:4/18:1
$[M + NH_4]^+$	982.6461	DGDG (38:6)	20:4/18:2 and 20:5/18:1
$[M + NH_4]^+$	980.6305	DGDG (38:7)	20:4/18:3 and 20:5/18:2
$[M + NH_4]^+$	978.6148	DGDG (38:8)	20:5/18:3 and 20:4/18:4
$[M + NH_4]^+$	976.5992	DGDG (38:9)	20:5/18:4
$[M + NH_4]^+$	748.3	MGDG (32:0)	16:0/16:0 and 14:0/18:0
$[M + NH_4]^+$	746.5765	MGDG (32:1)	14:0/18:1 and 16:0/16:1
$[M + NH_4]^+$	742.5479	MGDG (32:3)	16:0/16:3 and 14:1/18:2
$[M + NH_4]^+$	740.5309	MGDG (32:4)	16:0/16:4
$[M + NH_4]^+$	776.3	MGDG (34:0)	18:0/16:0

$[M + NH_4]^+$	774.3	MGDG (34:1)	18:1/16:0
$[M + NH_4]^+$	774.6074	MGDG (34:1)	18:1/16:0
$[M + NH_4]^+$	774.609	MGDG (34:1)	18:1/16:0
$[M + NH_4]^+$	772.5935	MGDG (34:2)	18:2/16:0 and 16:1/18:1
$[M + NH_4]^+$	768.5621	MGDG (34:4)	18:4/16:0 and 16:1/18:3
$[M + NH_4]^+$	804.5	MGDG (36:0)	18:0/18:0
$[M + NH_4]^+$	802.641	MGDG (36:1)	18:1/18:0
$[M + NH_4]^+$	800.624	MGDG (36:2)	18:2/18:0
$[M + NH_4]^+$	796.5929	MGDG (36:4)	18:1/18:3 and 20:4/16:0 and 18:2/18:2
$[M + NH_4]^+$	794.3	MGDG (36:5)	18:2/18:3
$[M + NH_4]^+$	794.3	MGDG (36:5)	20:5/16:0
$[M + NH_4]^+$	794.5772	MGDG (36:5)	18:2/18:3 and 20:5/16:0
$[M + NH_4]^+$	792.5614	MGDG (36:6)	18:3/18:3
$[M + NH_4]^+$	790.5459	MGDG (36:7)	18:3/18:4
$[M + NH_4]^+$	788.5307	MGDG (36:8)	18:4/18:4
$[M + NH_4]^+$	824.6235	MGDG (38:4)	20:4/18:0
$[M + NH_4]^+$	822.6073	MGDG (38:5)	20:4/18:1
$[M + NH_4]^+$	820.5926	MGDG (38:6)	20:5/18:1 and 20:4/18:2
$[M + NH_4]^+$	818.5766	MGDG (38:7)	20:5/18:2 and 20:4/18:3
$[M + NH_4]^+$	816.5608	MGDG (38:8)	20:5/18:3 and 20:4/18:4
$[M + NH_4]^+$	814.5546	MGDG (38:9)	20:5/18:4
$[M - H]^-$	737.4	SQDG (28:0)	14:0/14:0 and 12:0/16:0
$[M - H]^-$	765.4823	SQDG (30:0)	16:0/14:0
$[M - H]^-$	763.4666	SQDG (30:1)	16:0/14:1
$[M - H]^-$	793.5136	SQDG (32:0)	16:0/16:0 and 14:0/18:0
$[M - H]^-$	793.6	SQDG (32:0)	16:0/16:0 and 14:0/18:0
$[M - H]^-$	791.4979	SQDG (32:1)	16:0/16:1 and 14:0/18:2
$[M - H]^-$	789.4666	SQDG (32:2)	18:2/14:0
$[M - H]^-$	787.4666	SQDG (32:3)	18:3/14:0
$[M - H]^-$	821.5449	SQDG (34:0)	18:0/16:0
$[M - H]^-$	819.5292	SQDG (34:1)	18:1/16:0
$[M - H]^-$	819.6	SQDG (34:1)	18:1/16:0
$[M - H]^-$	817.5	SQDG (34:2)	18:2/16:0
$[M - H]^-$	817.5136	SQDG (34:2)	18:2/16:0
$[M - H]^-$	815.4979	SQDG (34:3)	18:3/16:0
$[M - H]^-$	813.4	SQDG (34:4)	18:4/16:0
$[M - H]^-$	813.4823	SQDG (34:4)	18:3/16:1
$[M - H]^-$	835.4	SQDG (35:0)	19:0/16:0 and 17:0/18:0
$[M - H]^-$	833.4	SQDG (35:1)	19:1/16:0 and 17:0/18:1
$[M - H]^-$	831.4	SQDG (35:2)	19:2/16:0 and 17:0/18:2
$[M - H]^-$	847.3	SQDG (36:1)	20:1/16:0
$[M - H]^-$	845.4	SQDG (36:2)	20:2/16:0
$[M - H]^-$	841.5136	SQDG (36:4)	20:4/16:0
$[M - H]^-$	839.4979	SQDG (36:5)	20:5/16:0

$[M - H]^-$	855.493	SQDG (36:5-OH)	20:5-OH/16:0
$[M - H]^-$	865.4	SQDG (38:6)	22:6/16:0
$[M - H]^-$	857.6	SQDG(36:4-OH)	20:4-OH/16:0
$[M - H]^-$	527.2525	SQMG (14:0)	
$[M - H]^-$	555.2838	SQMG (16:0)	
$[M - H]^-$	555.3	SQMG (16:0)	
$[M - H]^-$	555.4	SQMG (16:0)	
$[M - H]^-$	553.2688	SQMG (16:1)	
$[M - H]^-$	549.3	SQMG (16:3)	
$[M - H]^-$	567.3	SQMG (17:1)	
$[M - H]^-$	581.3	SQMG (18:1)	
$[M - H]^-$	579.2839	SQMG (18:2)	
$[M - H]^-$	577.2678	SQMG (18:3)	
$[M - H]^-$	597.3	SQMG (19:0)	

Ionization	***m/z***	**Molecular species (C:N)**	
$[M - H]^-$	908.6	IPC (*t*42:0)	*t*18:0/24:0
$[M - H]^-$	918.681	IPC (d44:1)	d18:1/26:0
$[M - H]^-$	810.5	IPC (*t*35:0)	*t*18:0/17:0
$[M - H]^-$	924.654	IPC (t42:0-OH)	t18:0/24:0-OH
$[M - H]^-$	922.639	IPC (t42:1-OH)	t18:0/24:1-OH
$[M - H]^-$	920.623	IPC (t42:2-OH)	t18:1/24:1-OH
$[M + H]^+$	496.3392	LPC (16:0)	
$[M + H]^+$	494.3241	LPC (16:1)	
$[M + H]^+$	524.37	LPC (18:0)	
$[M + H]^+$	522.3556	LPC (18:1)	
$[M + H]^+$	520.4	LPC (18:2)	
$[M + H]^+$	518.321	LPC (18:3)	
$[M + H]^+$	518.4	LPC (18:3)	
$[M + H]^+$	516.4	LPC (18:4)	
$[M + H]^+$	544.4	LPC (20:4)	
$[M + H]^+$	542.4	LPC (20:5)	
$[M + H]^+$	482.5	LPC (O-16:0a)	
$[M + H]^+$	536.6	LPC (O-18:1a)	
$[M - H]^-$	450.263	LPE (16:1)	
$[M - H]^-$	452.278	LPE (16:0)	
$[M - H]^-$	478.294	LPE (18:1)	
$[M - H]^-$	500.2779	LPE (20:4)	
$[M - H]^-$	498.2613	LPE (20:5)	
$[M - H]^-$	483.2733	LPG (16:0)	
$[M - H]^-$	481.2569	LPG (16:1)	
$[M - H]^-$	509.2887	LPG (18:1)	
$[M - H]^-$	525.3	LPG (19:0=	
$[M - H]^-$	535.3	LPG (20:2)	

$[M - H]^-$	533.3	LPG (20:3)	
$[M - H]^-$	531.3	LPG (20:4)	
$[M - H]^-$	507.3	LPG 18:2	
$[M - H]^-$	523.3	LPG 19:1	
$[M - H]^-$	597.306	LPI (18:1)	
$[M - H]^-$	619.433	PA (30:0)	14:0/16:0
$[M - H]^-$	645.4507	PA (32:1)	14:0/18:1
$[M - H]^-$	647.466	PA (32:1)	16:0/16:0
$[M - H]^-$	643.434	PA (32:2)	14:0/18:2 and 16:1/16:1
$[M - H]^-$	673.481	PA (34:1)	16:1/18:0 and 16:0/18:1
$[M - H]^-$	671.465	PA (34:2)	16:0/18:2
$[M - H]^-$	669.45	PA (34:3)	16:0/18:3 and 16:1/18:2
$[M - H]^-$	669.45	PA (34:3)	14:0/20:3
$[M - H]^-$	665.4184	PA (34:5)	14:0/20:5 and 16:1/18:4
$[M - H]^-$	701.513	PA (36:1)	16:0/20:1
$[M - H]^-$	699.497	PA (36:2)	16:0/20:2
$[M - H]^-$	697.481	PA (36:3)	16:0/20:3
$[M - H]^-$	695.466	PA (36:4)	16:0/20:4
$[M - H]^-$	693.4	PA (36:5)	16:0/20:5
$[M - H]^-$	691.434	PA (36:6)	16:1/20:5
$[M - H]^-$	721.4	PA (38:5)	18:0/20:5 and 18:1/20:4
$[M - H]^-$	719.4	PA (38:6)	18:3/20:3 and 18:2/20:4
$[M - H]^-$	717.4	PA (38:7)	18:3/20:4
$[M - H]^-$	745.3	PA (40:7)	20:3/20:4
$[M - H]^-$	743.3	PA (40:8)	20:4/20:4
$[M - H]^-$	741.3	PA (40:9)	20:4/20:5
$[M - H]^-$	681.3	PA (O-36:4)	O-18:1a/18:3
$[M + H]^+$	702.5	PC (30:2)	14:0/16:2
$[M + H]^+$	734.569	PC (32:0)	16:0/16:0 and 14:0/18:0
$[M - H]^-$	732.554	PC (32:1)	16:0/16:1 and 14:0/18:1
$[M + H]^+$	730.6	PC (32:2)	16:0/16:2 or 16:1/16:1
$[M + H]^+$	728.5	PC (32:3)	16:0/16:3 or 16:1/16:2
$[M + H]^+$	762.5	PC (34:0)	16:0/18:0
$[M + H]^+$	762.601	PC (34:0)	16:0/18:0
$[M + H]^+$	760.5835	PC (34:1)	16:0/18:1
$[M + H]^+$	758.569	PC (34:2)	16:0/18:2 and 16:1/18:1
$[M + H]^+$	758.6	PC (34:2)	16:0/18:2 and 16:1/18:1
$[M + H]^+$	756.554	PC (34:3)	14:0/20:3
$[M + H]^+$	754.538	PC (34:4)	14:0/20:4 and 16:2/18:2
$[M + H]^+$	752.523	PC (34:5)	14:0/20:5
$[M + H]^+$	788.616	PC (36:1)	18:0/18:1
$[M + H]^+$	786.5	PC (36:2)	16:0/20:2

$[M + H]^+$	786.6005	PC (36:2)	18:0/18:2 and 18:1/18:1
$[M + H]^+$	784.4	PC (36:3)	16:0/20:3 and 18:0/18:3
$[M + H]^+$	784.585	PC (36:3)	16:0/20:3 and 18:1/18:2
$[M + H]^+$	784.6	PC (36:3)	16:0/20:3 and 18:1/18:2
$[M + H]^+$	782.569	PC (36:4)	16:0/20:4 and 18:2/18:2
$[M + H]^+$	780.553	PC (36:5)	16:0/20:5 and 18:2/18:3
$[M + H]^+$	780.554	PC (36:5)	16:1/20:4
$[M + H]^+$	798.5	PC (37:3)	16:0/21:3 and 18:1/19:2
$[M + H]^+$	818.5	PC (38:0)	18:0/20:0 and 16:0/22:0
$[M + H]^+$	814.5	PC (38:2)	18:0/20:2 and 18:2/20:0 and 16:0/22:2
$[M + H]^+$	814.5	PC (38:2)	18:1/20:1
$[M + H]^+$	812.5	PC (38:3)	18:3/20:0
$[M + H]^+$	812.616	PC (38:3)	18:0/20:3 and 18:1/20:2
$[M + H]^+$	810.4	PC (38:4)	18:2/20:2 and 18:3/20:1
$[M + H]^+$	810.5	PC (38:4)	18:1/20:3 and 16:0/22:4
$[M + H]^+$	810.601	PC (38:4)	18:1/20:3
$[M + H]^+$	808.585	PC (38:5)	18:1/20:4
$[M + H]^+$	806.5683	PC (38:6)	18:3/20:3
$[M + H]^+$	806.569	PC (38:6)	18:2/20:4 and 18:1/20:5
$[M + H]^+$	804.554	PC (38:7)	18:3/20:4 and 18:2/20:5
$[M + H]^+$	808.5831	PC (38:7)	18:2/20:3 and 18:3/20:2
$[M + H]^+$	846.4	PC (40:0)	20:0/20:0 and 18:0/22:0
$[M + H]^+$	844.4	PC (40:1)	18:1/22:0
$[M + H]^+$	834.4	PC (40:6)	20:2/20:4 and 20:3/20:3 and 18:0/22:6
$[M + H]^+$	744.6	PC (O-34:2)	O-16:0a/18:2 or O-16:0e/18:1
$[M + H]^+$	774.5	PC (O-36:1)	O-18:0a/18:1 or O-18:1a/18:0
$[M + H]^+$	772.5	PC (O-36:2)	O-18:0a/18:2 or O-18:1a/18:1
$[M + H]^+$	770.5	PC (O-36:3)	O-18:0a/18:3 or O-18:1a/18:2
$[M + H]^+$	802.4	PC (O-38:1)	O-18:0a/20:1 and O-18:1a/20:0
$[M + H]^+$	800.4	PC (O-38:2)	O-18:0a/20:2
$[M + H]^+$	798.4	PC (O-38:3)	O-18:0a/20:3
$[M + H]^+$	796.4	PC (O-38:4)	O-18:0a/20:4
$[M + H]^+$	794.4	PC (O-38:5)	O-18:0a/20:5
$[M + H]^+$	830.5	PC (O-40:1)	O-18:0a/22:1
$[M + H]^+$	828.5	PC (O-40:2)	O-18:0a/22:2 or O-18:Oe/22:1
$[M + H]^+$	824.4	PC (O-40:4)	O-18:0a/22:4
$[M + H]^+$	822.5	PC (O-40:5)	O-18:0a/22:5 or O-18:Oe/22:4
$[M + H]^+$	758.5689	PC (34:2)	16:0/18:2 and 16:2/18:1
$[M + H]^+$	756.5	PC (34:3)	16:0/18:3 and 16:2/18:1
$[M + H]^+$	840.4	PC (40:3)	20:0/20:3 or 20:1/20:2 or 18:3/22:0 or 18:1/22:2
$[M - H]^-$	836.4	PC (40:5)	20:2/20:3 and 20:0/20:5
$[M - H]^-$	662.477	PE (30:0)	14:0/16:0

$[M - H]^-$	660.46	PE (30:1)	14:0/16:1
$[M - H]^-$	688.492	PE (32:1)	16:0/16:1
$[M - H]^-$	688.4923	PE (32:1)	14:0/18:1
$[M - H]^-$	686.4758	PE (32:2)	14:0/18:2
$[M - H]^-$	716.5227	PE (34:1)	16:1/18:1 and 16:0/18:2
$[M + H]^+$	718.3	PE (34:1)	16:1/18:0 and 16:0/18:1
$[M - H]^-$	714.5067	PE (34:2)	16:0/18:2
$[M - H]^-$	712.492	PE (34:3)	16:0/18:3 and 16:1/18:2
$[M - H]^-$	744.555	PE (36:1)	18:0/18:1
$[M + H]^+$	746.3	PE (36:1)	18:0/18:1
$[M - H]^-$	742.539	PE (36:2)	18:1/18:1 and 18:0/18:2
$[M + H]^+$	744.4	PE (36:2)	18:1/18:1
$[M - H]^-$	740.524	PE (36:3)	18:0/18:3
$[M + H]^+$	742.4	PE (36:3)	18:1/18:2
$[M - H]^-$	738.508	PE (36:4)	16:0/20:4
$[M + H]^+$	740.4	PE (36:4)	18:2/18:2
$[M - H]^-$	736.492	PE (36:5)	16:0/20:5
$[M - H]^-$	764.5232	PE (38:5)	18:1/20:4
$[M - H]^-$	762.5073	PE (38:6)	18:2/20:4
$[M - H]^-$	788.5218	PE (40:7)	20:4/20:3
$[M - H]^-$	786.5076	PE (40:8)	20:4/20:4
$[M - H]^-$	784.4918	PE (40:9)	20:4/20:5
$[M - H]^-$	691.456	PG (30:1)	14:0/16:1
$[M - H]^-$	721.502	PG (32:0)	16:0/16:0 and 14:0/18:0
$[M - H]^-$	719.4868	PG (32:1)	16:1/16:0 and 14:0/18:1
$[M - H]^-$	717.471	PG (32:2)	16:0/16:2 and 16:1/16:1
$[M - H]^-$	733.3	PG (33:1)	16:0/17:1 and 16:1/17:0
$[M - H]^-$	749.5335	PG (34:0)	16:0/18:0
$[M - H]^-$	747.5183	PG (34:1)	16:0/18:1 and 18:0/16:1
$[M - H]^-$	745.5018	PG (34:2)	16:0/18:2 and 16:1/18:1
$[M - H]^-$	745.503	PG (34:2)	16:1/18:1 and 16:0/18:2
$[M - H]^-$	743.4862	PG (34:3)	16:0/18:3 and 16:1/18:2
$[M - H]^-$	743.5	PG (34:3)	16:0/18:3
$[M - H]^-$	741.4	PG (34:4)	16:0/18:4
$[M - H]^-$	741.4713	PG (34:4)	16:1/18:3
$[M - H]^-$	763.3	PG (35:0)	17:0/18:0 and 19:0:16:0
$[M - H]^-$	759.4	PG (35:2)	17:0/18:2
$[M - H]^-$	775.549	PG (36:1)	18:0/18:1
$[M - H]^-$	773.5333	PG (36:2)	18:1/18:1 and 16:0/20:2
$[M - H]^-$	771.518	PG (36:3)	18:1/18:2 and 16:0/20:3
$[M - H]^-$	769.4	PG (36:4)	16:0/20:4 and 18:2/18:2
$[M - H]^-$	769.5017	PG (36:4)	16:0/20:4

$[M - H]^-$	769.503	PG (36:4)	8:1/18:3 and 18:2/18:2
$[M - H]^-$	767.3	PG (36:5)	16:0/20:5 and 18:2/18:3
$[M - H]^-$	767.487	PG (36:5)	16:0/20:5 and 16:1/20:4
$[M - H]^-$	765.471	PG (36:6)	16:1/20:5 and 18:3/18:3
$[M - H]^-$	787.3	PG (37:2)	17:0/20:2 and 19:0/18:2
$[M - H]^-$	803.58	PG (38:1)	16:0/22:1
$[M - H]^-$	801.565	PG (38:2)	16:0/22:2
$[M - H]^-$	807.4	PI (32:1)	16:0/18:2
$[M - H]^-$	837.5491	PI (34:0)	16:0/18:0
$[M - H]^-$	835.5339	PI (34:1)	16:0/18:1
$[M - H]^-$	833.5175	PI (34:2)	16:0/18:2 and 16:1/18:1
$[M - H]^-$	831.503	PI (34:3)	16:0/18:3
$[M - H]^-$	849.4	PI (35:1)	17:0/18:1
$[M - H]^-$	863.5674	PI (36:1)	18:0/18:1
$[M - H]^-$	861.5505	PI (36:2)	18:0/18:2
$[M - H]^-$	859.5352	PI (36:3)	18:0/18:3
$[M - H]^-$	857.5196	PI (36:4)	16:0/20:4
$[M - H]^-$	855.5041	PI (36:5)	18:4/18:4
$[M - H]^-$	877.4	PI (37:1)	19:0/18:1 and 18:3/20:5
$[M - H]^-$	875.4	PI (37:2)	19:0/18:2 and 18:4/20:5
$[M - H]^-$	873.4	PI (37:3)	19:0/18:3
$[M - H]^-$	883.534	PI (38:5)	18:0/20:5
$[M - H]^-$	907.4	PI (40:6)	18:0/22:6

Ionization	***m/z***	**Molecular species (C:N)**	
$[M + H]^+$	656.5465	DGTA (28:0)	14:0/14:0
$[M + H]^+$	684.5778	DGTA (30:0)	14:0/16:0
$[M + H]^+$	682.5622	DGTA (30:1)	14:0/16:1 and 16:0/14:1
$[M + H]^+$	680.5465	DGTA (30:2)	14:0/16:2
$[M + H]^+$	712.6091	DGTA (32:0)	14:0/18:0 and 16:0/16:0
$[M + H]^+$	710.5935	DGTA (32:1)	14:0/18:1 and 16:0/16:1
$[M + H]^+$	708.5778	DGTA (32:2)	14:0/18:2 and 16:0/16:2
$[M + H]^+$	706.5622	DGTA (32:3)	14:0/18:3 and 16:0/16:3
$[M + H]^+$	704.5465	DGTA (32:4)	16:1/16:3
$[M + H]^+$	738.6248	DGTA (34:1)	16:0/18:1
$[M + H]^+$	736.6091	DGTA (34:2)	14:0/20:2 and 16:0/18:2
$[M + H]^+$	734.5935	DGTA (34:3)	14:0/20:3 and 16:0/18:3
$[M + H]^+$	732.5778	DGTA (34:4)	14:0/20:4
$[M + H]^+$	762.6248	DGTA (36:3)	16:0/20:3
$[M + H]^+$	760.6091	DGTA (36:4)	18:1/18:3 and 16:0/20:4
$[M + H]^+$	656.5465	DGTS (28:0)	14:0/14:0
$[M + H]^+$	684.5778	DGTS (30:0)	14:0/16:0
$[M + H]^+$	682.5622	DGTS (30:1)	14:0/16:1

$[M + H]^+$	680.7	DGTS (30:2)	14:0/16:2
$[M + H]^+$	712.6091	DGTS (32:0)	16:0/16:0
$[M + H]^+$	710.5935	DGTS (32:1)	14:0/18:1 and 16:0/16:1
$[M + H]^+$	708.5778	DGTS (32:2)	16:0/16:2
$[M + H]^+$	706.5622	DGTS (32:3)	14:0/18:3 and 16:0/16:3
$[M + H]^+$	704.5465	DGTS (32:4)	16:1/16:3
$[M + H]^+$	740.7	DGTS (34:0)	16:0/18:0 and 14:0/20:0
$[M + H]^+$	738.6248	DGTS (34:1)	16:0/18:1
$[M + H]^+$	736.6091	DGTS (34:2)	16:0/18:2
$[M + H]^+$	734.5935	DGTS (34:3)	16:0/18:3
$[M + H]^+$	732.5778	DGTS (34:4)	16:0/18:4
$[M + H]^+$	752.6	DGTS (35:1)	16:1/19:0
$[M + H]^+$	750.6	DGTS (35:2)	15:0/20:2 and 16:0/19:2
$[M + H]^+$	748.6	DGTS (35:3)	15:0/20:3 and 16:3/19:0
$[M + H]^+$	766.5	DGTS (36:1)	16:0/20:1 and 16:1/20:0 and 18:0/18:1
$[M + H]^+$	764.6	DGTS (36:2)	18:1/18:1 and 16:0/20:2
$[M + H]^+$	764.6404	DGTS (36:2)	18:0/18:2
$[M + H]^+$	762.6248	DGTS (36:3)	18:0/18:3
$[M + H]^+$	760.6	DGTS (36:4)	16:0/20:4 and 18:0/18:4 and 18:1/18:3
$[M + H]^+$	776.5	DGTS (37:3)	18:3/19:0
$[M + H]^+$	794.5	DGTS (38:1)	18:0/20:1
$[M + H]^+$	792.5	DGTS (38:2)	18:0/20:2
$[M + H]^+$	790.5	DGTS (38:3)	18:0/20:3
$[M + H]^+$	784.5	DGTS (38:6)	18:1/20:5 and 18:2/20:4
$[M + H]^+$	818.5	DGTS (40:3)	18:0/22:3
$[M + H]^+$	808.5	DGTS (40:8)	18:2/22:6 and 20:4/20:4
$[M + H]^+$	446.3481	MGTA (14:0)	
$[M + H]^+$	474.3799	MGTA (16:0)	
$[M + H]^+$	472.3632	MGTA (16:1)	
$[M + H]^+$	468.3308	MGTA (16:3)	
$[M + H]^+$	500.3942	MGTA (18:1)	
$[M + H]^+$	498.3784	MGTA (18:2)	
$[M + H]^+$	496.3632	MGTA (18:3)	
$[M + H]^+$	494.3472	MGTA (18:4)	
$[M + H]^+$	526.4109	MGTA (20:2)	
$[M + H]^+$	524.3957	MGTA (20:3)	
$[M + H]^+$	522.3795	MGTA (20:4)	
$[M + H]^+$	520.3642	MGTA (20:5)	
$[M + H]^+$	446.347	MGTS (14:0)	
$[M + H]^+$	474.3792	MGTS (16:0)	
$[M + H]^+$	472.3632	MGTS (16:1)	
$[M + H]^+$	500.3943	MGTS (18:1)	
$[M + H]^+$	498.3796	MGTS (18:2)	
$[M + H]^+$	496.3634	MGTS (18:3)	

$[M + H]^+$	494.3477	MGTS (18:4)
$[M + H]^+$	528.5	MGTS (20:1)
$[M + H]^+$	524.5	MGTS (20:3)
$[M + H]^+$	554.3	MGTS (22:2)
$[M + H]^+$	470.5	MGTS (16:2)
$[M + H]^+$	516.4	MGTS (19:0)
$[M + H]^+$	514.5	MGTS (19:1)
$[M + H]^+$	512.5	MGTS (19:2)
$[M + H]^+$	522.5	MGTS (20:4)
$[M + H]^+$	520.5	MGTS (20:5)